NASA SP-83

CONFERENCE ON AIRCRAFT OPERATING PROBLEMS

LANGLEY RESEARCH CENTER
MAY 10-12, 1965

NATIONAL AERONAUTICS AND SPACE ADMINISTRATION

NASA SP-83

CONFERENCE ON AIRCRAFT OPERATING PROBLEMS

Langley Research Center
May 10-12, 1965

Scientific and Technical Information Division 1965
NATIONAL AERONAUTICS AND SPACE ADMINISTRATION
Washington, D.C.

For sale by the Clearinghouse for Federal Scientific and Technical Information
Springfield, Virginia 22151 – Price $3.00

PREFACE

This compilation includes papers presented at the NASA Conference on Aircraft Operating Problems held at the Langley Research Center on May 10-12, 1965. Contributions were made by representatives of the Ames Research Center, the Flight Research Center, and the Langley Research Center of NASA, as well as by representatives of the Federal Aviation Agency.

CONTENTS

GENERAL STUDIES

SUBSONIC AIRCRAFT

SUPERSONIC AIRCRAFT

GENERAL AVIATION AIRCRAFT

V/STOL AND STOL AIRCRAFT

1. RECENT STUDIES OF RUNWAY ROUGHNESS

By Garland J. Morris and Albert W. Hall

NASA Langley Research Center

SUMMARY

Recent studies of NASA research related to aircraft operating problems on rough runways are presented. Some of these investigations were conducted cooperatively with the airport operators, with the Federal Aviation Agency, and with the U.S. Air Force. The studies show that criteria based on power spectral levels of runway-profile data are not sufficient to define acceptable levels of runway roughness from the piloting viewpoint. Because of the large variation in response characteristics between various types of aircraft, a runway may be acceptable for some aircraft and unacceptable for others. A criterion for roughness, therefore, should be expressed in terms of aircraft response - preferably, cockpit acceleration. A criterion suggested is that the maximum vertical acceleration in the cockpit should not exceed ±0.4g for sections of the runway where precise aircraft control is required.

INTRODUCTION

For several years, the National Aeronautics and Space Administration has conducted research related to aircraft operating problems on rough runways. Most of the past research efforts have been concerned with the loads problems. These problems are of concern during all phases of ground operations - taxiing, take-off, and landing. Recently, the research efforts have been directed more to the piloting difficulties resulting from rough runways. These problems have generally occurred during the high-speed portion of the take-off run and, occasionally, during the high-speed portion of the landing.

On a rough runway, the cockpit environment is one of decreased instrument readability, pronounced pitching or plunging of the aircraft, and excessive accelerations. Such an environment seriously degrades the pilot's ability to control the airplane precisely during critical phases of the take-off or landing.

This paper presents a progress report on recent NASA research pertaining to the piloting difficulties caused by rough runways. Some of these investigations were conducted cooperatively with airport operators, with the Federal Aviation Agency, and with the U.S. Air Force.

DISCUSSION

Roughness Criteria Based on Profile Data

A considerable amount of work has been done in past years to define the characteristics of runway roughness. For this purpose, detailed runway elevation profiles were obtained for many runways. Short-section profiles, typical of the profiles that have been measured, are presented in figure 1. The three sections shown (designated runways A, B, and C) cover a range of roughness from smooth to rough. Each profile contains, in somewhat a random manner, waves of different wavelengths with the amplitudes generally becoming larger as the wavelengths increase. The order of magnitude of runway-profile deviations that can cause appreciable aircraft response is illustrated by the section from runway C, which has caused complaints of roughness. One rather well-defined depression has a distance of about 100 feet from peak to peak with a profile depression between peaks slightly greater than 0.1 foot.

Past work indicated that a more concise and convenient representation of the roughness characteristics could be obtained by converting the elevation-profile measurements to power spectral plots as shown in figure 2. The ordinate is the power spectral density, which indicates the relative amplitudes of the roughness corresponding to the wavelengths shown on the abscissa. The higher a curve is in the figure, the higher the indicated roughness level.

A study of the power spectral curves for a number of runways led to a proposal for power spectral criteria for runway roughness (ref. 1). The criteria included two power spectral levels, one for "new construction" and one for "needs repair." The spectral level for the new-construction criterion was established by the power spectral density of runway B which has caused no complaints of roughness. (See figs. 1 and 2.) It was felt that newly constructed runways would be satisfactory if their power spectrum fell below the line for new construction. Similarly, repairs were thought to be necessary if the spectrum of an existing runway exceeded the needs-repair criterion. Meeting the new-construction criterion apparently is not an unreasonable task, inasmuch as recently constructed runway A is much smoother than the new-construction criterion.

Shortly after attention was directed toward problems involving piloting difficulties, it became apparent that the power spectral criterion was not completely satisfactory to define an acceptable level of roughness for all operating problems (ref. 2). This conclusion was indicated, in one instance, where two runways having nearly identical power spectral levels caused complaints of roughness by pilots in one case and caused no complaints in the other case.

The inability of the power spectra to determine the relative level of roughness in all cases, particularly from the piloting viewpoint, is not too surprising when the characteristics of a power spectrum are considered to be as follows: The runway power-spectral-density variation with wavelength represents an average roughness over the entire runway length for various wavelengths, does not distinguish between many bumps of small amplitude and a few bumps of large amplitude at a given wavelength, and places no importance on

location of roughness along the runway. Because of the averaging and loss-of-roughness-location information, the power spectral representation does not have the ability to detect profile defects which might cause piloting problems. However, as originally intended, the runway spectral level is an indication of average roughness and for this purpose the spectra are still considered to be useful in analysis of loads and fatigue problems where a large number of runways are to be considered.

Aircraft Response Characteristics

Shortly after the jet transports were placed in service, it was found that runways which had been satisfactory for piston-engine aircraft were causing complaints by the jet pilots. Thus, the pilot's impression of the roughness of a given runway is dependent upon airplane type. Inasmuch as the pilot's impression of runway roughness comes from the manner in which a particular airplane responds to the runway, it is believed that for piloting problems, roughness criteria should be expressed in terms of aircraft response in the cockpit.

Figure 3 shows the spread in response characteristics of various types of aircraft ranging from a light jet trainer to a heavy jet transport. Each response curve was obtained by a power spectral analysis of the cockpit acceleration measured during a constant speed run along a runway. Each response curve presented in this figure was normalized to its own maximum value; therefore, these curves serve only to illustrate the difference in the low-frequency response modes for the aircraft types shown.

Several years ago, the available data on airplane response to runway and taxiway roughness indicated that practically all significant aircraft response occurred in a rather narrow frequency range of $1\frac{1}{2}$ to 2 cycles per second. The aircraft types shown in figure 3 have extended this frequency range. The most significant point to note is the trend toward lower frequencies for the larger aircraft. The trend to low response frequencies has been accompanied by an increase in runway speeds. These two factors have increased the range of roughness wavelengths of importance.

The relation between speed, frequency, and roughness wavelength is shown in figure 4 as the variation of wavelength with speed for several frequencies. At a given frequency, the wavelength increases with increasing speed and, at a given speed, the wavelength increases with decreasing frequency. The lowest resonant frequency for each aircraft and the highest runway speed (take-off speed) determines the maximum wavelength which would be expected to excite any significant response for that aircraft. For each aircraft, the shaded area encloses wavelengths capable of exciting aircraft response within the frequency spectrum of the particular aircraft. For example, the jet trainer would ride over 200- or 300-foot-wavelength bumps with little or no response. However, these same bumps would be expected to excite considerable response for a jet transport since these wavelengths are within the area shown for this airplane. It is this difference in response characteristics for various aircraft types which accounts for the fact that a runway can be satisfactory for some aircraft but cause trouble for others.

The wavelength, speed, and frequency relations are illustrated in figure 5 by actual measurements which were obtained during an investigation with a medium jet bomber. The small-amplitude bumps shown on the runway profile have about 100-foot wavelengths and amplitudes between 0.1 and 0.2 foot. At 75 knots, the 100-foot wavelengths result in a frequency of 1.2 cps which corresponds to the lowest resonant frequency for this airplane. (See fig. 6.) At 100 knots, the 100-foot wavelengths result in a frequency of 1.7 cps. The large difference in acceleration response measured at the two speeds shows the effect of a small frequency change near the resonant frequency (fig. 6). Thus, small changes in aircraft response characteristics, or small changes in operating conditions, can have a large effect on the resulting aircraft response.

Runway Repair

The problem facing the airport operators when they receive complaints of roughness from pilots is to determine whether the runway actually needs repair and, if so, where the particular areas are that need repair.

At the present time, it is thought that the most direct and practical method of establishing the repair requirements is to relate the magnitude of the cockpit acceleration to the runway profile and to note those sections of the runway which produce excessive accelerations. This approach is illustrated in figure 7. The lower plot shows the runway elevation for a 4000-foot section of the runway. The upper plot shows the maximum cockpit accelerations recorded at various runway locations and at three speeds during tests of a medium jet bomber.

In order to determine which areas are in need of repair, it is necessary to establish an acceleration level as a basis for separating the satisfactory from the unsatisfactory sections of the runway. Based on correlations of measured accelerations with pilot complaints during a number of investigations, it appears that an acceleration level of $\pm 0.4g$ is approximately the dividing line between satisfactory and unsatisfactory runways from the pilot's viewpoint. Consequently, a maximum vertical acceleration in the cockpit of $\pm 0.4g$ is suggested as a criterion for assessing whether a runway needs repair and also as a basis for locating the areas in need of repair. This criterion would be most applicable for portions of the runway where precision of control is most critical, such as during the high-speed portion of the take-off run.

In figure 7, all five of the runway locations identified by the acceleration measurements were considered to be in need of repair. This section of the runway is located near the middle of a military runway with the medium jet bombers generally lifting off in the region between 6500 and 7000 feet; therefore, the roughness is critical in this section. This investigation was initiated by complaints of a large pitching oscillation near lift-off causing the airplane to become prematurely airborne. During one of the take-offs made for this investigation, a rather severe pitching oscillation of $2\frac{1}{2}^{\circ}$ double amplitude was measured. The areas that caused this oscillation were the same as those located by the $\pm 0.4g$ criterion during the constant-speed tests. (See

fig. 7 at distances along runway of 5500, 6000, and 6600 feet.) Repairs to reduce the acceleration level for these three areas would also be expected to eliminate the pitching problem.

CONCLUDING REMARKS

This paper has presented a report of recent NASA research related to piloting problems caused by runway roughness.

It has been shown that criteria based on power spectral levels of runway-profile data are not sufficient to define acceptable levels of runway roughness from the piloting viewpoint.

Because of the large variation in response characteristics between various types of aircraft, a runway may be acceptable for some aircraft and unacceptable for others. A criterion for roughness, therefore, should be expressed in terms of aircraft response - preferably, cockpit acceleration.

A criterion suggested is that the maximum vertical acceleration in the cockpit should not exceed ±0.4g for sections of the runway where precise aircraft control is required.

REFERENCES

1. Milwitzky, Benjamin: Study of Taxiing Problems Associated With Runway Roughness. NASA MEMO 2-21-59L, 1959.

2. Coleman, Thomas L.; and Hall, Albert W.: Implications of Recent Investigations on Runway Roughness Criteria. AGARD Rept. 416, Jan. 1963.

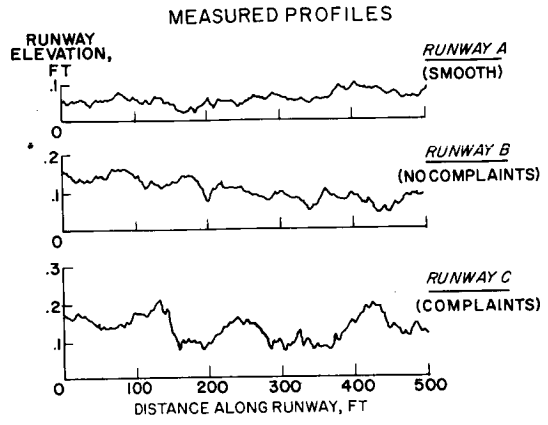

Figure 1

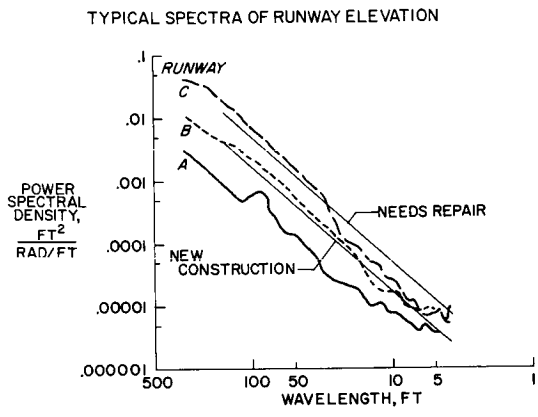

Figure 2

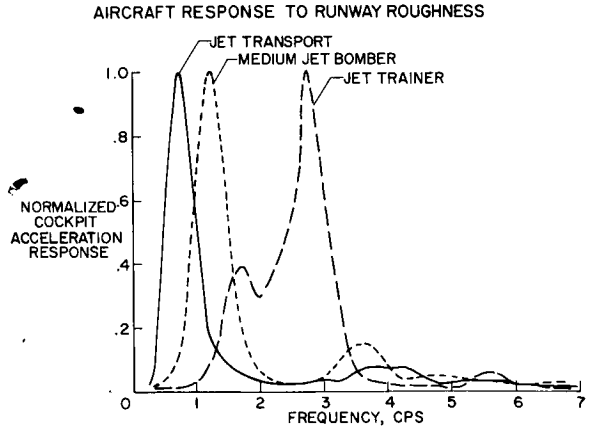

Figure 3

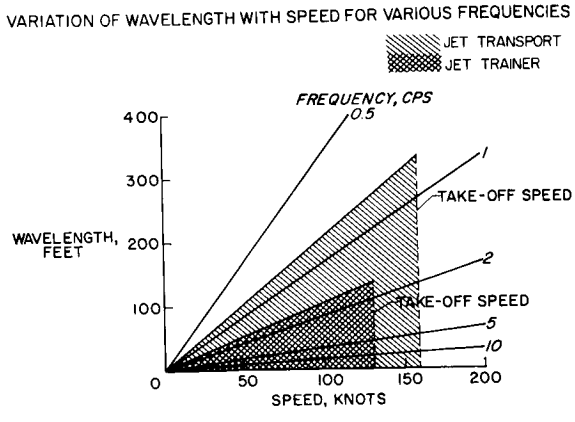

Figure 4

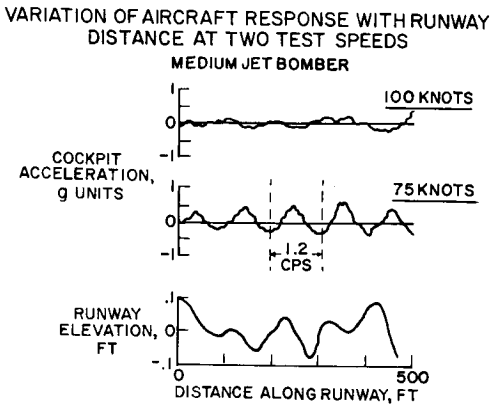

Figure 5

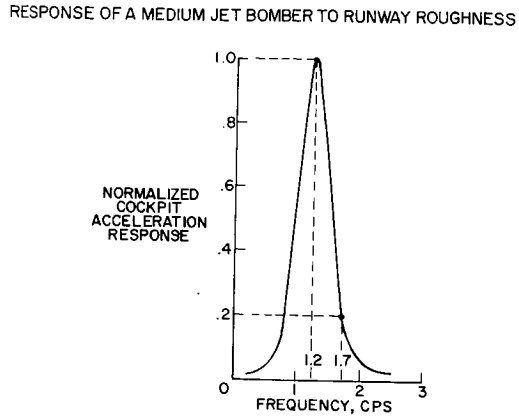

Figure 6

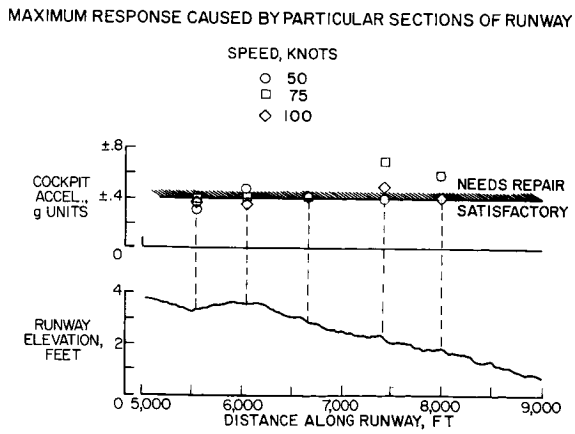

Figure 7

2. TRACTION OF PNEUMATIC TIRES ON WET RUNWAYS

By Walter B. Horne and Upshur T. Joyner

NASA Langley Research Center

SUMMARY

Recent work on the traction of pneumatic tires on wet runways is discussed, and it is shown that a loss of tire traction adversely affects cross-wind landings. The effect of runway surface texture is discussed, and a simple method for measuring surface texture is described. A preliminary correlation of tire traction with surface texture is shown. Results of work at Langley Research Center on the use of air jets to improve tire traction on wet or flooded runways indicate that this is a promising approach for alleviating the large losses in tire braking and sideways traction that occur when tire hydroplaning occurs on a flooded runway.

INTRODUCTION

The subject of traction of pneumatic tires on wet runways is important because of its effects on the landing, taxiing, and ground handling of airplanes. For example, when the phenomenon of hydroplaning occurs for an aircraft during landing on a flooded runway, tire-ground traction can drop to negligible values, and the pilot is confronted with the more difficult task of keeping the aircraft within the confines of the runway. From figure 1 the results can be seen of a case in which a cross wind caused an airplane to drift off the center of the runway, as shown by the light streaks proceeding from the foreground to the edge of the runway; in this instance, the airplane went off the side of the runway with a number of thousands of feet of runway left for stopping purposes. The white streaks are caused by high-velocity water, in the tire footprint areas, that scours the runway surface and cleans it of previously deposited dirt and other contaminants. This type of white streak has been noted for some years and was identified with water action in the footprint region at the Langley landing-loads track several years ago. It should be pointed out that for the incident referred to in figure 1, the pilot touched down near the runway center line. He did try the usual procedures but could not control the rightward drift of the aircraft. Figure 2 indicates why the pilot could not control the direction of the aircraft. At the top of the figure is shown an airplane making a cross-wind landing on a flooded runway with the side wind from the left, as indicated at the right side of the figure. The airplane touches down at a speed above the hydroplaning speed, and tire-ground traction is practically nil. Under this condition of very low traction, the airplane reacts like a sailboat without a keel, tends to weathercock into the wind, and drifts off the right side of the runway because of the cross wind. When an effort is made to slow the aircraft by use of reverse thrust, the vector diagram shown in figure 2 has to be considered. In this case the side component of reverse thrust is in a

direction which tends to augment the side force of the wind and to increase the airplane drift to the right side of the runway.

A cross-wind take-off on a flooded runway is not so severe a problem as a cross-wind landing. (See fig. 2.) The aircraft starts from rest with good tire-ground traction. The traction decreases as speed increases until hydroplaning speed is reached. At this point, traction again is nil and, if the pilot maintains heading as shown by the middle sketch, the cross wind will tend to drift the airplane off the right side of the runway. Drifting during take-off is normally controllable, as shown in the lowest sketch of the figure; the pilot simply yaws the airplane into the wind so that the side component of forward thrust, as shown by the lower vector diagram, cancels the cross-wind force, and the airplane then travels along the center line of the runway during take-off.

This example of the consequences of traction loss points out the need for some method or methods to improve tire traction on wet runways. Recent research on traction at Langley Research Center is so aimed, and several possibilities in this area are discussed in this paper.

SYMBOLS

V_p calculated hydroplaning speed, knots

μ_{AV} average friction coefficient

μ_{SKID} locked-wheel friction coefficient

RESULTS AND DISCUSSION

Effect of Runway Surface Texture on Tire Traction

Loss of traction is a phenomenon which occurs both in the sideways and braking directions nearly simultaneously and has been studied for several years by investigators to determine the best tire tread for traction on a wet runway. It has become increasingly obvious to investigators, however, that the runway surface itself is an important factor in determining the wet-runway traction which can be developed by any tire. (See refs. 1 to 3.) In a series of tests, which NASA is now conducting at the Langley landing-loads track in collaboration with the U.S. Air Force to develop a standard groove width and depth for Air Force tires, several different runway surfaces have been installed, all in a single line, so that every braking test is conducted over each of these surfaces and so that a braking cycle is initiated on each surface. The test-surface arrangement at the track is as follows: The first test surface, surface A, is a steel-troweled concrete surface 100 feet long that provided a very smooth surface finish similar to a table top. The second, surface B, is a

200-foot concrete section that was given a broomed finish to provide a moderately textured surface. The third surface, surface C, is a 300-foot-long section of small-aggregate asphalt which provides a medium-textured surface. Fourth, surface D, is a 300-foot-long section of large-aggregate asphalt that provides a very coarse-textured surface. Finally, a 200-foot-long refrigerated section was installed in the track; this section can be flooded and frozen so that wet ice can be obtained.

Figure 3 shows the braking friction results obtained on a smooth-tread 32 × 8.8, type VII, aircraft tire during braking runs performed on these test surfaces when in a water-flooded condition (water depth = 0.1 to 0.2 inch). The data shown were obtained for a vertical load of 22 000 pounds and an inflation pressure, acting on the tire, of 290 pounds per square inch. It should be pointed out that only the two concrete and the two asphalt surfaces were flooded; the ice surface during the tests was barely covered by a thin water film. It can be seen in figure 3 that as ground speed increases, the average friction coefficients on all surfaces tend toward minimal values at the hydroplaning speed indicated at 154 knots; this is the classic type of traction loss due to hydroplaning from fluid-density effects. At the lower speeds, however, for which fluid-density effects are negligible, the surface texture becomes all important. As can be seen from this figure, a surface must be textured in order to break through the viscous film separating the tire from the pavement even at speeds as low as 20 knots. In an effort to study the surface texture on a quantitative basis rather than resort to definition of the surfaces in terms of words, a method has been devised at the Langley landing-loads track in which a given quantity of material is worked into the runway voids to determine the average depth of texture; a known volume of stiff grease is worked into the runway voids, with a rubber squeegee, within an area of runway between two lines of masking tape. (See fig. 4.) (The rubber in the squeegee is of about the hardness of tire-tread material.) After the grease is worked into the runway voids over a certain length, between the lines, the area that has been covered is determined by simply measuring the distance along the lines, which are a known distance apart. Dividing this area into the known volume of grease gives an average depth of texture, which is given in millimeters. Admittedly this is not an exact basis for determining runway texture, but it is a simple method and shows some promise. Work along this line has been done by Kummer and Meyer (ref. 1) at the Pennsylvania State University and is being contemplated by R. W. Sugg at the Ministry of Aviation in England. The correlation obtained by using the grease technique for determining runway-surface average texture depth with wet-braking traction is shown in figure 5. Here, average friction coefficients obtained on the four flooded surfaces are plotted against average depth of texture (as determined by the grease technique) for velocities of 30, 60, and 90 knots. It can be seen that the friction coefficient on the wet surface coefficient improves at all velocities as the texture is increased in roughness. Above a certain texture depth, however, as from surface C to surface D, there seems to be little effect on friction coefficient of increasing harshness of the texture. This method of measuring runway texture and correlating it with friction coefficient will be pursued at Langley Research Center by using other surfaces with different tires. Also, it is planned to make measurements of various runways and roads, both new and used, to determine if, in fact, this simple method of measuring runway texture can be utilized to

infer from the texture alone, along with previously correlated data between friction coefficient and texture, whether a given runway-texture depth is below some value which would be considered satisfactory for wet-runway operations.

Use of Air Jets to Improve Tire Traction on Wet Runways

Air-jet research to improve tire traction was first performed at the Langley Research Center by E. N. Harrin in 1958. The results of this initial work, performed on a small wheel and belt arrangement, are reported in reference 4. Air-jet research at Langley was resumed at the landing-loads track during the summer of 1964, and some of the results obtained during this investigation are described.

Figure 6 shows a view of the test fixture and air jets used in the current test program. The test tire was a regular 6.50-13 automobile tire inflated to a pressure of 27 pounds per square inch. Both a smooth-tread and a 4-groove ribbed-tread tire were tested. Essentially, the air-jet arrangement, as shown here, was a tandem-nozzle arrangement with the trailing nozzle located about $7\frac{1}{2}$ inches behind the front nozzle and about 10 inches in front of the tire. The tire in this figure is resting on a glass plate which was located flush with the concrete surface in the test runway. From beneath this glass plate, pictures of the tire footprint were taken as the tire traveled across the plate. The water over the glass plate was colored with a green sea-marker dye to give better picture contrast. These pictures showed the very beneficial effect which can be obtained by completely clearing water from the footprint at speeds well above the hydroplaning speed. (For example, see fig. 7.) The left portion of figure 7 shows the tire in a completely hydroplaning condition when traveling at a speed of 62.7 mph. The right portion of figure 7 shows the good contact of the tire with the runway when the tire is traveling at a speed of 100.9 mph; this beneficial effect was obtained with the use of air jets. In addition, quantitative measurements were made of friction coefficient and hydrodynamic pressure developed between the tire and test runway surfaces.

The surface of the test runway shown schematically in figure 8 was very smooth, except for a 52-foot section in the middle which was sandblasted in order to have a surface texture somewhat more representative of highways and runways in use today. For example, the beginning of the sandblasted concrete surface had an average texture depth of 0.104 millimeter. This value is about half the texture depth of the broom-finished concrete surface described earlier.

Figure 9 presents values of locked-wheel friction coefficient and hydrodynamic pressure plotted against runway distance for one run. These values were obtained at a carriage speed of 90 knots, almost twice the hydroplaning speed of 47 knots, with the ribbed-tread tire and a runway water depth of 0.3 inch. The runway surface condition is as noted in figure 8; that is, there were three sections, a smooth concrete section, a sandblasted concrete portion, and another smooth concrete section. With the air jet off, it can be seen that hydrodynamic pressures above 40 pounds per square inch were developed on the

tire footprint and that very low values of μ_{SKID} were obtained. But with the air jet on, there is a reduction in hydrodynamic pressure to near zero on the tire surface. Note also the great improvement of values of μ_{SKID}, especially on the textured concrete section where the friction coefficient is greater than 0.4. The gradual decrease in μ_{SKID} shown here as the tire traveled over the sandblasted runway section is due to a nonuniform texture achieved in using the sandblasting technique.

Figure 10 presents wet-runway cornering-force data as a percent of dry-runway values plotted against the same runway distance as in figure 9. The yaw angle was 5°, the water depth was 0.3 inch, and the speed was 77 knots, which was once again greater than the critical hydroplaning speed. Note that with the air jet off, less than 5 percent of the dry-runway cornering force is achieved at this water depth; but, with the air jet on, more than 50 percent of the smooth-tire dry-runway cornering force is obtained in the textured concrete section.

Figure 11 summarizes results, such as those illustrated in figure 9, obtained with the locked wheel, the 4-groove ribbed-tread tire, and 0.3 inch of runway surface water. Here, the values of μ_{SKID} of both smooth and textured runway surfaces are plotted against forward speed in knots. It can be seen that on the smooth concrete surface there is not much difference between the curves obtained with the air jet off and the air jet on because of the inability of the air jet to remove the very thin fluid film which adheres to the smooth surface. On the roughened or textured surface, however, the many and minute surface irregularities puncture this thin surface film, and the result on friction coefficient is shown by the curves obtained on the sandblasted concrete. On this textured runway surface, which is more representative of actual runway surfaces in use today, much greater values of μ_{SKID} are obtained with the air jet on than with the air jet off.

CONCLUDING REMARKS

Some of the recent work on the traction of pneumatic tires on wet runways has been discussed and ways in which the loss of tire traction adversely affects aircraft cross-wind performance have been shown. Runway surface texture plays a most important role in determining the slipperiness of a pavement when wet. A simple method for determining the average depth of texture of pavements has been described, and measurements obtained on four test runway surfaces at the Langley landing-loads track by using this grease technique give a promising correlation with tire traction on a wet runway. Preliminary work at Langley Research Center on the use of air jets to improve traction on wet or flooded runways has been described and shows promise as a means of alleviating the large losses in tire braking and sideways traction that develop when hydroplaning occurs on flooded pavements.

REFERENCES

1. Kummer, H. W.; and Meyer, W. E.: Rubber and Tire Friction. Eng. Res. Bull. B-80, Pennsylvania State Univ., Dec. 1960.

2. Joyner, Upshur T.; Horne, Walter B.; and Leland, Trafford J. W.: Investigations on the Ground Performance of Aircraft Relating to Wet Runway Braking and Slush Drag. AGARD Rept. 429, Jan. 1963.

3. Gray, W. E.: Aquaplaning on Runways. J. Roy. Aeron. Soc. (Tech. Notes), vol. 67, no. 629, May 1963, pp. 302-304.

4. Harrin, Eziaslav N.: Investigation of Tandem-Wheel and Air-Jet Arrangements for Improving Braking Friction on Wet Surfaces. NASA TN D-405, 1960.

Figure 1 L-2411-2

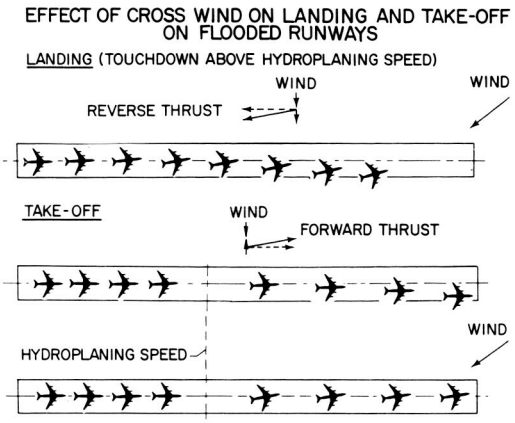

Figure 2

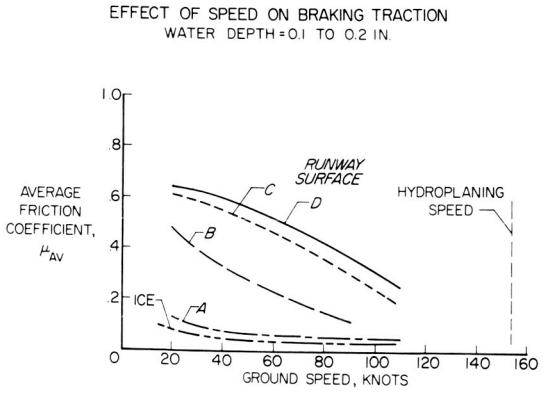

Figure 3

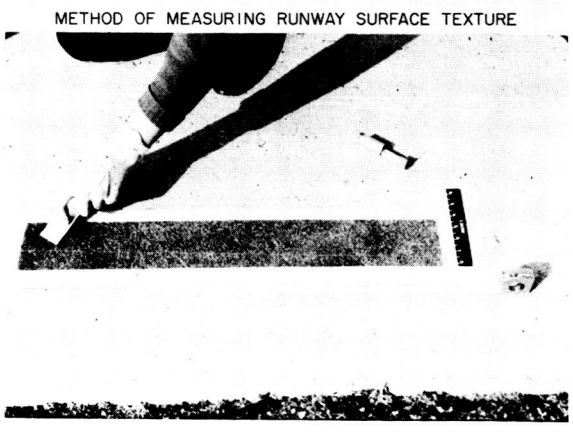

Figure 4 L-2411-5

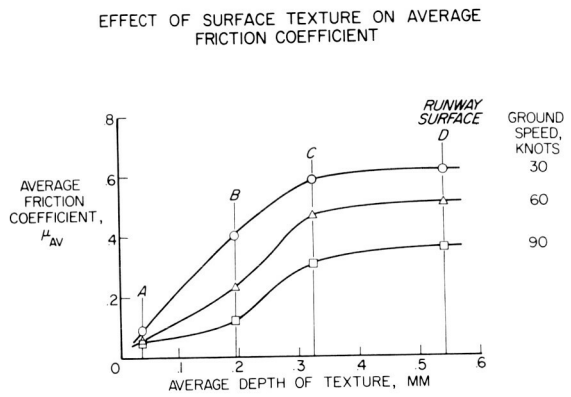

Figure 5

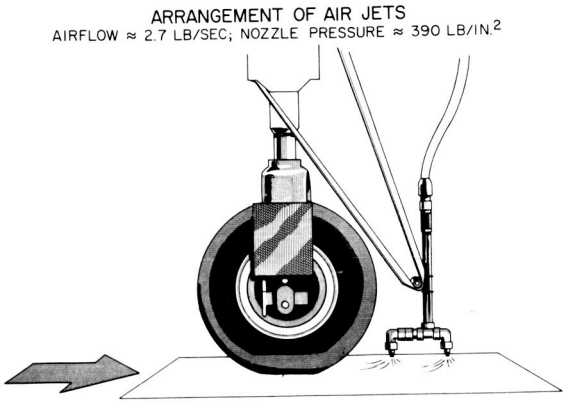

Figure 6

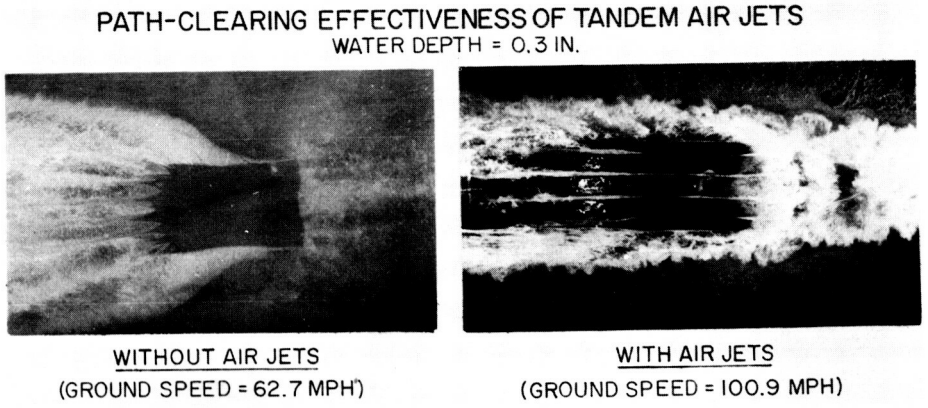

Figure 7 L-65-110

SCHEMATIC OF LEVEL RUNWAY SURFACES

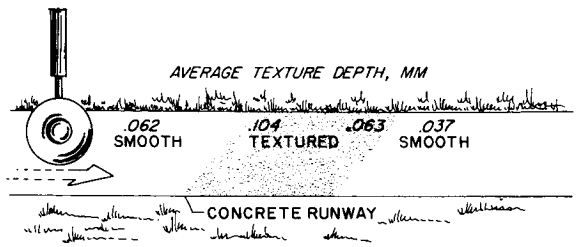

Figure 8

EFFECT OF AIR JETS ON BRAKING TRACTION
WATER DEPTH = 0.3 IN.; GROUND SPEED = 90 KNOTS

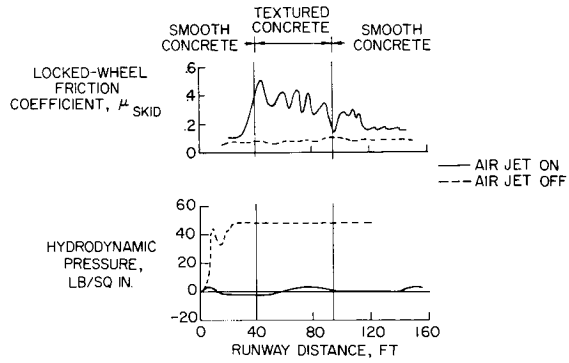

Figure 9

EFFECT OF AIR JETS ON CORNERING FORCE
WATER DEPTH=0.3 IN.; GROUND SPEED = 77 KNOTS

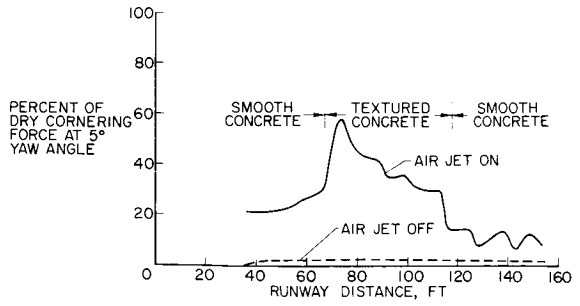

Figure 10

EFFECT OF GROUND SPEED ON AIR-JET PERFORMANCE
IN IMPROVING BRAKING TRACTION
WATER DEPTH=0.3 IN.

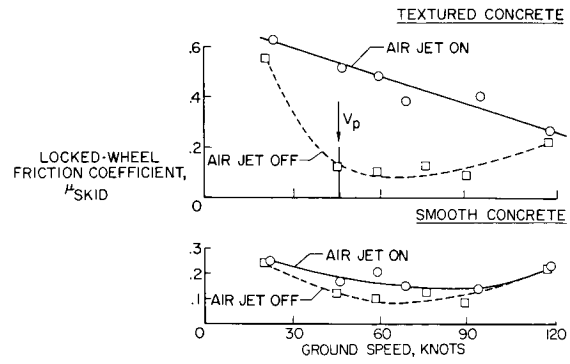

Figure 11

3. SUMMARY OF ATMOSPHERIC TURBULENCE DATA

By Roy Steiner

NASA Langley Research Center

SUMMARY

Turbulence data obtained from recent flights of the U-2 airplanes and from the National Severe Storms Project agree in general with the results obtained in previous investigations. The data show that nonstorm turbulence decreases in intensity and amount with increasing altitude. Less than 2 percent of the flight distance was in turbulence at altitudes above 50,000 feet. It also appears that the root-mean-square gust velocities of the composite turbulence patches may be 15 to 20 percent lower than previous estimates.

INTRODUCTION

In addition to the regular collection of turbulence data from routine airline operations, the NASA collects turbulence information through the use of special flight programs. From long experience in the study of the loads on aircraft in turbulence, it has been found that the airplane responses may be adequately defined if the turbulence is represented by two types: nonstorm and storm. It has become customary, therefore, to classify special flight programs in a similar manner. In this paper, two specialized sampling programs will be discussed. The first concerns nonstorm data obtained with the U-2 airplane at altitudes up to 75,000 feet; the second concerns measurements made in severe storms in Southwestern United States at altitudes up to 40,000 feet.

SYMBOLS

A	airplane response parameter relating rms input and output values
a_n	normal acceleration, g units
L	scale of turbulence, ft
N	average number of peaks per unit distance which exceed given level of response
N_0	average number of zero crossings per unit distance with positive slope
P	percent of total flight distance spent in turbulence

w_g vertical component of true gust velocity, ft/sec

x general response quantity

σ_c composite rms value of gust velocity

Subscripts:

1 nonstorm

2 storm

SAMPLE SIZES

The scope of the nonstorm turbulence data obtained from the U-2 airplane (ref. 1) and the B-36 airplane is given in table 1(a). The scope of the storm turbulence data (ref. 2) is given in table 1(b).

TABLE 1

SCOPE OF TURBULENCE MEASUREMENTS

(a) Nonstorm

Altitude, ft	Flight miles		
	To 1953 (B-36)	To 1960 (U-2)	To 1965 (U-2)
20,000 to 30,000	66,500	11,800	18,900
30,000 to 40,000	24,500	16,200	26,500
40,000 to 50,000	21,500	38,100	49,500
50,000 to 60,000		105,500	141,700
60,000 to 70,000		136,400	576,900
70,000 to 75,000		7,000	7,000
Total	112,500	315,000	820,500

(b) Storm

Altitude, ft	Flight miles	
	To 1953	To 1965
20,000 to 25,000	2,740	2,950
25,000 to 30,000	2,180	2,400
30,000 to 35,000	50	410
35,000 to 40,000		560
Total	4,970	6,320

By 1953, 112,500 miles of flight samples had been obtained with the B-36 airplane at altitudes up to 50,000 feet. Flight operations with the U-2 airplane started in 1956, and 315,000 flight miles had been accumulated by 1960. Since 1960, the high-altitude U-2 sample has more than doubled in size and now covers 820,500 miles. More than 700,000 miles, or 85 percent, of this distance is above 50,000 feet. Emphasis is being placed on the higher altitude programs, since they cover the expected cruising altitudes of the proposed supersonic transport.

The storm turbulence data obtained by 1953 covered about 5,000 flight miles, with only 50 miles above altitudes of 30,000 feet. The more recent samples have increased the sample size to more than 6,000 miles, with approximately 1,000 miles above 30,000 feet.

BASIC GUST RELATION

In order to establish a framework for discussing the results of the flight measurements, it might be well to consider a general relation between the gust characteristics and the airplane response. (See ref. 3.) This relation, based on power spectral techniques, is

$$N = P_1 N_0 e^{-\left(\frac{x}{\sigma_{c,1} A}\right)} + P_2 N_0 e^{-\left(\frac{x}{\sigma_{c,2} A}\right)}$$

This general equation is based on the concept of the response to nonstorm and storm turbulences as given by the first and second terms, respectively. Together, the two terms represent the total experience in atmospheric turbulence - the experience for both repeated and limit loads.

The relation is applicable to a given flight condition and yields the average number of peaks N which exceed a given level of airplane response x. The given number of peaks is a function of the percent of total flight distance in nonstorm and storm turbulences $(P_1$ and $P_2)$, the corresponding root-mean-square gust velocities $(\sigma_{c,1}$ and $\sigma_{c,2})$, and the airplane response parameters $(A$ and $N_0)$.

The center-of-gravity acceleration is a commonly measured response parameter. Since the derived gust velocity is proportional to the center-of-gravity acceleration, it may be considered as an airplane response function as well as a description of the intensity of the atmospheric turbulence. In the following sections of the paper, the derived gust velocities (a response, x) and the percent of turbulence for the nonstorm condition will be considered. Also, some information on the derived gust velocities for the storm condition and an evaluation of the root-mean-square gust velocities for the two turbulence conditions will be considered.

NONSTORM TURBULENCE

Intensity of Nonstorm Turbulence

In figure 1, the distributions of derived gust velocities are presented for flight of U-2 airplanes at altitudes above 20,000 feet. These data are for routine operations. Routine operations - in contrast to flights that seek out turbulent conditions - normally use turbulence avoidance procedures to reduce the flight distance in turbulence. The gust frequency per mile of flight is plotted against the values of gust velocity. The five distributions correspond to 10,000-foot-altitude brackets from 20,000 to 70,000 feet. The larger samples represent approximately 142,000 and 577,000 flight miles for the two highest altitude brackets.

The curves indicate that the frequency and velocity of the gusts generally decrease in an orderly manner with increasing altitude. The distributions for the two lower altitude brackets are nearly coincident. This correspondence in the turbulence at these altitudes is probably due to flights through the jet stream and the tropopause, which may vary from 25,000 feet to possibly 40,000 feet during the different seasons in the Northern Hemisphere.

In terms of the intensity of the turbulence, the results indicate that the maximum gust velocity experienced per mile of flight for higher altitude brackets is on the order of 1/3 or 1/2 that experienced per mile of flight for lower altitudes. The gust velocities, however, are quite low; for example, in 1,000 miles at an altitude of 50,000 feet, a gust velocity of only 4 ft/sec will be exceeded, as compared with 8 ft/sec at the lower altitudes. On the basis of airline data, a comparable value for an altitude of 15,000 feet would be 15 ft/sec. Current design values for airplanes are 50 and 66 ft/sec on this scale and would plot far to the right of the figure.

Eighty percent of the total flight distance represented in figure 1 was over the United States. The remaining 20 percent consisted of flights over Western Europe, Turkey, and Japan. The sample from Japan was not included in the altitude bracket of 50,000 to 60,000 feet, because of two unique patches of turbulence. Figure 2 shows the effect on the distribution of gust velocities if the Japanese sample is included. The distributions for the altitude brackets from 50,000 to 60,000 feet and from 20,000 to 30,000 feet have been included for comparison. The addition of the Japanese sample has shifted the frequency curve upward so that it is more nearly the same as that for the lower altitudes. It is believed that the interaction of moderately severe surface storms, the mountainous terrain, and strong jet streams at an altitude of 35,000 feet caused the unique patches of turbulence (ref. 1). The frequency of this unusual combination of conditions, probably over a rather localized area, and the method of integrating these data into the data for average conditions have not been determined.

Amount of Nonstorm Turbulence

The percent of the flight distance in nonstorm turbulence is presented in figure 3 as a function of altitude. The airplane was considered to be in turbulence whenever the accelerometer trace was disturbed and exhibited gust velocities greater than 2 ft/sec. The solid line represents a previous estimate (ref. 4) based on earlier data. The circled data points represent the present U-2 data. For altitudes between 50,000 and 75,000 feet, the U-2 airplane encountered turbulence less than 2 percent of the flight distance.

All sets of U-2 data show a peak in percent of turbulence at altitudes near 35,000 feet. The points for the present sample show a greater percentage of turbulence than given by previous estimates. The prevalence of turbulence at this altitude is probably due to the high winds and wind shears associated with jet streams. However, a note of warning is needed. The flights in the altitude range from 20,000 feet to the cruise altitude of the U-2 airplane represent, to some extent, a vertical sounding during climb and descent over rather localized areas, and the data may not indicate average conditions at these altitudes over the Northern Hemisphere.

COMPARISON OF DATA WITH PREVIOUS ESTIMATES

Figure 4 summarizes the nonstorm data previously discussed, the data from the National Severe Storms Project, and earlier estimates for nonstorm and storm conditions, which are shown as the shaded areas for altitudes of 20,000 to 60,000 feet. The gust frequency per mile of turbulence is plotted against the gust velocity. Again, a logarithmic scale is used on the ordinate. The range of the nonstorm U-2 data is shown for the five altitude brackets ranging from 20,000 to 70,000 feet. Note that a much compressed gust-velocity scale is used on the abscissa in order to cover both storm and nonstorm gust intensities. The turbulence data from the U-2 airplane flights are generally less severe than previously obtained data, but not to such an extent as to warrant a revision of the earlier estimates.

The solid square symbols represent the data for flight at an altitude of approximately 40,000 feet in storms. First impressions might lead to the conclusion that the earlier estimates are low. However, the storms in Southwestern United States are considered to be the most severe storms in the States. Of these storms, only the ones with sufficient energy to build to altitudes of at least 40,000 feet were investigated. Therefore, the severe-storm data would be expected to lie above the previously estimated curves. There is not sufficient justification, therefore, for revising the estimate at this time.

SPECTRAL REPRESENTATION OF ATMOSPHERIC TURBULENCE

In recent years considerable effort has been expended in describing atmospheric turbulence in terms of power spectra and in applying power-spectral

techniques to design problems. Typical spectra are presented in figure 5 for a severe-storm condition and for a nonstorm condition. The power spectral density is plotted against reduced frequency, which is given in radians per foot, and against wavelength which is given in feet. Each scale used in this plot is logarithmic. Each spectrum represents a given turbulent area. The spectra are similar in shape but vary in intensity. The square root of the area under the spectrum is the root-mean-square gust velocity given in the figure. Note that these rms gust velocities vary from about 14 to 4.5 ft/sec for the different meteorological conditions. The spectra for many turbulent patches in each condition would also cover a wide range. For example, in 11 storm traverses, the rms values varied from 6 to 16 ft/sec. A similar range of rms values would be expected for the nonstorm conditions. The values which describe this variation in the spectra for the nonstorm and storm turbulences are shown in figure 6 as a function of altitude. Earlier estimates of the rms gust velocities of storm and nonstorm turbulences are shown by the solid curves (ref. 4). These velocities were determined from airplane center-of-gravity response data by use of a rough approximation of the airplane response parameters. Only one degree of freedom was considered in the evaluation. More precise values of the airplane parameters have become available for a few types of airplanes and flight conditions (obtained from Lockheed-California Co.). The reevaluation of a few rms values by use of these revised airplane parameters indicates that the rms true gust velocities for the nonstorm and storm turbulences as shown by the dashed lines may range from 15 to 20 percent lower than the previous estimates.

For consistency, the reevaluation was based on the assumption that the scale of turbulence L is 1,000 feet. Should the scale value be larger, say 2,500 feet, as more recent investigations have indicated, both of the sets of curves would be shifted to the right.

MEASURED AIRPLANE MOTIONS DUE TO SEVERE TURBULENCE

The physical behavior of an airplane during flights through two storms is shown in figures 7 and 8. The vertical component of true gust velocity, the normal acceleration, and the altitude change of the airplane during flight are given in the figures. These traverses are flights of a fighter-type airplane. The pilot was instructed to correct only for the major changes in attitude.

Figure 7 indicates that the airplane encountered an updraft with a long gradient distance. The gust velocity changed from 0 to 170 ft/sec in 2,100 feet. The maximum velocity is approximately 210 ft/sec. Although the velocities are large, the airplane experienced only small acceleration. An altitude change of 1,600 feet, however, was experienced in 3 nautical miles. At the time the maximum gust velocity was encountered, the pilot had pitched the airplane down 13° in an effort to maintain the desired altitude. The vertical velocity of the airplane at this time was 80 ft/sec up.

Figure 8 indicates that the airplane was flying in an updraft which reached 70 ft/sec, and then suddenly encountered a downdraft of 90 ft/sec. This change in velocity of 160 ft/sec occurred over a horizontal distance of about 800 feet

in contrast to the 2,100 feet shown in figure 7. The airplane normal acceleration changed from about 0.5g to -2g. The change in altitude in this rather severe turbulence was only about 100 feet.

The pilot may believe that he is experiencing large altitude changes in turbulence of this nature. This impression would probably be caused by both the large accelerations and possible instrument response due to the changing angle of airflow over the static source. The large change in altitude illustrated in figure 7 may be undetected for a longer period because of the more quiescent flight conditions.

CONCLUDING REMARKS

In summary, turbulence data obtained from recent flights agree in general with the results obtained during previous investigations. Nonstorm turbulence decreases both in intensity and amount with increasing altitude. Less than 2 percent of the flight distance was in turbulence at altitudes above 50,000 feet. It now appears that the root-mean-square gust velocities of the composite turbulence patches may be 15 to 20 percent lower than previous publications.

REFERENCES

1. Coleman, Thomas L.; and Steiner, Roy: Atmospheric Turbulence Measurements Obtained From Airplane Operations at Altitudes Between 20,000 and 75,000 Feet for Several Areas in the Northern Hemisphere. NASA TN D-548, 1960.

2. Rhyne, Richard H.; and Steiner, Roy: Power Spectral Measurement of Atmospheric Turbulence in Severe Storms and Cumulus Clouds. NASA TN D-2469, 1964.

3. Houbolt, John C.; Steiner, Roy; and Pratt, Kermit G.: Dynamic Response of Airplanes to Atmospheric Turbulence Including Flight Data on Input and Response. NASA TR R-199, 1964.

4. Press, Harry; and Steiner, Roy: An Approach to the Problem of Estimating Severe and Repeated Gust Loads for Missile Operations. NACA TN 4332, 1958.

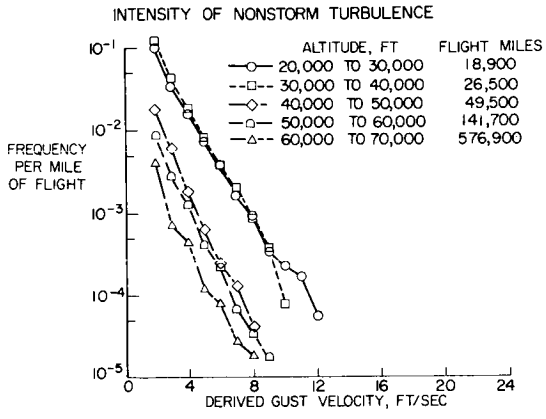

Figure 1

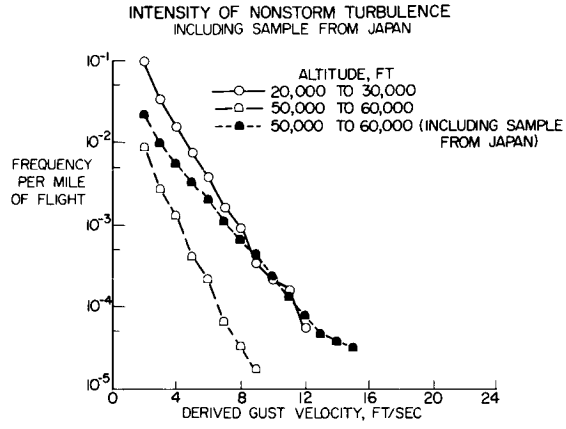

Figure 2

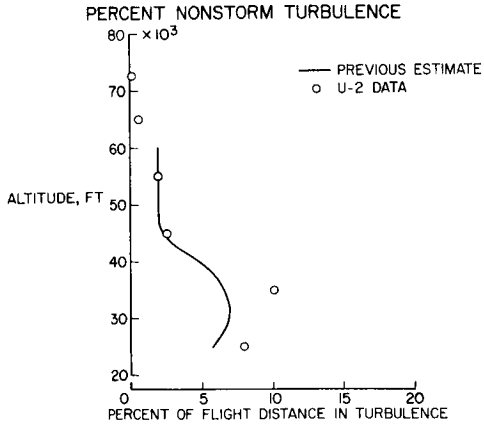

Figure 3

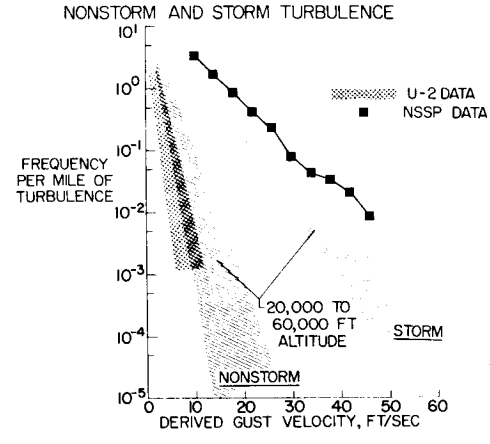

Figure 4

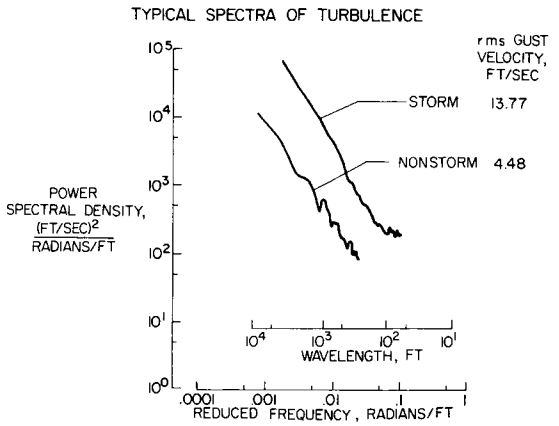

Figure 5

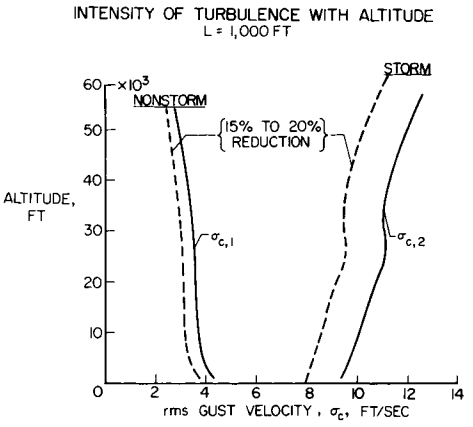

Figure 6

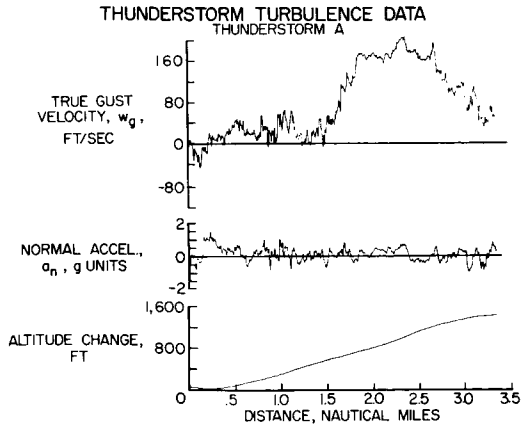

Figure 7

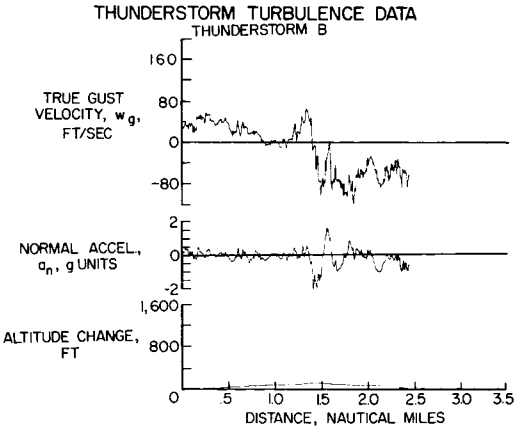

Figure 8

4. PRELIMINARY STUDY OF STEEP INSTRUMENT APPROACH OF THREE CONVENTIONAL AIRCRAFT

By Albert W. Hall, Robert A. Champine,
and Donald J. McGinley, Jr.

NASA Langley Research Center

SUMMARY

Preliminary studies of steep instrument approaches have been conducted with three conventional aircraft. Six-degree approach paths were found to be acceptable. A margin of 3° to 4° in maximum glide slope was available to allow for flight-path corrections. Control of the lateral-directional axis was the most difficult problem for pilots making either steep or conventional approaches; split-axis control reduced the pilot workload during this operation.

INTRODUCTION

The NASA Langley Research Center has recently completed a preliminary study on several aircraft to determine the capability of both aircraft and pilots to make steeper-than-normal instrument approaches. Steep approaches are attractive in that they offer the possibilities of reduced engine noise and reduced airspace requirements.

This paper reports the initial phase of a continuing program and covers studies made with C-47, T-33 (refs. 1 and 2), and DC-8F aircraft. The tests were conducted by making instrument approaches at increasing glide slopes until the maximum glide slope considered suitable for day-to-day operations was established on the basis of aircraft characteristics and pilot opinion. The scope of the initial studies is indicated in table I which shows for each of the aircraft the total number of approaches, the number of approaches at the maximum operational glide slope, and the number of pilots participating.

SYMBOLS

V_a	approach speed, knots
W	weight of airplane, lb
γ	glide-path angle, deg
$\Delta\gamma$	increment in flight-path angle, deg

TEST PROCEDURE AND EQUIPMENT

The approaches were flown with the evaluation pilot flying on instruments (simulated IFR, pilot under hood) while a safety pilot maintained visual contact and took control whenever conditions required a termination of the test. The instrument approach started in level flight about 5 to 8 miles from the runway threshold as shown in figure 1. The glide slope was intercepted about 4 miles from the runway for all tests. This approach distance was fixed by varying the initial altitude for each glide angle; for example, the 2.5° tests were started at an altitude of 900 feet and the 6° tests were started at an altitude of 2200 feet.

Special guidance equipment was used which allowed the glide slope to be adjusted to the desired angle by a simple adjustment. This equipment provided straight glide slopes (no bends) with conventional ILS sensitivity (±0.7°). In addition, this equipment could provide curved paths to give flare-path guidance from any desired altitude to touchdown.

The flight-path (glide-slope, flare, and localizer) information was displayed in the cockpit on the conventional ILS cross-pointer indicator for the C-47 and T-33 aircraft and on a flight director for the DC-8F. The DC-8F was fitted with a split-axis autopilot with which approaches could be made with the lateral-directional axis under autopilot control and with the glide slope under manual control.

DISCUSSION

Maximum Operational Glide Slope

All approaches were flown at the approach speeds recommended for conventional angles except the 9° approach for the T-33.

For a constant-speed approach with the airplane in the maximum-drag configuration, the maximum glide angle occurs with the lowest obtainable thrust.

A qualitative representation of the thrust-required curves is shown in figure 2 for the C-47. As shown in figure 2, the maximum angle obtained with the C-47 was 10° with throttles closed and the propellers windmilling. The 10° angle is not usable for a constant-speed instrument approach because the pilot cannot get the airplane back to the glide slope from an inadvertent high position without diving and gaining speed.

For the C-47 airplane, a 6° glide slope was determined to be the maximum glide slope suitable for day-to-day use in an instrument approach. At this glide slope, by reducing power, the pilot has a 4° margin available to steepen the flight path without gaining speed. The pilots believed that this margin would be sufficient to take care of gusty conditions, windshear, and other inadvertent flight-path deviations.

The thrust-required curves for the T-33 are shown in figure 3. Maximum angles of 9° were flown with the approach speed increased about 10 knots and with the engines about 57 percent of design rpm. Here again, the pilots picked 6° as the maximum angle suitable for operational use. At the 6° angle, the engine speed was about 65 percent of design rpm. Because of the poor acceleration characteristics of this engine, the pilots did not want to operate continuously below this rpm. However, power could be reduced below this level for short intervals, as needed for flight-path control, so that there was a capability of steepening the flight-path angle as much as 3° with only a small increase in aircraft speed.

A maximum operational glide slope for the DC-8F transport was also found to be 6°. At this angle, the engine speed was about 75 percent of design rpm. This airplane had turbofan engines and the pilots did not like to reduce the engine speed below this value; in fact, they tended to accept a slight airspeed increase during flight-path corrections rather than reduce power. It should be pointed out here (as is described subsequently) that the flare path started at an altitude of 260 feet and, from this point, the pilot had to add power so that the engine speed was increased as the airplane came nearer the ground.

Flare Paths

Part of the C-47 and T-33 investigation was to determine flare paths suitable for transition from the steep slopes to a shallow angle at touchdown. Early in the C-47 and T-33 programs, it was evident that good approaches could be flown down to 200 feet; therefore, a more demanding task of attempting an instrument landing was initiated. The guidance equipment provided flare paths as shown in figure 4. The flare path was started at 6000 feet from the touchdown point for both slopes shown. It should be noted that these flare paths are long and change slope rather gradually, and thus, allow considerable distance and time to accomplish the transitions from the glide slope to the landing.

There were only a few cases where the approaches were flown with enough accuracy that the safety pilot would allow the hooded pilot to complete the approach to touchdown. However, the safety pilots felt that the approaches, both at 6° and 2.5°, were flown with sufficient accuracy to allow visual landings to be made from altitudes as low as 100 feet under good visibility conditions. It should be pointed out that at 100-foot altitude the glide slopes and flare paths used in these tests place the airplane in a better position relative to the desired touchdown than the conventional ILS glide slope shown in figure 4.

Flare-path geometry was determined for the DC-8F by extending the 3° flare-path curvature upward to a point where the 6° slope was tangent to the path. (See fig. 5.) Instrument touchdowns were not attempted with the DC-8F. The pilots' task was to simulate instrument flight to 100-foot altitude and touch down visually from this position. Here again, the 6° flight-path geometry appears to be better related to the desired touchdown spot than the conventional ILS path. In this case, the airplane is in almost the same position at 100-foot altitude for both the 3° and 6° path. Based on the conditions of the tests,

clear weather, good visibility, and with flare-path guidance, the pilots felt that 6° approaches could be flown consistently down to 100-foot altitudes. The qualifying conditions of good visibility and special guidance equipment are to be noted.

Lateral-Directional Control

Another important aspect of this steep approach study was the effect of lateral-directional control of these aircraft on the steep-approach problem.

The lift, drag, and engine characteristics determined the maximum operational glide slope for each airplane investigated. Lateral-directional characteristics did not limit the steep-approach capability for any of these aircraft. However, the instrument approach is a very demanding pilot task, and good lateral handling qualities reduce the pilot workload and result in more precise flight-path control. This condition is equally true for both the steep and conventional slopes.

The C-47 had the poorest handling qualities of any of the airplanes investigated. The high lateral-control forces and large wheel displacements made small heading corrections difficult. It took considerable effort to start the airplane in the desired direction, and the same effort was required to stop it; thus, overshoots were commonplace. When approaches were flown in gusty air, the heading correction became a very difficult task.

An example of the deterioration of the smooth flight path along the glide slope after the pilot had to concentrate on a lateral deviation is shown in figure 6. By using the ordinary ILS cross-pointer display, the pilot had to decide how much bank was needed, when to take it out, and then repeat this procedure in the opposite direction in order to come out on course with the proper heading. In this case, rather than ending up on course, he overshot to a greater localizer deflection in the opposite direction. The concentration and effort required to make these corrections detracted from the glide-path control and resulted in larger glide-slope deviations during this time.

The T-33 and DC-8F had more desirable handling qualities than the C-47 and generally the time histories of localizer variation did not show the oscillatory variations which were found to be typical of the C-47 aircraft.

However, even with good lateral-directional characteristics, the pilots' workload was still too great to allow both glide-slope and localizer needles to be flown with the precision required for consistent touchdowns while under the hood. It is recognized that a zero-zero touchdown is not a realistic operational task, particularly with only basic ILS cross-pointer guidance display; but the extreme difficulty of this task tends to emphasize the differences in flight-test results, such as those given in table II.

Table II illustrates the improvement in touchdown capability achieved by eliminating the lateral-directional task. During some of the approaches with the T-33, the safety pilot controlled the lateral-directional path while the

hooded pilot only had to follow the glide slope and flare path. Only one touchdown was made out of 16 approaches with complete control by the hooded pilot. Six touchdowns were made out of seven approaches with split-axis control.

The DC-8 had the capability of split-axis autopilot control; that is, coupled approaches could be made with autopilot control of the lateral-directional axis and manual control of the glide slope.

The pilots found this mode of operation to be very effective in giving better localizer tracking and in reducing the pilot workload and, thereby, allowing more effort to be put on glide-path control. Very good approaches were flown down to 100 feet. For several years various groups have indicated the desirability of using some form of split-axis autopilot. Some airlines are presently using this split-axis operation in their fleet as part of the overall program to reduce ILS minimums.

CONCLUDING REMARKS

An investigation of steep instrument approaches has indicated the following results for the C-47, T-33, and DC-8F aircraft:

1. Six-degree glide slopes can be flown with reasonable precision. Under conditions of good visibility and with special flare-path guidance, these approaches can be flown to 100-foot altitudes.

2. The maximum glide slope suitable for operational use was 3° to 4° less than the maximum glide slope attainable. This margin is needed to allow flight-path corrections to be made without increasing speed.

3. Control of the lateral-directional axis was the most difficult problem for either conventional or steep approaches. Split-axis autopilot control of this axis relieved the pilot workload considerably and resulted in better flight-path control of all axes.

REFERENCES

1. Hall, Albert W.; and McGinley, Donald J., Jr.: Flight Investigation of Steep Instrument Approach Capabilities of a C-47 Airplane Under Manual Control. NASA TN D-2559, 1965.

2. Hall, Albert W.; and McGinley, Donald J., Jr.: Flight Investigation of Steep Instrument Approach Capabilities of a T-33 Airplane Under Manual Control. NASA TN D-2775, 1965.

TABLE I

INSTRUMENT APPROACHES USED IN EVALUATION

AIRPLANE	NUMBER OF RUNS	NUMBER OF RUNS AT MAXIMUM OPERATIONAL SLOPE	NUMBER OF EVALUATION PILOTS
C-47	85	54	5 NASA
T-33	107	49	5 NASA
DC-8F	47	30	2 AIRLINE

TABLE II

IMPROVEMENT IN ZERO-ZERO TOUCHDOWN CAPABILITY BY ELIMINATION OF LATERAL-DIRECTIONAL CONTROL TASK

T-33 AIRPLANE; GLIDE SLOPES, 2.5° AND 6°

FLIGHT-PATH CONTROL	NUMBER OF APPROACHES	NUMBER OF TOUCHDOWNS
FULL CONTROL BY HOODED PILOT	16	1
SPLIT-AXIS CONTROL	7	6

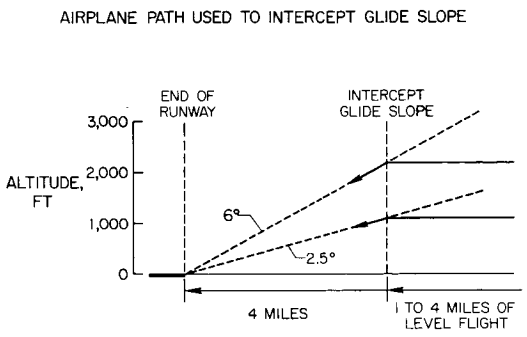

Figure 1

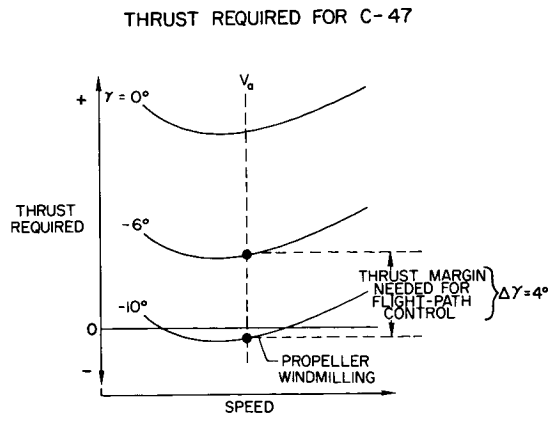

Figure 2

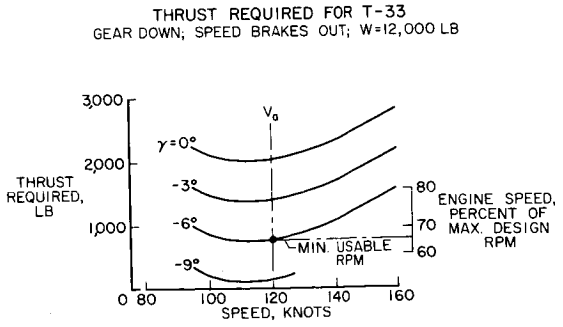

Figure 3

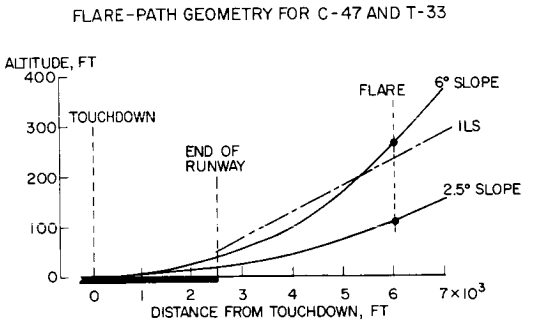

Figure 4

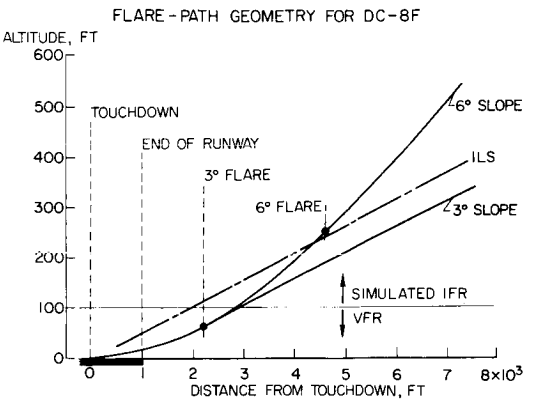

Figure 5

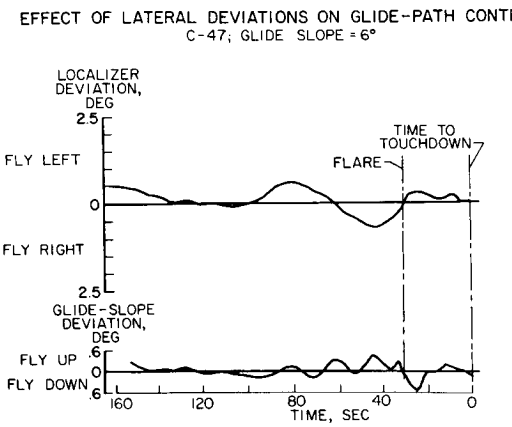

Figure 6

5. SOME FACTORS AFFECTING FATIGUE OF AIRCRAFT STRUCTURES

By Herbert F. Hardrath

NASA Langley Research Center

SUMMARY

Several points of interest to the operator of aircraft are reviewed. Rates of crack propagation tend to increase and residual static strength tends to decrease as the strength of the materials increases. Ground-air-ground and other negative loadings accelerate the damage to certain critical sections so that in first approximation, the fatigue life in these areas should be estimated on the basis of the number of flights, rather than the flight miles or flight hours. Regular inspection for cracks is necessary to assure safe operation of existing flight structures.

INTRODUCTION

The belief that a well-designed aircraft may be operated with no concern about fatigue difficulties is gradually becoming recognized as the myth it is. The review of some recently developed information may help to place fatigue in proper perspective, particularly for operators; for it is they who, more than anyone else, must live with the problem.

SOME PARAMETERS OF THE FATIGUE PROBLEM

Several important factors influence the fatigue life of aircraft structures. Rather obviously, the behavior of the material of which the structure is made, the details of design and manufacture, and the chemical, thermal, fretting, and load environments are the commonly recognized primary factors. Much of the fatigue research carried out over the past 100 years has been devoted to establishing methods for anticipating the influence of these factors analytically. In spite of this effort, current design procedures cannot depend completely on analytical predictions, and considerable testing is used to evaluate particular configurations. Recently, more attention has been devoted to the study of the accumulation of damage under the complex loadings encountered in service, the rate of fatigue-crack propagation, and residual static strength. The present paper deals mainly with these topics.

The observed scatter in fatigue life data under identical loading conditions and the varied loads experienced by individual aircraft of a given type raise considerable doubt regarding the predictability of the fatigue life of a given aircraft even after full-scale tests have been performed. For example,

recent examination of military aircraft of a certain type led to the discovery of cracks which had developed in one-fourth to one-tenth of the time estimated from a full-scale test. The application of a sufficiently high scatter factor to insure against such failures in service would lead to prohibitive weight penalties under present design methods.

How then, can the operator proceed to operate an aircraft with reasonable safety? It is the purpose in the following discussion to consider the steps that can be taken to insure safer operation. The remarks are intended especially for users of aircraft that have parts designed for so-called "safe life" in contrast to the "fail safe" concept.

As indicated previously, the emphasis is on the rate of fatigue-crack propagation and residual static strength; thus, the need for diligent inspection is developed. The way in which fatigue life is affected by the number and severity of loads is discussed.

FATIGUE OF SIMPLE SPECIMENS AND STRUCTURES

Fatigue behavior is generally characterized by S-N curves of the type shown in the left side of figure 1. Such curves have occupied the attention of a host of investigators over the years and have become the yardstick by which the influence of any of a dozen or more parameters is evaluated. The parameter illustrated in figure 1 is the effect of stress concentrations. Many papers have been written to develop empirical or semiempirical relations to relate the S-N curves of unnotched specimens with those of notched or simulated structural specimens.

If one considers the observable propagation of a fatigue crack in a simple unnotched specimen, he will find a behavior such as is indicated by the lower curve on the plot on the right in figure 1. However, for the same overall life of a notched specimen, the applied stress is lower, the effective rate of crack propagation is slower, and the critical crack length is longer for these structural parts than for simple specimens. Thus, the crack is present for a larger proportion of the total life in structural parts. In practical situations, cracks are frequently present for well over one-half of the total life. On the one hand, this is fortunate, in that damage may be found by inspection and corrected. This fact makes feasible the incorporation of fail-safe characteristics in the design of a structure. On the other hand, such cracks reduce the residual static strength so that the structure becomes more vulnerable to sudden failure under high loads.

CRACK GROWTH

The rate of propagation of cracks and their effects on residual strength are getting more attention in recent years and this trend is likely to lead to more satisfactory methods for producing reliable structures. An example of

how a systematic study of crack growth and residual strength may lead to an improved understanding of fatigue behavior is illustrated in figure 2.

The failures of three sheet panels, each made of a different aluminum alloy, are compared. The panels are all the same width but the thicknesses are proportioned in such a way that the original tensile failing load P_U is the same in each case. Each panel contains an initial hole in the center. Each curve in the figure was calculated to illustrate the progress of a fatigue crack during tests in which each panel is loaded in fatigue at the same proportion $\frac{P}{P_U}$ of its ultimate tensile strength. The end of the curve represents failure when the panel is subjected to a high static load (60 percent P_U) at which time that static load is just sufficient to produce failure. It is quite obvious that the weakest of the three alloys (2024-T3) has the lowest rate of fatigue-crack propagation and tolerates the longest crack at failure; the strongest material (7178-T6) is at the other end of the scale. With this sort of insight, one can readily understand why structures made of some of the new high strength materials appear much more vulnerable to failure than do those made of moderate strength materials.

The picture is even more dramatic in steels where heat treating to high strength levels S_U has become quite common in recent years, particularly for landing gears and actuating mechanisms. The same kind of crack growth as shown in figure 2 is shown in figure 3 for two pieces of steel heat treated to two different strength levels. The lower strength material again exhibits a lower rate of crack growth and tolerates a much longer crack before failure. Note that even this longer crack is only one-fifth as long as that tolerated by the 2024-T3 aluminum alloy in figure 2. The curves represent the behavior that might be observed in tests conducted in a clean laboratory at room temperature. However, the situation is much worse in the environment encountered in service. A crack as short as 1/16 inch may propagate to failure under low static loads in just a few hours on a wet day.

The same kind of phenomenon has been responsible for the failure of landing gears that become "cold-soaked" during flight and become wet or even frosty from condensation during descent or landing.

Obviously, the variations of behavior just discussed are partly attributable to choice of material and that choice is up to the designer. However, the operator should be aware of the size of crack that may be serious if he owns a structure made of one of these materials.

Perhaps some examples of cracks that have caused difficulties would be of interest. Figure 4 shows a crack in the skin of an aircraft wing. The material was 7075-T6 aluminum alloy about 1/2 inch thick. Failure occurred at approximately 90 percent of limit load with a crack less than 1 inch long. The disconcerting feature of this crack was that it was not detectable from the outside and an internal doubler plate covered the inside surface to within 1/4 inch of the tip of the fatigue crack.

Had this wing been made of 2024-T3 aluminum alloy the crack would have grown at a slower rate for at least 2 more inches before failure and thus would have enhanced its chances of being observed before final failure occurred. This particular crack was observed in a full-scale fatigue test and subsequent inspections in the fleet led to installation of a reinforcement of this location. Thus, the full-scale test can be a most informative means for identifying potential crack locations. It also provides information regarding the rate of fatigue-crack propagation and serves as a test bed for the development of specific crack-detection apparatus and techniques for a given structure.

An example of a manufacturing defect that can lead to fatigue difficulties is given in figure 5. The part shown was taken from the corner of an access cutout in the same wing structure in which the previous crack was found. The designer wisely called for a radius of about 3 inches, all rough edges were carefully beveled, but the machinist permitted his milling cutter to dwell, leaving a small indentation. It was from that small defect that the fatigue crack grew. This is probably not representative of failure locations in this particular type of aircraft. Rather, it illustrates the need for thorough repeated inspection of every aircraft to discover cracks starting from manufacturing or service-induced flaws. Obviously, not every such blemish can be polished out of every aircraft, but inspection must be thorough and regular to prevent trouble. Only the operator is in a position to conduct such inspections.

EFFECTS OF GROUND-AIR-GROUND CYCLE ON FATIGUE LIFE

It was pointed out previously that fatigue life was related to the number and severity of loads encountered. A few points of interest to the operator should be discussed.

The influence of the so-called ground-air-ground (GAG) cycle has been studied in some detail in recent years. This is the average load cycle that occurs once per flight when the aircraft is lifted off its landing gear during take-off and is then returned to the gear upon landing. The bar graph in figure 6 shows the result of a systematic series of tests in which identical specimens were subjected to programs of fatigue loads simulating, in one case, the gust-load cycles alone and, in the other, the gusts and ground-air-ground cycles. The ground-air-ground cycles caused a decrease in life to less than one-fourth of that for gust-load cycles alone. The influence of the GAG cycle was found to be more severe when it was simulated at appropriate intervals; that is, once per flight, rather than in groups as is often done in simulated service tests.

From these observations one may conclude appropriately that, at least for certain critical sections, ground-air-ground cycles can produce more damage than all other normal operating loads experienced by transport aircraft. This observation may be rationalized in a qualitative sense by considering that the negative phase of the load cycles systematically removes beneficial residual stresses. The more frequently this happens, as in each flight, the more serious is the effect.

EFFECTS OF FREQUENCY OF OCCURRENCE

Figure 7 is a comparison of the number of times a given load is encountered in transport aircraft. In the left plot in the figure the data are normalized on a per-mile basis and in the right plot, on a per-flight basis. It should be emphasized that, for this purpose, a flight includes only one take-off and one landing. The data were accumulated on scheduled airlines ranging from feeder-line transports to transcontinental jets. The same data are used for both plots. Quite obviously the variation in the data is much smaller when compared on a per-flight basis.

The trend observed is easily understood when one considers that most maneuvers are performed and most turbulence is found at low altitudes. Once the aircraft reaches cruise altitude, turbulence is much reduced, maneuvers are usually gentle, and the pilot has freedom to select a route that avoids storms. If one considers, in addition, the predominant effect of the ground-air-ground cycle, the variation in the damage produced per flight is even less than indicated in figure 7.

Thus, the operator should be aware that, in first approximation, fatigue life is determined by the number of flights, rather than by flight miles or flight hours. This fact is of real interest inasmuch as the trend in the airline operations seems to be to use aircraft designed for medium range for ever shorter routes.

Obviously, if the speed, gross weight, altitude, or other mission characteristics are changed, as is frequently the case for military aircraft, the fatigue life will be influenced directly. Probably no factor has been so potent in this respect as the current trend toward low-level operations. In some cases, such operation has resulted in an increase of two orders of magnitude in the frequency of occurrence of a given load-level per flight. Fatigue difficulties under such conditions should come as no surprise.

CONCLUDING REMARKS

The information presented in this paper emphasizes the following points of interest to the operator of aircraft:

Rates of crack propagation tend to be higher and residual static strength lower in higher strength materials than in lower strength materials.

Ground-air-ground and other negative phases of the loadings produce more average damage than ordinary gust loadings.

In first approximation, fatigue life in some critical sections is determined by the number of flights, rather than by the flight miles or flight hours.

Regular inspection for cracks is necessary to insure safer operation of flight structures.

FATIGUE BEHAVIOR OF SIMPLE SPECIMENS AND STRUCTURES

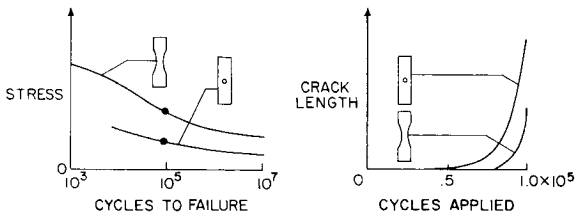

Figure 1

CRACK GROWTH IN TYPICAL ALUMINUM-ALLOY SHEETS

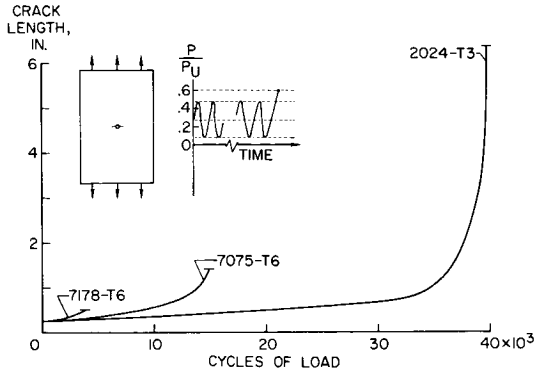

Figure 2

CRACK GROWTH IN HEAT-TREATED AIRCRAFT STEEL

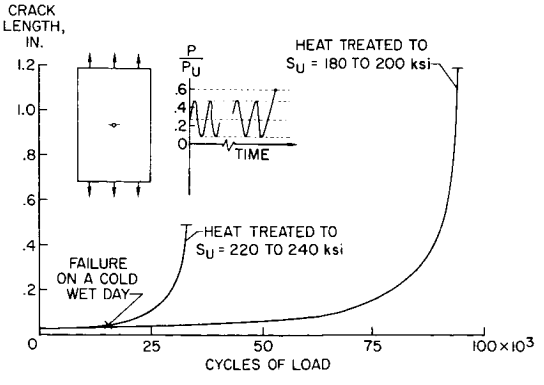

Figure 3

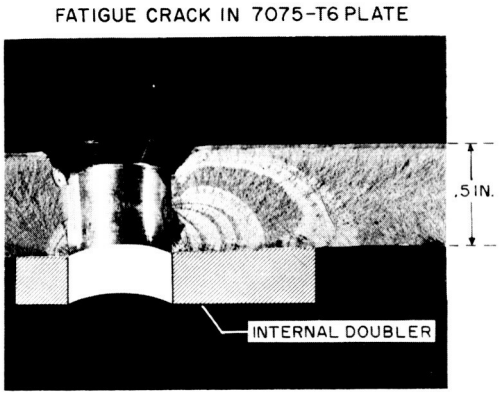

Figure 4 L-2416-6

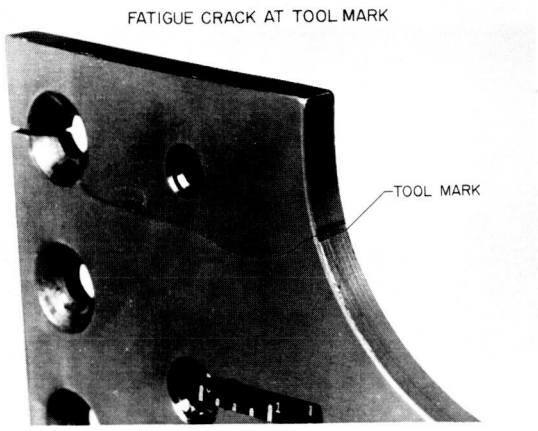

Figure 5 L-59-2980

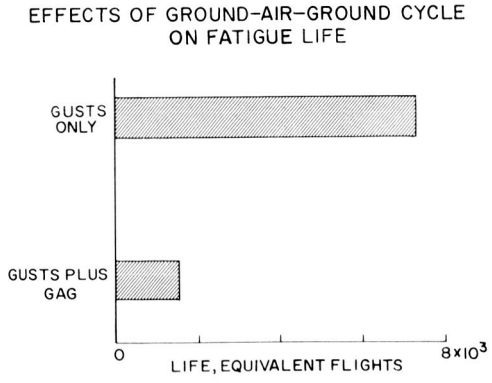

Figure 6

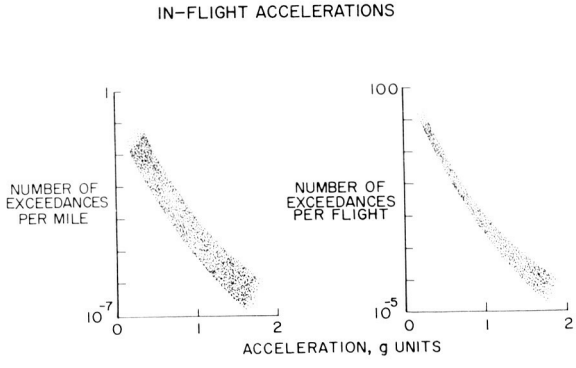

Figure 7

6. USE OF VERY WEAK RADIATION SOURCES TO DETERMINE AIRCRAFT RUNWAY POSITION

By Fred J. Drinkwater III and Bernard R. Kibort

NASA Ames Research Center

SUMMARY

Various methods of providing runway information in the cockpit during the take-off and landing roll have been proposed. The most reliable method has been to use runway distance markers when visible.

Flight tests were used to evaluate the feasibility of using weak radioactive sources to trigger a runway distance counter in the cockpit. The results of these tests indicate that a weak radioactive source would provide a reliable signal by which this indicator could be operated.

INTRODUCTION

An investigation was conducted to determine the feasibility of using weak radioactive transmitters to provide position information to the crew during take-off and landing. The transmitters were spaced along the runway and detected by equipment in the aircraft. This information is similar to that which is provided by runway distance markers except that the transmitters are not affected by outside visibility. The need for more precise runway distance information becomes apparent when the basic four-engine jet take-off condition is examined. The airspeed-distance relationship during a take-off is shown in figure 1. When all four engines are operating, the acceleration proceeds as shown by the solid curve. There is one point at which, should an engine failure occur, the distances required to come to a complete stop or to continue accelerating to take-off speed (V_2) on three engines are equal. This point on the runway is the critical engine failure point and the associated airspeed reached at this position under normal acceleration conditions is called the critical engine failure speed or basic V_1.

Although the concept of a critical engine failure speed is supposed to account for the sudden loss of an engine, there is no effective way, presently, using speed alone to detect reduced performance resulting from an underthrust engine condition, a dragging brake, drag due to slush or puddles on the runway, or a miscalculation of gross weight for a critical runway length. Under these conditions the critical engine failure speed is reached at a point further along the runway than was expected; thus, speed alone is hazardous to use as a decision point. However, several factors have permitted this lack of information to exist. First, unless the airplane is loaded to the maximum allowable weight for the runway to be used, the refusal condition given the crew is conservative

since this condition is based on the maximum allowable weight for the particular runway. Secondly, the reliability of jet engines is extremely good, and lastly, the stopping distances are demonstrated without reverse thrust which provides an additional margin of safety in an actual emergency.

Obviously, a measurement of aircraft acceleration would provide a satisfactory solution. The measurement could be made either directly with accelerometers or indirectly by noting the time or distance required to reach a chosen airspeed. Direct measurements of acceleration have been used in experimental take-off monitor systems as noted in references 1, 2, and 3. However, none of these methods are in general use. Time checks of acceleration to a reference airspeed have been used but the technique is not considered accurate enough by the pilots; thus, few operators have retained it. Airspeed and distance checks of take-off acceleration are used by the military because most military runways have distance markers spaced 1000 feet apart. These markers are useful in daylight to provide an airspeed-distance decision point even for single-engine aircraft. However, few civil runways are equipped with distance markers. Since distance information is an important part of a complete take-off performance monitor system, several types of wheel rotation pick-offs are being developed for this purpose, for example, the systems described in references 4, 5, and 6.

The purpose of a take-off monitor system is to provide an indication of unsatisfactory performance as early as possible. The attendant problems are several. For example, too early a prediction raises the possibility of unnecessary refused take-offs. In addition, the accuracy and reliability of accelerometers and wheel pick-offs in this environment are still not adequate and these systems usually require the inclusion of aircraft gross weight, runway temperature, runway slope, and altitude into a computation which adds to the possibility of error. Since these developmental problems have delayed the introduction of a true take-off performance monitor system, a less ambitious system is to provide the pilot with runway distance information under all conditions of visibility. Take-off performance is then checked by using airspeed and distance just as performance is checked on a runway which has distance markers. The decision to refuse a take-off can then be made with the knowledge that sufficient distance is available for stopping. The reference reports discuss several ways of obtaining distance during the take-off and this paper presents still another method.

Preliminary studies indicated that weak radioactive sources spaced along the runway as distance markers could be readily detected by simple airborne equipment. The runway installation of sources has advantages such as low initial cost, simple installation, negligible maintenance, and high reliability since the runway units required no power and would not be affected by runway surface conditions. Subsequent to these studies, NASA negotiated a contract for the design and fabrication of a two-transmitter runway installation and the airborne components.

RUNWAY POSITION MONITOR EQUIPMENT

Runway Installation

Gamma radiation transmitters, each of which consisted of a 10-millicurie source of Cesium 137 (Cs^{137}), were installed in containers which shaped the radiation pattern (fig. 2) and were located along the center line of the runway. The Cs^{137} in the container has a half-life of 30 years, no electrical power or periodic maintenance is required, and the transmitter units are not a source of radio or magnetic interference. The containers were designed to provide security for the small radioactive source and to allow de-activation by the insertion of a lead plug. For this investigation two transmitters were embedded along the center line of the runway on the dry lakebed at Edwards Air Force Base (fig. 3). The transmitters were spaced 200 feet apart, since it had been determined from earlier tests that for the source strength used, 200 feet would be the minimum spacing for separate detection of each source; the spacing could, of course, be greater. For example, 1000-foot spacing would still allow adequate acceleration checks and provide braking distance information. The hardened dry lake surface has radiation shielding characteristics similar to those of concrete. However, the natural background radiation present over the lakebed was several times greater than would be present on a conventional runway.

Airborne Equipment

A correlation between the actual aircraft position and the position indicated by the radiation sources was determined photographically. The essential airborne components are shown in figure 4. The scintillating probe is a 3-inch thallium-activated sodium iodide crystal, coupled to a 3-inch photomultiplier tube. The largest unit contains the amplifier discriminator, binary counter, timer circuit, logic gates, and an indicator driver. A conventional impulse counter, shown in the figure, was the only component required in the cockpit. The power used was 115 VAC 60 cps. Since the large unit was a prototype, no effort was made to reduce its size. In fact, the only units which could not readily be reduced in size were the scintillating probe and photomultiplier tube.

A symbolic diagram showing the complete installation of the airborne equipment is shown in figure 5. There was no external probe or antenna. The only requirement was to minimize the mass of aircraft material or structure interposed between the scintillating probe and the runway. The recorders indicated in figure 5 were part of the test instrumentation used to obtain a continuous record of the radiation level. The runway distance meter or counter was located between the pilots for coordinated use.

RESULTS AND DISCUSSION

The aircraft was flown over the sources in addition to the normal take-off tests. This was done to obtain the higher speed and altitudes required to determine the limiting conditions. A recording made during a typical pass is shown in figure 6. The upper trace is from a count rate meter in counts per minute. The lower signal corresponds to the upper trace but is in a form to operate the cockpit indicator. Each vertical step is 8 counts which are totaled approximately each 1/3 second as indicated by the return to zero on the trace. The background level is seen to provide 24 to 32 counts before resetting. When a transmitter is approached, it is seen that the count rate increases and when the total exceeds 64, 8 steps up, before the reset time, a signal is passed to the indicator driver. Successive counts in excess of 64 are blocked by the and-or gates until the total count drops below 64 during the 1/3-second time interval. This return to zero indicates that the beam has been passed and another step is sent to the cockpit indicator by the driver. In this way the mechanical counter is stepped two times for each radiation source, once on entering and once on leaving the beam. The scale on the indicator mounted in the cockpit in the case of this test registered 100 feet for each pulse sent by the indicator driver. However, only the odd 100-foot indicator pulses were found to measure an accurate distance between the sources. (That is, the distance between the pulses, at the points where the 64 count gate was entered, was proportional to the 200-foot spacing between the sources.) The run shown in figure 6 was made at a measured 155 knots ground speed 35 feet above the center line. As can be seen in figure 6, the signal over each source is readily detectable and the probability of receiving an inadvertent count or of not counting when over the source at signal levels such as shown in this figure can be estimated to be less than one chance in one million. During these tests reliable detections of the sources were achieved at distances of 50 feet and speeds of over 150 knots. If the sources were spaced further apart the speed of passage would have a less significant effect. The source detection at heights of 50 feet was evaluated for possible consideration of the use of this signal to indicate to the pilot his touchdown point after landing.

The radiation level of the source installed in the container was lower than the predicted value because of excessive shielding by the container. This value indicates that improvements can be made in the container design. In addition the hazards associated with the radiation sources can be further reduced by a design which distributes the sources more uniformly across the runway. The ultimate in distribution would be obtained by painting stripes of an epoxy-type base containing the radiating material. The radiation level of such a stripe could be less than 1 mR per hr at a distance 4 inches from the surface. This rate can be compared with the radiation level of a luminous dial watch which has a rate between 1.0 and 2.0 mR per hr at a distance of 1/2 inch. Another method would be to install aluminum tubing in slots in the runway. The tubing would contain a homogeneous mixture of the source material and an inactive filler which would again reduce the local concentration of radioactive material.

Under the present rules of the Atomic Energy Commission, upon application permission may be obtained to install sources in unrestricted areas if the

radiation levels are such that an individual is not likely to receive a radiation exposure in excess of 500 mR per yr. A person would have to remain within 1-1/2 feet of the source used in this experiment for more than 40 hours per year in order to exceed this exposure. By using the improved installation the distance would have to be in the order of several inches for several hundred hours per year. Since this is unlikely, especially on an active runway, it is considered probable that the U.S. Atomic Energy Commission or the applicable State regulating agencies would approve the use of radioactive sources for the purposes set forth in this report, provided satisfactory precautions are taken to secure the sources from accidental or malicious removal from the site.

CONCLUDING REMARKS

Operational tests have shown that aircraft distance traveled during the take-off roll can be determined by using relatively simple airborne equipment to count nonhazardous radiation sources located in the runway. The detection of the sources was reliable at heights of up to 50 feet above the runway. With this information provided in the cockpit under all runway conditions, the pilot can not only determine whether his take-off acceleration is satisfactory by using an airspeed-distance check, but also make the decision to continue or refuse the take-off at a point which assures sufficient stopping distance.

REFERENCES

1. Kolnick, Joseph J.; and Rind, Emanuel: Investigation of the Characteristics of an Acceleration-Type Take-Off Indicator in a Large Jet Airplane. NASA MEMO 4-21-59L, 1959.

2. Morris, Garland J.; and Lina, Lindsay J.: Description and Preliminary Flight Investigation of an Instrument for Detecting Subnormal Acceleration During Take-Off. NACA TN 3252, 1954.

3. Swindle, Elro M.: Flight Test of Sperry Gyroscope Company Takeoff Monitor in a B-47 Airplane. WADC TN 59-360, U.S. Air Force, Jan. 1960.

4. Various contributors: Towards Safer Take-Offs. Flight Intern. (Letters), vol. 86, no. 2899, Oct. 1, 1964, pp. 600-602.

5. Fearnside, K.: Instrument Aids for Take-off. J. Roy. Aeron. Soc., vol. 67, no. 633, Sept. 1963, pp. 544-551.

6. Rush, D. A.: Ground Run Prediction. AGARD Rept. 422, Jan. 1963.

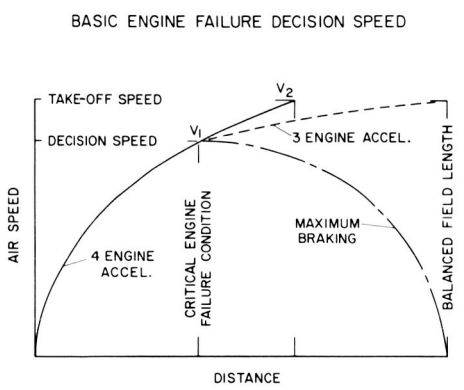

Figure 1

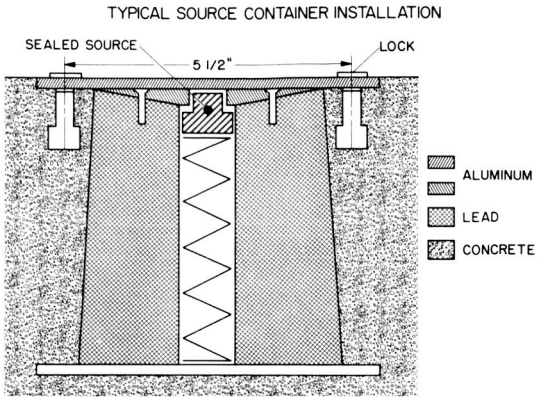

Figure 2

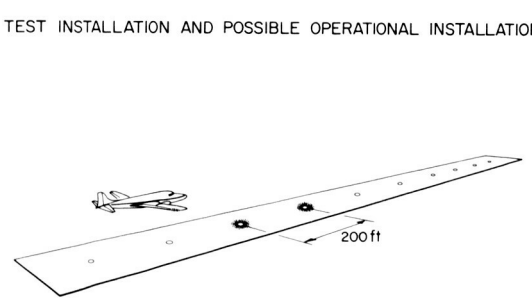

Figure 3

Figure 4 A-33993

AIRBORNE RADIATION DETECTION EQUIPMENT

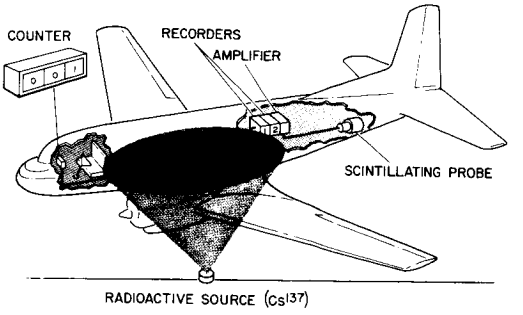

Figure 5

TAKE-OFF RADIATION MEASUREMENTS

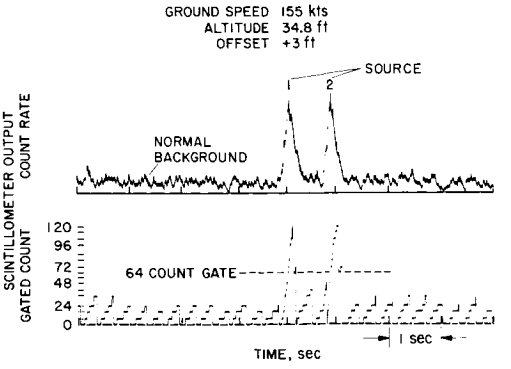

Figure 6

7. A LABORATORY INVESTIGATION OF TURBULENCE DETECTION USING A LASER

By Kent Bourquin and Fred H. Shigemoto

NASA Ames Research Center

SUMMARY

Calculations and experiments have been undertaken to determine the property of the backscattered laser-return signal that undergoes the most significant change in a turbulent region as compared with a nonturbulent region. If the turbulent region is composed mainly of air molecules, the detection of a shift in the frequency property appears to be the most promising. Therefore at this time the main effort at the Ames Research Center is focused on the implementation and laboratory evaluation of a clear-air turbulence detector utilizing a laser source and observing the frequency change.

INTRODUCTION

The unexpected penetration of clear-air turbulence has increased greatly in recent years because of the increased number of flights and the lack of any reliable detection methods. Clear-air turbulence presents itself in different forms and has been reported at altitudes from sea level to 100,000 feet where it has been encountered by U-2 and X-15 flights. Turbulence, however, has most often been encountered near the jet stream at altitudes of 20,000 to 40,000 feet. The region of turbulence is small compared with the overall air volume; it is usually less than 3,000 feet in vertical depth, 20 miles in width, and 50 or more miles in length along the direction of the wind. This localized nature of clear-air turbulence makes it very difficult to predict from normal meteorological observations. Still it would be extremely valuable to be able to detect clear-air turbulence regions and, as yet, there are no suitable devices available. Several different approaches to the detection of turbulence are presently being pursued. Some of these devices rely on the detection of temperature or electric-field gradients in the vicinity of turbulence. Since these effects occur near clear-air turbulence, there exists a limit to the maximum advance warning time available to the pilot to execute a maneuver to avoid the area. A fundamental requirement of a clear-air turbulence detector is that the device must give the pilot enough warning to make avoidance possible.

The success of a conventional radar in detecting storms has led to considerations of its use in detecting turbulence. However, the extreme ratio of wavelength to particle size makes its effective use appear extremely doubtful. An optical radar using a laser appears more promising owing to its much shorter wavelength. Ames Research Center is conducting laboratory experiments in order to determine the feasibility of using an onboard laser as a probe to detect clear-air turbulence.

An investigation is being carried out to determine whether the laser light backscattered from a turbulent region will be modified as compared with light backscattered from a nonturbulent region. Laboratory experiments, rather than actual onboard experiments, were chosen in order to correlate the results with a controlled atmosphere.

DISCUSSION

The backscatter consists of three phenomena: Rayleigh scattering from gas molecules and microscopic particles that are small compared with the wavelength of light, Mie scattering from dust particles that are comparable in size to the wavelength of light, and refractive scattering due to inhomogeneities of the refractive index. An analytical study of the latter phenomena has revealed it to be insignificant compared with the first two.

Before discussing the results of the experiment, some background material is presented that justifies the choice of a laser system as a possible clear-air turbulence detector. The background material will also include the properties of the laser source and a description of the experimental setup. A laser detection system would be similar to a conventional microwave radar, except that it would operate at a much higher frequency, one that is in the visible region. A comparison of the two systems, Rayleigh scattering being assumed, shows that there is a 10^{20} increase in scattered return and a 10^{-5} reduction in beam angle owing to the 10^{5} difference in frequency. In order to make a preliminary determination of the feasibility of an optical radar, calculations were made of the received signal-noise ratio, a region free of high particle content being assumed and, as a result of this assumption, the air molecule scattering is predominant. The calculations show that the currently available pulsed lasers are feasible but that the currently available continuous-wave lasers at their best are borderline.

For use of either a pulsed or a continuous-wave laser, consideration would have to be given to the effect of the laser beam on the eye of occupants in other aircraft that might be located along the laser line of sight. The high-power pulsed laser would certainly require special safety precautions, whereas the continuous gas laser might be tolerated for short exposures. This area will require further investigation.

A study of the effects of turbulence on the characteristics of backscattered radiation requires an understanding of the properties of the laser light contained in the backscattered signal. Important properties to be considered are amplitude, polarization, coherence, and frequency. The amplitude is an indication of the power in the beam. Polarization of the wave refers to the orientation of the electric-field vector in a plane perpendicular to the direction of propagation. The path described by the tip of the electric-field vector in the plane defines the polarization. For example, a straight-line path would be called linear polarization.

One of the most important laser characteristics is coherence. It is this property which allows the laser to be radiated in a narrow beam and focused into an intense spot. It also causes a granular appearance when the light is incident on a surface. There are two kinds of coherence. One is spatial coherence, the other is temporal coherence (or monochromaticity). These two coherence characteristics in reality form a three-dimensional coherence function where temporal coherence describes phase correlation of the radiation in the direction of propagation, and spatial coherence describes phase correlation across the wavefront.

The frequency is of the order of 10^{14} cycles per second. The frequency determines the color of the laser light. The laser output can be composed of one or several discrete frequencies, depending on the optical cavity length and laser power input.

Laboratory experiments have been designed to determine which properties of the scattered laser-return signal have the most significant change in a turbulent region as compared with a nonturbulent region. The experimental equipment is not designed to simulate actual clear-air turbulence phenomena, but only to provide a gross air motion and to introduce aerosol particle concentrations. This experimental technique provides a means for evaluating the properties of the return signal under controlled conditions. One of the main reasons for not attempting to simulate clear-air turbulence is that the actual phenomena is not thoroughly known. In particular, the particle content is not known. Some meteorologists speculate that silt and clay are distributed in the eddies around the jet stream.

Figure 1 shows a photograph of the laboratory setup. The laser output passes through a fused-quartz window and into the test section. The portable enclosure is sealed and bolted to the bulkhead and allows the test section to be evacuated for initial calibration. The ports located on the side of the enclosure allow air flow to be introduced through the ports by an external clean-air source with a 0.3-micron filter.

Figure 2 shows more detail of the system. A continuous-wave gas laser is located on one end of a 17-foot aluminum T-beam. The output of the laser passes through a fused-quartz window at Brewster's angle, the collimating apertures, and the test section, and is finally absorbed. The absorber consists of a cone lined with a smooth gelatin filter material that absorbs or diverts the wide-angle rays into the main section containing a filter. The filter, set at Brewster's angle, causes maximum transmission and minimum reflection of the polarized light; therefore the laser light is transmitted through the filter and rapidly absorbed. The collimator and absorber are required to prevent the laser light from being scattered off the walls of the chamber and into the optical receiver.

The test section is determined by the intersection of the laser beam and the receiver field of view. Figure 3 shows the geometry involved. The detector is a photomultiplier tube which has an S-20 surface.

It should be noted that most of the experimental equipment would not be used in an actual detection system. The main equipment needed in an actual

clear-air turbulence detection system would be a laser and an optical receiver. The other equipment shown in the figures merely permits evaluation of the previously discussed properties in a laboratory environment. The most difficult design requirement was complete absorbance of the laser light at the end of the chamber since the received light at the detector from molecular scattering is only 10^{-10} times the initial light power of the laser. Any light reflected from the chamber must be kept well below this value.

The initial experiments verify that when the atmosphere is removed from the chamber, stray light signal is negligible. Under vacuum condition the photomultiplier output is essentially only the noise current of the photomultiplier. The magnitude of the detected signal is 6.00 millivolts because of the photomultiplier noise current, 8 millivolts with the chamber under vacuum, 350 millivolts with normal room air in the chamber, and 100 volts when a high concentration of water vapor is passed through the test section.

Preliminary experiments and calculations based on Rayleigh scattering have shown that the amplitude property of the returned signal is not significantly modified in a turbulent region. On the other hand, calculations show that if the turbulent region contained significantly larger particle concentrations than the surrounding nonturbulent region, a change of amplitude could be detected. However, even in this case, the amplitude property might not be a reliable property to detect, since absorption and scattering from clouds and other phenomena other than clear-air turbulence would affect the amplitude during transmission.

The results, as expected, have indicated no first-order effects on polarization due to turbulence. The effect of polarization was examined by rotating a linear sheet of polaroid in front of the receiver optics. The results showed the return to have polarization identical to that transmitted. However, further investigations using different particle sizes with different indices of refraction will be considered with various laser output polarizations.

The spatial coherence of the return wave can be studied by use of an experiment similar to Young's double-slit experiment. If the phase difference between the waves entering the two slits changes, the interference fringe pattern will shift according to this change. Investigation of this property has not, as yet, been undertaken by the Ames Research Center.

One of the more promising properties for detection, which calculations show changes significantly in a turbulent region as opposed to a nonturbulent region, is that of frequency shift due to velocity gradients. This frequency shift is an effect analogous to the change in pitch of a moving train whistle as it passes a stationary observer. Detection of this property is complicated by the Brownian motion of molecules due to temperature. The effect of Brownian motion is to spread the frequency spectrum of the return signal from air molecules. In a turbulent region, the air mass is moving in a random fashion and thus the frequency spectrum is spread still further, or the whole spectrum is displaced. Most particles are not affected by Brownian motion and backscatter from them will only display a spread in the frequency spectrum due to turbulence. If the air mass were moving in only one direction, a shift in frequency

would result. Detection is limited to velocity components parallel to the direction of travel. One method for detecting a frequency shift is by photomixing a local laser oscillator and the scattered return signal. The use of a local reference oscillator imposes the problem of critical alinement of the reference oscillator and the return signal. Photomixing also required both signals to have essentially the same polarization and spatial coherence. The velocity of the aircraft also causes the Doppler frequency shift to be outside the bandwidth of conventional photomultipliers and the types of photomultipliers now being developed for laser photomixing would be required.

Another detection method recently proposed uses a laser in an operating mode which contains two frequencies in the output. By photomixing the return scattered signal, which still contains the two frequencies, a frequency shift should be detected. This frequency shift would be proportional to the difference between the two frequencies which is about 1.5×10^8 cycles per second instead of being proportional to the single laser frequency of 10^{14} cycles per second. The advantage of this technique is that the signal bandwidth is within that of conventional photomultipliers and the bandwidth of the electronics can be narrow; hence, the noise in the system is reduced. Another advantage is there should be no critical alinement or spatial coherence problems, such as matching with a local oscillator. However, there is still the main practical disadvantage of the inadequate power of current gas lasers.

Both methods of Doppler frequency-shift detection are being investigated at the Ames Research Center. Optical equipment is being assembled and electronic spectrum-analysis-amplifier-filter combinations are being designed in order to carry out an experimental program in the test chamber.

CONCLUDING REMARKS

Calculations and experiments have been undertaken to determine the property of the backscattered laser-return signal that undergoes the most significant change in a turbulent region as compared with a nonturbulent region. If the turbulent region is composed mainly of air molecules, the detection of a shift in the frequency property appears to be the most promising. Therefore, at this time the main effort at the Ames Research Center is focused on the implementation and laboratory evaluation of a clear-air turbulence detector utilizing a laser source and observing the Doppler frequency change.

LABORATORY SETUP

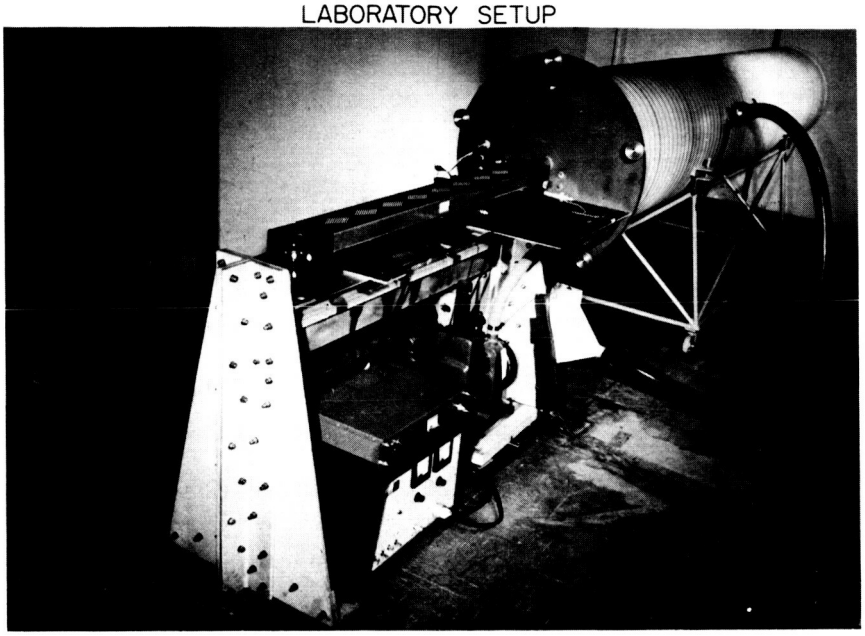

Figure 1 A-34386-4

DETAILED SYSTEM DIAGRAM

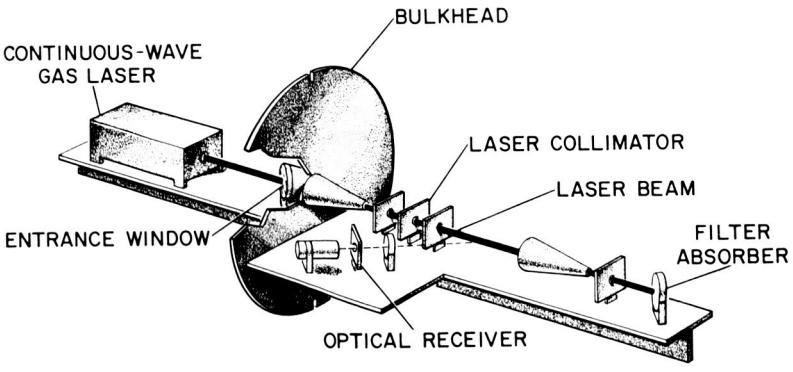

Figure 2

GEOMETRY OF EXPERIMENTAL SETUP

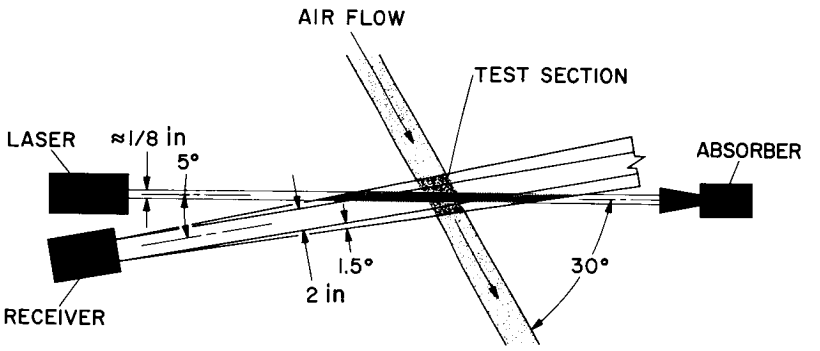

Figure 3

8. SIMULATOR EVALUATION OF A DISPLAY FOR MANUAL ZERO-ZERO LANDINGS

By Joseph G. Douvillier, Jr.

NASA Ames Research Center

SUMMARY

A research program to study in flight the display, sensor, and computer requirements for airborne, manually piloted zero-zero landing systems is being undertaken at the Ames Research Center. An evaluation has been made, on a flight simulator, of the display which will be used in the flight tests. Results show that on the simulator the pilots performed at least as well when they used the display for zero-zero approaches and landings as they did when they made simulated ILS approaches followed by simulated VFR breakouts and landings. In some aspects, particularly in the presence of crosswind, performance for the zero-zero display landings was somewhat better than for the ILS-VFR landings.

Eight configurations of the display were studied in an attempt to evaluate the several elements in the display. There was no evident difference among the eight display configurations. The pilots who participated in the simulator program doubt that this result will carry over into flight.

INTRODUCTION

The Ames Research Center is conducting a research program on the concept of manually piloted zero-zero landing systems. This paper is a report of some results of the evaluation on a flight simulator of the pilot's display which will be used in the flight program. The particular concept which will be explored is that of an airborne, manually piloted system: airborne, because to be independent of ground installations would allow zero-zero capability to airplane operators using small, relatively unequipped airports - for example, to short-haul, commuter airlines or to general aviation operators; manually piloted, because a manual system would likely be simpler than an automatic one and, therefore, probably lighter and more reliable - always two important considerations. Furthermore, even with an automatic system, provision for manual landings would be desirable as a safety measure. Manual capability, therefore, is fundamental.

The objectives of the program are: First, to document quantitatively the performance of pilots in making manual zero-zero landings by using a synthesized landing display, compared with their performance in making landings in VFR conditions and, second, to determine the degree of accuracy which must be provided in the sensors and the computers as well as in the display. This paper pertains only to the first objective.

Concurrently with the preparations for the in-flight research, a ground-based flight simulator was used to develop and make a preliminary evaluation of a display.

DISCUSSION

The basic display which will be used in the flight tests is shown in figure 1. Based on what had been learned in previous display research, the approach taken was to make the display as VFR-like as possible - in other words, such that the pilot could use it much as he does the outside world when making visual landings. There would be no numbers explicit in the display and no director information. The elements of this basic display are shown in figure 1. There is a horizon line which behaves the same as the horizon in the conventional attitude gyro. There is a runway, depicted by four lines - like tar strips across the real runway. The symbolic runway moves about in the display and has the same perspective as would the real runway viewed from the pilot's position. The velocity circle encloses the point on the ground toward which the airplane is flying. It is the point of intersection of the total velocity vector and the ground. There is also the fixed vertical index representing the nose of the airplane.

It was reasoned that these elements contained all the information a pilot needs to land his airplane, presented in a way that could be interpreted as VFR-like as a symbolic display can be. He can discern from it his position in relation to the runway by the asymmetry of the runway symbol; his path by the location of the velocity circle; his altitude by the amount of separation between the horizon line and the runway lines; and his attitude by the displacement and the angle of the horizon line.

However, an early subjective evaluation suggested the need for more information. The pilots wanted better lateral-displacement information when relatively far out on the approach and better height and height-rate information when close to the ground.

For better lateral-displacement information a centerline indicator was added, as shown in figure 2. It behaves essentially as would the fuselage of another airplane in front of and slightly below the pilot's own airplane, but this other airplane is always lined up with the runway centerline. It has been named a "ghost" airplane. Essentially, it gives the pilot a magnified indication of lateral displacement. It behaves like a lead airplane as seen from the pilot's position. For example, in figure 2 the airplane is far out on the approach; the runway symbol is too small for the pilot to perceive any asymmetry. But he can tell from the ghost airplane that he is off to the left a bit. He can also tell, from the velocity circle, that he is correcting the error. He is flying toward a point to the right of the runway. He has to fly toward the right of the runway if he wants to get lined up. When he is lined up, he will be right behind the ghost airplane; that is, the ghost airplane will be between his own airplane and the runway. But the pilot does not want to fly past the ghost airplane; so, as he closes on being lined up - as the ghost airplane drifts in front of his own airplane - the pilot makes a turn into position

behind the ghost airplane. In other words, he flies toward the ghost airplane and the runway.

For better height and height-rate information another symbol, a small dash, was added. This altitude indicator is shown in figure 3. The displacement of the dash below the velocity circle is proportional to airplane height above the runway, scaled at 1 inch per 10 feet. It does not appear in the display until the airplane is down to an altitude of about 50 feet. The position and the rate of change of position of the altitude indicator give the pilot a more compelling signal than does the perspective of the runway. The dash is somewhat like the airplane shadow on the ground. When the airplane is descending, the shadow comes up to meet the airplane; if the airplane balloons upward, the shadow sinks away. When the shadow coincides with the point toward which the airplane is flying (the velocity circle), the airplane is on the ground.

The scaling of the display is one to one with the real world. That is, the visual angles associated with a particular element of the display are the same as the corresponding visual angles associated with the object in the real world which the particular element of the display represents. For example, the visual angle between the horizon line and the runway threshold line in the display is the same as the visual angle between the actual horizon and the actual runway threshold. As a result, the sensitivity of the display changes as the airplane gets closer to the ground, just as the effective sensitivity of the real world changes. The pilot has information to larger scale as he gets close to the ground - with the display just as with the real world.

The pilot can, as he chooses, make shallow approaches or steep approaches. Figure 4 shows a comparison of the display for two angles of approach. In each, the airplane is at the same distance from the threshold. In each, it is flying toward the same point on the runway. But in the left display the pilot is making a more shallow approach than in the right. The different runway perspectives show this; but the primary indication is in the velocity circle. Its distance below the horizon in the display subtends a visual angle equal to the flight-path angle and is about three times greater in the right display than in the left.

The experiment was made in such a way that pilots' performance in landing when they used the display could be compared with their performance in landing when they used a televised facsimile of the visual landing scene in conjunction with an ILS approach - all on a flight simulator. Not only was the complete display, as shown in figures 3 and 4, studied but, in order to get a measurement of the values of the several elements, the display was tested without the velocity circle, without the altitude indicator, and without the ghost airplane, each removed singly and in combination with the other two. In this way the separate and the interacting effects of these elements on the pilots' performance could be measured relative to the complete display and to the visual picture. Therefore, eight configurations were tested of this display, which varied in completeness from the one in figures 3 and 4 to one containing just the horizon and the runway lines.

In addition, runs were made both with and without crosswind so that the effect of this variable on each of the displays could be examined. The flight

characteristics simulated were those of a Breguet 941 STOL airplane in the landing configuration.

The flight-simulator configuration is such that a televised picture of the simulated visual landing is projected on an 8- by 6-foot screen attached to the front of the simulator cockpit and about 8 feet in front of the pilot as shown in figure 5. The simulator can be rolled, pitched, and translated vertically. This simulator has been used in several Ames research programs, so the Ames pilots are "well-calibrated" to its similarities and its dissimilarities to flight.

Figure 6 is a drawing of the view from inside the cab during an oscilloscope-display run. The pilot can see nothing outside the cab. Shown in the figure are the oscilloscope on which the display was generated, and the viewing mirror with the image of the display. During the ILS-VFR runs the display was off. The pilot made an ILS approach down to an altitude of about 350 feet, at which time the projected televised picture of the simulated runway appeared on the screen outside the cockpit, and the pilot made a simulated visual landing by using the picture.

The simulator is fitted with a complete set of cockpit instruments, typical of a large transport airplane. All panel instruments were operating during all runs, so that the pilots could gather whatever information they wanted from them, as they would in an actual airplane.

Although the analysis of the data is not yet complete, enough has been done to discover the trends. The preliminary analysis indicated that, on the average, the pilots did at least equally well at touchdown with any of the displays as they did with the visual simulation. According to significance tests the differences which did appear at touchdown were scatter in the data and not due to any real difference among the displays and the visual simulation.

Not only were data recorded at touchdown but throughout the entire approach. The next three figures (figs. 7, 8, and 9) show average time histories during the 30 seconds before touchdown for three of the parameters measured. In these figures the results associated with the eight configurations of the scope display are presented in a shaded band, and the results associated with the ILS-visual runs are shown by a solid line. The results for the scope displays are presented this way not only because the measured differences among them are not large enough to be due, probably, to anything other than experimental variation but also because there was no discernible tendency for one scope display to be different from the other scope displays (to be at the high end or the low end of the band). However, on some of the curves there is a tendency for the performance with the visual simulation to be different from performance with the scope displays.

Figure 7 shows rates of descent. The upper curves show rates of descent averaged over all the runs with no crosswind; the lower curves, with crosswind. As can be seen, there is virtually no difference between the visual runs and the scope-display runs, either with or without crosswind. Moreover, the crosswind

curves are almost the same as the no-crosswind curves; therefore, there appears to be no effect of crosswind on the rate of descent for either the visual simulation or the scope displays.

All this indicates that the pilots controlled their rate of descent in the same way with any of the scope displays as with the ILS-visual simulation, under both no-crosswind and crosswind conditions. The rate of descent was about 13 ft/sec during the approach; they started to break the glide at about 10 seconds before touchdown, and the rate of sink was about 5 or 6 ft/sec at touchdown. All these values are typical of actual landings with the Breguet 941.

Figure 8 shows time histories of average drift angle. Averages of the runs with no crosswind, the upper curves, show essentially zero drift angle - as might reasonably be expected with no crosswind. However, the averages of the runs with crosswind, the lower curves, show that the pilot flew differently when he used the visual simulation from the way he did when he used any of the scope displays, for which averages tend to group. On the ILS-visual runs, breakout occurred at about 28 seconds before touchdown, so the curve is for the visual portion of the ILS-visual runs. (Of course, the curves for the displays represent only zero-zero conditions.) Obviously, the effect of crosswind tends, during the approach, to be greater when the pilot used the visual simulation than when he used any of the scope displays. This result was not surprising because, in a crosswind, the pilots used a technique with the scope displays that was different from the one they used with the ILS-visual simulation.

This different technique, although it resulted in slightly better performance, was actually necessary because of a shortcoming in the display. The horizontal visual range of the scope display was from 10° to -10°. The crab angle necessary to correct for the crosswind used was 9°. Therefore, if the crosswind were corrected for by crabbing, the runway (and the ghost airplane and the velocity circle when they were in the display) would be well over on one edge of the display, almost out of sight. Any small deviation would drive it off the scope. So, with the scope displays, as soon as the approach began the pilots held the heading of the airplane so that the runway stayed essentially in the center of the scope and compensated for the crosswind by holding a wing down. The airplane was more nearly decrabbed throughout the approach with the scope displays than with the visual simulation, and no large last-second corrections had to be made.

On the ILS-visual runs the pilots would crab the airplane to compensate for crosswind, until breakout, and then gradually feed in some sideslip. In fact, on the average, they let the drift build up again beginning at about 10 seconds before touchdown and then decrabbed during the last 3 seconds. However, at the instant of touchdown, the amount of drift was not large in any case; and the spread is, in fact, statistically not significant.

It is interesting to note that none of the curves indicate a tendency for the pilots to overcompensate for drift. All the end results are on the undercompensating side of zero.

Figure 9 shows a time history of lateral displacement from the runway centerline. The upper curves, the averages over the runs with no crosswind,

again show almost no difference, either among scope displays or between scope displays and visual simulation. There is an average error of about 35 feet at breakout on the ILS-visual runs, but the spread at touchdown is about 8 feet.

The lower curves show the effect of crosswind on lateral displacement. Obviously, the pilots flew differently with the ILS-visual simulation from the way they did with the scope displays. On the ILS-visual runs, breakout occurred at about 28 seconds. It appears that the average error at the end of the ILS portion of the approach was about 80 feet, in the direction the crosswind tended to carry the airplane away from the centerline. At breakout, the pilot detected the misalinement and was able to correct it easily enough by using the televised picture. On the other hand, with the scope displays the pilot was able to stay more nearly alined through most of the approach and did not have to make any appreciable correction. Again, the differences at touchdown were insignificant.

Several other parameters were measured during the experiment, but these have yet to be examined in detail. The brief analysis which has been made suggests that the same trends which were apparent in the rate of descent, the drift angle, and the lateral displacement can be expected: essentially no average difference among the scope displays, and little practical average difference between scope displays and ILS-visual simulation.

It is surprising that there was no difference among the eight configurations of the scope displays. One would expect that, as the explicit information provided by the velocity circle, the altitude indicator, and the ghost airplane was removed, the pilots' performance would deteriorate. On the other hand, all the information provided by those three elements is still in the display when it contains only the horizon line and the four runway lines. It is apparent, from the results and also from the pilots' comments during the experiment, that they learned to use this implicit information. Also, while using the complete display they learned to recognize the behavior of the runway symbol, relative to the horizon and to the scope frame, in successful landings. They could successfully reproduce that behavior, on the average, even with the three elements missing. However, the pilots do not believe that this would carry over into even the most mildly stressful situation in flight - and perhaps not even into an unfamiliar simulation.

Remember that all the results shown here are averages. It may well be that even though pilots can, on the average, do as well with the minimum scope display as with the most complete, perhaps their performance is less consistent from run to run. Therefore, the data will also be analyzed to show the variability from run to run, with the eight display configurations and the ILS-visual simulation.

The conclusions reached here are tentative, both because they are the results of simulator tests and because the data analysis is not yet complete. Whether or not they hold up in flight will be finally determined in the research airplane.

The display described in this paper is not unique. Other similar displays are described in references 1, 2, and 3. Reference 3 is a comprehensive discussion of the kinds of information which must be contained in a landing display

and the way in which this information should be presented. It contains a comparison in particular of five existing and proposed displays and makes recommendations for flight and simulator test programs. Reference 3 is recommended reading for anyone interested in flight displays in general, and landing displays in particular.

EQUIPMENT FOR FUTURE FLIGHT RESEARCH

The flight research part of the program will be conducted in a Convair 340 airplane. This airplane is being prepared as a general-utility flying laboratory, especially for conducting research on the required characteristics of sensors, computers, and displays for airborne zero-zero landing systems.

Figure 10 shows briefly how this research airplane is being equipped. The system is basically a distance-measuring system (DMS). Because current state of the art does not permit a completely airborne system, there will be three DMS transponders on the ground at known positions relative to the runway. The airborne DMS components interrogate the transponders; and the airborne computer, using the DMS signals, calculates the position and rate of change of position of the airplane relative to the runway. These data, together with airplane attitude information fed to the computer from onboard sensors, are used to compute the display. The display is generated on a cathode-ray tube (CRT), and the reflection of it in a mirror is viewed by the pilot. When the airplane is near touchdown, the position information from the DMS is augmented with height information from a radar altimeter. References 4 and 5 contain detailed descriptions of this research equipment and its operation.

At present the DMS, the computer, and the display-generating equipment are being tested on the ground and prepared for installation in the airplane. The support equipment has already been installed and checked in flight. When this flying laboratory is completed, Ames will have a flexible research facility for in-flight studies of display concepts as well as of the attendant sensing and generating equipment. The first program to be undertaken on this flying laboratory is the one which has been described in this paper.

REFERENCES

1. Noxon, Paul A.: Microvision. Eclipse-Pioneer Div., Bendix Corp., July 1964.

2. Snodgrass, Reuben P.: Head-Up Display - A New Form of Avionics. Sperry Eng. Rev., vol. 17, no. 3, Fall 1964, pp. 10-19.

3. Baxter, J. R.; and Workman, J. D.: Review of Projected Displays of Flight Information and Recommendations for Further Development. Human Eng. Rept. 2, Aeron. Res. Lab., Australian Defense Sci. Service, Aug. 1962.

4. Robinson, Gilbert G.; and Johnson, Norman S.: An Airborne Zero-Zero Landing Laboratory. Presented at Inst. Navigation, Low-Cost Navigation Symposium (Los Angeles, Calif.), Nov. 6-7, 1963.

5. Robinson, Gilbert G.; and Johnson, Norman S.: Subsystem Requirements for an Airborne Laboratory To Study Zero-Zero Landing Systems. Presented to 25th Meeting of Flight Mechanics Panel of AGARD (Munich, Germany), Oct. 12-14, 1964.

BASIC ELEMENTS OF THE DISPLAY

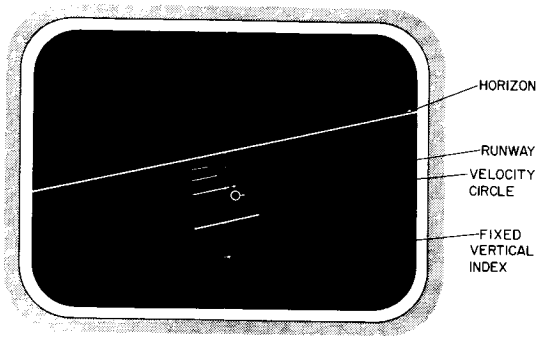

Figure 1

DISPLAY WITH CENTERLINE INDICATOR

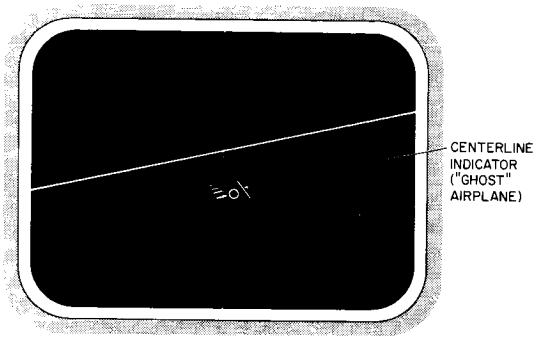

Figure 2

THE COMPLETE DISPLAY INCLUDING ALTITUDE INDICATOR

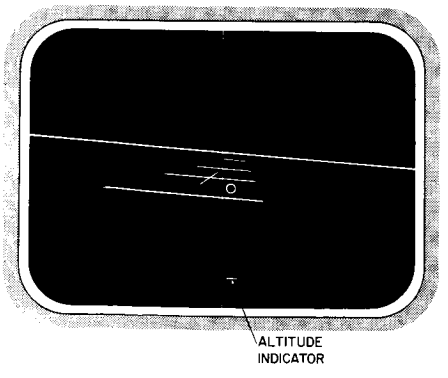

Figure 3

TWO VIEWS OF DISPLAY SHOWING DIFFERENT ANGLES OF APPROACH
SAME DISTANCE OUT

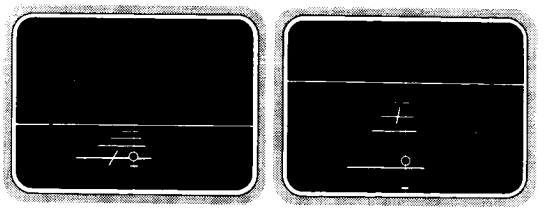

Figure 4

THE AMES TRANSPORT LANDING SIMULATOR

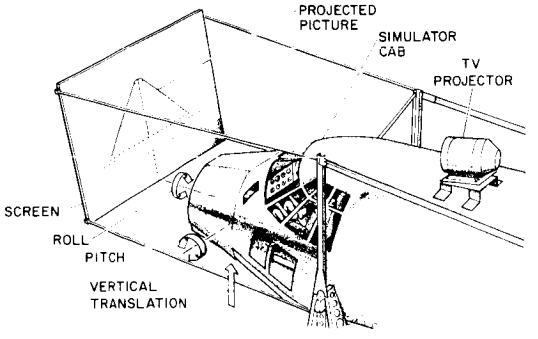

Figure 5

THE INTERIOR OF THE SIMULATOR CAB

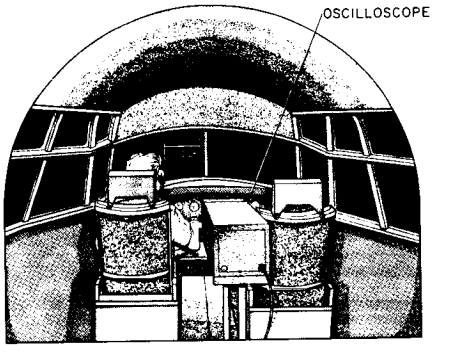

Figure 6

TIME HISTORIES OF AVERAGE RATE OF DESCENT DURING LAST 30 sec BEFORE TOUCHDOWN

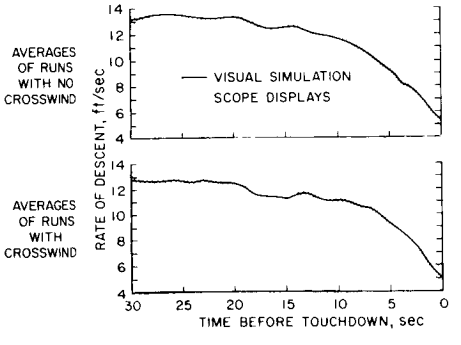

Figure 7

TIME HISTORIES OF AVERAGE DRIFT ANGLE DURING LAST 30 sec BEFORE TOUCHDOWN

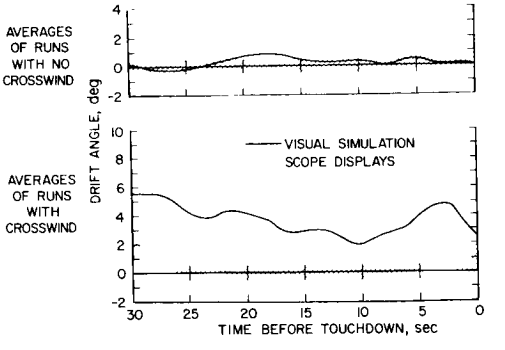

Figure 8

TIME HISTORIES OF AVERAGE LATERAL DISPLACEMENT FROM RUNWAY CENTERLINE DURING LAST 30 sec BEFORE TOUCHDOWN

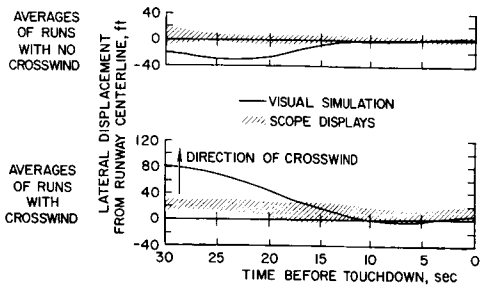

Figure 9

AIRBORNE SYSTEM FOR ZERO-ZERO LANDING RESEARCH

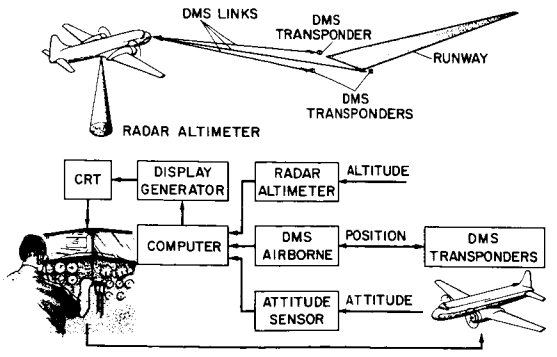

Figure 10

9. FACTORS RELATING TO THE AIRPORT-COMMUNITY NOISE PROBLEM

By Harvey H. Hubbard, Jimmy M. Cawthorn,
and W. Latham Copeland

NASA Langley Research Center

SUMMARY

Factors relating to the airport-community noise problem are discussed herein. The noise problems are associated with aircraft landing approaches, take-offs, and climbouts in communities near commercial airports. The main objectives are to identify the significant factors involved in the problem, to define some of their interrelationships, and to present recent related research information from NASA in-house and contract studies. Changes in the types of aircraft power plants, the aircraft operating procedures, and the community itself are all judged to be important; however, these changes should not be made without understanding the associated human-response implications.

INTRODUCTION

Factors relating to the airport-community noise problem which are discussed herein are illustrated in figure 1. These factors relate to noise associated with landing approaches, take-offs (ground operations), and climbouts in communities near commercial airports. The main objectives of this paper are to identify the significant factors involved in the problem, to define some of their interrelationships, and to present recent research information from NASA in-house and contract studies.

The significant factors in the airport-community noise situation are presented in figure 2. At the heart of the problem, as indicated in the center of the figure, is the fact that humans respond unfavorably to noise. Since there is very little possibility of such human responses changing markedly in the near future, it is important that aircraft operators understand these adverse responses and, particularly, what features of the noise are most objectionable. There are several means of obtaining an overall solution, all of which fall into the three categories identified by the shaded areas in figure 2. (See also refs. 1 and 2.) Noise sources refer, of course, to aircraft power plants and involve both the type of engine cycle and its operating conditions. Aircraft operations include such factors as aircraft gross weight, flight path, frequency of operations, preferential runways, and time of day. Community considerations involve such items as size and location of the areas affected, type of activity existing in the community, the social structure, background noise level, and types of construction of the buildings.

The main objective is, of course, to obtain a more favorable human response to the noise. This objective might be achieved by means of any one of the factors in figure 2, or preferably by some combination of them. It should be noted

that no physical changes should be made, however, without an understanding of the associated human-response implications.

There is first a review of some of the recent results of subjective response studies performed under contract by Bolt, Beranek & Newman, Inc. (refs. 3 and 4). Then there is a brief discussion relating to each of the physical factors represented by the shaded areas of figure 2.

HUMAN RESPONSE

The perceived noise level which is a measure of human response to noise (see refs. 3 and 4) is at present widely used, both in this country and abroad. One of the basic concepts of this response rating procedure is that high-frequency noise is generally more objectionable than low-frequency noise. Spectrum shape is thus an important influence in human reaction to noise. This is especially important where discrete frequencies are involved, as illustrated in figure 3 which is taken from unpublished work done under contract to Bolt, Beranek & Newman, Inc. The basic spectrum at the bottom of the figure has a discrete-frequency component superposed on the broad-band random noise. Such a discrete frequency might be produced by the compressor of a jet engine and, for the case of the illustration, extends about 10 dB above the background (basic) noise level of the octave band in which it resides. The net effect of such a pure tone is to increase the perceived-noise-level value noticeably. For the example shown, the net effect of the single pure tone is the equivalent of a 6 dB across-the-board increase in all octave bands of the basic spectrum, as illustrated in the curve at the top of the figure. Since pure tones have an adverse effect on acceptance, much research effort is being directed toward eliminating such noise components during aircraft operations near airports. (Decibels are referred to 0.0002 dynes/cm^2.)

There has recently become available some information on the effect of time duration of the noise on its acceptability. (See ref. 3.) This effect is illustrated in figure 4 for the flyover-noise situation. The two noise-level time history plots at the bottom of the figure might represent the noise exposures at a community observation point for two different flyover conditions, as illustrated in the sketch at the top of the figure. On the left, path A is shown as an example for which the time t (measured between the points that are 10 dB down from the maximum levels) is relatively short (about 10 seconds), but the peak noise levels are higher than those for path B on the right where the time is $2t$. Laboratory experiments under controlled conditions suggest that the longer exposure time is detrimental. For path B to be equally acceptable, it would be necessary to reduce the peak noise level by about 4.5 dB to compensate for doubling the time exposure. The two noise-exposure time histories shown in the figure are thus judged to be about equally acceptable.

NOISE REDUCTION AT THE SOURCE

Jet Exhaust Noise

One of the main objectives of research on exhaust-noise reduction is to find acceptable methods of producing less noise per unit thrust. The fan, or bypass, engine offers the possibilities for lower exit velocities and hence lower noise levels. (See ref. 5.) The data of figure 5 are included to show the ranges of perceived noise levels associated with both current and proposed engines. Maximum perceived noise levels at a sideline distance of 200 feet have been estimated for all engines by the methods of references 6 and 7. These levels have been arbitrarily normalized to a thrust of 21,000 pounds for comparison and, for convenience, have been plotted as a function of bypass flow ratio.

Data for current turbojets are plotted at the zero location on the abscissa scale and fall in the narrow hatched region. Current turbofans are represented by the larger hatched region and are seen to have somewhat lower perceived noise levels. Some proposed high-bypass-ratio engines are represented by the stippled region at the right, and it is seen that by this means, substantially lower perceived noise levels may be realized. It should be noted that this lower boundary is well defined, but the upper boundary is not well defined. The vertical extent of the stippled region represents some of the uncertainties regarding the importance of jet-stream turbulence, combustion noise, compressor noise, and turbine noise for these proposed engines. Research effort is being focused on minimizing the noise from these sources so that the full potential of these engines can be realized.

Compressor Noise

Several recent research studies (refs. 8 to 14) have been directed toward ways of minimizing the discrete-frequency compressor noise radiation from inlets. Samples of the results obtained are shown in figure 6. These studies have involved changes to the inlet geometry, the compressor geometry, and the inlet flow conditions. Noise-level reductions (i.e., the differences between those for the modified compared with those for the unmodified configuration in each case) are shown for various azimuth angles in one of the front quadrants. The use of resonators arranged in a peripheral array around the inlet provided the results shown on the left. For the case where the spacing between the rotor and stator of the front stage was changed, a rather complex pattern of noise reduction was obtained, as indicated by the center diagram. On an inlet for which it was possible to establish choked-flow conditions, the greatest noise reductions were obtained as shown in the right-hand diagram.

The results are summarized briefly in figure 7 by means of a bar graph which illustrates the maximum noise reductions obtained for each of four different approaches. The first three of these approaches represent the results obtained in NASA research studies, whereas the last item represents the results achieved with configurations suitable for application to current aircraft designs. The ranges of noise reductions obtained with resonators, spacing

changes, and inlet flow choking are generally consistent with the results of other known experience. Results have varied from one particular investigation to another, and thus the conclusion is drawn that such results are sensitive to configuration details. The experience with absorptive treatment is also believed to be strongly influenced by the configuration for which the work was done, since there is reason to believe that configurations having longer duct lengths available for treatment would produce larger noise reductions than those illustrated in the figure.

It is not known whether or not some of these modifications may be successfully used in combination. Contract research studies are under way for the purpose of optimizing compressor-noise-reduction procedures for a full-scale engine nacelle.

AIRCRAFT OPERATIONS

Landing Approach

With regard to aircraft operations, one of the most difficult aspects is related to the landing approach, during which time the airplane flight path is shallow and the aircraft is quite close to the observers on the ground. One obvious scheme to improve this situation would be to use a steeper approach-path angle as shown in figure 8. Some related performance studies are described in paper no. 4 by Hall, Champine, and McGinley, and some of the noise-level time histories for a fan-powered transport aircraft are shown in figure 8. The solid curve represents a conventional approach at a 3° geometric angle, whereas the dashed curve applies to a 6° approach. The data were obtained at a measuring station about 6900 feet from the end of the runway. An obvious beneficial result of the steep approach is that the maximum noise levels are lower because of the increased distance of the aircraft and the somewhat lower power setting. There is a trend noted, however, that the aircraft is audible for a somewhat longer total time during approach at the higher angle probably because of the more favorable sound-propagation-path conditions at this higher altitude.

Take-off and Initial Climb

There has been much discussion also about the use of steeper initial climb rates in order to increase the distance to the aircraft and thus reduce the noise on the ground. In the plot at the top of figure 9 are shown schematically two altitude-distance profiles. The lower profile is representative of the operation of a current, long-range, fan-powered aircraft. The upper profile, on the other hand, represents a hypothetical high-performance aircraft of about the same gross weight but with twice the installed thrust and with advanced-design fan engines.

At the bottom of the figure the plot shows the estimated 100 PNdB contours on the ground for the associated take-off operations. These contours are plotted at appropriate longitudinal and lateral distances with reference to the runway. The reference rectangle of dashed lines is drawn at a 1/2-mile

distance in all directions from the runway, and therefore is representative of the size of some commercial airports.

The current airplane, because of its lower thrust-to-weight ratio, has a longer take-off run, a slower climb rate, and thus an associated ground-noise contour that is relatively long and slender. The hypothetical high-performance aircraft, on the other hand, has a shorter take-off run, a more rapid climbout, and an associated ground-noise pattern that is relatively short in the take-off direction as indicated by the shaded area. A shaded area is included to show the range of results obtainable, depending on the exhaust conditions of the proposed engine. For a high-velocity exit (duct heating), the outer extremes of the area apply, whereas for a high-bypass-ratio engine without duct heating, the inner extremes apply. For this latter condition, the perceived noise levels above 100 PNdB all occur within the airport boundaries.

COMMUNITY COMPATIBILITY CONSIDERATIONS

It is obvious that normal activities in many communities near airports are not, for one reason or another, compatible with the noise exposures from airport operations. (See ref. 15.) Some changes in the noise characteristics of the power plants or in the manner of aircraft operation, as have been discussed, might be beneficial in reducing noise. Of equal importance to the overall compatibility problem are possible changes in the community itself to better adapt itself to its environment. Some of the possible considerations in such a community undertaking could be: zoning, tax incentives, financial assistance, building and housing codes, land acquisition, eminent domain, and urban renewal. Each of these considerations is not discussed, but it should be pointed out that they have already been used successfully to bring about desired changes in some specific situations. A contract study is currently under way for the purpose of gathering together the latest information relative to the application of these procedures to communities with airport noise problems. The use of such instruments by the proper authorities as part of a sound overall plan for community development could be very beneficial and would complement other efforts to minimize noise exposures.

CONCLUDING REMARKS

Three types of approaches to solving the airport-community noise problem which are closely interrelated with the phenomena of human responses are discussed. These approaches include changes in the types of aircraft power plants, the aircraft operating procedures, and the community itself. Because there are many facets to this problem, a coordinated, multipronged approach to a solution is required.

REFERENCES

1. Tyler, John M.: A New Look at the Aircraft Noise Problem. [Preprint] 911B, Soc. Automotive Engrs., Oct. 1964.

2. March, Alan H.; and McPike, A. L.: Noise Levels of Turbojet- and Turbofan-Powered Aircraft. Sound, vol. 2, no. 5, Sept.-Oct. 1963, pp. 8-13.

3. Kryter, Karl D.; and Pearsons, Karl S.: Some Effects of Spectral Content and Duration on Perceived Noise Level. NASA TN D-1873, 1963.

4. Kryter, K. D.; and Pearsons, K. S.: Modification of Noy Tables. J. Acous. Soc. Am. (Letters to Ed.), vol. 36, no. 2, Feb. 1964, pp. 394-397.

5. Kantarges, George T.; and Cawthorn, Jimmy M.: Effects of Temperature on Noise of Bypass Jets as Measured in the Langley Noise Research Facility. NASA TN D-2378, 1964.

6. Anon.: Definitions and Procedures for Computing the Perceived Noise Level of Aircraft Noise. ARP 865, Soc. Automotive Engrs., Oct. 15, 1964.

7. McPike, A. L.: Recommended Practices for Use in the Measurement and Evaluation of Aircraft Neighborhood Noise Levels. [Preprint] 650216, Soc. Automotive Engrs., Apr. 1965.

8. Tyler, J. M.; and Sofrin, T. G.: Axial Flow Compressor Noise Studies. [Preprint] 345D, Soc. Automotive Engrs., 1961.

9. Copeland, W. Latham: Inlet Noise Studies for an Axial-Flow Single-Stage Compressor. NASA TN D-2615, 1965.

10. Bateman, David A.; Chang, Stephen C.; Hulse, Bruce T.; and Large, John B.: Compressor Noise Research. Tech. Rept. ADS-31, FAA, Jan. 1965.

11. Carmichael, R. F.: Analyses of Dynamic Measurements Obtained During the J79-13 Engine Installation Test for the NB-66D Laminar Flow Control Aircraft. Rept. NOR-62-163, Norair Div., Northrop Corp., July 1962.

12. Copeland, William L.; and Crigler, John L.: Rotor-Stator Interaction Noise Studies of a Single-Stage Axial-Flow Research Compressor. NASA paper presented at Sixty-Eighth Meeting of the Acoustical Society of America (Austin, Texas), Oct. 21-24, 1964.

13. Bragg, S. L.; and Bridge, R.: Noise From Turbojet Compressors. J. Roy. Aeron. Soc., vol. 68, no. 637, Jan. 1964, pp. 1-10.

14. Advanced Eng. and Technol. Dept., Gen. Elec. Co.: Research Investigation Into Fan Noise Prediction and Alleviation. Contract No. DA 44-177-AMC-72 (T), U.S. Army Transportation Res. Command, Sept. 1964.

15. Anon.: Land Use Planning Relating to Aircraft Noise. Tech. Rept., Bolt, Beranek & Newman, Inc. [Cambridge, Mass.], Oct. 1964.

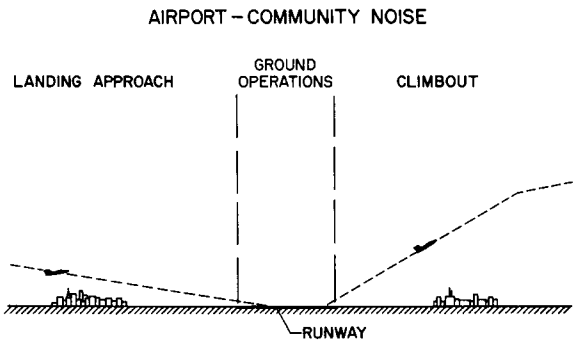

Figure 1

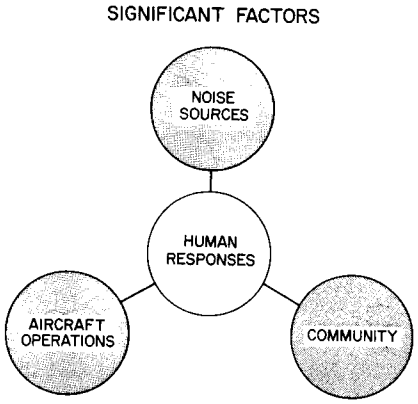

Figure 2

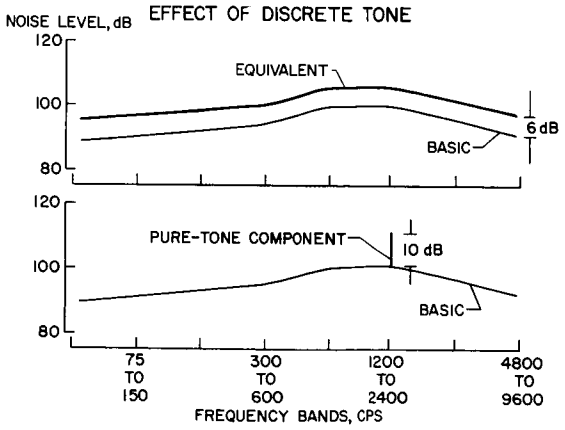

Figure 3

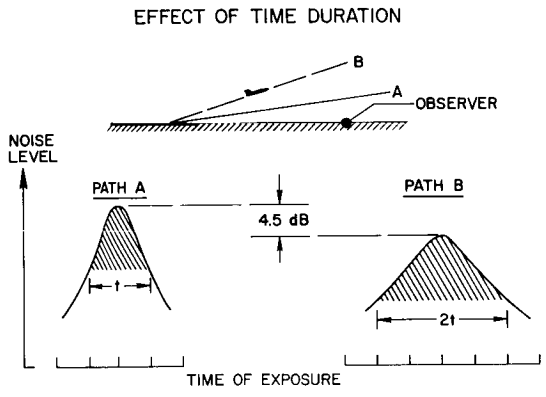

Figure 4

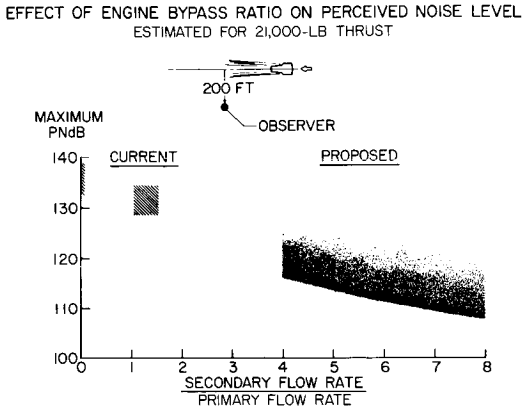

Figure 5

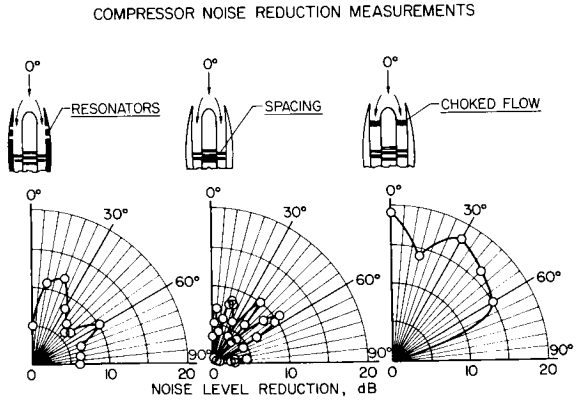

Figure 6

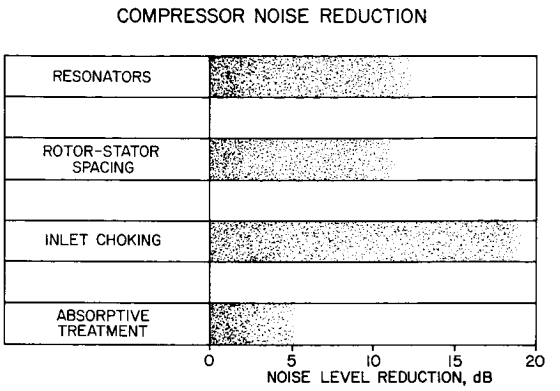

Figure 7

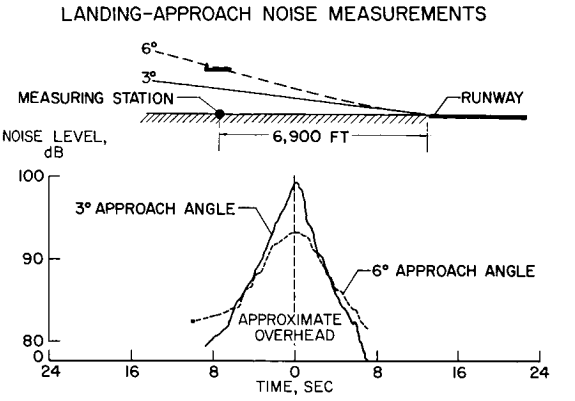

Figure 8

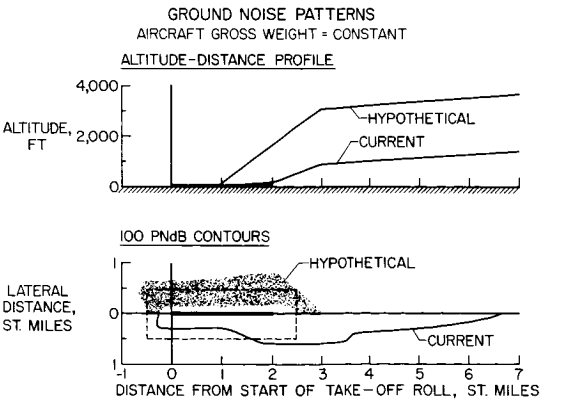

Figure 9

10. PRELIMINARY MEASUREMENTS OF TAKE-OFF AND LANDING NOISE FROM A NEW INSTRUMENTED RANGE

By Carole S. Tanner and Norman J. McLeod

NASA Flight Research Center

SUMMARY

This paper describes the NASA noise-survey instrumentation system presently in use at Edwards Air Force Base, California, and presents preliminary noise data from an F-104 airplane. Also presented are noise measurements of the XB-70 and 707-131B airplanes obtained with essentially the same equipment at another location. The difference between measured noise levels for the XB-70 and 707 is illustrated and comparisons of perceived noise levels are made. The adequacy of noise predictions is discussed briefly.

INTRODUCTION

Excessive noise in and near airports has become an increasing problem with the development of commercial jet airplanes. Considerable research on this noise problem has been undertaken in the past but the results have been less than conclusive. Some factors compounding the problem are differences in engine installations, engine types, wind, temperature, humidity, and airplane operating parameters such as flight path and velocity.

The relationship between these factors and noise from advanced engine/airframe configurations presents the airplane designer and operator with serious difficulties since safe and economically feasible operating conditions must be combined to obtain acceptable noise levels. In view of the availability of the most advanced airplanes at Edwards Air Force Base, a noise study under actual operational conditions has been undertaken by the NASA Flight Research Center with the assistance of the Air Force Flight Test Center. This paper describes an acoustic measuring system installed along the main runway at Edwards Air Force Base and presents some of the initial data obtained from this facility. In addition, XB-70 and 707 noise data obtained with essentially the same equipment temporarily installed at Palmdale, California, are presented.

DESCRIPTION OF TEST INSTRUMENTATION

Noise data for the F-104 were obtained at Edwards Air Force Base, California; XB-70 and 707 data were obtained at Palmdale, California. The Edwards instrumentation layout is shown in figure 1. Twelve microphone

stations are positioned symmetrically in pairs at 5000-foot intervals along and beyond the runway. Total distance between microphone pairs varies from 310 feet to 1000 feet. Each microphone station consists of a 1/4-inch microphone/cathode follower unit, an integrated microphone power supply and line-driving amplifier unit, and a battery operated ac power supply. The noise measured by each microphone is amplified and transmitted via an underground cable system to a tape recorder in the van.

The instrumentation layout at Palmdale, shown in figure 2, consists of eight NASA microphone stations (circles with numbers) and three microphone stations (circles with letters) provided by North American Aviation. The NASA microphone stations, the same as those used at Edwards, were installed along the 200-foot-wide, 12,000-foot-long runway. The three North American microphones were located 3 miles from airplane brake release. Two separate cable systems and recording vans were used.

The Edwards instrumentation for data acquisition and reduction and the Palmdale system were completely electrically and acoustically calibrated. The only deviation was the extrapolation of system response to 31.5 cps. Typical response characteristics shown in figure 3 indicate that system frequency response is flat within 1.8 dB and 2.5 dB for the Edwards and Palmdale systems, respectively. Corrections applied to data obtained with the Edwards instrumentation and the eight NASA microphones at Palmdale are for system response and the energy acceptance of the data-reduction filters. Evaluation of these corrections indicates that these data are accurate to ±1.5 dB. Unfortunately, complete system and data-reduction corrections are not available for the three North American microphones used at Palmdale; however, the data are considered accurate to within ±3 dB. (Decibels are referenced to 0.0002 dyne/cm^2.)

SYSTEM TESTS

The Edwards system was placed in operation in December 1964. Initial operation consisted of repeated test flights using a single-engine F-104 airplane to determine the extent and effect of space-positioning accuracy and data repeatability. Noise data from the test flights were time correlated with airplane location which was obtained by using Air Force radar. Evaluation of the test results indicates that the location of the aircraft in relation to the microphones could be determined within the limits of a box having a base of 14 feet, a height of 16 feet, and a length of 50 feet. Since skin tracking was used, larger airplanes may have a larger position error.

The F-104 noise-data repeatability is shown in figure 4. The data are from four consecutive flybys having the minimum ranges between airplane and microphone for the weather conditions shown.

To minimize near-field effects, data from microphone 3 (fig. 1) were selected for presentation. The octave band sound pressure levels show excellent repeatability up to 500 cps except for the one point at 250 cps. Data repeatability is not as good at the higher frequencies where a scatter of ±3 dB occurs.

Since higher frequencies would be affected by slight changes in engine thrust, the larger variation of those frequencies is attributed in part to changes in engine thrust as gross weight decreased from one flyby to the next. However, the variation in noise at the higher frequencies is not believed to be significant, and since the overall sound pressure levels agree quite well, data repeatability is considered satisfactory for all octave bands.

XB-70 AND 707 NOISE

In an effort to provide take-off noise data from the largest supersonic airplane available, preliminary data were obtained from the XB-70.

The data presented were obtained on one of the earlier flights which originated from Palmdale, California. In order to obtain the data at the earliest possible time the Palmdale layout (fig. 2) was used.

In order to help place XB-70 noise in proper perspective, arrangements were made with the Air Transport Association for a 707 fan-jet airliner to operate from the Palmdale runway approximately 1 hour after the XB-70 take-off. Noise data presented for these two airplanes are for the take-off profiles and weather conditions shown in figure 5. Illustrated are the actual take-off profiles of the XB-70 and 707 and representative take-off profiles of the supersonic transport (SST) obtained from NASA Technical Note D-423 which is an early summary report.

The XB-70 take-off was made with all engines at maximum afterburner thrust, but the programed rate of climb was rather low. The 707 take-off is typical of operation from a commercial airport. It should be noted that the SST will have different engines and higher climb profiles resulting in noise levels lower than those of the XB-70.

The magnitude of the noise levels measured from the XB-70 and 707 for these take-off profiles is illustrated in figures 6 and 7. Figure 6 shows the noise spectra along the runway for the XB-70 and the 707. Data from microphones 3 and 8 (fig. 2) are shown.

The XB-70 maximum spectrum levels occur in the 125 cps band. The spectrum from microphone position 3 had a higher noise level than the spectrum from microphone 8. This difference is between 20 and 25 dB over all frequencies. The inverse-square-law attenuation for the difference between the microphone locations is approximately 9 dB; therefore, it is concluded that microphone 3 is in the near field of the XB-70 engines.

The 707 data at the bottom of figure 6 show that the maximum spectrum levels occur in the 125 cps band. The spectrum level at microphone 3 is higher than the level at microphone 8 and the difference is approximately 10 dB. This noise-level difference approaches the inverse-square-law attenuation, which leads to the conclusion that both microphones were in the far field of the 707 fan-jet engines. Far-field noise data are more consistent than near-field data,

therefore the difference between noise along the runway is best determined by comparing the spectra from microphone 8 for each airplane.

The XB-70 spectrum is, on the average, 15 dB noisier than that for the 707. This difference is due to the larger number of engines as well as the higher thrust of the XB-70. The remarkable similarity between the spectrum shapes was not expected and more research is needed before the exact reasons for this similarity can be determined.

The airplane noise at the 3-mile point is also of interest from the standpoint of community response to noise. A direct comparison of the noise spectra of the XB-70 and 707 airplanes at the 3-mile point is shown in figure 7. Spectra for both airplanes at similar slant ranges show that the XB-70 noise levels are considerably higher than those of the 707. It is significant that the difference between these two spectra is an average of 25 dB for all frequencies, whereas the difference in spectra along the runway was 15 dB (fig. 6).

The larger difference in spectra at the 3-mile point indicates that further research is needed to ascertain the effects of airplane attitude, source size, and airplane motion on the noise produced.

PERCEIVED NOISE LEVELS

The noise spectra at the 3-mile point, as well as the spectra along the runway, can be used to calculate perceived noise levels. The perceived noise level is a judgment of the noisiness or annoyance of a sound and is obtained by weighing the octave band levels with factors determined from the response of the human ear. Perceived-noise-level calculations were made by using the conversion tables in reference 1 and the following formula:

$$N_T = N_M + 0.3\left(\Sigma N_N - N_M\right)$$

where

N_T total noisiness, noys

N_M noisiness in noisiest band, noys

ΣN_N sum of noisiness of all bands, noys

Perceived noise levels for the XB-70 and the 707 are shown in figure 8. The circles represent the positions for which perceived noise levels were calculated.

The perceived noise levels for the XB-70 are higher in all cases than are those for the 707. The point of interest is the comparison of the magnitude of perceived noise levels from a commercial airliner operated to be quiet with a

military airplane whose design and operation did not consider the alleviation of noise as a prime factor. The question of whether or not the XB-70 could be operated in a manner resulting in perceived noise levels comparable with those of the 707 is at present unknown.

NOISE PREDICTIONS

The perceived noise levels shown are calculated from data obtained by a frequency analysis of the measured overall sound pressure levels. However, if no measured data were available, a designer would have to use the methods presented in reference 2 or 3, for example, to predict the overall sound pressure levels. The following table shows a comparison between the predicted and measured overall sound pressure levels for the XB-70:

Maneuver	Slant range, ft	Predicted noise from proposed SAE method, (ref. 3), dB	Predicted noise from Handbook of Noise Control (ref. 2), dB	Measured noise, dB
Take-off roll (1-mile point)	1410	120	121.5	118.5
Climbout (3-mile point)	1200	126	125	119.5

The XB-70 noise prediction is based on a single static turbojet engine with afterburning.

The predicted overall sound pressure level was corrected for six engines and divergence. The results from the table indicate that there are small differences between the predicted noise levels for both airplane positions. The measured levels are lower than the predicted ones. It should be noted that the predicted results, in this case, were based on effective nozzle area and its associated flow velocity. It would seem that in the final analysis, the designer or operator must presently resort to flight-testing to obtain a true indication of aircraft noise levels and to check on the noise predictions.

CONCLUDING REMARKS

The data presented in this paper illustrate some of the problems involved in accurately determining engine noise for flight conditions. The acoustic-noise measuring system operated by the NASA Flight Research Center has been developed to acquire data useful in ascertaining the relative importance of the various parameters involved. Present program plans involve the measurement of noise from advanced aircraft and engine configurations. Data from these studies will aid in the establishment of better prediction methods and will help in further assessing the relationship between airplane operating parameters and the noise produced.

REFERENCES

1. Kryter, K. D.; and Pearsons, K. S.: Modification of Noy Tables. J. Acoust. Soc. Am., vol. 36, no. 2, Feb. 1964, pp. 394-397.

2. Von Gierke, Henning E.: Aircraft Noise Sources. Handbook of Noise Control, ch. 33, Cyril M. Harris, ed., McGraw-Hill Book Co., Inc., 1957, pp. 33-56.

3. McPike, A. L.: Recommended Practice for Use in the Measurement and Evaluation of Aircraft Neighborhood Noise Levels. [Preprint] 650216, Soc. of Automotive Engrs., Apr. 1965.

NOISE-SURVEY INSTRUMENTATION LAYOUT

EDWARDS MAIN RUNWAY - ELEVATION 2300 FT

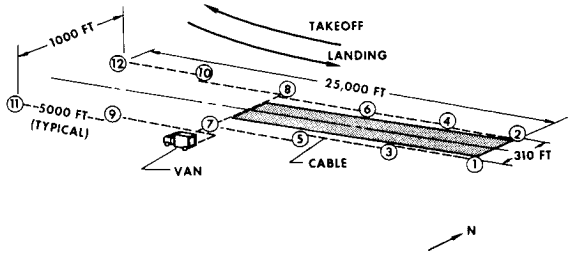

Figure 1

NOISE-SURVEY INSTRUMENTATION LAYOUT

PALMDALE, CALIF.-ELEVATION 2200 FT

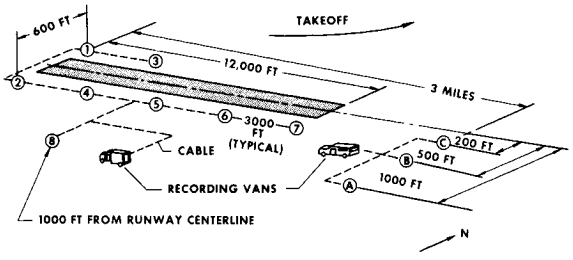

Figure 2

TYPICAL SYSTEM RESPONSE

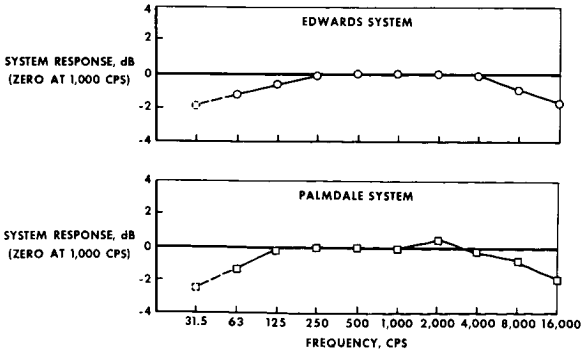

Figure 3

F-104 DATA REPEATABILITY

MICROPHONE 3

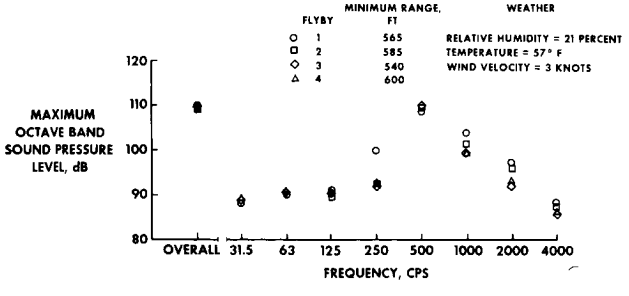

Figure 4

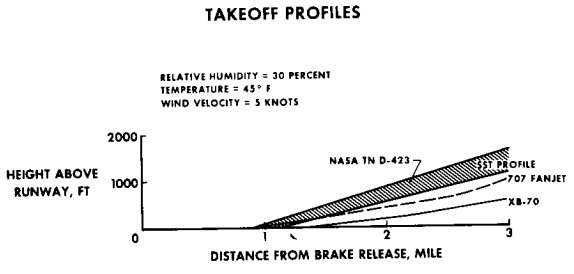

Figure 5

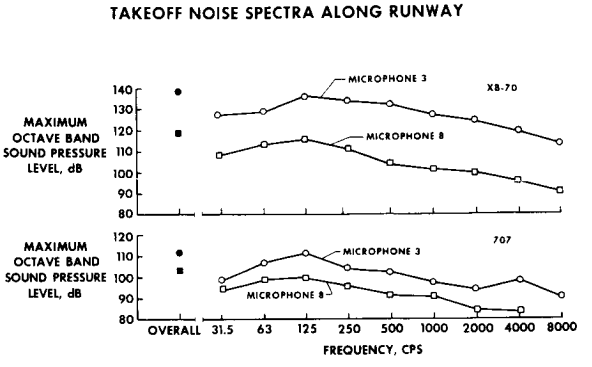

Figure 6

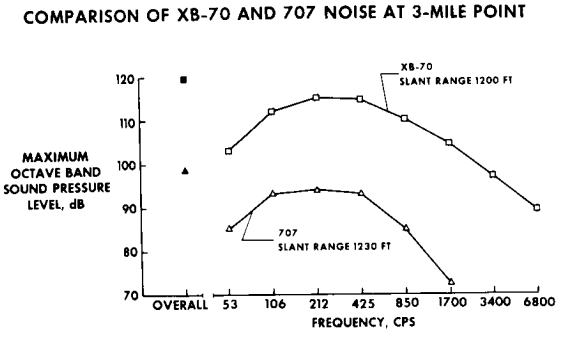

Figure 7

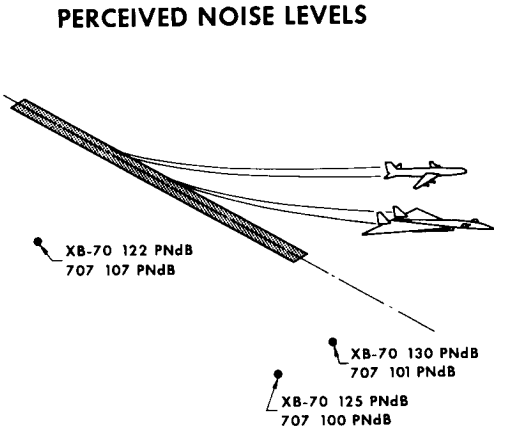

Figure 8

11. OPERATIONAL EXPERIENCES OF TURBINE-POWERED COMMERCIAL TRANSPORT AIRPLANES

By Paul A. Hunter and Walter G. Walker

NASA Langley Research Center

SUMMARY

Recent results obtained from NASA V-G and VGH recorders installed on commercial turbine-powered transports have indicated that exceedances of placard speeds appear to have been significantly reduced since the placard speeds have been redefined and changes made in the aural warning. Oscillatory accelerations and unusual events, such as large or rapid departures from the planned flight profile, occur less frequently. Landing-impact accelerations are higher for turbine transports than for piston transports and vary with operator. The total in-flight acceleration experiences for turbine transports, however, are not significantly different from those for four-engine piston transports.

INTRODUCTION

The NASA V-G/VGH program was initiated on turbine-powered transports concurrently with their introduction into commercial service. A summary of preliminary results of the program was presented at meetings with various segments of the aviation industry in 1961. At that time, some concern was expressed in regard to airspeed practices relative to placard speeds, aircraft oscillations, landing impact accelerations, and unusual events. These preliminary results, including information on in-flight accelerations and gust velocities, were published in 1962. (See ref. 1.) The purpose of this paper is to present information obtained since that time.

INSTRUMENTATION AND SCOPE

In the program, information on operational experiences of turbine aircraft is obtained by means of NASA V-G and VGH flight recorders. The V-G recorder (ref. 2) provides an envelope of airspeed and normal acceleration experience, whereas the VGH recorder (ref. 3) provides time histories of airspeed, normal acceleration, and altitude.

The scope of the program is indicated in table I which shows the number of turbojet and turboprop airplanes on which VGH and V-G recorders were installed and the number of airlines involved. The turbojet airplanes were the Boeing 707, Douglas DC-8, and Convair 880, and the turboprop airplanes were the Lockheed Electra, Vickers Viscount, and Fairchild F-27A. In terms of the accumulated flight time of U.S. commercial turbojet and turboprop aircraft

corresponding to the closing of the various recording programs, the VGH and V-G samples are rather small, as is indicated by the percentage values shown. In terms of number of aircraft, the recorded samples vary from about 4 to 6 percent of the domestic fleet. Despite the small samples in terms of the fleet, it is believed that the careful selection of the operations sampled result in data representative of general airline operations.

Most of the programs on the first line of turbine aircraft have been completed. However, other programs are underway or will be initiated in the near future on the Sud Caravelle, Boeing 727, Douglas DC-9, and BAC-111 transports. A total VGH program involving about 30 aircraft from both domestic and foreign airlines is contemplated.

DISCUSSION

Placard Speed Exceedances

Early samples of VGH data indicated that the turbine-powered transports were exceeding certain limit speeds more frequently than the piston transports. (See ref. 4.) The particular limit speeds were: the normal operating limit speed V_{NO} and the never-exceed speed V_{NE} at which an aural warning was provided. As a result of continued overspeeds, the V_{NO} speed was redefined as a maximum operating limit speed V_{MO} and an aural warning was provided within a 6-knot margin above this speed rather than at the higher never-exceed speed. (See ref. 5.)

Table II shows a comparison of turbojet overspeed experience before and after the change in aural warning. Before the change, Airline A averaged 61 flights between exceedances of V_{NO}, whereas Airline B averaged only 2.7 flights between exceedances. For this comparison, a flight is defined as extending from take-off to landing. The percent of total time spent over V_{NO} was two one-hundreths and eighteen one-hundreths for Airlines A and B, respectively. Both of these samples show better limit speed observance than did some earlier samples. Most of the overspeeds occurred in descent at the lower altitudes where the limit speeds are determined by dynamic-pressure considerations rather than by Mach number.

After the change in aural warning was made, however, no speeds over V_{MO}, the maximum operating limit speed, were recorded for either airline. The sample sizes for these overspeed analyses varied from 200 to 450 hours but for both airlines the second sample was the larger by about 50 percent. The results from the samples taken after the change in aural warning are highly encouraging. Although sampling of speed practices on the older turbine-powered transports is being phased out, the sampling will be continued on new turbojets in the short- and medium-range categories.

Oscillatory Accelerations

Aircraft oscillations in the longitudinal-lateral mode proved to be one of the unanticipated aspects of turbine operations. Oscillations seldom occurred on piston-engine transports but apparently occur on turbine transports because of decreased damping at the higher speeds and altitudes being flown and because of increased sophistication of equipment. Figure 1 shows examples of two types of oscillations - one, a constant-amplitude oscillation and the other, a divergent oscillation. The constant-amplitude type of oscillation was found to continue from several minutes to as much as several hours. The divergent type of oscillation generally lasted less than 2 minutes. The acceleration oscillations shown in these examples have peak-to-peak values of 0.4g for the constant-amplitude type and 0.8g for the divergent type. Other VGH samples are available which show even greater variations. For example, peak-to-peak oscillatory accelerations as high as 0.8g for the constant-amplitude type and 1.8g for the divergent type have been recorded. Variations in the airspeed and altitude were negligible for the constant-amplitude type of oscillation but reached values of 17 knots and 900 feet, respectively, for the divergent oscillation shown here. Every turbine aircraft from which VGH data have been collected showed oscillations to exist, the frequency of occurrence varying from about 0.2 to 26 percent of total flight time. Inasmuch as most of the occurrences of oscillations were traced to control-system or autopilot components, they were a source of concern regardless of amplitude. Oscillations showed up in the initial year of operation of the turbine aircraft but, as a result of a cooperative effort by airlines, and airframe and autopilot companies to improve maintenance procedures and equipment, recent data samples indicate that the amplitudes and frequency of occurrence have been considerably reduced. New airplanes now being phased into the recording program also experience some oscillations, but the amplitudes and frequency of occurrence seen thus far are fairly low.

Landing-Impact Accelerations

Turbine-powered transports have, in general, shown a trend towards higher landing-impact accelerations than the piston transports. This trend has been confirmed by measurement of sinking speeds made from motion pictures of transport landings. In addition, large differences have also been noted between some operators of turbine aircraft of the same type. These differences are illustrated in figure 2 which shows the probability of exceeding given values of landing-impact accelerations for two different operators of the same type of turbojet transport. The landing-impact accelerations experienced by Airline K were about 40 percent higher than those of Airline E. This difference, which is greater than differences generally found between airplane types, is attributed to differences in techniques and crew training between the two airlines.

Unusual Events

Routine examinations of VGH records in the past have, on occasions, shown events not normally associated with passenger-airline operations. Examples of such unusual events, which were reported to the airlines and the aircraft

industry several years ago, were: pitch-up when the aircraft flew at too high an altitude for its weight, collision-avoidance maneuvers, large acceleration oscillations during landing approach, and an upset in which the aircraft recovered from a spiral dive with 4.4g maximum normal acceleration at an airspeed of about 405 knots.

Figure 3 shows one such unusual event recorded during a routine passenger-carrying flight. The nonlinear airspeed scale results from the nonlinear variation between dynamic pressure and airspeed. The salient point of this time history is the indicated airspeed of 100 knots reached at an altitude of about 23,000 feet. The pilot apparently reduced altitude and airspeed in order to reduce the airplane response to the turbulence shown by the acceleration trace. Based on take-off weight and estimated fuel consumption, it appears that the airplane was very near the stall.

The frequency of appearance of such events on VGH records from the older turbine transports has dropped considerably during the past 18 months. During this period, however, the program on these transports was being largely phased out and it is not known how much this reduced frequency of unusual events is associated with the diminishing number of aircraft in the program.

In-Flight Accelerations

Figure 4 compares the gust, operational maneuver, and check-flight maneuver accelerations for turbojet, four-engine turboprop, and four-engine piston aircraft in the form of cumulative frequency per nautical mile to exceed various values of incremental accelerations. Each curve represents the average of the experience of a number of individual airplanes. Relative to the four-engine piston airplanes, gust accelerations were experienced less often by the turbojets and slightly more often by the turboprop aircraft. The operational maneuver experience of the three types of transports is essentially the same. Over most of the acceleration range, turbojet and turboprop airplanes show more frequent check-flight maneuver accelerations than the piston aircraft.

Figure 5 shows a comparison of total gust and maneuver accelerations for the three types of aircraft. The distributions shown here are a combination of distributions obtained from VGH and from V-G records. As may be seen, the total in-flight accelerations for turbojet, four-engine turboprop, and four-engine piston aircraft are not significantly different.

The relative contributions of acceleration sources to the total number of accelerations equal to or greater than 0.6g for each aircraft type are shown in figure 6. For the piston and turboprop aircraft, the gust accelerations predominate, check-flight maneuver accelerations being a secondary source. For the turbojet aircraft, however, the order is reversed and check-flight maneuver accelerations provide the largest portion of the total accelerations. For all three types, operational maneuver accelerations contribute a relatively small number of accelerations equal to or greater than 0.6g. As was indicated earlier, oscillatory accelerations are an additional source for turbine aircraft, but this contribution is negligible at the larger values of incremental acceleration.

Gust Velocities

In figure 7, distributions of derived gust velocity (that is, derived from acceleration, airspeed, altitude, and weight as indicated in ref. 6) in 10,000-foot altitude intervals for turbine transports are compared with estimated distributions (ref. 7) based on past investigations. The estimated distributions represent a model atmosphere widely used to estimate gust-velocity experience. A reduction in gust velocity by a factor of 20 percent had been made in the estimates of reference 7 to account for airplane flexibility. In order that the comparison between the present data and the estimates of reference 7 be more compatible, this 20 percent has been restored to the estimates. The data are in reasonably good agreement with the estimates made about 7 or 8 years ago.

CONCLUDING REMARKS

Recent results from NASA V-G and VGH recorders installed on commercial turbine-powered transports have indicated the following conclusions:

Exceedances of placard speeds, considered to be a serious problem in the early period of turbine transport operation, appear to have been significantly reduced by the redefining of the placard speeds and the changes in the aural warning.

Oscillatory accelerations, which were one of the unanticipated aspects of turbine transport operations, have become much less frequent but have not been eliminated.

The landing-impact accelerations for turbine transports are, in general, higher than for piston transports and vary substantially between operators. Unusual events, such as large departures from the planned flight profile, appear to occur less frequently than in the earlier period of turbine transport operation.

Although the relative contributions of gust and maneuver accelerations to the total in-flight accelerations have changed somewhat from those of piston transports, the total in-flight acceleration experiences for turbine transports are not significantly different from those for four-engine piston transports.

REFERENCES

1. Staff of Langley Airworthiness Branch: Operational Experiences of Turbine-Powered Commercial Transport Airplanes. NASA TN D-1392, 1962.

2. Taback, Israel: The NACA Oil-Damped V-G Recorder. NACA TN 2194, 1950.

3. Richardson, Norman R.: NACA VGH Recorder. NACA TN 2265, 1951.

4. Coleman, Thomas L.; Copp, Martin R.; and Walker, Walter G.: Airspeed Operating Practices of Turbine-Powered Commercial Transport Airplanes. NASA TN D-744, 1961.

5. Anon.: Airworthiness Standards: Transport Category Airplanes. Federal Aviation Regulation Part 25, Rules Service Co. (Washington, D.C.), Feb. 1, 1965.

6. Pratt, Kermit G.; and Walker, Walter G.: A Revised Gust-Load Formula and a Re-Evaluation of V-G Data Taken on Civil Transport Airplanes From 1933 to 1950. NACA Rep. 1206, 1954. (Supersedes NACA TN's 2964 by Kermit G. Pratt and 3041 by Walter G. Walker.)

7. Press, Harry; and Steiner, Roy: An Approach to the Problem of Estimating Severe and Repeated Gust Loads for Missile Operations. NACA TN 4332, 1958.

TABLE I

SCOPE OF PROGRAM

	TURBOJET	TURBOPROP
VGH		
NUMBER OF AIRPLANES	22	9
NUMBER OF AIRLINES	8	5
DATA SAMPLE, HR	47,058	12,484
PERCENT OF U.S. AIRLINES FLIGHT TIME	0.88	0.41
V-G		
NUMBER OF AIRPLANES	24	10
NUMBER OF AIRLINES	7	3
DATA SAMPLE, HR	127,796	48,506
PERCENT OF U.S. AIRLINES FLIGHT TIME	3.41	1.60

TABLE II

SPEED LIMIT EXCEEDANCES

AIRLINE	FLIGHTS TO EXCEED V_{NO}	PERCENT TIME OVER V_{NO}
AURAL WARNING AT V_{NE}		
A	61	0.02
B	27	0.18
AURAL WARNING AT V_{MO} (V_{NO})		
A	—	0
B	—	0

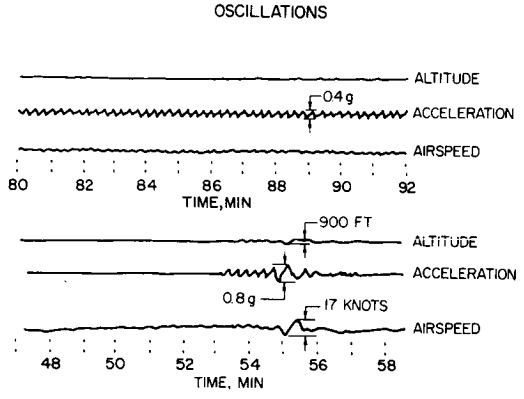

Figure 1

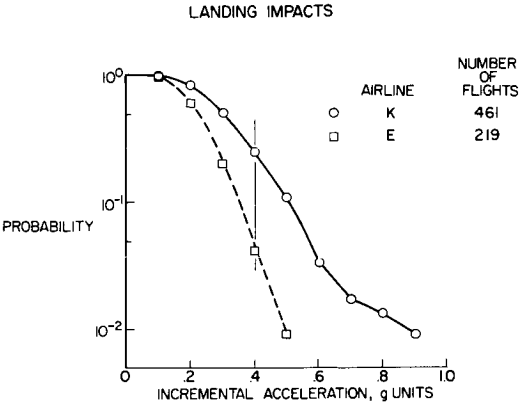

Figure 2

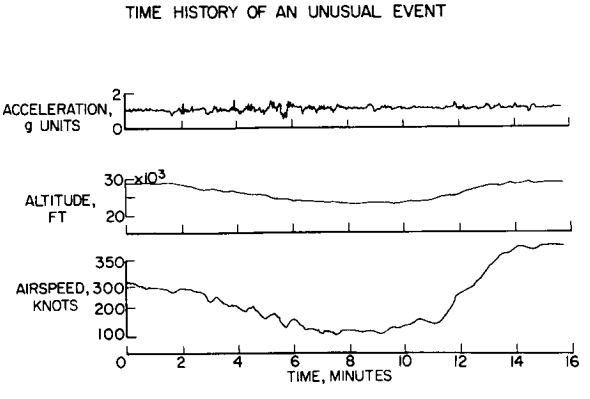

Figure 3

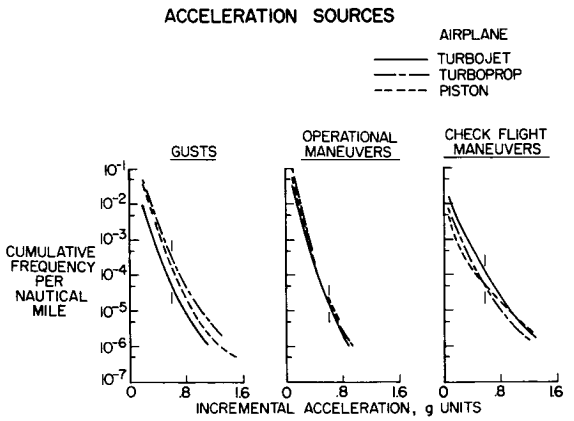

Figure 4

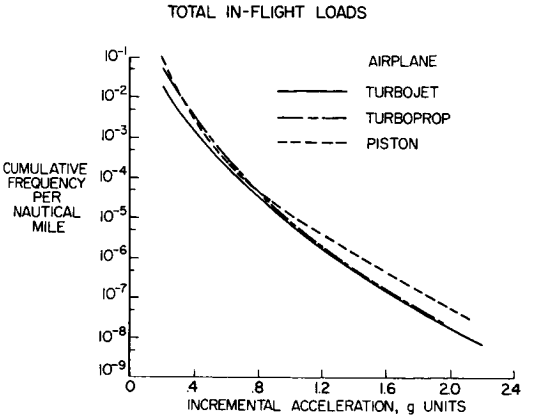

Figure 5

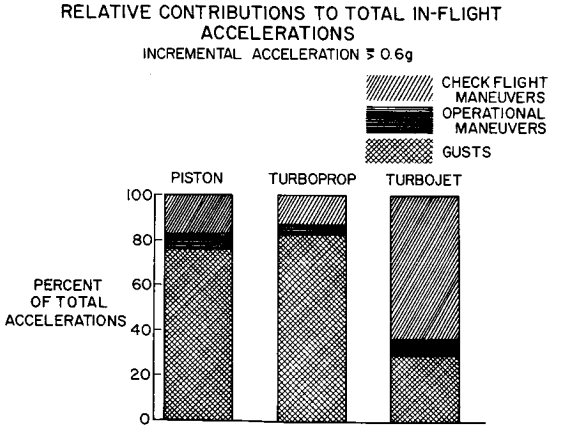

Figure 6

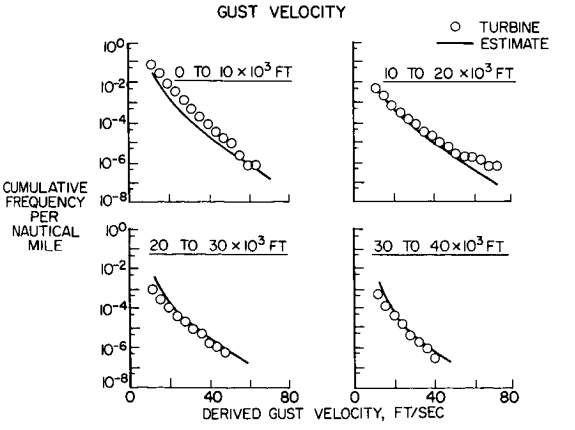

Figure 7

12. SIMULATOR STUDIES OF THE DEEP STALL

By Maurice D. White and George E. Cooper

NASA Ames Research Center

SUMMARY

Simulator studies of the deep-stall problem encountered with modern airplanes are discussed. The results indicate that the basic deep-stall tendencies produced by aerodynamic characteristics are augmented by operational considerations. Because of control difficulties to be anticipated in the deep stall, it is desirable that adequate safeguards be provided against inadvertent penetrations.

INTRODUCTION

Renewed concern has recently developed over an aircraft handling-qualities problem that had received extensive treatment about 10 years ago, namely, the pitch-up. Because of some differences in the character of the problem, it has come to be identified differently, either as a "deep-stall" or a "T-tail" problem. The term "deep stall" refers to the very large angles of attack that are developed after the stalling angle has been exceeded. A popular definition of the term "deep stall" associates it with a locked-in condition where recovery is impossible. In this paper the former more general definition is accepted. The term "T-tail" refers to the tail arrangement that tends to produce pitching-moment variations that would encourage deep stalls, the horizontal tail being located high on the vertical tail. The widespread use of this tail arrangement on modern airplane designs is one of the factors that prompted the current concern over this problem.

Safeguards against dangerous stall penetrations are included in the requirements of existing civil and military regulations. However, since some testing of these airplanes in the stall is required and since a possibility of inadvertent stall penetration (however remote) does exist, a further understanding of the nature of the problem is necessary. Accordingly, the National Aeronautics and Space Administration has started a number of investigations to study this problem. The present paper describes some of the results of simulator studies that were conducted at the Ames, Langley, and Flight Research Centers.

SYMBOLS

C_L lift coefficient

C_m pitching-moment coefficient

h altitude, ft

V airspeed, ft/sec

α angle of attack, deg

θ angle of pitch, deg

δ_e elevator deflection, deg

SIMULATOR STUDIES

The variation of the pitching-moment coefficient with angle of attack that is typically identified with deep-stall tendencies is illustrated in figure 1. On the lower part of the figure is shown a corresponding lift curve. The initiation of unstable slopes is usually identified with the maximum lift coefficient. In the stall of an airplane having a pitching-moment curve of this type, the angle of attack tends to increase rapidly as the stall is penetrated as a result of the unstable variation of pitching moments. A further contribution to increased angles of attack results from the accompanying drag increases and lift decreases, which produce a descending flight path.

Simulator studies of the deep stall that were performed at the three Centers are indicated in table I and will be described in this paper. As shown in this table, the nature and scope of the various studies were different.

TABLE I.- SIMULATOR STUDIES AT NASA RESEARCH CENTERS

Center	Piloted	Degrees of freedom in motion	Motion	Scope
Flight	No	3	-----	Longitudinal recovery performance with wide range of variables, including time for initiation of recovery control.
Langley	Yes	6	Fixed	Piloted study of general longitudinal recovery performance with emphasis on control power and pitch-damping effects.
Ames	Yes	6	Roll and pitch	General investigation of factors influencing deep-stall acceptability from pilot's standpoint, longitudinal and lateral-directional modes.

In the piloted studies, no consideration was given any stall-warning effects or stall-prevention effects other than those resulting from the basic aerodynamic characteristics. Stall tests were conducted as deliberate maneuvers from straight, wings-level flight, and no turbulence effects were introduced. However, in the interpretation of the airplane responses, the pilots would, of course, consider realistic operating conditions.

GENERAL NATURE OF THE PROBLEM

A great many aerodynamic and operational elements define the deep-stall problem. Some of the important elements other than the pitching-moment curve are itemized in table II.

TABLE II.- ELEMENTS OF DEEP-STALL PROBLEM

1. Depth of angle-of-attack penetration
   (a) Higher drag
   (b) Limited control power
   (c) Unsatisfactory lateral-directional characteristics
   (d) Delay in recovery control application

2. Steep flight-path angles
   (a) Large altitude losses
   (b) Steep nose-down attitudes

3. Inadequacy of conventional instrument display
   (a) Lack of cues to identify stall entry
   (b) Misleading information for timing recovery pull-out

The interrelationships among the various elements are complex; some represent causes, some effects, and some act as both the effect of one element and the cause of another.

Consider first the depth of angle-of-attack penetration; it has been found that, with initial entry into the stall, the drag increases and the lift decreases, and these effects together cause the airplane to descend. This angle of descent contributes a further increase in angle of attack which further accelerates the pitch-up. This effect is illustrated in figure 2 where the flow-angle relationships before the stall and in the stall are shown.

With penetration to deep-stall angle of attack there frequently occurs a decrease in longitudinal control power, which compromises the ability of the pilot to arrest the stall penetration and delays recovery. As a result, the pilot is committed to flight at deep-stall angles of attack for a considerable time period, during which an altitude loss is suffered, and it may be necessary

to control unsatisfactory lateral-directional characteristics that occur in many airplanes at these angles of attack.

The depth of stall penetration is also sensitive to delay on the part of the pilot in initiating recovery control, and this problem will be discussed in more detail in a subsequent section.

The remaining elements of the deep-stall problem listed in table II are discussed with the aid of figure 3, which shows two typical deep-stall time histories that were obtained during operations on the Langley simulator. The dashed curves were recorded during the initial experience of a pilot with the deep-stall pitching-moment and control effectiveness characteristics. The solid curves were recorded after the pilot had obtained some familiarity with the problem.

On the first try, as the airplane pitched up, the pilot failed to do more than return the elevator to zero deflection. The nose dropped to a horizontal attitude, and the pilot awaited recovery. Recovery seemed to be progressing satisfactorily because the airspeed started to increase. The angle of attack, however, continued to increase to 50° and thereafter stabilized at about 45°. As a result, when the control was pulled back to resume level flight, it served only to maintain the stall.

With practice and understanding of the problem, the pilot applied full nose-down corrective control to initiate recovery, with little effect on the initial attitude changes. This time, however, the pilot held full control, despite the misleading attitude and airspeed indications, and finally recovery was completed.

Note the large altitude losses and the steep nose-down attitudes that were indicated in figure 3 to be required for recovery. Attention has also already been directed to the misleading information that led to a premature pull-out attempt. In the particular case illustrated, the attitude changes at stall entry were large enough to give a strong indication of stall entry. In many cases the attitude change is much smaller, and the cue is correspondingly weaker. In fact, in some cases studied in the Ames investigations, where only minimal pitch-up instabilities existed on the pitching-moment curves, the lack of any warning cue resulted in the airplane drifting into a deep stall unobtrusively because of only the drag increase.

EFFECTS OF MARGINAL RECOVERY CONTROL

One of the most disturbing aspects of the deep stall is the length of time for which the pilot is committed to the stalled region once the stall has been entered. As already discussed a number of different factors contribute to delay in recovery, but one of the most obvious is the fact that, even with full nose-down control, the pitching-moment curve approaches a balance point at deep-stall angles of attack, leaving little pitching-moment margin for recovery. This effect is illustrated in figure 4 where, at $\alpha \approx 35°$, a minimal

margin of pitching-moment increment is available for recovery. It will be noted in figure 4 that, if the curve for full-forward stick crosses into the region of positive values of C_m, it would be possible for the airplane to become "locked" into the stall so that elevator alone cannot effect recovery. Less extreme cases might still represent serious recovery problems. In order to define what degree of controllability is required, studies were conducted in both the Langley and Flight Research Center simulations. The results are indicated in figures 5 and 6.

Figure 5 shows some of the variations in the pitching-moment curves that were examined in the Flight Research Center studies. These range from curves for which full-forward stick would be inadequate for recovery if the angle of attack reached approximately 45° to those for which positive control margin were available. Figure 6 shows the results in terms of two parameters, the maximum angle of attack developed and the altitude lost. For different control margins these parameters are plotted against another important variable, time delay in initiating recovery. In the case of curve A, recovery can be accomplished by prompt control application but a complete lock-in would occur for a 4-second time delay. For curves B and C, progressively larger stall penetrations and altitude losses with increasing delay in applying recovery control are evident, but, interestingly, for the data shown there does not seem to be much effect of differences in control margin available. It appears to be important only that some margin be available.

These specific results were obtained in analog computer studies conducted at the Flight Research Center. The importance of the second variable, time delay in initiation of recovery, was also repeatedly emphasized by pilots who participated in the studies at Langley and Ames, and these reactions stress the requirement for adequate cues to identify the stall onset.

STALL PREVENTION BY STABILITY INCREASE PRECEDING PITCH-UP

In operational service it is, of course, basically undesirable to have the capability of penetrating into a pitch-up that would lead to a deep stall, even if positive recovery control were provided. This problem is widely recognized, and attention is being directed to the development of safeguards against such penetrations. One such safeguard would be the existence of a sharp increase in static longitudinal stability immediately preceding the pitch-up, and studies were conducted at Ames to obtain some indication of the stability increase that would have to be provided.

The first part of the study involved piloted operation for the conditions represented by the three curves shown in figure 7.

The indications from the tests were that the increase in stability represented by the "bump" in curve (b) did not, of itself, provide a positive enough indication or warning of the impending pitch-up. It appeared to be partly a question of the magnitude of the slope change that occurs in approaching the bump from lower angles of attack, and partly a question of how deep the bump

was in terms of the amount of control required to pull up through the stable slope. The condition represented by curve (c) was considered to provide the minimum amount of warning that would assure no penetration of the pitch-up region; with the control effectiveness and control-force gradient provided, this curve required a stick movement from 40 to 80 percent of the full aft control and a control-force change from 20 to 40 pounds to pass the peak of the bump. One interesting inference of these results was that complete protection against stall entry may not depend entirely on limiting elevator authority.

This class of stable bump was also examined for its ability to protect against inadvertent deep-stall penetrations due to atmospheric turbulence. As a part of the analog computer study conducted at the Flight Research Center, the airplane was balanced at the angle of attack corresponding to the knee of the pitching-moment curve (see insert, fig. 8) and then was exposed to turbulence as represented by a vertical-velocity variation measured in flight. This test was repeated for different levels of turbulence amplitudes and different shapes of the stable bump, with the results shown in the main part of figure 8. The ordinate of the main part of figure 8 is an empirical parameter $(\Delta C_m) \times (\Delta\alpha)$ that roughly measures the magnitude of the stable bump. (The increments ΔC_m and $\Delta\alpha$ are identified in the insert in fig. 8.) For a given turbulence level, the larger values of this parameter should provide more protection against angle-of-attack reactions that exceed the stable range of pitching moments. And, of course, with only small values of the parameters the protection is less, and there is more likelihood of the critical angle of attack being exceeded to project the airplane into the unstable pitch-up range. The boundary curve then represents the minimum bump size that will prevent pitch-up into the stall. It is of interest to note that in the analog-computer studies, the critical part of the turbulence time history that triggered pitch-ups (of which only a small section is shown) was the sustained updraft that occurred at the region noted. For the particular curve that had been identified from the earlier piloted tests as providing adequate protection, the corresponding limiting turbulence amplitude would be about 25 percent of the full-scale turbulence.

FLIGHT-TEST PHILOSOPHY

The simulator studies reported here have provided considerable insight into the nature of the deep-stall problem but have not provided a schedule for rating acceptability of a given set of characteristics. On the contrary, it appears that unless an airplane happens to have unusually mild lateral-directional and longitudinal problems in the stall, measures are likely to be required to limit prolonged penetration or exploration of the stall. However, as noted earlier a certain amount of deliberate stall penetration must be assumed in development and training, in order to establish and demonstrate safeguards for operation. To accommodate to this situation some philosophy of operation is necessary, and figure 9 illustrates such a philosophy.

The important innovation of this suggested philosophy is that it provide a positive cue to impending stall, in addition to (and removed from) the usual

stall warning. The locations of the stall warning and positive cue with respect to the angle of attack of deep-stall entry are indicated in the top part of figure 9, with the pitching-moment curve defining the angle-of-attack scale.

Two kinds of airplane operation are of concern, as noted in figure 9. One is standard operational service. For the pilot in this case the stall warning must be demonstrated in training, but positive protection should be provided against deliberate or inadvertent deep-stall entries or penetration. The other kind of operation is test flying for development or certification where the test pilot may explore the deep-stall region.

The stall warnings suggested would be of the same kind for either type of operation - buffeting, perhaps, as a natural form, or a stick shaker as an artificial form. As a positive cue to preclude further angle-of-attack increase, a strong increase in longitudinal stability would be desirable for either operational service or developmental testing. Lacking a natural cue, an artificial positive cue of the nature of a stick pusher is proposed for operational service. For test flying, the artificial cue could be in the form of an angle-of-attack indicator, so that exploration at higher angles of attack was possible, but under conditions that kept the pilot clearly informed of the status of the stall. Finally, it is fairly obvious that in flight investigations of the deep stall, provision should be made for artificial recovery augmentation if there is any question about the effectiveness of natural methods for recovery.

It should be noted that in the foregoing discussion, the various devices indicated as safeguards are identified as typical and are designated only for illustrative purposes. Other methods or devices could be used and might possibly prove superior to those discussed.

CONCLUSIONS

From the simulator studies of the deep-stall problem, the following conclusions are reached:

1. In airplanes that are identified with deep-stall pitching-moment curves, other aerodynamic and operational factors would tend to prolong the time that the airplane is committed to stalled flight. If the stall is penetrated, the pilot should be given positive cues to recognize it; he should then apply full corrective control promptly and should maintain full control despite misleading information, if the stall duration is to be effectively limited.

2. Adequate safeguards against penetration of the deep stall are needed to avoid the possible severe consequences of prolonged stalled flight. These consequences include large altitude losses, steep nose-down recovery angles, and possible unsatisfactory lateral-directional controlability. It is suggested that these safeguards include an additional positive cue between the stall warning and the actual stall.

3. Attitude and airspeed information were much less valuable than angle-of-attack information for detecting stall entry and for completing longitudinal recovery.

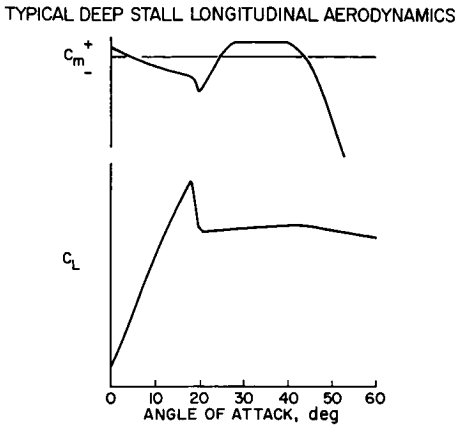

Figure 1

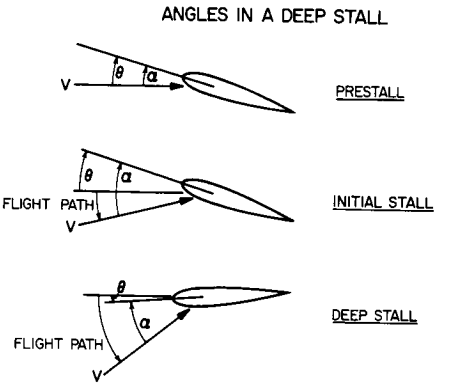

Figure 2

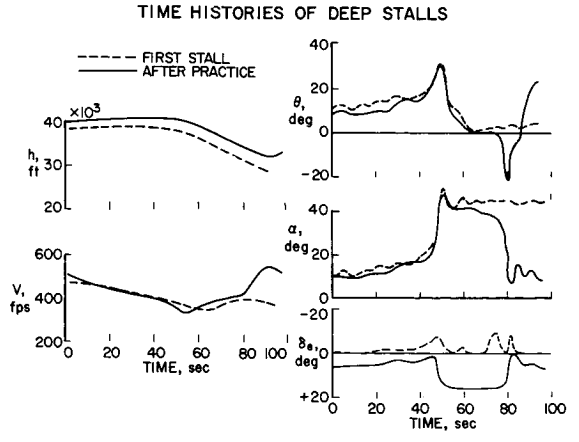

Figure 3

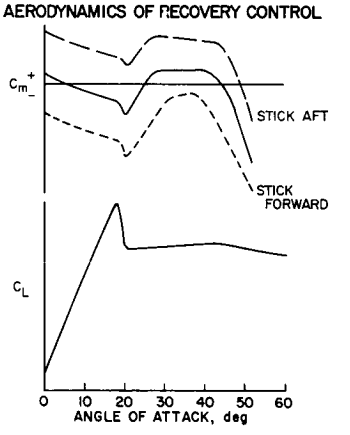

Figure 4

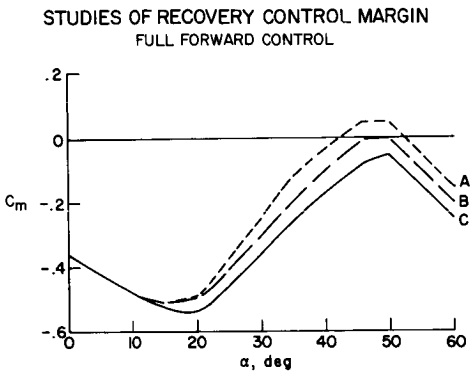

Figure 5

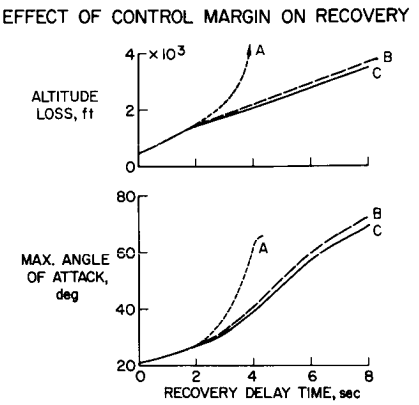

Figure 6

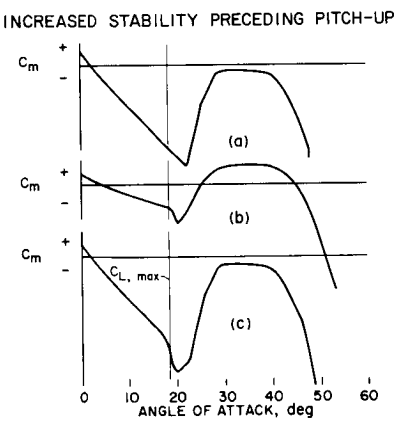

Figure 7

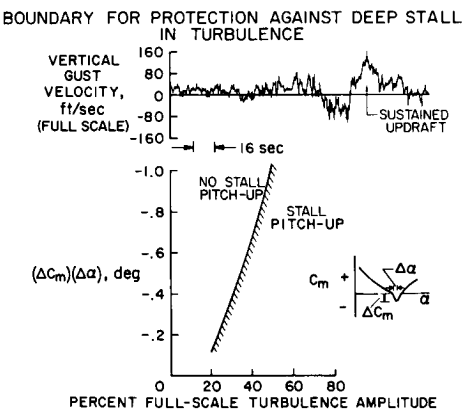

Figure 8

SUGGESTED OPERATIONAL PHILOSOPHY FOR AIRPLANES WITH DEEP-STALL TENDENCIES

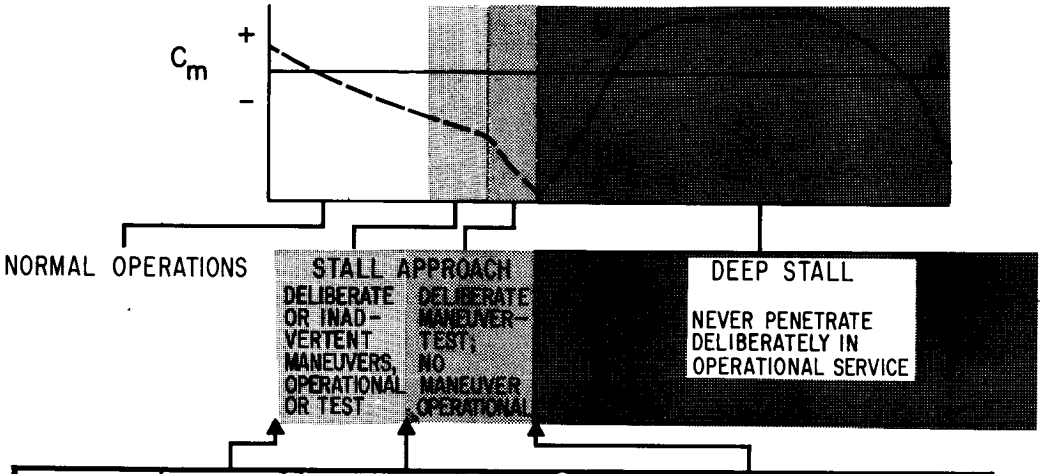

OPERATION	WARNING REQ'D (TYPICAL)	POSITIVE CUE REQ'D (TYPICAL)	RECOVERY AUGMENTOR REQUIRED (TYPICAL)
OPERATIONAL SERVICE	BUFFET	UNMISTAKABLE STABILITY INCREASE	NOT APPLICABLE
	STICK SHAKER	STICK PUSHER	
DEVELOPMENT FLIGHT TEST	BUFFET	UNMISTAKABLE STABILITY INCREASE	TAIL PARACHUTE
	STICK SHAKER	ANGLE OF ATTACK INDICATOR	

Figure 9

13. DEEP-STALL AERODYNAMIC CHARACTERISTICS OF T-TAIL AIRCRAFT

By Robert T. Taylor and Edward J. Ray

NASA Langley Research Center

SUMMARY

A wind-tunnel research program has been undertaken by the NASA to study the aerodynamic characteristics of T-tail aircraft at high angles of attack. The program was designed to show the effects on longitudinal stability and control of several configuration variables.

The results to date do not allow the formulation of general design rules, but the effects of several configuration variables have been noted to have a prime influence on the post-stall characteristics..

An increase in tail size, changes in the location of fuselage-mounted engine nacelles, and reduced fuselage-forebody lift were all found to have a beneficial effect on static longitudinal stability at high angles of attack.

INTRODUCTION

Recently, both here and abroad, several transport aircraft have appeared in service which employ a horizontal stabilizer mounted on top of the vertical fin. Many others, including executive as well as commercial transports, are in the design or certification stages. Past research on the T-tail problem has given an indication of the general design rules for providing good pitch characteristics in the angle-of-attack range prior to wing stall. At angles of attack above the stall angle, however, there is a distinct lack of data on the pitch characteristics of T-tail aircraft.

The NASA has, therefore, undertaken a wind-tunnel research program to investigate the post-stall, or high-angle-of-attack, behavior of transport-type configurations employing the T-tail. Table I shows, in general, the scope of the wind-tunnel tests. The program was designed to study the effects on longitudinal stability and control of many configuration variables, primarily at low speed. The studies have not yet progressed to the point which would allow the formulation of general design rules, but several interesting facts have come to light. It is the purpose of this paper to show the aerodynamic origin of the instabilities at high angles of attack of T-tail airplanes, and this discussion is concerned with only those items and variations which appear underlined in the table.

SYMBOLS

A	cross-sectional area
A_{BASIC}	cross-sectional area of basic configuration
b	wing span
C_L	lift coefficient
$(C_m)_{.40\bar{c}}$	pitching-moment coefficient at $0.40\bar{c}$
$\Delta C_{m,t}$	tail contribution to stability
$\bar{c}$	wing mean aerodynamic chord, in.
i_t	tail incidence, deg
Δi_t	change in tail incidence, deg
l	tail arm, in.
M	Mach number
S	wing reference area
S_t	tail surface area
z	tail height, in.
α	angle of attack, deg
α_{STALL}	stall angle of attack, deg

DISCUSSION

Basic Configuration

Figure 1 shows a line drawing of the model used in the investigation. It was typical of the current T-tail airplanes in that it had a wing with moderate sweepback and aft-mounted engine nacelles. Some pertinent model dimensions are given in terms of the wing mean aerodynamic chord $\bar{c}$ and the wing span b. The model was constructed so that the configuration changes listed in table I could be readily accomplished. In this discussion the aerodynamic characteristics of this model will be used as a standard of comparison and the model will be referred to as the basic configuration.

Effect of Horizontal-Tail Height

Figure 2 shows data for two horizontal-tail heights in terms of the pitching-moment coefficient as a function of angle of attack. The reference point for pitch data, here and throughout the paper, is 40 percent of the mean aerodynamic chord, which is a typical aft center of gravity for the current T-tail aircraft. The shaded portion of the figure below an angle of attack of 20° has received a great deal of attention in the past. The smaller shaded region between 15° and 20° denotes an angle-of-attack region for which these data are not believed to be applicable to full-scale aircraft because of the low Reynolds numbers of the tests.

Effect of Tail Incidence

At low angles of attack the low horizontal tail contributes much less to stability, because of its position in a region of high downwash behind the wing. As the angle of attack increases, however, the tail moves below the high downwash region, becomes more effective, and remains effective to high angles of attack. The high horizontal tail, on the other hand, starts in a region of low downwash at low angles of attack and thus shows greater stability. As the angle of attack approaches the stall angle, the high horizontal tail moves into the high downwash field created by the wing and its contribution to stability tends to lessen. If the tail location is high enough, this decrease in stability can be delayed until after the stall angle has been exceeded. At very high angles of attack the high horizontal tail becomes even less effective as it penetrates deeper into the airplane-wake system. The influence of high-angle-of-attack wakes on the airplane pitch-control effectiveness is shown in figure 3. Here pitching-moment coefficient is plotted as a function of angle of attack. The solid curve represents data for the basic configuration trimmed at an angle of attack of 10°. A stable trim point is evident near an angle of attack of 40°. The dashed curve represents a more positive stabilizer incidence ($\Delta i_t = 4.1^\circ$) and serves to illustrate what happens to the control effectiveness with increasing angle of attack. If the two curves are compared where the arrows are shown, it can be seen that the amount of control available from a given stabilizer or elevator angle is reduced to a small percentage of its low-lift value due to the wake system at the high angles. The implication is that the amount of control available for recovery from high-angle-of-attack penetrations is seriously limited for some configurations which use the T-tail and that the reduction of control power and stability at high angles of attack is a function of the wake system of the airplane.

Effect of Engine Nacelles

In this study of post-stall pitching problems the effect of the aft-engine-nacelle placement must be examined. Figure 4 shows the effect of removing the nacelles from the basic configuration. On the left in figure 4 are curves of pitching-moment coefficient against angle of attack for the model with the tail off (upper plot) and with the tail on (lower plot). The nacelles-on curves are solid and the nacelles-off curves are dashed. Notice that the addition of the

nacelles is stabilizing at all angles of attack with the tail off. With the T-tail on, the addition of the nacelles is destabilizing past an angle of attack of about 20°. This result suggests the presence of a wake off the nacelles which masks the T-tail and reduces its effectiveness; comparison of the tail-increment curves on the right in the figure shows this effect more directly. The tail-increment curves are simply the difference between the tail-on and tail-off curves and represent a measure of the tail contribution to stability. There is a break in the nacelles-off curve at the angle of attack at which the wing-fuselage wake crosses the T-tail. When the nacelles are added, a marked reduction is seen in the tail contribution. The inference is that at high angles of attack the T-tail has entered the nacelle wake and the tail contribution to stability is degraded to the point that the complete configuration becomes unstable at an angle of attack of about 20°. In addition to this reduction in stability, the nacelles were found to have a large effect on the control power available at the higher angles of attack. The effect of the nacelles appears in the wake system of the aircraft and can affect the tail only if the tail is mounted high on the vertical fin.

With this information in mind a series of tests was made in which the nacelles were moved to various locations on the model; results of some of these tests are shown in figure 5. The small sketches at the top of the figure show the nacelle locations. The curves again are pitching-moment coefficient as a function of angle of attack; each complete-configuration (nacelles-on) curve is solid and each nacelles-off curve, dashed. The difference between the nacelles-on and the nacelles-off curves is, in general, an indication of the size of the nacelle wake at the higher angles of attack. The solid curve on the left shows data obtained when the nacelles were moved to wing pylons, as seen in the sketch, at a spanwise location about in line with the tips of the horizontal stabilizer. A stabilizing influence is apparent prior to stall and deteriorates between angles of attack of 20° and 30°. This effect at the higher angles of attack is not fully understood at this point but is presumed to be due to the nacelle wake, shed forward and above the wing at high angles, crossing over the tips of the horizontal tail. As a means of hiding the nacelles in the aft-fuselage wake they were moved on top of the fuselage close to the vertical tail. Nacelles added in this location caused essentially no change in the pitch curve.

The other plots in figure 5 are for nacelle locations which vary only in longitudinal position; that is, the nacelle span and vertical position were unchanged and the nacelles were in a forward, a basic, and an aft location. For the nacelles in the basic location, note again the marked deterioration of the pitch curve past $\alpha = 20°$ due to the nacelles and a stable trim point at $\alpha = 40°$. With the nacelles in the forward position, not much influence is shown on pitch prior to wing stall and a destabilizing trend is shown after $\alpha = 20°$. However, the nacelle is quickly enveloped in the stalled-wing wake and near $\alpha = 40°$ the two curves merge. As the nacelle is moved aft from the basic location, notice the heavy stabilizing contribution from $\alpha = 10°$ to 20°. The nacelle contribution in this angle range is presumed to be due to its acting as a low horizontal tail. Beyond $\alpha = 20°$, however, the pitching-moment-coefficient curve deteriorates as the nacelle wake crosses the T-tail, and beyond $\alpha = 40°$ the pitch increment due to the nacelles is even

worse than for the basic configuration. It appears that aft movement of the basic nacelle improves the pitching-moment coefficient at low angles of attack and tends to shed a worse wake at very high angles of attack. Moving the nacelle forward does not appear to have much effect on the data for low angles of attack and improves the pitch curve at very high angles of attack. It should be remembered that no fixed set of criteria exist which will allow the designer to choose, on the basis of these tests, the best location for engine nacelles when the T-tail is employed; the data shown are only indicative of some effects which need further exploration. (Wind-tunnel testing at high angles of attack is the only safe way of developing the required stability and control data.)

Effect of Horizontal-Tail Size

If the foregoing discussion of nacelle effects may be interpreted as showing the influence of the nacelle-wake size on a fixed size of the horizontal tail, the effect of increasing the size of the T-tail with relation to the basic nacelle wake should be shown. Figure 6 illustrates the effect of increased tail size on the pitching-moment coefficient as a function of angle of attack. On the left in figure 6 data are repeated for the basic configuration with the horizontal-tail area of 22 percent of the wing area. The plot on the right in the figure is for the model with the tail size increased to 30 percent of the wing area and the tail span, to 40 percent of the wing span. The solid curves are for both models trimmed at an angle of attack of 10°. The addition of the larger tail has increased the stability at low angles of attack and has eliminated the stable trim point at $\alpha = 40^{\circ}$ noted previously for the basic configuration. The dashed curve is added, for a fixed incremental incidence of 4.1°, to illustrate the degradation in control effectiveness with increasing angle of attack. Comparing the arrows again shows that increasing tail size has produced a small increase in control power at low angles of attack; at high angles of attack the control power is still reduced to a small percentage of its low-lift value. Whether or not curves such as these are what would be termed acceptable is a subject for further simulator studies.

Effect of Fuselage Size

The effect of the fuselage-forebody length and size was also studied during the wind-tunnel program. It has been learned from experience and wind-tunnel tests in the past that the effect of increasing the fuselage-forebody volume will, in general, decrease the stability. The point in question concerning the T-tail layout has been the influence of the fuselage wake at the T-tail location. Figure 7 shows a line drawing of the basic model and of a version with a small fuselage. The smaller fuselage differed in depth as well as in width and had a cross section which, although similar in shape, was only 55 percent as large as that of the basic body. All other dimensions for the two models were identical. Figure 8 shows the effects of fuselage cross-sectional size. Here again are plotted the pitching-moment coefficients for the model with tail off, tail on, and a tail increment, each as a function of the angle of attack. Note that the smaller fuselage, represented by the solid

curve, is more stable with the tail off as well as with the tail on. Note further that the tail-increment curves are nearly the same regardless of fuselage size. The reduction of tail contribution at the higher angles of attack is again due to nacelles. Based on the same reasoning as was used previously, since the tail increment remains relatively constant the fuselage size can be said to have little or no influence at the tail plane. The benefits in pitching moment are primarily due to decreased lift on the fuselage forebody which in turn is due to decreased cross-sectional size. Fuselage-forebody length has an effect similar to the cross-sectional-size effect shown in this figure - that is, increases in the fuselage-forebody length tend to destabilize the moment curves - and this effect occurs regardless of the location of the horizontal tails.

Effect of Mach Number

The data presented thus far were obtained at a Mach number of 0.21. Figure 9 shows some results of tests at higher Mach numbers made in the Langley transonic dynamics tunnel. Results are shown as lift and pitching-moment coefficients as a function of angle of attack for the basic configuration. It is obvious from the pitching-moment-coefficient curve that the high-angle-of-attack nonlinearities have not disappeared as a result of increased speed; in fact, they may be somewhat more severe. The lift coefficient shows the characteristic depression in initial stall angle and the associated initial maximum C_L. At the higher angles of attack, however, an increase of 15 percent in the post-stall maximum lift is noted from a Mach number of 0.21 to 0.86.

CONCLUSION

An increase in horizontal-tail size, changes in the location of the fuselage-mounted engine nacelles, and reduced fuselage-forebody lift were all found to have a beneficial effect on static longitudinal stability at high angles of attack.

TABLE I

SCOPE OF THE WIND-TUNNEL RESEARCH PROGRAM

• ITEM	• VARIATIONS
HORIZONTAL TAIL	SIZE, VERTICAL POSITION, PLANFORM, AND INCIDENCE
NACELLE	SIZE AND LOCATION
WING	SECTION, STALL CONTROL DEVICES, FLAPS, ASPECT RATIO, AND SWEEP
FUSELAGE	CROSS-SECTION SIZE, CROSS-SECTION SHAPE, FOREBODY LENGTH
MACH NUMBER	0.21 TO 0.90
REYNOLDS NUMBER	0.78×10^6 TO 1.8×10^6

GENERAL ARRANGEMENT OF BASIC CONFIGURATION

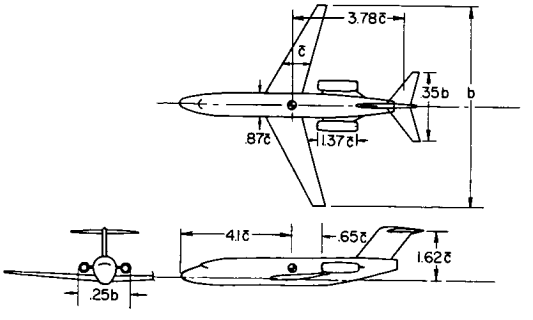

Figure 1

EFFECT OF HORIZONTAL-TAIL HEIGHT
$i_t = 0$; $l/\bar{c} = 3.78$; $M = 0.21$

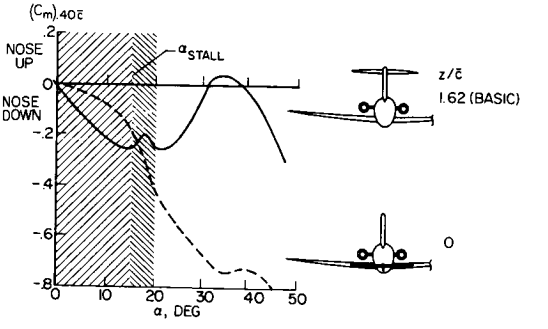

Figure 2

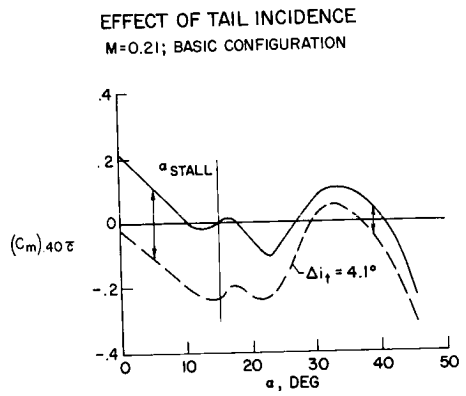

Figure 3

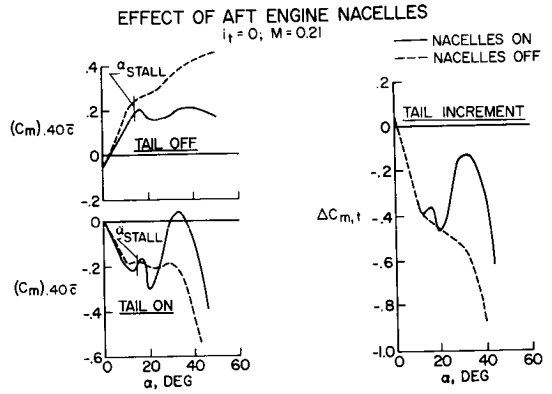

Figure 4

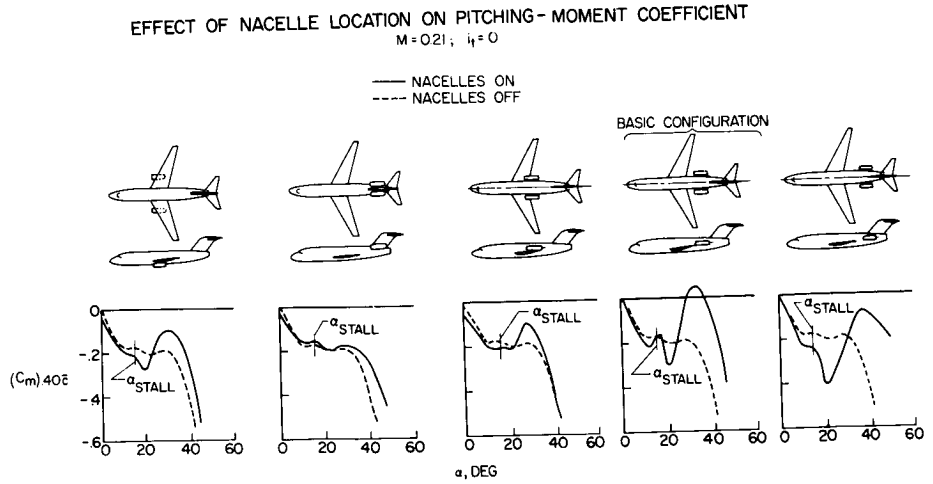

Figure 5

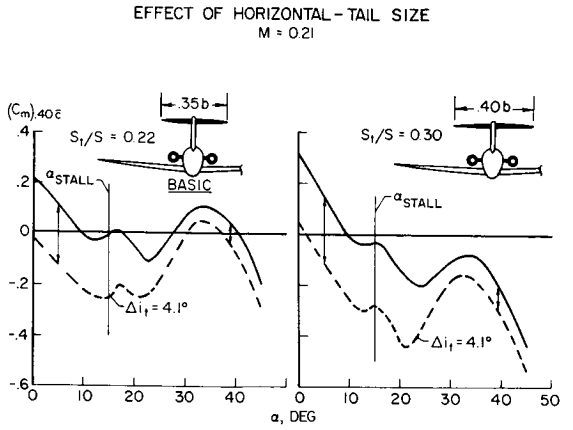

Figure 6

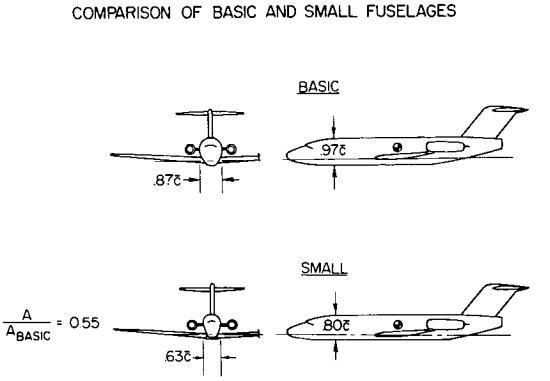

Figure 7

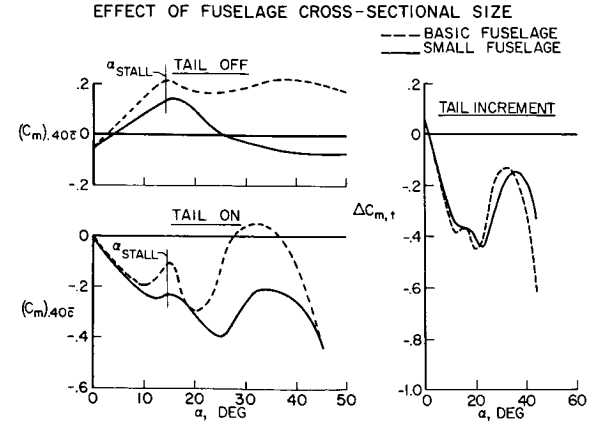

Figure 8

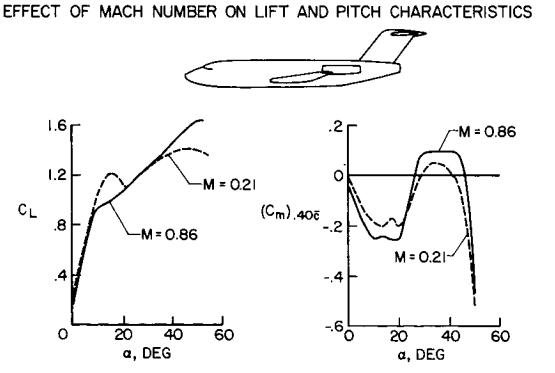

Figure 9

14. FLIGHT TESTS RELATED TO JET-TRANSPORT UPSET AND TURBULENT-AIR PENETRATION

By William H. Andrews, Stanley P. Butchart,
Thomas R. Sisk, and Donald L. Hughes

NASA Flight Research Center

SUMMARY

A flight program, utilizing a Convair 880 and a Boeing 720 airplane, was conducted in conjunction with wind-tunnel and simulator programs to study problems related to jet-transport upsets and operation in a turbulent environment. During the handling-qualities portion of the program the basic static stability of the airplanes was considered to be satisfactory and the lateral-directional damping was considered to be marginal without damper augmentation. An evaluation of the longitudinal control system indicated that this system can become marginal in effectiveness in the high Mach number and high dynamic-pressure range of the flight envelope. From the upset and recovery phase of the program it was apparent that retrimming the stabilizer and spoiler deployment were valuable tools in effecting a positive recovery; however, if these devices are to be used safely, it appears that a suitable g-meter should be provided in the cockpit because the high control forces in recovery tend to reduce the pilot's sensitivity to the actual acceleration loads. During the turbulence penetrations the pilot noted that the measured vibrations of 4 to 6 cps in the cockpit considerably disrupted their normal scan pattern and suggested that an improvement should be made in the seat cushion and restraint system. Also it was observed that the indicator needles on the flight instruments were quite stable in the turbulent environment.

INTRODUCTION

Within the past few years, the turbine-powered jet-transport airplanes have experienced a series of incidents which, in the majority of cases, have been associated with the penetration of a region of turbulent air. The reports of the flight crews, as well as the analysis of data derived from onboard crash recorders, have been consistent in that the airplanes were initially disturbed from stabilized flight to the extent that a period of uncontrolled flight developed and in several cases the airplanes involved did not recover stability.

To study this problem, the Flight Research Center of the National Aeronautics and Space Administration has initiated a flight-test program, in conjunction with simulator and wind-tunnel studies conducted by other NASA Research Centers on this subject. The prime objectives of the flight program were to document the airplane handling characteristics in support of ground-based simulator studies and to document the airplane characteristics and

operational experience during controlled upset maneuvers and flight in a turbulent environment.

A major portion of the data was derived from flights within the normal operational boundaries and illustrates some of the salient features related to the longitudinal control system, longitudinal upset, and lateral-directional dynamics in turbulence of these airplane types. It is recognized that these characteristics may be common knowledge to the majority of those who have a working relationship with this class of airplane. However, it is believed that, in consequence of the series of incidents which have occurred, a reemphasis of these inherent characteristics, particularly to the operational pilots, is appropriate.

TEST AIRPLANES

The airplanes used in the investigation were a Convair 880 and a Boeing 720 which were provided by the Federal Aviation Agency Facility at Oklahoma City, Oklahoma. Both airplanes incorporated standard airline equipment and were considered to be representative airplanes in the turbine-powered jet-transport class.

The only deviation from the standard configuration was that related to the longitudinal control system in the Boeing 720 during the early portion of the program. At the conclusion of the basic handling-qualities evaluation of this airplane, several features became apparent which indicated that the longitudinal control system was not responding as predicted by the manufacturer. Initially, it was not possible for the pilot to stall the stabilizer jack screw motor in moving the stabilizer in or out of the trim position except in the airplane nose-up direction at high dynamic pressure (Mach number, 0.75 at 15000 feet). Furthermore, the data indicated that the predicted maximum elevator deflection was not being obtained during tests which were performed to establish the maximum elevator available with a critically "mistrimmed" stabilizer (that is, stabilizer at a position other than trim). A detailed inspection of the cove gaps related to the aerodynamic balance system (shown in fig. 1) indicated that some of the balance-panel seals had been improperly installed. At the completion of the inspection, it was determined that 5 of the 10 balance panels shown in figure 2 were outside of the specified tolerance limits of the cove-gap spacing by as much as 0.28 inch at certain elevator settings. (TEU signifies trailing edge up.) As a result of this condition, flight tests were repeated after the system was reworked to the specified tolerances and some of the comparative flight results are presented in the discussion to follow. It should be stated that although there was a measurable change in the longitudinal wheel-force characteristics, the system modification did not reveal an apparent change in the stall characteristics of the stabilizer jack screw motor and, as will be shown, the maximum elevator conditions were only slightly improved.

INSTRUMENTATION

The Convair 880 instrumentation was limited to provide those measurements necessary to document responses of the airplane, the flight instruments, and the pilot in turbulence. The instrumentation consisted of two cameras mounted in the cockpit and at the center of gravity to record the respective pilot, flight-instrument, and wing response to turbulence. Also included were a standard NASA airspeed-altitude recorder, three-component linear accelerometers at the pilot, center-of-gravity, and tail positions, and angular velocity recorders and accelerometers at the center of gravity.

The instrumentation included in the Boeing 720 airplane was consistent with that required for a complete handling-qualities investigation. The measured quantities consisted of the following:

Airspeed/altitude
Three-component linear accelerations (pilot, center of gravity, and tail position)
Angular displacement (pitch and roll)
Angular velocity and accelerations (pitch, roll, and yaw)
Control forces (longitudinal, lateral, and directional)
Control positions (longitudinal, lateral, and directional)
Cockpit and wing cameras (similar to those used in the Convair 880)

Recording accuracies were consistent with standard NASA instrumentation.

TEST PROGRAM

The flight program was divided into two phases. In the initial phase, a Convair 880 airplane was flown for a total of 15 hours to record the pilot and cockpit flight-instrument response and the associated accelerations along the fuselage during the penetration of thunderstorm turbulence.

The second phase of the program consisted of flying a Boeing 720 airplane for a total of 40 hours, during which time the basic handling qualities were recorded for standard flight-test maneuvers, for conditions of controlled upsets, and for flights into regions of turbulence. Most of the data presented herein was derived from this program. Figure 3 presents the variation of altitude with Mach number covered during this program. Data were obtained from Mach numbers of 0.25 to 0.79 at 15000 feet, from Mach numbers of 0.53 to 0.91 at 35000 feet, and at a Mach number of 0.75 at 42000 feet. During the controlled upset maneuvers, the high-speed boundary was penetrated only slightly during the recovery portion of the maneuver. A limited amount of data was acquired at 18000 feet for comparison with available manufacturers' information and for an evaluation of the effects of the stabilizer jack screw stall characteristics. The weight of the airplane ranged from 190,000 to 140,000 pounds and the center of gravity varied from 16 to 29 percent of the mean aerodynamic chord.

As the investigation of several of the turbulence-associated accidents indicated that the stabilizer may have been in the setting for airplane full nose down at impact, a significant part of the program was devoted to investigating the longitudinal control characteristics with this trim setting and the pilot's ability to recover from a longitudinal upset through elevator alone, stabilizer retrimming, and manipulation of the spoilers.

DISCUSSION

Consideration of the basic airplane characteristics and the comments which have been obtained from various pilot reports of upset, turbulence penetration, and the associated recoveries indicates a lack of appreciation of the longitudinal-control-system limitations, particularly in unfamiliar regions of the flight envelope. Consequently, the next series of figures are shown to illustrate the various aspects of the system operation and potential limitations, particularly in the high Mach number and high dynamic pressure range.

Longitudinal Maneuvering Data

Figure 4 presents a typical variation of the stick force and elevator position for longitudinal control as a function of normal acceleration at an altitude of 34500 feet and a Mach number of 0.84. The data illustrated by the open symbols were obtained with the previously mentioned out-of-tolerance cove gaps on the elevator-balance panels, and the solid symbols present the stick-force variation indicative of the reduction of force that was obtained when the clearances were brought within the specified tolerances. The maximum apparent force reduction was between 18 and 20 pounds for this flight condition and ranged to as high as 40 pounds in other conditions tested.

The general trend of the data covering the acceleration range between 0.1g and 2.25g shows that at the extreme levels of acceleration, the stick-force gradient is considerably reduced and the variation of elevator position appears to be unfavorable and nonlinear.

These nonlinear characteristics are more pronounced at the higher altitude and Mach numbers where cruise flight is normally performed. It is realized that these characteristics are not unusual for a control system of this type. However, the inherent characteristics do present problems to the pilot, particularly when he is subjected to extreme levels of acceleration in either smooth or turbulent air conditions.

Longitudinal Control Effectiveness

Another feature of this longitudinal control system is that related to the loss of control effectiveness of the tab-actuated elevator in the transonic speed range. Figure 5 presents the control tab-elevator relationship at an indicated Mach number M_i of 0.54 and 0.84 at an altitude of 35000 feet.

From the data at $M_i = 0.54$, it may be seen that the variation of the elevator tab with elevator deflection is essentially linear and the ratio is approximately 1 to 1 for the trailing-edge-up (TEU) elevator positions. At the conditions shown for the higher Mach number of 0.84 the tab-to-elevator ratio is still about 1 to 1 between elevator deflections of about 5.0° TEU and 8° TED (trailing edge down). However, beyond these limits it may be observed that this tab-to-elevator ratio is reduced by about one-half. This loss in control-tab effectiveness may be associated with a shock stall, which may occur on the control-tab—elevator combination as the tab deflection is increased and the local flow becomes supersonic. It is appreciated that this explanation is not new; however, when the overspeed boundary is inadvertently penetrated, it is believed that the pilots operating the aircraft, in many cases, do not have a full appreciation of this influence.

Elevator Available for Recovery

In conjunction with the loss in control effectiveness at the high speed, another item of interest is that related to the maximum elevator available for recovery from an upset with a mistrimmed stabilizer. Figure 6 presents the maximum elevator deflection attained during the flight test over the predicted Mach number range of 0.62 to 0.89 at an altitude of 35000 feet. The estimated boundary curve shown represents the maximum elevator deflection that should be attained with a maximum deflection of the elevator tab. The flight-test data represented by the open and solid symbols show the actual elevator deflection that was obtained with the stabilizer trimmed in the full airplane-nose-down (A.N.D.) position of 3.5° and with the pilot applying a maximum pull force as the airplane decelerated from $M_i = 0.89$ to $M_i = 0.62$.

The open and solid symbols represent the results before and after the elevator-balance-panel cove gaps were corrected to the specified tolerances. Initially, it may be seen that the out-of-tolerance cove gap cost about 2.0° to 2.5° in elevator deflection over the speed range. Furthermore, the solid symbols indicate that under the specified trim conditions at $M_i = 0.89$ approximately 8.5° of elevator deflection are available for trim maneuvering. As the speed is reduced to $M_i = 0.76$ the elevator available increases to approximately 10.5°. A major portion of the test data represented by the solid symbols was obtained with both pilots pulling on their respective control wheels.

The apparent deviation between the estimated and the maximum elevator attained during the flight tests represents a reduction in longitudinal recovery control available for the airplane used in this test. From consideration of the fact that the maximum recovery capability of the airplane is dependent upon the elevator deflection per g relationship and the elevator available, a limitation in the elevator available becomes of primary concern. The significance of this relationship is further illustrated in the discussion of the controlled upset maneuvers.

Recovery by Elevator and Stabilizer

At the completion of the basic handling-qualities evaluation of the airplane, a series of controlled upset maneuvers were performed at the test altitudes of 15000 and 35000 feet. The method employed to upset the airplane was either to push over to the overspeed warning or to execute a stabilizer "runaway" in either the full-nose-down or the nose-up direction. At the overspeed warning, the throttle was reduced to idle and the recovery was initiated.

Figure 7 presents a stabilizer runaway performed at 35000 feet at an initial Mach number of 0.78. At time 1 second, the stabilizer was activated in the full-nose-down direction and at 6 seconds, was driven to 3.5° airplane nose down. In this period of 5 seconds the airplane went from level flight to approximately -0.2g. At the time 10.7 seconds the throttle was reduced to idle and at 12 seconds the pilot initiated recovery through the elevator. At time 18 seconds the full elevator available had been applied and a maximum of 1.3g was attained. At the time of 20 seconds the stabilizer was activated toward the trim position and as the normal acceleration increased the elevator input was reduced until a time of 26 seconds, when the full recovery had been effected and the airplane had reached an acceleration of 2.3g. The elevator and acceleration traces between the increment of time of 18 and 20 seconds indicate a loss in elevator effectiveness. The elevator remains essentially constant in this region while the acceleration decreases from approximately 1.3g to 1.0g. Also, at the time 18 seconds it is not apparent that the airplane rate of descent is at all reduced. However, after the stabilizer is returned to the trim position, the acceleration increases, the rate of descent is reduced, and the airplane returns to a level-flight condition.

Elevator-Stabilizer Trade

For the purpose of illustrating the horizontal-stabilizer power and the effects of a mistrimmed stabilizer, figure 8 presents a summary of the trades in elevator and stabilizer for 1 g flight at altitudes of 15000 and 35000 feet. The ratio of the elevator deflection to stabilizer deflection and of the stick force to stabilizer deflection are presented over the Mach number range from 0.38 to about 0.85. The ratio of elevator angle to stabilizer angle indicates that approximately 2° to 2.5° of elevator are required for every degree of mistrimmed stabilizer over the speed range tested. The corresponding stick forces required to maintain level flight vary from approximately 15 to 35 pounds per degree at 35000 feet and 18 to 70 pounds per degree at 15000 feet. From these data it is apparent that the available elevator for maneuvering is considerably reduced. Also the increased workload associated with the high stick forces tends to reduce the pilot's sensitivity to the actual accelerations experienced in maneuvering.

In general, pilots have been taught to minimize stabilizer manipulation while maneuvering. As shown in the previous time history, once the airplane has been upset with a corresponding change in stabilizer setting and a recovery is initiated, the retrimming of the stabilizer can be a valuable tool in effecting a positive recovery. However, to use the stabilizer intelligently

under these circumstances, the pilot needs some acceleration reference through a suitable g-meter to prevent overstressing the airplane.

Recovery by Elevator and Spoiler

Figure 9 presents a stabilizer runaway where the initial recovery is effected through the elevator control and the final recovery is accomplished through the deflection of the spoiler system. The general operational procedures used in performing the upset were the same as those employed in the previous maneuvers. As noted on the previous upset time history, there is a loss of elevator effectiveness showing up between time 15 and 19.5 seconds. In this region the elevator remains fixed at approximately 8° while the acceleration decreases from 1.5g to 1.1g. Also it may be observed, through the airspeed and altitude traces, that the rate of descent has not been checked until after the spoilers have reached their maximum deflection of about 30°. In this maneuver the spoiler handle was moved to the full spoiler position of 60°. Regardless of the fact that only 30° of spoiler deflection were obtained, because of the blowdown effect at high speed, this much spoiler, in conjunction with the elevator, allowed complete recovery of the airplane to a level-flight condition while the stabilizer remained in the full nose-down setting.

In similar maneuvers performed with the stabilizer in the trim setting, there was no problem in recovery with the elevator alone. However, in the upsets that were performed with the mistrimmed stabilizer, it is obvious that supplemental recovery control is required if additional elevator deflection cannot be provided.

Dynamic Lateral-Directional Stability

During the evaluation of the basic handling qualities, the dynamic, lateral-directional stability characteristics were measured in smooth air in order that the influence of the Dutch roll mode could be more intelligently assessed in the flights where turbulence was penetrated. Figure 10 presents a summary of the dynamic lateral-directional characteristics measured in terms of the reciprocal of the time to damp to half amplitude over the speed range at an altitude of 35000 feet. Results are shown for conditions both with the damper on and off.

The general observation in the comparison of these damping characteristics is that the damping without augmentation is quite low and the engagement of the yaw damper considerably improves the Dutch roll damping. On the basis of these data and experience acquired in the turbulence flights, it was apparent that the low level of Dutch roll damping increases the pilot workload when the airplane is upset or disturbed by gusts or turbulence, particularly with the yaw damper inoperative. Also, as has been shown in reference 1, the utilization of the yaw damper in turbulence, in general, relieves the tail loads by about 50 percent. Consequently, it is believed that the yaw damper should be considered an essential operational system on all transport airplanes of this type.

Turbulent-Air Penetrations

During the turbulent-air portion of the Boeing 720 program, an attempt was made to penetrate either wave turbulence generated by terrain or high-altitude clear-air turbulence. The initial conditions investigated were at the high altitude during cruising flight. However, very little or no turbulence was experienced at the levels between 33000 and 39000 feet. On the other hand, in the region of Denver and Colorado Springs, mountain-wave turbulence, which was classified by the pilots to be light to moderate, was encountered at 22000 feet. The technique employed in penetrating the turbulent air was to stabilize at an initial indicated airspeed of 350 knots and, once the turbulence was encountered, to reduce the power and attempt to maintain a constant attitude and an airspeed of 300 knots.

Figure 11 presents a 5-second portion of the time histories acquired during three of these tests. The first test was made with the autopilot and yaw damper on, the second was with the autopilot off and the yaw damper on, and the final test was made with both the autopilot and yaw damper off. The respective normal accelerations show that the peak value ranges from 0.3 to 2.3g at the pilot's station, 0.3 to 2.0g at the center of gravity and 0.1 to 2.6g at the tail. These peak accelerations are of a magnitude similar to those measured from flight recorders of airplanes involved in turbulence incidents; however, the persistence experienced in the illustrated tests was not as long. In addition to the acceleration, it may be seen that there is an apparent oscillation measured at the pilot's station of approximately 4 to 6 cps. This superimposed motion was noted by the pilots to be quite disconcerting and disrupted their normal scan pattern. These studies indicate the need for improvements in the seat cushion and restraint system to reduce these motions.

The effects of the yaw damper and autopilot may be observed through motion of the pitch, roll, and yawing velocity traces. The progressive decay in Dutch roll damping is apparent as each of the systems is turned off and with both the yaw damper and autopilot off, the Dutch roll, previously discussed, becomes quite pronounced even though the general level of accelerations is considerably reduced.

Convair 880 Turbulence Penetration

In the Convair 880 test program a series of turbulence flights were accomplished at an altitude of about 29000 feet and the penetration was into a thunderstorm. The flights made through this region of turbulence were made with the autopilot off and the yaw damper on and off. The pilot's task was essentially the same as that required on the Boeing 720 airplane. The overall magnitude of turbulence was not much greater than that experienced with the Boeing 720; however, because of the persistence of the disturbance, the pilots at times classified the turbulence as moderate to severe. The transverse acceleration experienced during these flights was in the range from ±0.5g and was considerably greater than that evidenced in the Boeing 720 airplane. This result, however, could be due to the nature of the turbulence that the airplane was flown through.

CONCLUDING REMARKS

With regard to the basic airplane characteristics, the analysis of the overall static stability characteristics of the airplanes tested appears to be satisfactory and acceptable to the pilots. Considering the inherent characteristics of the longitudinal-control system design and the flight envelope where the airplanes are being operated, the system can become marginal in the high Mach number and high dynamic-pressure range. The operational pilot should be thoroughly acquainted, either through simulator or in-flight demonstration, with the effectiveness of the longitudinal control system under adverse flight conditions beyond the normal operational boundary. Regarding the lateral-directional dynamics, the data obtained during the test program serve to reemphasize the low damping of these airplanes, particularly without the operation of the yaw damper system; and the system should be considered, if it is not currently the practice, to be an operational item.

In the upset and recovery category, it is believed that the stabilizer or spoiler system can be effectively employed to assist the pilot in recovering from an upset attitude in the longitudinal mode. However, the increased pilot workload associated with the high control forces tends to reduce the pilots' sensitivity to the increased accelerations during recovery. Consequently, it is believed that a suitable g-meter should be provided in order that all systems available, such as the stabilizer and spoilers, can be safely employed without overstressing the airplane.

From the turbulence data acquired during the test program it was observed that the pilot is subjected to frequency ranges around 4 to 6 cps. Also it appeared that an improvement in the seat cushion and restraint system may be essential to reduce the shaking of the pilot and firmly anchor him in his seat. In this regard, it is believed that the pilot motion in the seat is obviously the main contributor to the fact that his scan pattern is considerably disrupted. Finally an observation of the camera data, which were obtained in the cockpit, indicates that the flight instruments and panel are relatively steady and there is no apparent shaking of the indicator needles.

REFERENCE

1. Funk, Jack; and Cooney, T. V.: Some Effects of Yaw Damping on Airplane Motions and Vertical-Tail Loads in Turbulent Air. NASA MEMO 2-17-59L, 1959.

CROSS SECTION OF ELEVATOR BALANCE SYSTEM

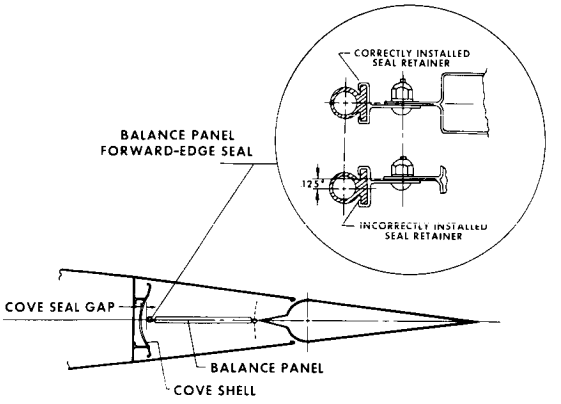

Figure 1

RESULTANT TOLERANCES FROM MISRIGGED ELEVATOR BALANCE PANELS

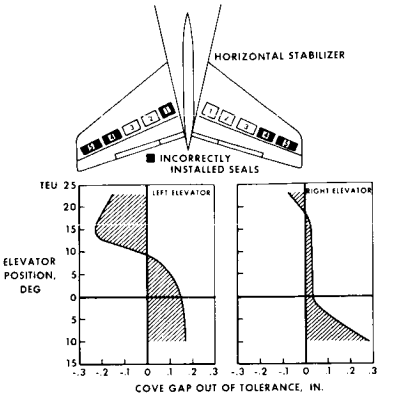

Figure 2

FLIGHT-TEST LIMITS

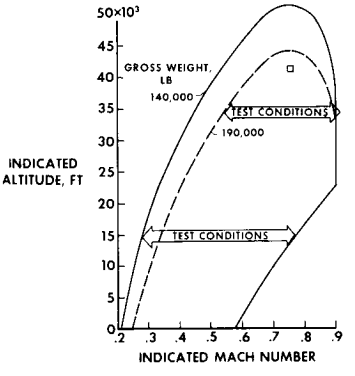

Figure 3

LONGITUDINAL-CONTROL-SYSTEM MANEUVERING CHARACTERISTICS

MACH NUMBER = 0.84, ALTITUDE = 34,500 FT

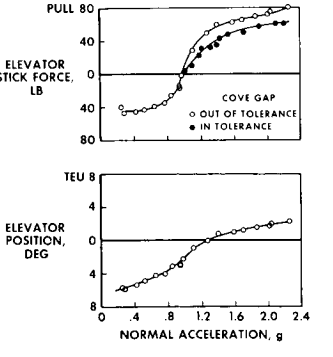

Figure 4

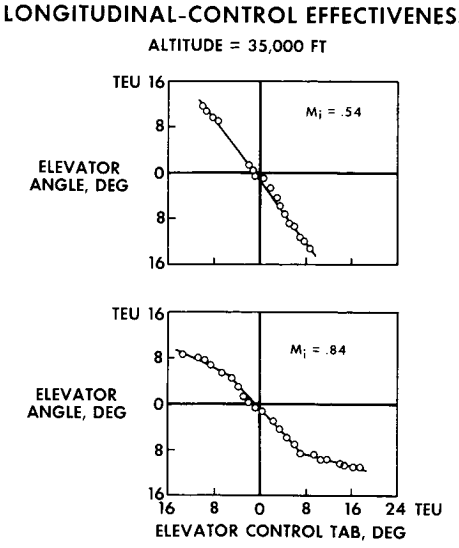

Figure 5

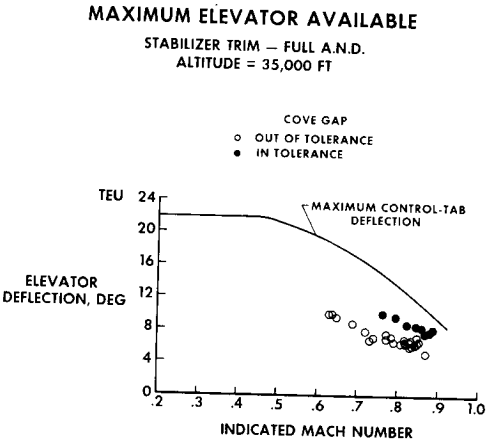

Figure 6

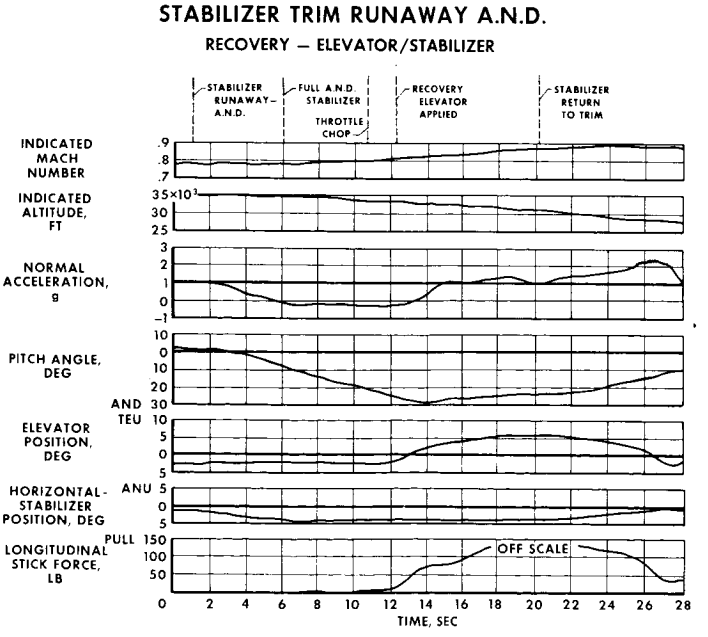

Figure 7

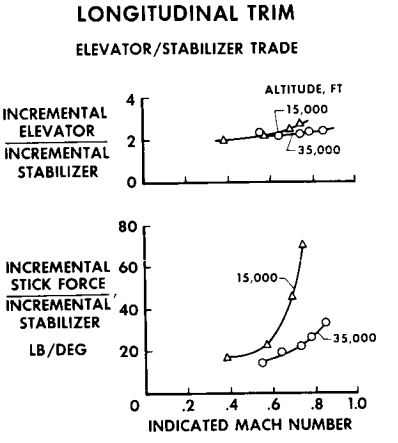

Figure 8

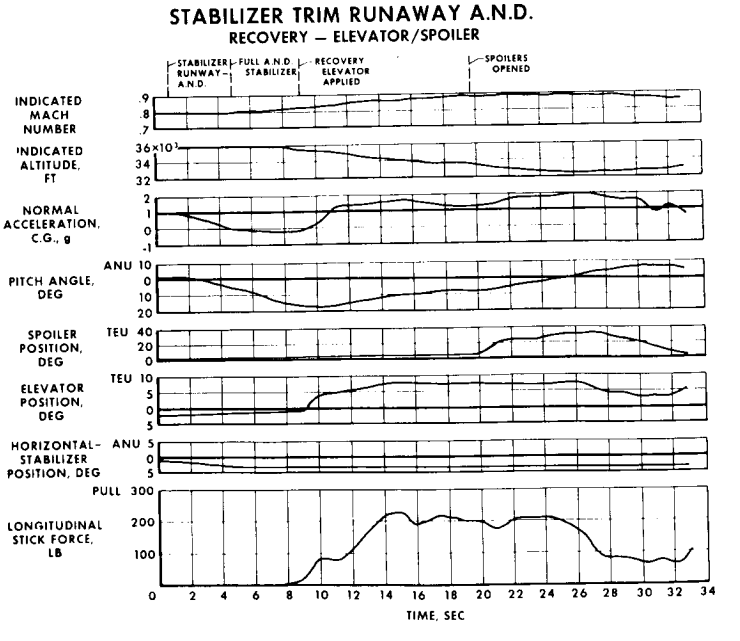

Figure 9

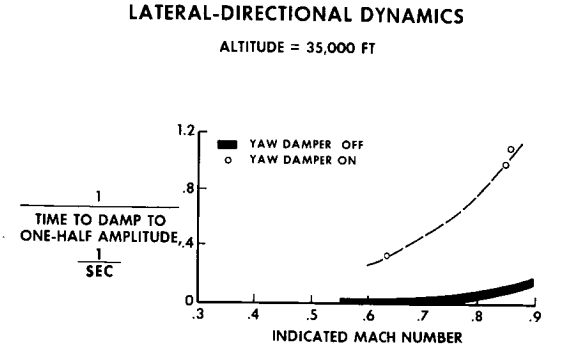

Figure 10

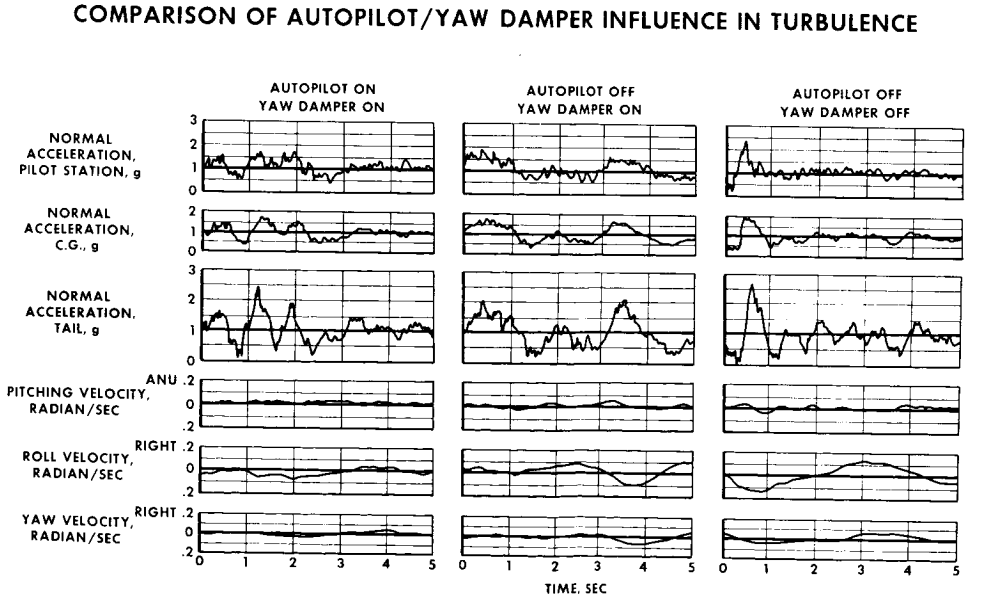

Figure 11

15. SIMULATOR INVESTIGATIONS OF THE PROBLEMS OF FLYING A SWEPT-WING TRANSPORT AIRCRAFT IN HEAVY TURBULENCE

By Richard S. Bray and William E. Larsen

NASA Ames Research Center

SUMMARY

An investigation of several factors which may contribute to the problem of piloting jet transport aircraft in heavy turbulence was conducted by using a piloted simulator that included the most significant airplane response and cockpit vibrations induced by rough air. Results indicated that the primary fuselage structural frequency contributed significantly to a distracting cockpit environment, and there was obtained evidence of severely reduced instrument flight proficiency during simulated maneuvering flight in heavy turbulence. It is concluded that the addition of similar rough-air response capabilities to training simulators would be of value in pilot indoctrination in turbulent-flight procedures.

INTRODUCTION

During the past 3 or 4 years, jet transport aircraft have been involved in a number of serious incidents resulting from encounters with heavy atmospheric turbulence. These experiences fall into two categories: those resulting from encounters with clear-air turbulence that caused structural damage and personal injury, and those that involved encounters with storm turbulence, while in instrument flight, that resulted in partial or complete loss of control of the aircraft. The clear-air turbulence problem indicates the need for meteorological detective work, but the storm turbulence presents a less defined problem and has inspired a review of turbulent-flight procedures among all segments of the airline industry. In response to this general concern, the National Aeronautics and Space Administration instituted a program of investigations to examine several factors which might contribute to piloting problems in severe turbulence. Wind-tunnel tests of a transport model at the Langley Research Center and flight tests of a Boeing 720 airplane conducted by personnel of the Flight Research Center were performed for the purpose of augmenting aerodynamic and stability and control data for the swept-wing transport category of airplane. Concurrently, at the Ames Research Center, an investigation of rough-air piloting problems was conducted by using a piloted simulator that has unique capabilities regarding creation of the physical environment in the cockpit during flight in turbulence. This paper summarizes the results and observations obtained in the Ames investigation.

The simulation program was intended to pursue the following objectives:

(a) Examine aircraft response to turbulence

(b) Evaluate handling qualities in turbulence

(c) Study effects of cockpit accelerations on conduct of flight tasks

(d) Evaluate the simulator as a training device

AIRPLANE SIMULATION

Cockpit.- Since many of the first-hand accounts of incidents in heavy turbulence stressed the distracting aspects of cockpit accelerations and vibrations, the simulation used in the Ames program was designed to utilize a device known as the height control simulator. The simulator cab is mounted on a vertical track that provides 100 feet of travel. (See fig. 1.) High-performance electrical servomotors drive the cab through a cable system. The simulator cockpit, illustrated in figure 2, employed basic controls and instruments similar to those installed in jet transport aircraft. White light was used for instrument illumination. The occupant was seated on a cushion of the type used on Boeing 707 airplanes, and was restrained by a military-type lap belt and shoulder harness.

Computer program.- The computer program utilized aerodynamic and stability and control characteristics that were generalized to be typical for a medium-weight swept-wing jet transport airplane at midcruise loading (about 175,000 lb). All stability and control derivatives other than lift, drag, pitching-moment, and longitudinal-control gradients were linearized and were invariant with Mach number. The operating envelope provided by the computer program extended from 25,000 feet to 45,000 feet in altitude and allowed for speeds up to a Mach number of 1.0. Although the computational program was simplified in many respects, it did include the following qualitative representations of those characteristics that were believed to be significant to the flight tasks being simulated:

(a) Performance reduction with altitude

(b) Reduction in longitudinal control power at high indicated airspeeds and Mach numbers

(c) Reduction in longitudinal stability at the stall

(d) Speed instability, or "tuck," at high Mach numbers, together with a simulated Mach trim compensator

(e) Cockpit vibrations at the stall and at high Mach numbers

Simulation of structural vibration.- Accelerations measured in the cockpits of several jet transport airplanes during flight in turbulence revealed the existence of a predominate frequency of vibration of about 4 cycles per second. This value is presumed to reflect the first bending mode of the fuselage. The upper portion of figure 3, which is a sample of the flight records, gives evidence of the 4-cycle-per-second cockpit vibration that appears to be constantly excited by the turbulence. This frequency can hardly be noticed at the center-of-gravity location. Measurements taken in smooth air in response to sharp elevator pulses defined the low value of damping inherent in this bending mode. The effects of this bending mode were adequately simulated by including in the computational circuitry for cockpit acceleration a simple resonant circuit, tuned to 4 cycles per second and appropriately damped. The amplitude of accelerations at this frequency in relation to the general root-mean-square level of accelerations was adjusted to agree with the results of an analysis of the flight records. The lower portion of figure 3 presents for comparison the center-of-gravity and cockpit accelerations computed in the simulation program in response to simulated turbulence inputs.

Turbulence simulation.- Turbulence was introduced into the analog computation as incremental angles of attack and sideslip resulting from vertical and lateral gusts. The turbulence inputs used in this initial phase of the study were derived by appropriately filtering the output of a Gaussian noise generator. In subsequent phases of the program, extensive use was made of gust profiles that had been recorded during actual penetrations of thunderstorms with a T-33 jet chase airplane, which was operating as part of the National Severe Storms Project of 1960 and 1961. These profiles contained large-scale draft velocities of up to 200 feet per second.

Simulator capabilities.- The drive system of the simulator cab is capable of reproducing the computed accelerations up to a frequency of 5 cycles per second, and because of its large vertical travel is capable of reproducing acceleration frequencies as low as the airplane short-period frequency of about 1/4 cycle per second. Frequencies below this value are rapidly attenuated by the necessary "wash-out" circuitry.

The unique aspects of this jet-transport-airplane simulator, particularly in comparison with training simulators, are

(a) Capability to reproduce a significant portion of the cockpit vertical-acceleration environment of flight in turbulence

(b) Flexibility in programing of rough-air inputs

(c) Representation of airplane characteristics beyond normal operating limits

TESTS

The observations discussed in this paper are based on several periods of operation of the simulator. The investigation was exploratory in nature, and

a total of 26 NASA, FAA, and industry pilots were exposed to the simulator. Research pilots made repeated runs in simulated heavy turbulence in order to assess the relative significance of the various factors that bear on the task of flying in turbulence. At the conclusion of the program, the simulation was used in a demonstration program for 16 pilots involved with the airline industry.

RESULTS AND DISCUSSION

Response to Large-Scale Turbulence

Because several of the serious turbulence incidents culminated in steep dives, concern has been expressed regarding the longitudinal response of the jet transport airplane to large vertical drafts and the adequacy of the control available to the pilot in this large-scale turbulence environment. The simulation showed no unusual characteristics, and longitudinal control was more than adequate if speeds were maintained within the normal operating boundaries. Figure 4 illustrates the behavior of the aircraft in response to vertical drafts. The left-hand side of the figure illustrates the normal weather-vaning response of the longitudinally stable airplane to a very large (200 feet per second) sustained updraft. With no intervention on the part of the pilot, the aircraft is pitched nose down through an angle of 11°. For the rate of gust onset shown in figure 4, a maximum of about 50 feet per second per second, the acceleration transient is very small, but it does initiate a positive rate of climb. Of course, with the nose-down attitude, there is a rapid buildup in speed. In 20 seconds the aircraft has accelerated from a Mach number of 0.79 to a Mach number of 0.88. As the aircraft leaves the region of the updraft and progresses into a downdraft, the reverse behavior is indicated.

The time history on the right-hand side of figure 4 indicates the course of events if the pilot intervenes to return the pitch attitude to its original value. Substantial acceleration increments are required, and a rate of climb equal to the gust velocity is attained. This action by the pilot does, however, minimize speed variations. The point to be gained from this figure is that the energy imparted to the aircraft by such a large draft must show up as either a speed or an altitude increase. The pilot has that choice, but he has no means of rapidly dissipating the energy.

Figure 5 illustrates the longitudinal behavior of the aircraft, without pilot input, in response to a vertical gust profile that was recorded in an actual thunderstorm penetration. Although at several points in the exposure, incremental accelerations of nearly ±1 g are shown, they are not sustained. In fact there is little evidence of acceleration frequencies lower than the natural frequency in pitch - about 1/4 cps. Speed and altitude deviations are gradual, and except for the early portion of the encounter, where large sustained drafts were present, these changes could easily be accepted as the phugoid oscillation. Figure 5 is offered as additional evidence that a normally stable aircraft will not be longitudinally "upset" to the point of flight-path divergence, even by very heavy turbulence.

Handling Qualities in Turbulence

Assessments of handling qualities of the simulated aircraft in heavy turbulence indicated that there were no marked deficiencies within the normal operating boundaries and with the yaw damper and pitch trim compensator operating. Dutch roll was a constant annoyance, but good lateral control mitigated its significance. Control characteristics were considered satisfactory to speeds as low as 230 knots at the aircraft loading conditions assumed for the tests. The changes in trim and control power above a Mach number of 0.85 were considered unsatisfactory in heavy turbulence. Because these changes are difficult to recognize quickly in turbulence, they add confusion to an already demanding task.

Cockpit Accelerations

The cockpit-acceleration environment in the heaviest turbulence was considered to be detrimental to instrument flight proficiency. The pilots agreed that the instruments generally remained readable, but only with increased effort, and that this requirement for increased concentration tended to disturb the normal "scan" pattern that is the key to proficient instrument flight. Several pilots were exposed to the simulation of heavy turbulence with the structural frequency removed - that is, without a 4-cycle-per-second resonance. The resulting cockpit-acceleration environment was considered much more tolerable even though the root-mean-square level of accelerations was not significantly decreased. This observation, together with a desire to substantiate available physiological data, inspired tests to determine pilot tolerance to vertical vibrations as a function of frequency. In figure 6, acceleration measurements at a pilot's head are compared with cockpit accelerations for frequencies up to 5 cycles per second. For the pilot seated on a standard seat cushion, there is indicated an amplification factor of more than 2 at frequencies between 3 and $4\frac{1}{2}$ cycles per second. Slightly lower amplifications are noted at these frequencies with no cushion at all, but the attenuating effects of the cushion do become apparent above $4\frac{1}{2}$ cycles per second. There was good correlation of a decrease in subjective tolerance to the vibrations with the increase in head accelerations. As indicated in the figure, the fuselage bending frequencies of the aircraft lie in a most sensitive range, and the present seat cushions are ineffective, at best, in reducing the stress on the pilot.

It was interesting to note that the level of physical discomfort and concern expressed at initial exposures to the highest turbulence levels tended to lower with subsequent exposures. These facts point to the benefits that might be obtained by providing a similar environment in training simulators.

Pilot Performance

During the portion of the program in which research pilots were evaluating the rough-air flight task, there were no indications in their performances of

severe control difficulties; that is, there were no incidents or "upsets," even under the most severe conditions of turbulence and task. However, it must be remembered that their familiarity with the objectives of the test, and their background of test flying reduced the elements of surprise and distraction from the environment. More significant variations of pilot performance became evident during the demonstration program for the industry pilots. The primary objectives of this phase of the program were to demonstrate the simulated rough-air environment, to exchange ideas and opinions on the subject of operations in turbulence, and to obtain professional assessments of the value of this type of simulator in airline training.

Each pilot averaged about 2 hours in the simulator, with most of the first hour devoted to familiarization and demonstration of the characteristics of the simulated aircraft, including stalls and flight beyond a Mach number of 0.9. The rest of the time was devoted to simulated thunderstorm penetrations and demonstrations pertinent to rough-air flight techniques.

Reactions of the visiting pilots were favorable. The vertical motion appeared to minimize the tendency to overcontrol in pitch that bothers most pilots in fixed-cockpit simulation. The stability and control characteristics were accepted as typical for the aircraft category, except for the longitudinal instability or "tuck" which was considered exaggerated. However, this characteristic was demonstrated to be completely controllable. Many of the pilots believed that the highest levels of simulated turbulence were within their flight experiences, but that such encounters were very rare.

The most critical task posed for each pilot was introduced during his third turbulence encounter. He was requested to descend 5,000 feet and change heading simultaneously. Unknown to the pilot, his pitch trim compensator was rendered inoperative so that an unstable longitudinal trim change would accompany any acceleration past a Mach number of 0.84. With this task, five of 14 pilots experienced some form of control difficulty. Figures 7, 8, and 9, are examples of performances recorded in this task.

The performance illustrated in figure 7 is typical of that of most of the pilots. With relatively low control forces, the pilot maintained a reasonably steady rate of descent and good control of his speed. In comparison, the pilot whose performance is illustrated in figure 8 demonstrated difficulties in his control of the descending flight path. Although he did prevent the airplane from accelerating beyond a Mach number of 0.84 and into the "tuck" region, his attempts to stabilize at 33,000 feet resulted in large flight-path excursions. Two momentary stalls were induced in attempts to arrest undesired rates of descent. Note the control activity shown by figure 8 in comparison with that shown by figure 7. In figure 9 is presented what might be considered an "upset." An initial speed divergence was compounded by the "tuck," and recognition of the seriousness of the situation apparently was delayed long enough for the aircraft to accelerate into the region where elevator control was relatively ineffective. Confidence in the validity of these performances was heightened by the fact that no evidence of similar difficulties was noted during the familiarization period, when each of the pilots was required to do a similar task in the absence of simulated turbulence.

The upper portion of figure 10 illustrates the performance, in the simulator, of a research pilot who intentionally deprived himself of pitch-attitude information and placed exaggerated emphasis on control of airspeed. As shown in figure 10, the pilot induced a flight-path oscillation with a period of about 40 seconds. Several stalls occurred at the highest speeds as an effort was being made to reduce airspeed and rate of descent. This behavior may be compared with that illustrated in the lower portion of this figure, which is a transcription of a portion of a record from a flight recorder of one of the more celebrated flight incidents. It is interesting to note that the simulator performance of figure 8 demonstrates very similar flight-path variations. These similarities do not merit extensive and detailed interpretive efforts, but they can support the contention that pilot techniques and cockpit environment are as significant to the problem of flying jet transport airplanes in turbulence as are the mechanics of large-scale turbulence or the aerodynamic characteristics of the aircraft.

CONCLUDING REMARKS

The experiences with the simulation, together with opinions offered by the visiting airline personnel, lead to the primary recommendations resulting from this program; that is, that the capabilities of training simulation be extended to include the most significant cockpit environmental effects and the aircraft response induced by heavy turbulence. In addition, the training simulator should have the capability of accurately representing the stability and control characteristics of the airplane at and beyond the normal operating boundaries.

The demonstrations that the cockpit environment in heavy turbulence can seriously degrade the capabilities of pilots in tasks demanding integration of information from a number of instruments lead to these concluding recommendations:

1. In heavy turbulence, the pilot should make every effort to minimize deliberate flight-path changes so as to keep his task as simple as possible.

2. The pilot should avoid imposing large angular rates on the aircraft; in other words, he should try to limit his job to that of a low-gain attitude stabilizer.

3. Consideration should be given to modifying overspeed warning systems to include rate of speed buildup. This modification could be effected by including pitch-attitude information in the warning system.

4. Consideration should be given to the possibility of isolating the pilot from the most distracting vibration frequencies through modification of the seating and restraint systems.

5. Increased attention should be directed toward attitude presentations that can be interpreted with the ease with which the view of the outside world is used in VFR flight.

SIMULATOR CAB

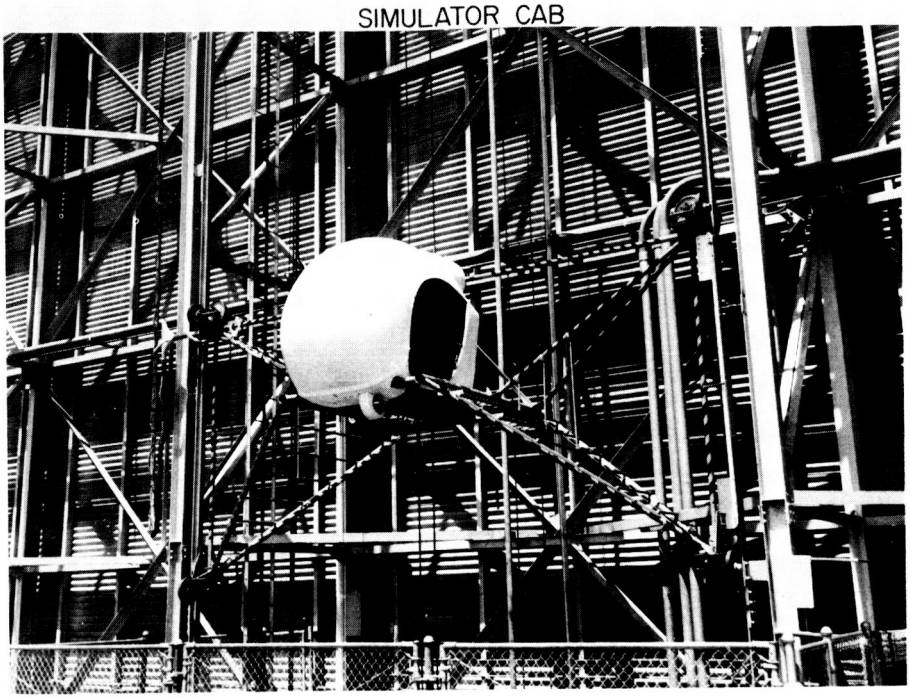

Figure 1 A-33492

SIMULATOR COCKPIT

Figure 2 A-33497

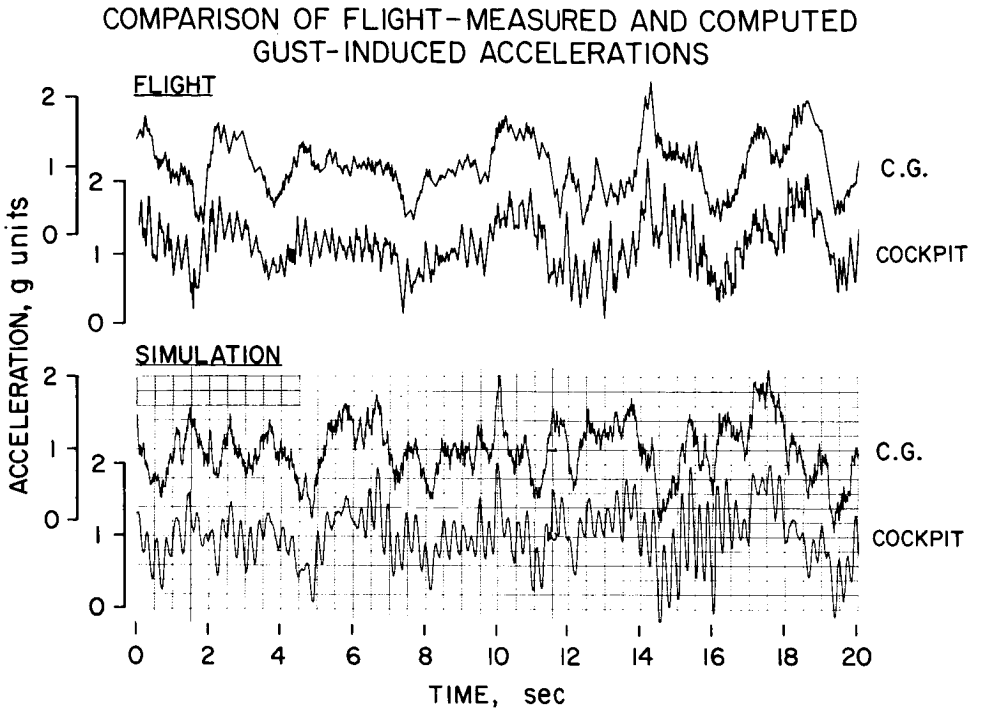

Figure 3

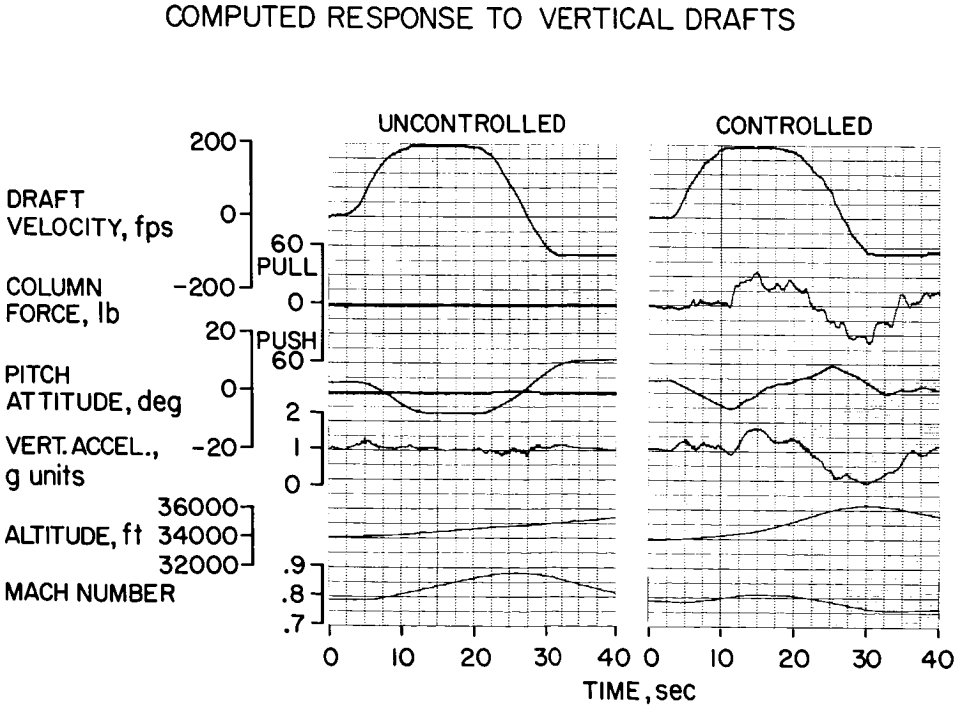

Figure 4

COMPUTED RESPONSE TO THUNDERSTORM TURBULENCE

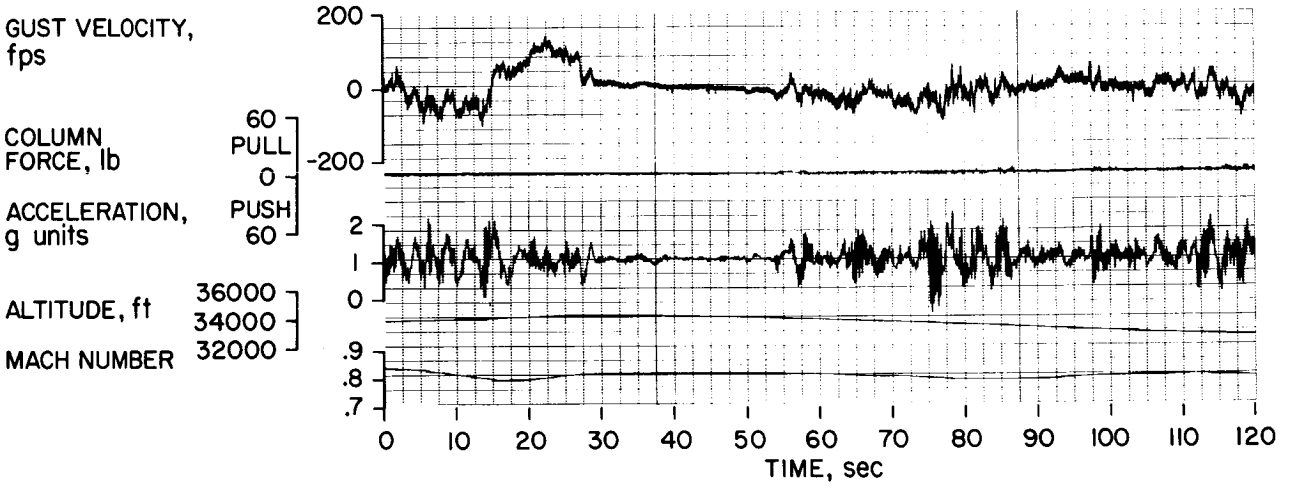

Figure 5

EFFECT OF VIBRATION FREQUENCY ON ACCELERATION AMPLIFICATION AT PILOT'S HEAD

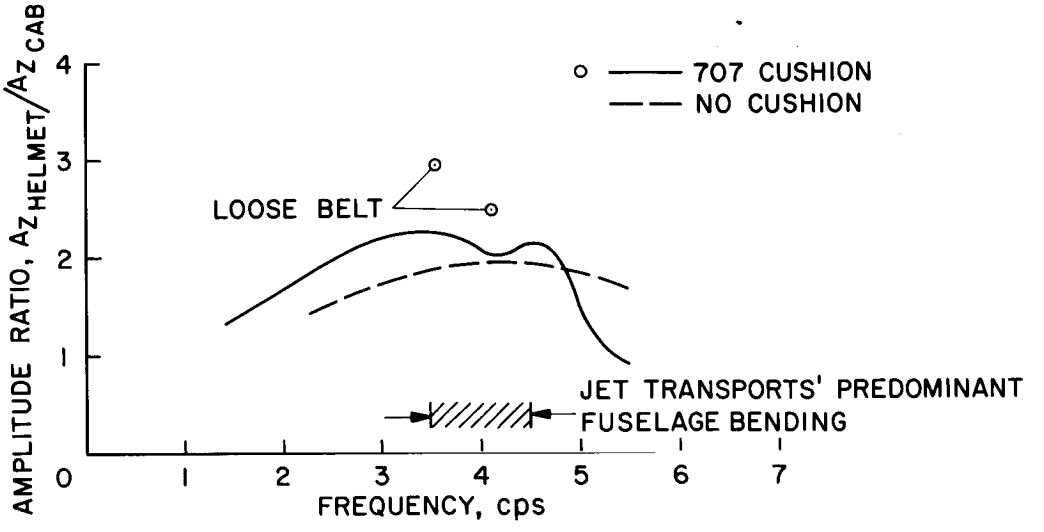

Figure 6

GOOD FLIGHT-PATH CONTROL DURING TURNING DESCENT IN SIMULATED TURBULENCE

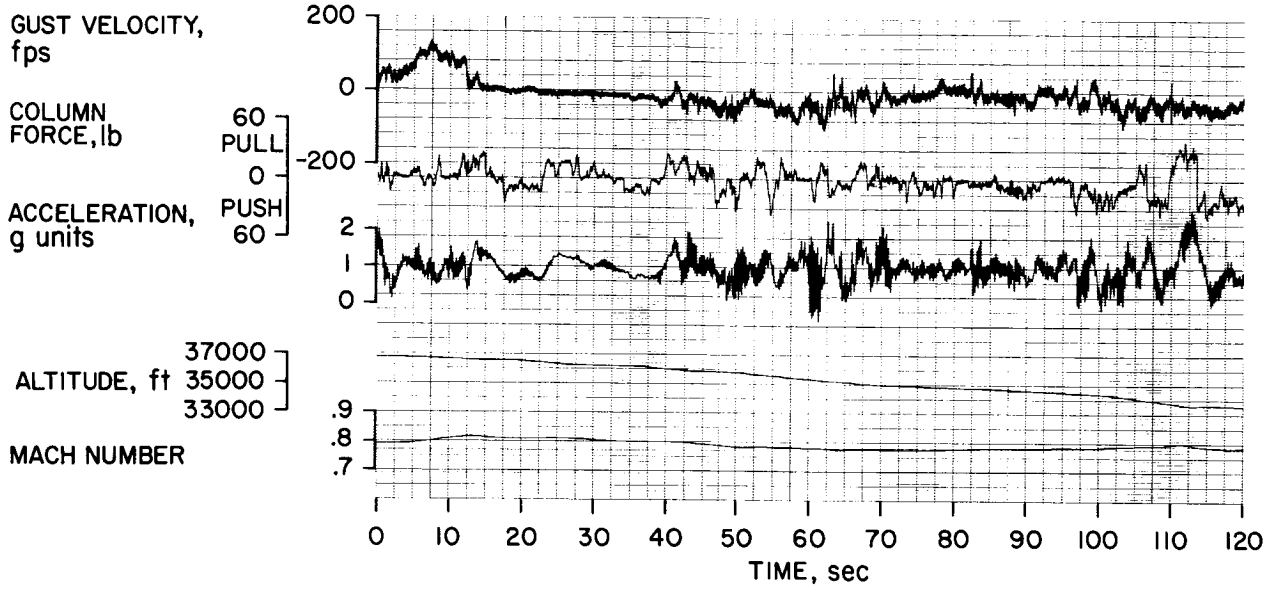

Figure 7

MARGINAL FLIGHT-PATH CONTROL DURING TURNING DESCENT IN SIMULATED TURBULENCE

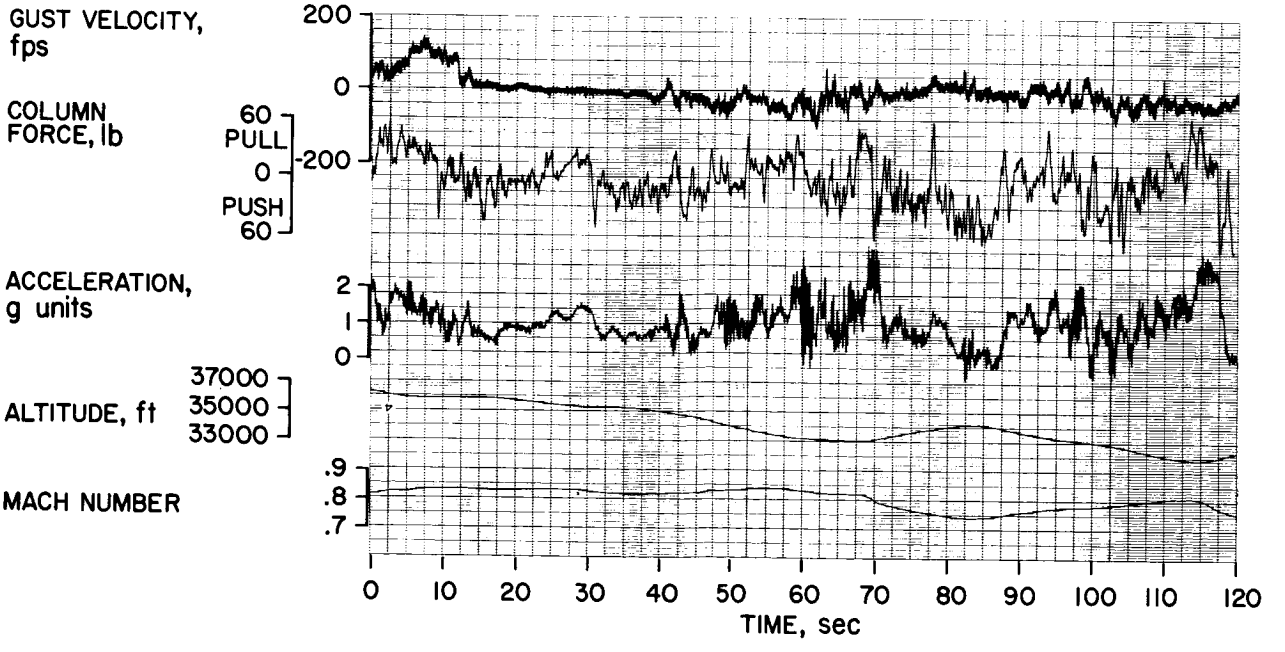

Figure 8

FLIGHT-PATH DIVERGENCE DURING TURNING DESCENT IN SIMULATED TURBULENCE

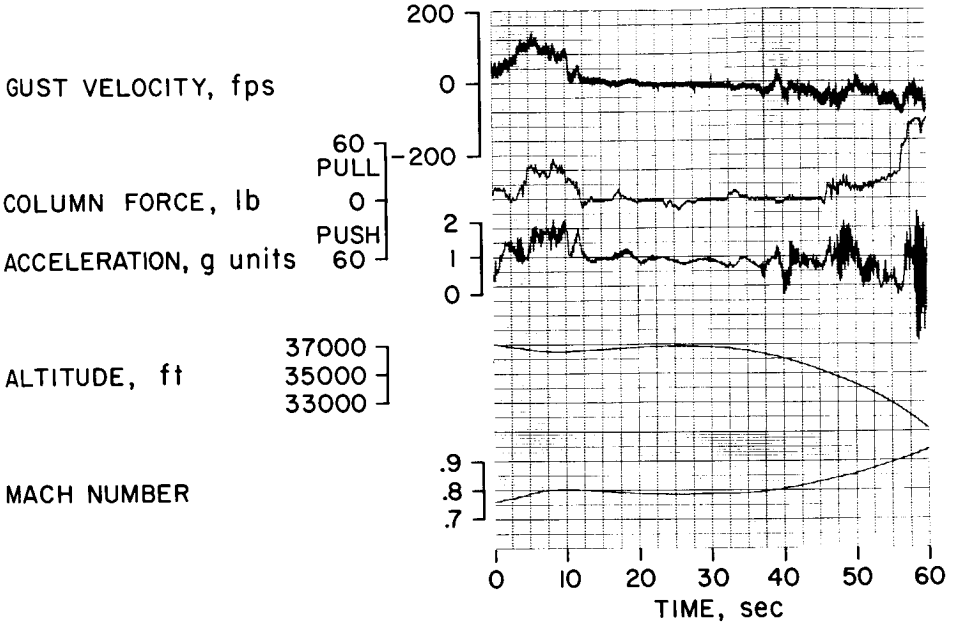

Figure 9

FLIGHT-PATH OSCILLATIONS IN TURBULANCE IN THE SIMULATOR AND IN FLIGHT

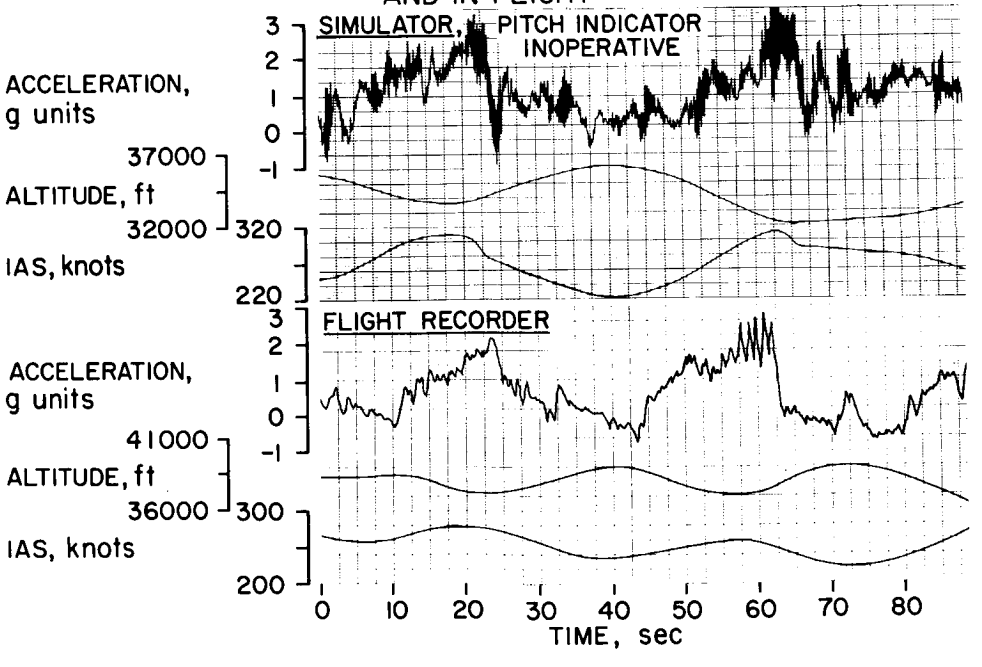

Figure 10

16. A SIMULATOR STUDY OF TAKE-OFF CHARACTERISTICS OF PROPOSED SUPERSONIC TRANSPORTS

By Charles T. Jackson, Jr., and C. Thomas Snyder

NASA Ames Research Center

SUMMARY

Fixed-cockpit piloted simulator studies of delta-planform and variable-wing-sweep supersonic transport configurations are being conducted at the Ames Research Center to investigate the handling qualities and certification requirements related to the take-off maneuver.

Validation of the simulation was achieved by duplicating the take-off certification program of a subsonic jet transport. Evaluation of the simulator was made by NASA pilots as well as company and FAA pilots involved in the actual certification flights of the airplane. The present paper is limited to a discussion of normal take-off, minimum control speed (ground), rotation characteristics, and initial climbout.

Comparisons of the take-off characteristics are made between the supersonic transport and the current class of subsonic jet transports.

Results indicate that minimum control speed (ground) characteristics are a function of thrust-weight ratio, the time provided for SST rotation should be at least as long as that for the subsonic jet transports, abused take-offs are more likely to result in tail scrapes, and climbout below the minimum drag speed requires that the pilot carefully monitor airspeed.

INTRODUCTION

In the interest of providing technical assistance for the National Supersonic Transport Program, fixed-cockpit simulator studies of delta-planform and variable-sweep-wing supersonic transports (SST) are being conducted at the Ames Research Center to investigate flying qualities and airworthiness criteria.

The first of these simulations is devoted to the study of take-off characteristics. At present only preliminary studies have been made; however, certain conclusions can be drawn at this time which apply to the SST program in general. This paper summarizes a few of the more interesting observations based on the delta SST studies.

SYMBOLS

T/W	thrust-weight ratio
V_{LO}	lift-off speed, knots
V_{MC_G}	minimum control speed (ground), knots
V_R	rotation speed, knots
V_2	take-off safety speed, knots
W/S	wing loading, pounds per square foot
α	angle of attack, degrees
γ	climb angle, degrees
θ	pitch attitude, degrees
A.N.D.	airplane nose down
A.N.U.	airplane nose up

AIRPLANES SIMULATED

The basic characteristics of the two SST's under study as well as those of a reference subsonic transport used for simulator validation are given in table I. One SST has a variable-sweep wing with a horizontal tail; the other has a tailless delta planform with a low wing loading.

Both SST's are larger than the subsonic jet transport and have greater maximum take-off gross weights. These characteristics, in combination with a high-fineness-ratio fuselage, contribute to pitch and yaw inertias several times greater than those of the subsonic jet. The low-aspect-ratio delta SST has a roll inertia less than that of the subsonic jet, and the variable-sweep SST has a roll inertia greater than that of the subsonic jet while in the high-aspect-ratio take-off configuration. Of particular interest in take-off are the larger thrust-weight ratios of the SST.

The center-of-gravity location of the SST permits only small static margins because of supersonic cruise considerations that require low trim drag. Both SST's are "geometry-limited" in that the maximum lift coefficient cannot be attained with the main wheels on the runway.

The SST values simulated are not necessarily representative of a final SST design.

SIMULATOR DESCRIPTION AND FIDELITY

Figure 1 illustrates the basic arrangement of the simulator. The pilot is seated in a fixed transport cockpit equipped to pick off electrical signals proportional to his control movements. These signals, along with the geometric and aerodynamic characteristics of the airplane, are processed by an analog computer to produce voltages which represent airplane motion and to drive the cockpit instruments, visual-system camera, and data recorders. Permanent records of the visual scene as seen by the pilot are recorded on videotape.

The pilot's view from the cockpit is shown in figure 2. Instrumentation includes angle-of-attack, sideslip, control-force, sensitive airspeed, and tail-clearance indicators. The five-digit counter is used for data correlation.

Fidelity of the simulator was checked with duplication of a large portion of the take-off certification program of a subsonic jet transport by NASA pilots as well as company and FAA pilots who were involved in the actual certification of the airplane.

Typical certification maneuvers flown during the investigation included

normal four-engine take-offs
three-engine take-offs
"mistrim" take-offs
accelerate-stops (rejected take-offs)
minimum unstick speed determination, V_{MU}
minimum control speed tests

Each maneuver involved realistic piloting techniques in order to achieve satisfactory assessment of the task involved. Most maneuvers were accomplished with an acceptable level of performance when compared with the maneuvers of the subsonic jet; increased margins of maneuvering capability, as well as certain performance parameters, were evident. A few of the tasks involved, however, uncovered characteristics which may indicate a need for changes in piloting technique and training. The full implication of these characteristics warrants further study. The present paper is limited to a discussion of normal take-off, mimimum control speed (ground), rotation characteristics, and initial climbout.

DISCUSSION

Normal Take-Off

Two types of normal take-offs were conducted: One involved maximum available thrust and the other involved less than maximum thrust as may be required in order to minimize airport and/or community noise. Immediately obvious to the pilot is the excellent performance of the SST in comparison with the subsonic jet, as indicated by the higher acceleration on the ground run, shorter time to accelerate through 100 knots, shorter distance to lift-off, and larger

available climb gradient. Main gear lift-off was not obvious from the visual scene alone due, in part, to the height of the cockpit in the rotated attitude. Ground handling characteristics on the take-off run appeared to be good.

Ground Minimum Control Speed

The ground minimum control speed was determined by plotting the results of a number of take-off ground runs, each involving an outboard engine failure. The pilot applied full corrective rudder upon recognition of the engine failure.

The simulator results are shown in figure 3 where the maximum unavoidable deviation from runway centerline is plotted against the corresponding airspeed at which the engine was failed, both with and without rudder-pedal-actuated nose wheel steering. For the reduced T/W, directly comparable to that of subsonic jet transports, the minimum control speed is rather sharply defined, in that a small decrease in the speed at which the engine failed causes a significant increase in deviation from runway centerline. By comparison, the curve obtained by using "normal" SST T/W indicates comparable controllability at lower airspeeds.

During certification of the subsonic jets, the speed at which an outboard engine could be failed and at which the maximum lateral deviation from runway centerline not exceed 15 feet was taken as V_{MC_G}. Figure 3 shows little variation in V_{MC_G} (based on a 15-foot deviation) with T/W since the curves coincide. But if, for example, a 40-foot deviation could be tolerated, a significant reduction in V_{MC_G} would be realized.

The benefits due to rudder-pedal-actuated nose wheel steering are indicated by the curve labeled "nose wheel steering operative," which shows that deviations from runway centerline may be held to less than 10 feet with outboard engine failures at speeds as low as 40 knots. This curve applies only for dry runway tire friction coefficients.

Rotation Characteristics

The speed V_R at which take-off rotation is initiated was varied over a wide range during the simulator tests. Initially a 17-knot speed spread was used between the rotation input and the target lift-off speed, a value comparable with the 10- to 15-knot spread used with subsonic jets. Because of the higher longitudinal acceleration of the SST, a rapid rotation was required to reach the proper lift-off attitude before overshooting the designated lift-off speed. As might be expected, this, aided by the low static stability of the airplane, resulted in a tendency to either overrotate or "hunt" for the desired attitude. As tests progressed the rotation speed was gradually reduced until a more satisfactory rotation time of $3\frac{1}{2}$ to 4 seconds was used. (Values for the

subsonic jet averaged about $3\frac{1}{2}$ seconds.) However, this slower rotation rate required that rotation be initiated 20 to 30 knots before lift-off.

Figure 4 shows a comparison between a time history for the subsonic jet simulation and one for the delta SST. Note the higher ground run acceleration, higher pitch attitude after lift-off, and shorter distance to a 35-foot altitude for the SST. Also note the longer duration elevator input for rotation, followed by an abrupt forward control column motion to arrest the rotation rate. The 4-second rotation resulted in satisfactory and reasonably accurate rotations and more consistent take-off performance. Lift-off occurred 24 knots after rotation was started.

Frequent tail scraping occurred during initial familiarization tests with the SST simulation. In part, this resulted from the low margin of pitch attitude between normal lift-off and tail scrape, a margin which is less than that for the subsonic jet. Slower rotations and increased simulator experience minimized the tendency to strike the tail.

Figure 5 shows the effect of rotation attitude on longitudinal acceleration as determined from simulator take-offs. While the SST has more acceleration than the subsonic jet, its remaining acceleration after rotation drops off faster with pitch attitude. While the geometry limitation of the tail striking the runway prevents excessive attitudes before lift-off, nothing mechanically prevents the pilot from attaining excessive pitch attitude, with large attendant loss in acceleration, immediately after lift-off. Poor readability of the attitude indicator also contributed to difficulty in performing accurate rotation.

Initial Climbout Characteristics

Normal take-offs of the delta SST followed by climbout at a four-engine V_2 speed of 180 knots were conducted by a number of different pilots. The flight path and airspeed were generally controlled in a satisfactory manner. Some pilots reported increased difficulty in maintaining the desired airspeed, while others reported no difficulty but admitted that increased attention was devoted to speed control. In figure 6 the characteristics are presented which contribute to this situation and which may suggest changes in the use of instrument information. Plotted against speed are climb angle, angle of attack, and pitch attitude for the subsonic jet transport, the variable-sweep SST, the delta SST, and, for comparative purposes, the F5D, a small delta-wing airplane.

With the subsonic jet and the variable-sweep SST, the result of the pilot's holding a discrete pitch attitude is the attainment of a unique airspeed. However, for the delta SST, pitch attitude remains constant over a wide range of airspeeds, and a single attitude can satisfy several combinations of α and γ and, therefore, will not guarantee a single speed. This suggests that pitch attitude is an insensitive indication of speed for the delta SST during initial climb. The curves for the F5D show a similar slope trend as those for the delta SST. A slight change in piloting technique with more attention given to airspeed may be all that is required. Additional benefits are indicated,

however, by supplying the pilot with suitably processed angle-of-attack information, which, in turn, will define airspeed. Should a more sophisticated approach be desired it is possible to reshape the airplane's climb-angle and pitch-attitude curves through operation of a speed-controlled throttle, sacrificing excess gradient for speed stability. Alteration of obstacle clearance and noise abatement constraints which force initial climbout below the minimum drag speed would permit immediate acceleration to speeds where the airplane is "speed-stable" and higher aerodynamic efficiencies could be attained. Regardless of the alternative chosen the attitude indicator still serves as a sensitive indicator of rate-of-speed change, and pilots familiar with backside operation had no difficulty during climbout.

CONCLUSIONS

The following conclusions are based on simulator studies of the delta-planform SST:

1. The SST displays good performance on normal take-off.

2. Ground minimum control speed characteristics are influenced by higher thrust-weight ratios.

3. The time provided for the rotation maneuver should be at least as long as that for the subsonic jet transports.

4. The lift-off attitude tolerance is less than that of the subsonic jet.

5. Improved readability of attitude indicators may result in improved rotation accuracy.

6. The abused take-off results indicate a higher probability of tail scrapes with abrupt rotations than with the subsonic jets.

7. There is an increased dependence on airspeed information during initial climbout of the delta SST.

TABLE I

BASIC CHARACTERISTICS OF SIMULATED AIRCRAFT

	SUBSONIC TURBOJET TRANSPORT 	TAILLESS DELTA 	VARIABLE SWEEP 
max T/W	0.21	0.44	0.30
WING LDG W/S, lb/ft^2	107	64	100
ROLL INERTIA, slug - ft^2	5.7 x 10^6	2.5 x 10^6	7 x 10^6
PITCH INERTIA, slug - ft^2	4 x 10^6	21 x 10^6	22 x 10^6
YAW INERTIA, slug - ft^2	9.5 x 10^6	24 x 10^6	28 x 10^6

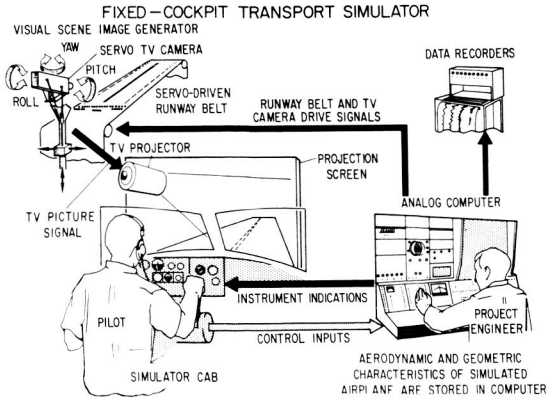

Figure 1

PILOT'S VIEW FROM SIMULATOR COCKPIT

A-32752-5.1

Figure 2

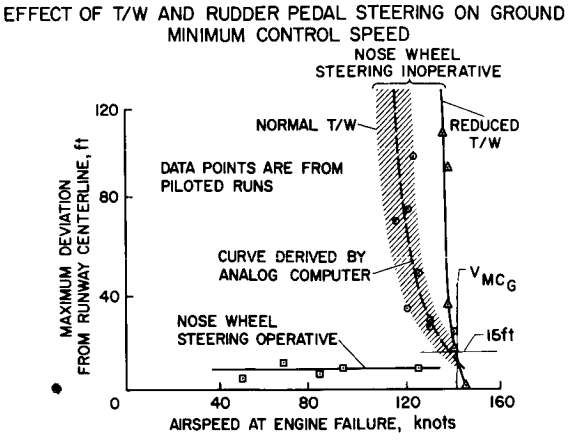

Figure 3

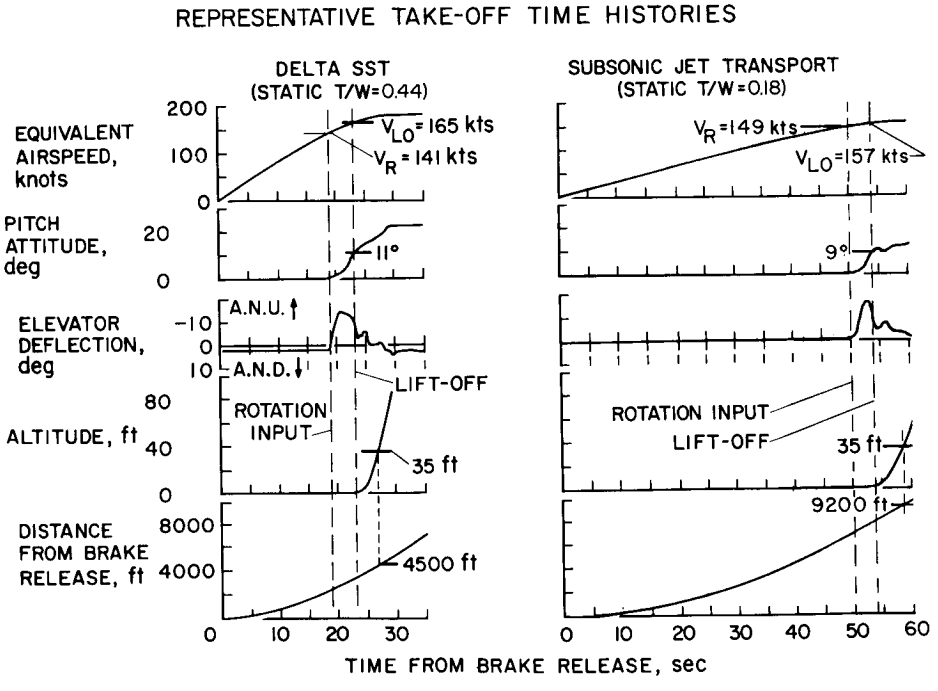

Figure 4

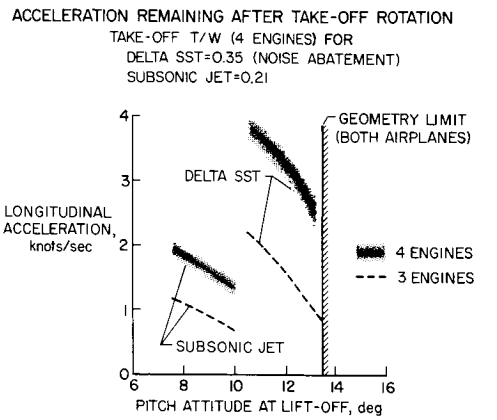

Figure 5

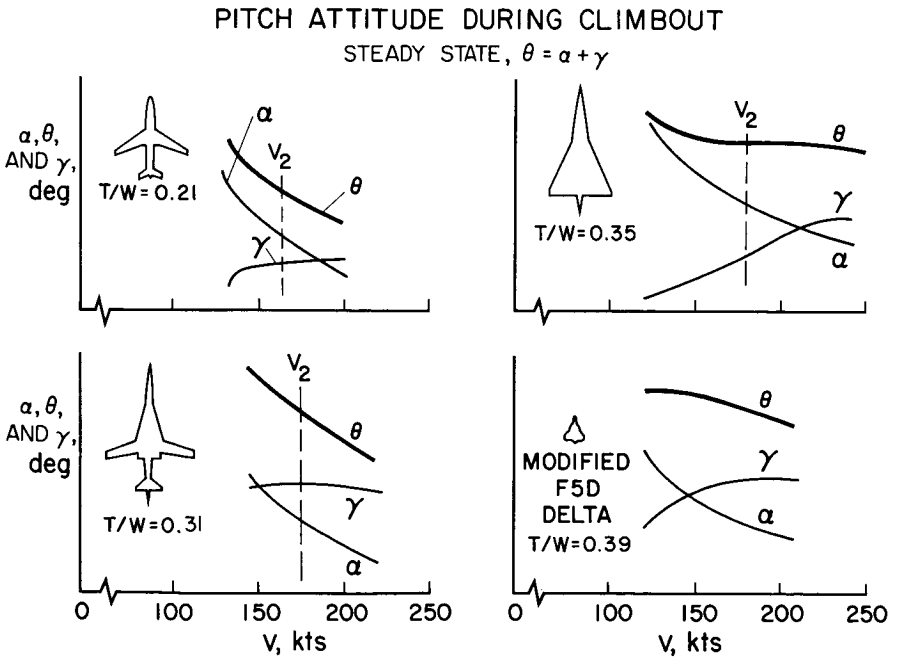

Figure 6

17. INTRODUCTION TO SST-ATC STUDY PROGRAM

By Thomas A. Toll

NASA Langley Research Center

The two papers to follow present results from a program being carried out as a joint effort by the NASA Langley Research Center and the FAA National Aviation Facilities Experimental Center (NAFEC) at Atlantic City, New Jersey. The purpose of this brief introduction is to define the objectives of the program and to describe the manner in which it is being pursued.

The study is directed toward problems anticipated with the introduction of the supersonic transport into the air-traffic-control system. The primary objectives are:

(1) The determination of the effects of the SST (supersonic transport) on requirements of the ATC (air traffic control) system

(2) The determination of the effects of the ATC system on requirements for the SST design and for its equipment

Basically, the program is a simulation effort involving equipment both at Langley and at the NAFEC facility. A block diagram illustrating the manner in which the equipment of the two agencies has been integrated to carry out the program is shown in figure 1. The blocks on the left represent NASA equipment at the Langley Research Center, Hampton, Va., and those on the right indicate the FAA equipment at Atlantic City. The Langley equipment includes a cockpit, or flight compartment that is generally representative of transport equipment, and an analog computer for solving the six-degree-of-freedom motion equations for an aircraft having the characteristics of the SST design under study.

The Langley cockpit has been linked through leased telephone lines to the ATC simulator at Atlantic City. The telephone lines transmit SST position data to NAFEC and permit two-way voice communication. Traffic simulation, consisting of a variety of airplane types, also is provided by NAFEC.

The simulation program is expected eventually to cover many aspects of the problem, including variations in design parameters and operating procedures for the SST, as well as planned improvements in the ATC system. The results reported in the following two papers have been derived only from the early stages of the program so far completed. Responsibility for interpretation of the results of the program is

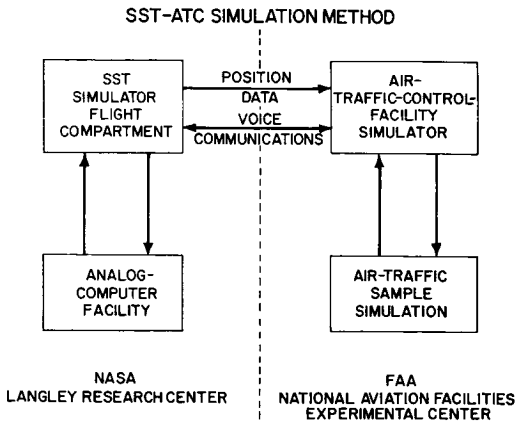

Figure 1

divided between the two agencies involved, with the FAA having responsibility for effects of the SST on the ATC system, and NASA Langley having responsibility for effects of the ATC system on SST design and operations.

18. EFFECTS OF THE SUPERSONIC TRANSPORT ON THE AIR TRAFFIC CONTROL SYSTEM

By Joseph P. O'Brien and Andrew L. Sluka

Federal Aviation Agency

SUMMARY

The current joint NASA-FAA simulation program is designed to study problems anticipated in the integration of the supersonic transport (SST) into the present and future Air Traffic Control (ATC) System. The initial tests conducted consisted of simulated departure and arrival operations in the New York terminal area under high-density traffic-flow conditions with as many as six SST operations per hour. Several types of radar and altitude-separation standards and handling concepts were investigated with the present ATC System. Results have shown that for the ATC System, in operations in which the SST was given priority, subsonic traffic incurred excessive radar vectors and excessive holding and ground delays. Further, airport acceptance rates were reduced substantially when the high separation standards and priority conditions were applied. Present voice communications procedures appear to be adequate for SST operations. Future studies will include other potential designs for the SST, and updating of the ATC system concepts to those envisioned for the time period 1970-1975.

INTRODUCTION

In order to study problems anticipated in connection with the introduction of the supersonic transport (SST) into the air traffic control (ATC) system, the Federal Aviation Agency (FAA) and the National Aeronautics and Space Administration (NASA) established a joint simulation program. The FAA program is a three-phase program to develop new air traffic control procedures, techniques, and concepts for handling (1) current and future supersonic military aircraft, (2) the interim (Concorde) SST, and (3) the Mach 3 SST. (See fig. 1.) The program calls for a series of simulation studies which began in May 1963 and will continue through 1966.

The objective of the dynamic simulation studies conducted was the investigation of problems anticipated in connection with the integration of the supersonic transport into the present air traffic control system. To aid in studying the problems, a supersonic transport flight simulator located at NASA Langley Research Center, Hampton, Va., and the ATC Simulator located at the FAA National Aviation Facilities Experimental Center (NAFEC), Atlantic City, N.J., were utilized. The ATC Simulator consists of 60 simplified pilot control consoles, each capable of simulating aircraft performance that duplicates performance of fixed-wing and supersonic aircraft. Each console generates primary and secondary

radar returns which can be displayed on any of the current airport surveillance, long range, and precision approach radars. It is possible to duplicate authentically a system consisting of 1 to 4 radars, 20 control displays, and 40 control positions. By means of telephone landlines connecting these facilities, projected designs of the supersonic transport and various air traffic control concepts are being tested in a real-time air traffic control environment.

The objectives of the initial phase of the program are to study the supersonic transport in the current air traffic control system to:

(1) Determine the effects of the ATC system on SST design and equipment requirements

(2) Determine the effects of the SST on ATC system requirements

(3) Provide a comparison base for further tests and for possible improvements to the SST and the ATC system

In this paper, results of studies of simulated departure and arrival operations of a variable-sweep SST configuration (NASA SCAT 16) from and to the John F. Kennedy International Airport are presented.

AIR TRAFFIC CONTROL FACILITIES

The real-time simulated ATC environment is created by means of representative air traffic control facilities. The facilities simulated consisted of portions of the New York, Cleveland, and Boston Air Route Traffic Control Centers, the New York Oceanic Control Sector, and the John F. Kennedy Approach Control and Tower complex. Figure 2 depicts the layout of the Air Traffic Control Facilities as used in these studies. These facilities were operated by 30 experienced air traffic controllers. The controllers were provided with modern TV type bright radar displays with video maps showing navigation aids, route structures, and holding pattern areas - as well as the usual flight progress strips, interphone, and radio communication equipment.

TEST DESIGN

Tests for the initial phase of the program were designed to study SST oceanic flights which arrived at and departed from John F. Kennedy International Airport. These flights traversed portions of the New York and Boston Air Route Traffic Control Centers and New York Oceanic Control Areas. Routes used by the supersonic transport are shown in figure 3. A mixed traffic sample representing conditions of high-density traffic flow (148 per hour) including 6 supersonic transports, one of which is the NASA supersonic flight simulator, was used. All traffic was under positive control of the respective facilities.

EXPERIMENTAL CONCEPTS

Tests were made in real time as follows:

(1) Concept I - High priority for supersonic transports (that is, clear track, no restrictions, delays, or holding)

(2) Concept II - No priority for the supersonic transport (current ATC system)

Concept I

Concept I was the investigation of experimental procedures for handling supersonic transports on a priority basis. Basic changes in handling were in radar and altitude-separation standards and the priority of sequencing with respect to other aircraft. Present-day standards (fig. 4) are 1,000 feet vertical or 3/5 nautical miles (N.Mi.) radar separation below flight level 290 (FL 290). Above FL 290, aircraft are provided 2,000 feet vertical separation (because of altimeter error) or 3/5 N.Mi. radar separation. Rules for applying radar separation are as follows: 3 N.Mi. radar separation if aircraft are less than 40 N.Mi. from the radar antenna site; if more than 40 N.Mi., 5 N.Mi. radar separation.

Two experimental standards tested (fig. 5) were 1,000 feet vertical or 5/10 N.Mi. radar separation to FL 230. From FL 240 to FL 540, 2,000 feet vertical or 5 N.Mi. radar separation and also 3,000 feet vertical or 10 N.Mi. radar separation were tested. At FL 550 and above, 5,000 feet vertical or 10 N.Mi. radar separation was tested.

For all ATC tests, a standard 1-minute separation standard for arrivals and departures was employed because of vortices expected with the SST. The 1-minute separation was also applied to cross runway operations, until such time as additional study may indicate a more reasonable standard.

It was assumed under Concept I that the supersonic transports were parked in a position for easy access to the runway and after "engine start" could taxi unrestricted to a runway for an immediate take-off, and after landing could proceed without delay to a parking area.

During the simulation of this concept, the following SST ground handling procedures were used:

(1) Flight plans were filed 1 hour prior to estimated time of departure (ETD).

(2) SST requested ATC clearance 15 minutes prior to ETD.

(3) ATC clearances were delivered no later than 5 minutes prior to the proposed take-off time.

(4) There was no ground delay in taxiing and no departures were released or arrivals sequenced 1 minute prior to the arrival of the SST. Departures were restricted when an SST was 8 N.Mi. out on final approach.

Arrival and departure priorities and handling under this concept were:

(1) No en route or outer fix holding

(2) Assured landings and programed departures

(3) No altitude restrictions in climb or descent

(4) Minimum radar vectoring unless to the advantage of the SST

(5) No ground delays

Concept II

Normal ramp parking was assumed and taxiing to the active runway was accomplished by using the same taxiway as other aircraft. All procedures and separation standards used were as outlined in the Manual of Air Traffic Control Procedures (AT P 7110.1A) with the following exceptions:

(1) The 1-minute standard separation for supersonic transports for vortex dissipation was used

(2) The supersonic transports had to await their turn for take-off and abide by local departure restrictions but were not held longer than 10 minutes when at the runway and ready for departure

(3) Arrival delays for supersonic transports did not exceed 30 minutes.

A 300-nautical-mile area was found to be adequate for the oceanic runs with SST arrivals entering the problem at cruise altitudes of 60,000 to 70,000 feet and at Mach 3.

It was assumed that adequate radar and communications existed throughout the area, that VORTAC facilities provided good navigational capability at all altitudes, that dual or parallel instrument landing system (ILS) approaches were authorized to permit simultaneous landings, and that an all-weather landing system existed, the latter capability particularly for the later program phases.

GENERAL PROCEDURES

Generally, departures operating under Concept I or Concept II were radar vectored to a radial of a departure route navigational aid and climbed to cruising altitude as soon as possible or as dictated by a programed profile. Figure 6 depicts a typical supersonic transport departure profile.

Generally, as depicted in figure 7, an inbound SST contacted the appropriate center sector, was identified and was decelerated to 340 knots indicated airspeed (KIAS). Then, subject to departing supersonic transports, descent was made to flight level 500 where the aircraft was decelerated to Mach 0.9 and usually occurred between Nantucket and Hampton. The supersonic transport was cleared to Deer Park (DPK) at altitudes from 15,000 to 25,000 feet. At or approaching Deer Park, a handoff was made to John F. Kennedy (JFK) Approach Control for a radar vector to the instrument landing system.

For obtaining air traffic control results, measurements were made of the following:

(1) Airport movements per hour

(2) Communications
  (a) Number of contacts
  (b) Duration

(3) Subsonic aircraft delays
  (a) Departures, ground
  (b) Arrivals, holding

(4) Supersonic aircraft delays
  (a) Departures, ground
  (b) Arrivals, holding

(5) Total SST time in system
  (a) Concept I
  (b) Concept II

Controllers, with at least 8 years of ATC field experience, manned the control sectors and positions of operation. A sufficient number of exploratory runs with different teams of controllers were used to become familiar with the procedures to be used.

AIR TRAFFIC CONTROL RESULTS

From the air traffic control measurements (figs. 8 and 9) and controllers' observations, the following results were obtained:

(1) When supersonic transports were given priority (Concept I), subsonic traffic incurred excessive radar vectors and excessive holding and ground delays. Subsonic delays were 13 percent higher in priority system Concept I than in the current system Concept II.

(2) Delays incurred by supersonic transports in the current system Concept II resulted in increasing SST time in the system of approximately 7 percent over that incurred in priority system Concept I. Some of this increase can also be attributed to the wide range of fluctuations in adherence to climb and descent profiles by SST flight crews.

(3) Airport operations per hour were reduced in the priority system Concept I. Under this concept with a theoretical possibility of 60 operations and an average current system of 55 operations per hour, the operations rate ranged from a low of 48 operations to a high of 50 operations per hour. Under the current system Concept II and the same theoretical and average figures of 60 and 55 per hour, the operation rate ranged from a low of 53 to a high of 54 operations per hour.

(4) There was no appreciable difference in the number of communication contacts with supersonic transports although duration of contacts was longer under both concepts. This condition may be attributed to controller requests to SST pilots for additional information. Voice communications appear to be adequate for SST operation.

(5) Increased airspace use and difficulty in predicting proper lateral spacing is encountered when a lead turn is not used by the supersonic transports at supersonic speeds. This condition may result in a possible increase in lateral-separation standards, an increased dependence on altitude separation, and possible changes in navigational procedures.

(6) More expeditious ATC handling of supersonic transports and subsonic traffic is possible through segregated approach and departure routes. Previous NAFEC simulation studies indicate that the combined use of an off-course computer and pictorial navigation display (PD) would provide a significant operational advantage to supersonic transports.

(7) Controller subjective opinion was that radar and altitude-separation standards in Concept I were too high and could be reduced.

PLANNED AREAS OF INVESTIGATION

There is a need for much study and research to introduce the SST into the Air Traffic Control System. The Jet Operational Requirements Panel (JORP) committee work which preceded the introduction of the subsonic jets had an immeasurable effect on the fairly smooth introduction of these aircraft. Similar early action with regard to the SST is needed to facilitate their introduction into the ATC system.

Transcontinental and overocean flights operating in the current ATC system are planned to investigate the following operational parameters:

(1) SST holding and entry into holding patterns

(2) Response time for radar vectors at various speeds

(3) ILS turn-on distances

(4) Departure performance
    (a) Straight out or turns for noise abatement
    (b) Altitude restrictions or tunneling

(5) Pictorial displays
    (a) Discrete routes for arrivals and departures
    (b) Route flexibility

(6) Airspace blocks, military missions, and air refueling

Succeeding test series will examine the SST in a 1970 ATC system having radar and flight plan tracking, alphanumerics on the controllers display, partial sequencing, and computer-assisted final approach spacing.

In the 1975 ATC system series, in addition to the 1970 system capabilities, full departure and arrival sequencing, automatic transfer of control data between ATC facilities, conflict prediction, and other sophistications will be examined.

CONCLUSIONS

As a result of preliminary tests of the supersonic transport in the present-day air traffic control (ATC) system, the following conclusions may be made:

1. Limited preferential treatment can be provided the supersonic transport (SST) without major adverse effects on the current ATC System.

2. More expeditious ATC handling for the SST is possible by provisions of segregated approach and departure routes through use of a pictorial navigation display.

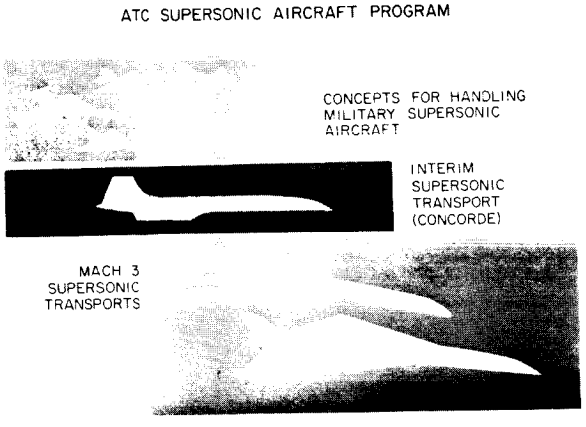

Figure 1

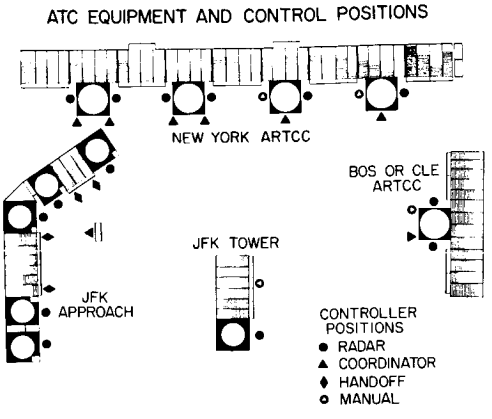

Figure 2

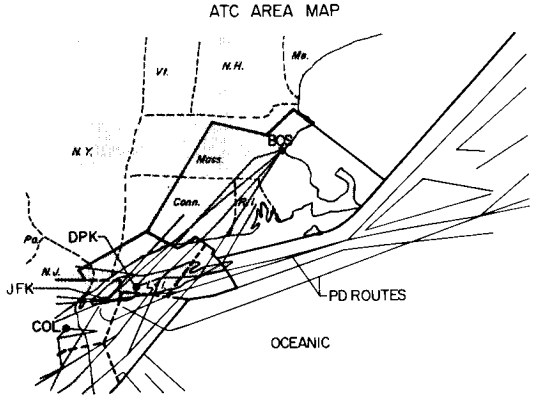

Figure 3

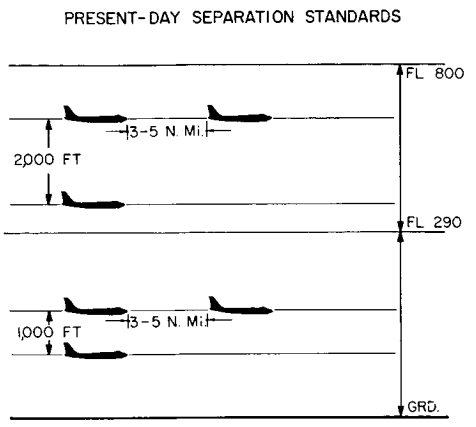

Figure 4

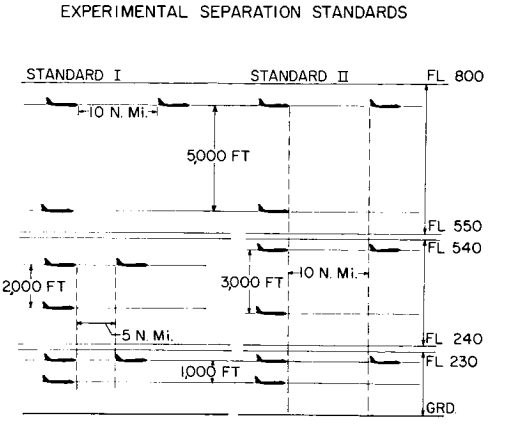

Figure 5

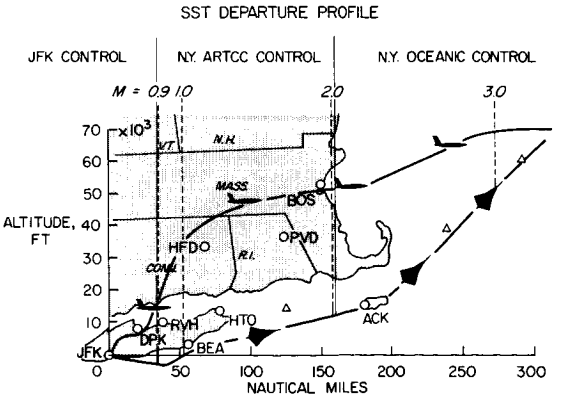

Figure 6

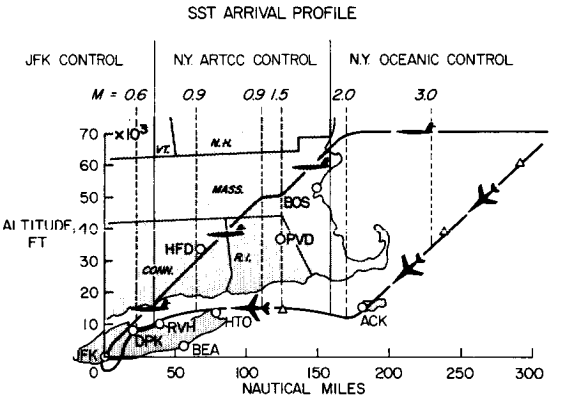

Figure 7

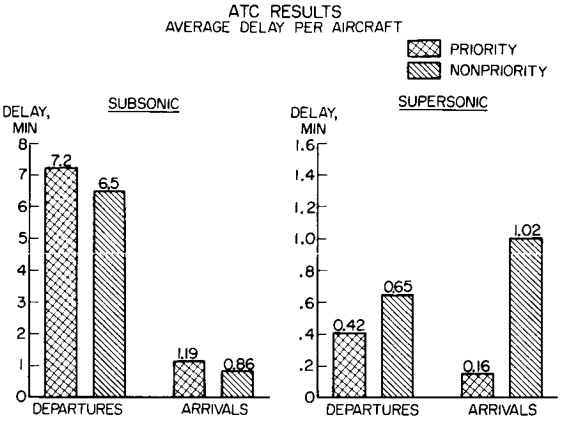

Figure 8

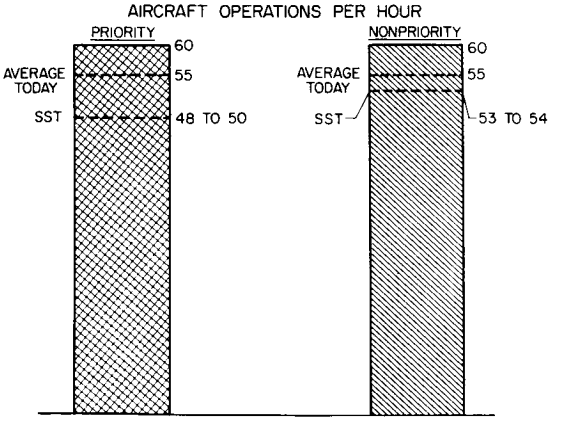

Figure 9

19. EFFECTS OF THE AIR TRAFFIC CONTROL SYSTEM ON THE SUPERSONIC TRANSPORT

By Norman S. Silsby, Milton D. McLaughlin, and Michael C. Fischer

NASA Langley Research Center

SUMMARY

A study of the problems anticipated with the introduction of the supersonic transport into the air traffic control system indicated that supersonic transport design allowances for time and fuel for maneuvering during climbouts may not be sufficient, that there is a greater communications-navigation workload for the supersonic transport than for the subsonic jet transport during descent, and that use of a flight director to command pitch control guidance for the pilot would be helpful.

INTRODUCTION

In order to study the problems anticipated with the introduction of the supersonic transport (SST) into the air traffic control (ATC) system, the National Aeronautics and Space Administration and the Federal Aviation Agency have initiated a cooperative research program.

The objectives of the program are: (1) to determine the effects of the air traffic control system on the design and equipment requirements for the supersonic transport, and (2) to determine the effects of the supersonic transport on the requirements for the air traffic control system.

EQUIPMENT AND INSTRUMENTATION

The physical layout of the simulation equipment is shown by the block diagram in figure 1. The blocks on the left represent the equipment at NASA Langley Research Center and those on the right represent the FAA equipment at the National Aviation Facilities Experimental Center (NAFEC), Atlantic City, N.J. The block at the upper left depicts the flight compartment of the SST simulator which is similar to that for a current four-place subsonic jet transport aircraft as shown in the photograph in figure 2. The flight panel instrumentation is similar to present-day displays, but with the ranges modified to cover the higher altitude and Mach number M of supersonic transport operations. The block at the lower left (fig. 1) shows the analog computers which are used to solve the six-degree-of-freedom equations of motion for an aircraft having the characteristics of the SST design under study. A photograph of the analog computer is shown in figure 3. The block on the upper right (fig. 1) depicts the

ATC facility simulator which is manned by about 30 experienced traffic controllers, as shown in the photograph in figure 4. The block at the lower right (fig. 1) depicts the air traffic sample which is made up of a mixture of supersonic transports and piston- and turbine-powered subsonic transports. This traffic sample is created by means of the radar target generators which are shown in figure 5. The purpose of the supersonic transport simulator at Langley Research Center was to provide a realistic cockpit environment for experienced airline crews and utilizing real controls and instrument displays. This simulator permitted studies of the effects of ATC on fuel and time, crew workload, and instrumentation requirements.

TEST CONDITIONS AND CONFIGURATIONS

With regard to general conditions for the tests, the simulation was conducted in real time and utilized instrument flight rules for both departures and arrivals and for both oceanic and domestic (transcontinental) operations during present-day peak-traffic conditions in the New York area. Two aircraft configurations were simulated: configuration A used a variable-sweep wing with an afterburning turbojet engine, and configuration B utilized a fixed delta wing with a duct-heating turbofan engine.

Pertinent general characteristics, as well as longitudinal control characteristics, are given in table I for the two configurations. In tests conducted to date, there have been no significant differences in the results due to differences in performances of the two configurations.

CLIMB AND DESCENT PROFILES

The ascent and descent profiles utilized in the tests, together with some operational limitations are shown in figures 6 and 7 for configurations A and B, respectively. The engine limitation and structural limitation define a corridor through which the SST must operate. For configuration A (fig. 6) after take-off and initial acceleration, ascent is made at a constant indicated airspeed of 360 knots, then follows along the 2.0-pounds-per-square-foot ground overpressure sonic-boom profile, is followed by a further accelerated climb at constant indicated speed of 570 knots to cruise altitude. The descent profile consisted of deceleration at cruise altitude to an indicated speed of 340 knots which was maintained in descent to 50,000 feet, at which altitude deceleration was continued down to a Mach number of 0.9. This Mach number was held constant in descent until indicated speed again reached about 360 knots. For configuration B, the ascent profile followed was very similar to that for configuration A except that the indicated speeds were 325 knots and 500 knots for the lower and higher altitude ranges of the ascent, respectively. The descent profile differed in that initial descent speed was 300 knots and there was no intermediate level off at 50,000 feet altitude.

DEPARTURE AND ARRIVAL ROUTES

Oceanic

The oceanic arrival routes used in the present tests are shown in figure 8. The solid straight lines are airways intersections, the circles are VORTAC radio navigational aids, and the triangles are navigational fixes. The dotted lines show two actual arrival tracks flown which were initiated at both South Bangor (SBG) and Cod (COD), with end-cruise points shown. The descents were made passing over Nantucket Island (ACK), then over Long Island, and descending into John F. Kennedy International Airport (JFK). The tracks shown were selected to illustrate that the maximum deviations from airway center lines experienced were of the order of 3 or 4 nautical miles.

Arrivals from Cod posed no significant problems.

Arrivals from South Bangor required a Mach 2.0 supersonic turn with a heading change of about 45° at Nantucket. This area at Nantucket, showing both a nonlead and a lead turn, is shown at a large scale for better detail in figure 9. The turn labeled "nonlead turn" was initiated at the intersection, and resulted in considerable overshoot and difficulty in regaining the desired route outbound because of the large radius of turn existing at this speed. Regular operation in this manner would require a wider buffer zone by ATC. The upper track shows a lead turn (ref. 1) in which the turn was initiated 15 to 20 nautical miles before the intersection in order to follow a track inside the corner and to become tangent to the desired track outbound. This lead turn is much more satisfactory from an ATC point of view. Either type of turn at supersonic speed, however, intensifies sonic booms. Tests with fighter-type aircraft have indicated amplification factors from 2 to 4. (See ref. 2.) The alternative methods of ending cruise earlier to avoid the supersonic turn would be inefficient in both time and fuel for the SST. A solution that appears desirable, however, would be to provide special straight-in high-altitude routes for the SST, the present routes not being joined until some point close to Long Island where the subsonic speeds and altitudes of the present jet transports have been attained.

The oceanic departure routes are shown in figure 10. The upper route is the standard instrument departure route, which requires two substantial heading changes - one left and one right - at transonic speeds which compromise the climb-accelerate capability. This route is undesirable from a pilot's point of view because, at the speed attained, it is essentially an "S" turn. The lower route, which was utilized as a test route, eliminated one turn but the other turn still occurred at transonic speeds. Experience with these oceanic routes made it appear desirable, when setting up transcontinental or domestic routes, to provide some experimental, straight acceleration tracks for the SST from 100 to 170 nautical miles long and beginning as close as possible to the airport.

Domestic

The domestic departure and arrival routes are shown in figure 11. Arrival routes start at Cleveland (CLE) and come in on airway J60 to Philipsburg (PSB), then over either Allentown or Yardley (ARD) to Colts Neck (COL). Two standard instrument departure routes were used: one to the north through Huguenot (HUO) airway J70 to Erie (ERI), and one to the south which was a Dutch 7 to Coyle (CYN) using the uppermost route which required a transonic turn at Coyle going out either airway J80 or to Philipsburg. The two experimental routes are shown to the south of the standard departure route on which speed was held to a Mach number of 0.9 until turns were completed to the desired route heading along which a 170-nautical-mile-long straight-accelerate track was available.

RESULTS

Maneuver Time and Fuel

Departures.- The results of maneuver time and maneuver fuel for departures for both domestic and oceanic routes are shown in figure 12. The ordinate, maneuver time, is the difference in times between that required for a straight climbout and that required in operating in the ATC system and influenced by (a) following airways, (b) radar vectoring by ATC, and (c) ATC altitude restrictions. The dotted line is the SST design ground rule currently specified in the national supersonic transport development program which provides for 5 minutes operation at 250 knots at an altitude of 5000 feet. Application of the Air Transport Association (ATA) method of calculating direct operating costs for a subsonic jet would provide 10 minutes for an aircraft of this weight and is shown by the solid line. The extent of the shading on the bar graphs represents the range from minimum to maximum values for the test runs. No bar graph appears for the oceanic experimental route because of insufficient data.

Comparison of domestic and oceanic maneuver times shows substantially greater maneuver times for the domestic routes as a whole compared with the oceanic routes. The main reason for this result is that a substantial amount of flying to the east is required before turns can be made to head westward on the domestic routes. This figure also indicates that maneuver times for the domestic routes exceed the SST design ground rule for the greater portion of the test runs. The experimental runs evidenced consistently greater maneuver times, on the average, than those for the present-day routes - the price paid for restraining speed until the straight transonic acceleration track was available in order not to focus the boom in supersonic turns.

There was little difference in maneuver fuel for the domestic and oceanic present-day routes, whereas, for the experimental routes, the maneuver fuel was somewhat greater on the average. For all routes flown, maneuver fuel for many test runs exceeded that provided by the SST design ground rule. However, for the present-day routes, the average maneuver fuel used only slightly exceeded the design ground rule allowance. On this average basis, the design ground rule appears to be adequate if allowance for cases exceeding the average is accounted for in reserve requirements.

Arrivals.- Arrival maneuver times were somewhat greater for the domestic routes than for the oceanic routes. (See fig. 13.) Part of this difference could be due to the use of different runways, but insufficient runs precluded isolating this effect. No holding times are contained in these maneuver times, but holding times varied from 0 to 14 minutes. There was little difference in maneuver fuel used between domestic and oceanic arrivals, the values averaging 3 to 4 percent of mission fuel. There appears to be no specific allowance for arrival maneuver fuel in the supersonic transport design study requirements against which to compare the measured values. Arrival maneuver fuel would, thus, have to be accounted for in the reserve fuel.

Communications-Navigation Workload

A comparison of the communications-navigation workload for the supersonic transport and for a subsonic transport for an arrival is shown in figure 14. The lower portion of the figure shows, as the ordinate, the number of operations which are defined in the upper part of the figure for various 10-minute intervals from touchdown. The bar heights indicate a substantially greater workload for the supersonic transport crew in both the 30- to 20-minute and 20- to 10-minute intervals before landing. At the lower altitude and speeds - comparable to those for the subsonic transport - the workload is, of course, about the same. Pilots' comments have been that the communications-navigation workload is high; it could be handled but continued effort toward its reduction is recommended. For departures, the communications-navigation workload for the supersonic transport was essentially the same as that for subsonic jet transports.

Operating Problems in Climb Profile

An area in which there has been one of the more interesting operating problems with the supersonic transport has been that of operation in the ascent along the 2.0-pounds-per-square-foot overpressure climb profile. (See figs. 6 and 7.) The task is made difficult with normal instrumentation displays because the pilot has no constant instrument indication to monitor in this region since Mach number, airspeed, and altitude are increasing and rate of climb is decreasing. For the initial guidance task with present instrumentation, the pilot was given about a dozen Mach number-altitude target points defining the profile. Because of the difficulty of flight-path control with this type of guidance, substantial excursions in altitude, penetrating the sonic-boom boundary, occurred. Pilots' comments were that the workload for this task was too high for routine operations. As an aid to the pilot in performing this task, the command bar of a flight director was programed to display the pitch trim required to return to the scheduled profile.

A comparison of the excursions in altitude of several SST simulator flights along the sonic-boom profile for a range of Mach numbers from about 1.2 to 2.0 utilizing the two methods described (with and without the flight director) is shown in figure 15. The figure shows that, with use of the flight director, altitude excursions are reduced from 1000 feet or more to ±300 feet on the average with an occasional excursion to 500 feet. What is not evident

from the figure, however, and what is, perhaps, even more significant are the pilots' comments concerning the difference in the difficulty of performing the task by the two methods. Whereas the pilots considered the task with basic instrumentation to be unsatisfactory for routine daily operations, with the flight director they considered the task much easier and satisfactory for daily operations.

CONCLUDING REMARKS

In initial phases of simulation tests to determine the effects of air traffic control on the supersonic transport, the following results have been indicated:

1. Supersonic transport design allowances for time and fuel for maneuvering during climbouts may not be sufficient, based on results of operations in the present-day air traffic control system in the New York area.

2. There was a somewhat greater communications-navigation workload indicated for the supersonic transport compared with that for the subsonic jet transport during part of the descent.

3. Use of a flight director to command pitch-control guidance for the pilot eased his task substantially in vertical flight-path control along the sonic-boom boundary portion of the climbout and was considered to be acceptable by the pilots for routine daily operations.

REFERENCES

1. Sawyer, Richard H.: A Simulator Study of Airspace Requirements for the Supersonic Transport. NASA TN D-1964, 1963.

2. Maglieri, Domenic J.; and Lansing, Donald L.: Sonic Booms from Aircraft in Maneuvers. NASA TN D-2370, 1964.

TABLE I.- SUPERSONIC TRANSPORT CONFIGURATIONS

	Airplane A		Airplane B	
General characteristics:				
Thrust weight ratio at take-off with no afterburner, $(T/W)_{TO}$	0.32		0.32	
Minimum transonic acceleration, ft/sec^2	1.6		1.4	
Wing loading, lb/sq ft	107		56	
Longitudinal control characteristics:				
Mach number	0.4	3.0	0.4	3.0
Longitudinal control force required for lg, lb	20	20	9	27
Elevator deflection required for lg, deg	2.5	4.5	4	14
Longitudinal short-period oscillation, sec	5.7	6.3	3.3	4.2
Cycles to half-amplitude	0.17	0.16	0.11	0.37

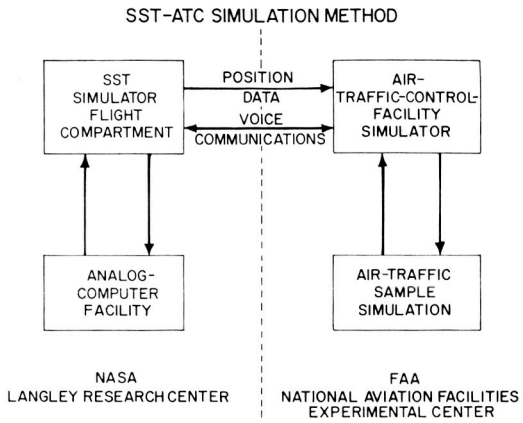

Figure 1

LANGLEY FIXED-BASE SST SIMULATOR COCKPIT

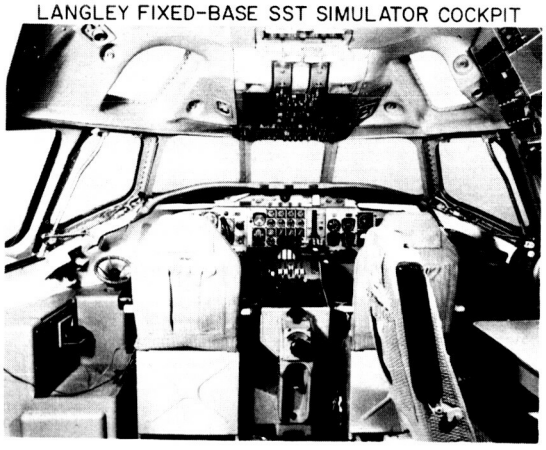

Figure 2 L-64-1743

ANALOG COMPUTER

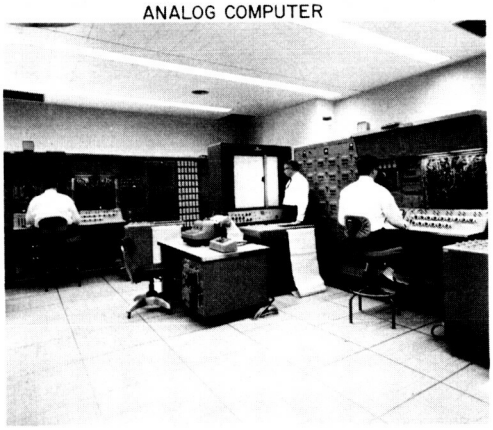

Figure 3 L-64-2220

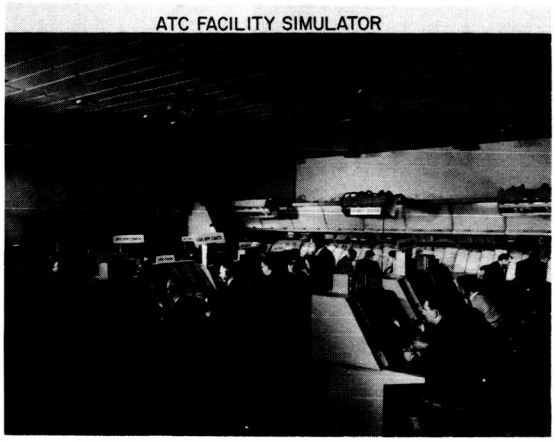

Figure 4 L-64-3249

Figure 5 L-64-3251

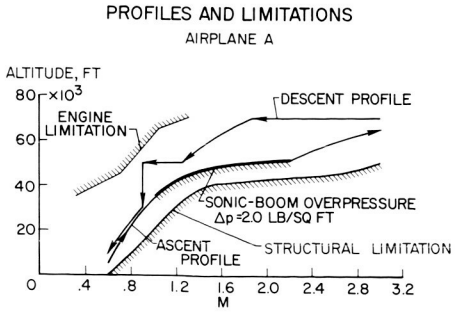

Figure 6

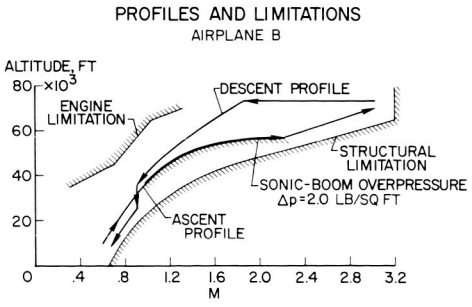

Figure 7

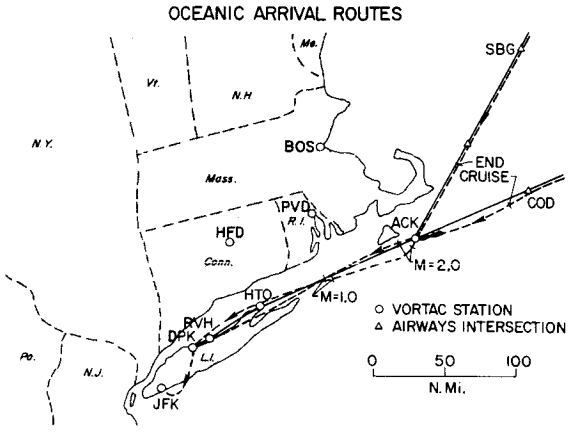

Figure 8

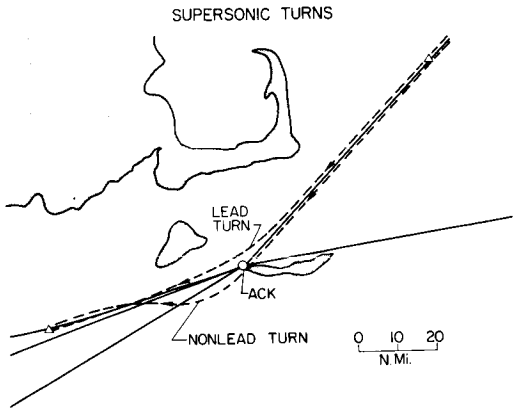

Figure 9

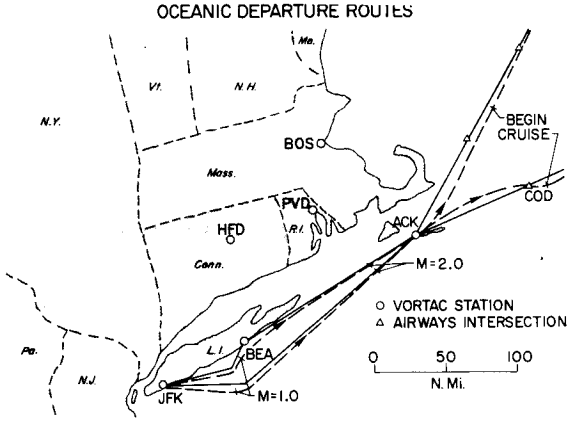

Figure 10

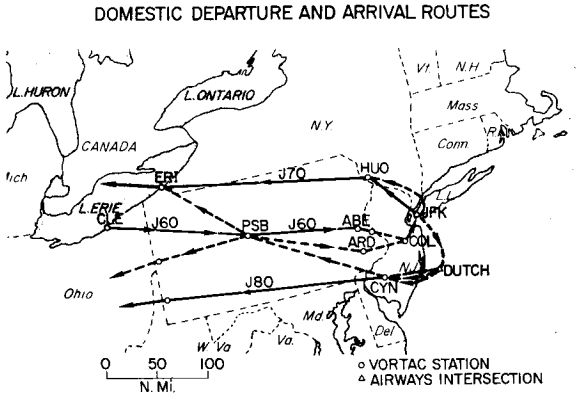

Figure 11

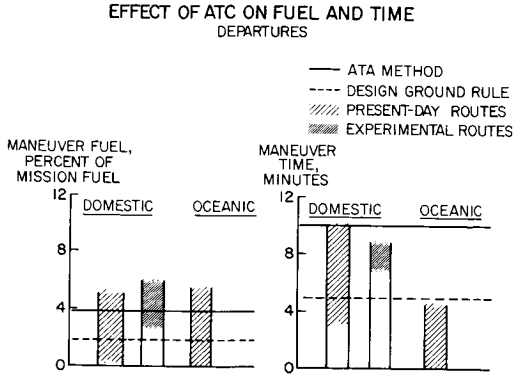

Figure 12

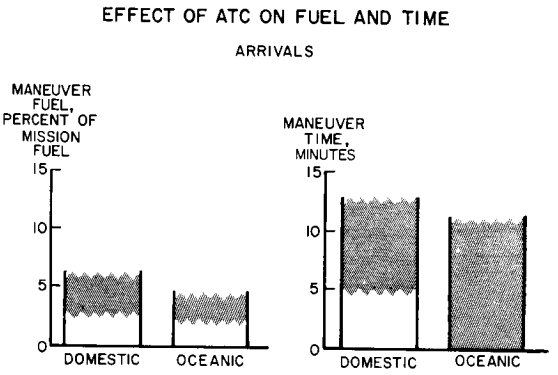

Figure 13

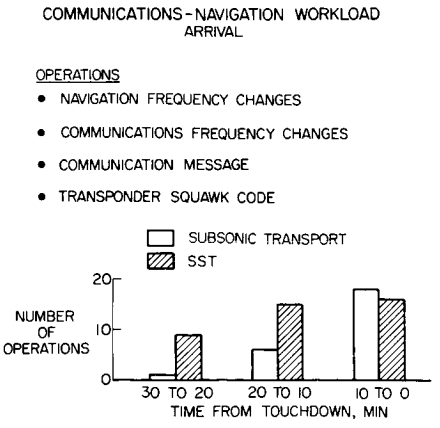

Figure 14

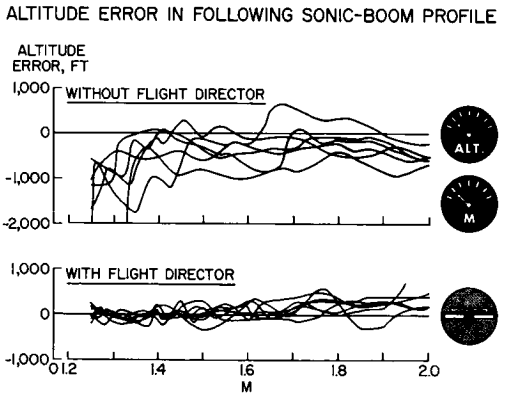

Figure 15

20. REVIEW OF THE XB-70 FLIGHT PROGRAM

By Thomas R. Sisk, Kirk S. Irwin, and James M. McKay

NASA Flight Research Center

SUMMARY

Although the major NASA research effort is directed toward XB-70-2, which will not enter its flight program until the summer of 1965, a limited amount of information is available from the early flights of the XB-70-1 airplane.

Initial take-off and landing performance data have generally substantiated predictions and indicate no unforeseen problems for this class of vehicle. Vertical velocities at impact are of the same order of magnitude as those being experienced by present-day subsonic jets. The XB-70 distances from brake release to lift-off graphically illustrate the advantage of the increased thrust-weight ratio of the supersonic cruise vehicle. The landing loads are well within the design limits up to the highest vertical velocities encountered to date, and recorded data show the response at the pilot station to be somewhat greater than that recorded at the center of gravity. Persistent shaking has been encountered in flight at subsonic speed. The cause of the excitation is not known at present but the oscillation does not appear to be conventional buffeting. The oscillation occurrence drops off appreciably at supersonic speeds and can be correlated with atmospheric turbulence. The stability and control characteristics at subsonic speeds appear satisfactory with stability augmentation on and off. A longitudinal trim discrepancy from predictions has been noted in the transonic region which appears to be decreasing with increasing supersonic speed. The supersonic handling qualities are considered adequate with stability augmentation off; however, sensitive lateral control has resulted in small pilot-induced oscillations.

INTRODUCTION

The XB-70 is a large, supersonic cruise vehicle with the performance and flexibility representative of the supersonic transport and, as such, can contribute information toward the design and development of the SST as well as other future supersonic and hypersonic cruise vehicles.

Because of the NASA role in technical support of the national supersonic-transport effort, and in recognition of the potential contributions of the XB-70 aircraft to development of the supersonic-cruise concept, the NASA began formulating a research program around this aircraft in 1962. A review of the military XB-70 program by NASA personnel at that time showed that it was desirable to supplement the program in several areas to achieve maximum benefits. The NASA arranged to have instrumentation installed (primarily on XB-70-2) to augment the basic airplane instrumentation and permit investigation of these

areas in some detail. An outline of the NASA research program and the prime vehicle for each investigation is shown in the following table:

Research area	Airplane	Investigation
Flight control	1 and 2	General handling qualities Stability derivatives Control-system evaluation
Performance	1 and 2	Air-induction system Induction-system—engine interaction Performance and mission analysis Operational margins
	2	Skin-friction evaluation Base pressure study
Structural loads	1	Landing loads Panel response
	1 and 2	Flight loads
	2	Boundary-layer noise
Environmental	1	Sonic boom Take-off and landing noise
	2	Vehicle internal environment Crew biomedical

These investigations cover some of the fundamental flight-control, performance, and structural-loads aspects of a large, Mach 3 cruise vehicle. Definition of the environmental problems, such as sonic boom and take-off and landing noise, will be obtained in the course of the other investigations.

Although the major NASA research effort is directed toward XB-70-2, which will not enter its flight program until late in the summer of 1965, a limited amount of information is available at this time from the program for XB-70-1. It is the purpose of this paper to review the flight program to date and present some of the preliminary results from the first nine flights. Among the items to be discussed are handling qualities, take-off and landing performance, and landing loads. The data on take-off and landing noise are presented in paper no. 10 by Tanner and McLeod.

Before proceeding with the discussion of program results, some information regarding the size of the airplane would be helpful. Figure 1 illustrates the size of the XB-70 as compared with a Boeing 707-320 airplane, referenced to a common main-gear location, and shows the fuselage to be 32 feet longer than the 707 whereas the wing span, because of the delta configuration, is some 40 feet

less. The XB-70 stands 20 feet to the pilot's eyeball as opposed to 14 feet for the 707 with the airplanes in the three-point attitude. Note the cockpit overhang distance ahead of the main and the nose gear of the XB-70 compared with the conventional subsonic jet.

DISCUSSION

Program Status

The status of the program of the XB-70-1 airplane is summarized in figure 2 which shows the maximum points reached on each flight in terms of Mach number and altitude. Lines of constant dynamic pressure and a typical subsonic jet operating envelope are superimposed on this chart as points of reference. Supersonic flight was achieved for the first time on flight 3. The highest point reached to date is Mach 2.43 at 64,500 feet, attained during flight 11. Flights 6 and 9 were terminated prematurely because of various systems difficulties. The flight program to date has expanded the performance envelope as rapidly as possible, consistent with flight safety. These early flights have concentrated on flutter and vibration testing and basic airworthiness and systems evaluation. Considerable engine and inlet dynamics work is being performed at the higher Mach numbers. In general, the airplane has performed well and the program has progressed rapidly.

Take-Off and Landing Performance

One area of interest in which the XB-70 is already shedding information concerns the take-off and landing characteristics of supersonic cruise vehicles.

Figure 3 shows the take-off performance obtained to date in terms of lift-off velocity and distance from brake release. The velocity is plotted against wing loading and the distance from brake release is presented as a function of the thrust-weight ratio. Data for a Boeing 707-320C intercontinental are included to provide a familiar point of reference. The XB-70 lift-off velocities are not unusually high when it is remembered that the airplane was designed as a weapons system and did not take advantage of the most favorable wing loadings for low-speed operation. Note that the heavier XB-70 take-offs have approached the operational wing loading of the swept-wing 707. The XB-70 distances from brake release, on the other hand, present the same order of magnitude as the 707 even though the XB-70 has very nearly twice the gross weight of the 707. This plot graphically illustrates the advantage of the increased thrust-weight ratio of the supersonic cruise vehicle. The initial XB-70 flights indicate that take-off performance of a supersonic cruise vehicle poses no unusual problems.

Several points concerning the landing performance are made in figure 4. The upper portion of the figure shows the touchdown velocity as a function of wing loading and, again, Boeing 707-320C data. The XB-70 touchdown velocities are high, which is not surprising considering the newness and experimental nature of the aircraft. The second highest point represents a touchdown on

the dry lakebed where there was unlimited roll-out distance, whereas the minimum-speed touchdown was made at Palmdale Airport where the pilot made an effort to get the airplane on the runway as early as possible. This range of touchdown velocity at approximately the same wing loading indicates that, in general, the airplane is not landing at its minimum speed and, therefore, some decrease in the touchdown velocity can be anticipated as the landing operation becomes routine. The extreme right-hand point was achieved on flight 9 when systems difficulties forced an early landing. It is interesting to note that the touchdown velocity was not significantly higher than for the lower wing-loading landings; however, the pilot did bounce this one.

The fact that the XB-70 uses a drag chute in place of thrust reversers makes a roll-out-distance comparison meaningless and these data are not shown. Instead, the vertical velocities at touchdown as a function of touchdown velocity are shown in the lower portion of the figure. Included in this figure are the results of a statistical analysis for 331 landings of subsonic jet transports at New York International Airport as reported by Stickle in 1962 in reference 1. The mean vertical velocity for these landings was found to be 1.8 feet per second while the maximum was 4.7 feet per second for touchdown airspeeds between 104 and 150 knots. These data show that a statistical boundary for 95 percent of all landings will be less than 3.5 feet per second. Although the XB-70 data are extremely limited, it is interesting to note that they are about the same level as the data of reference 1. Also noteworthy is the fact that the landing studies in which the XB-70 fixed-base simulator was used produced appreciably higher vertical velocities than are actually being experienced in flight.

From the landings to date, it may be noted that the anticipated problems associated with pilot location at main-gear contact have not materialized. In the XB-70, the pilot is 106 feet ahead of the main gear and approximately 38 feet in the air at main-gear contact for a landing at a 10° angle of attack. These distances are nearly twice those of present-day subsonic jets. The XB-70 pilot has stated that landing visibility is acceptable (about like that for a B-58) and his location at main-gear contact has little detrimental effect on height judgment. The pilot has commented that although the XB-70 is a relatively easy airplane to land, it appears that a great deal of practice will be required before precise touchdowns on the first 1000 feet of runway at predetermined speeds can be made. It would be well to remember that the XB-70 pilot enjoyed the assistance of chase aircraft calling out height above the runway for these landings.

A look at the glide slopes of four early landings on the Edwards Air Force Base runway has shown them to average approximately 2°, slightly lower than the standard ILS glide slope. The altitude at runway threshold for these four landings was just under 20 feet and the average touchdown distance was less than 1900 feet from the end of the runway. As mentioned for take-off, it would appear that the landing performance of the supersonic cruise vehicle is not likely to offer a problem.

Landing Loads

It is appropriate at this point to summarize the results of the landing-loads investigation to date. The landing-loads evaluation is limited to the XB-70-1 airplane because this aircraft has strain-gaged landing gear. The landing gear has been instrumented to measure loads, deflections, and accelerations, and accelerometers have been installed at the airplane center of gravity and the pilot station to measure the dynamic response at these fuselage locations. Additional instrumentation for the NASA landing loads and dynamics investigation includes three cameras to record the behavior of the main and the nose gear during touchdown, a down-pointing camera for a measure of the drift angle, trailing-arm devices installed on each main and nose gear to measure the sinking velocity at landing, and magnetic pickups to measure the wheel rotational velocities and accelerations during the spin-up.

Figure 5 shows typical landing loads experienced for all landings where data have been recorded. The upper portion of the figure presents the ratio of measured peak gear loads to the design load as a function of vertical velocity at touchdown. It is significant that up to the highest vertical velocities encountered, the loads are well within the design limits.

The solid symbols at the left of the figure indicate the magnitude of nose-gear loads at nose-gear impact. Note that nose-gear vertical velocities have been on the order of 1 foot per second or less, showing the excellent control available after main-gear contact.

A consequence of the landing impact on the fuselage is shown in the lower portion of the figure. In this figure, normal acceleration at two fuselage stations, the center of gravity and the pilot station, is given as a function of vertical velocity. These data show the response at the pilot station to be somewhat greater than that recorded at the center of gravity. It is interesting to note that even with average accelerations of $1\frac{1}{2}g$ at main-gear impact, the pilots have indicated that they have not been sure of main-gear contact for a number of these landings. The solid symbols in this portion of the figure again represent nose-gear impact and show the pilot-station and center-of-gravity response to be of the same order of magnitude as the response to main-gear impact.

Landing loads on the XB-70 will be measured in a continuing effort to permit evaluation of gear loads and upper fuselage response for a complete range of gross weights. Special effort will be directed toward obtaining loads incurred during taxiing for comparison with predictions.

Oscillation Characteristics

It has been emphasized in this paper that the XB-70 is a large, flexible aircraft and it is of interest to note that persistent shaking has been encountered in flight at subsonic speed. Figure 6 presents a summary of acceleration data obtained during the first nine flights. Although the figure may

raise more questions than it answers, it does provide a basis for comments on a number of important points.

The lower portion of the figure presents the flight envelope covered to date in terms of altitude and Mach number. The degree of shading indicates the percentage of time that fluctuating normal-acceleration levels were measured with a recorder located near the center of gravity. (Similar amplitudes were obtained at a location near the cockpit.) The upper portion of the figure is a companion plot of half-amplitude of oscillating normal acceleration.

Note that the airplane experiences a persistent shake, or oscillation, over the subsonic speed range to a Mach number of approximately 0.85. This oscillation varies from ±0.03g at the higher subsonic Mach numbers to more than twice that value at the lower speeds as shown by the curve in the upper portion of the figure. Oscillations of larger amplitude than this level have been measured and are indicated by the symbols in this figure. The oscillation has a predominant frequency of 12 cps at the center of gravity and 2.5 cps at the cockpit. (The first bending mode of the fuselage is approximately 2.5 cps.) The periodic nature of the oscillation, coupled with its failure to show significant trends with lift coefficient, indicates that it is not conventional buffeting. The cause of the excitation is not known at present. The pilot has reported that these oscillatory conditions have not degraded airplane handling qualities.

The oscillation occurrence drops off to 25 percent above a Mach number of 0.85 and, above 1.6, it is reduced to the point that disturbances are recorded in less than 10 percent of the total flight time for flight conditions of mild turbulence. It has been noted that the XB-70 crew report a significantly greater turbulence severity than is reported for the B-58 and other chase planes flying through the same air mass.

Additional emphasis is being placed on this study to determine the cause of the subsonic vibration. Later studies will also determine the conventional buffet boundary as well as examine response to turbulence in some detail.

Handling Qualities

The primary objective of the program to date has been to expand the performance envelope as rapidly as possible, and a minimum amount of time has been spent in obtaining systematic stability and control data. A gross picture is beginning to emerge, however.

Neither take-off nor landing with stability augmentation off presents a problem, and trim changes with canard-flap and gear actuation are small. Low-speed handling qualities are satisfactory with stability augmentation off. Pitch and yaw control are both excellent whereas the initial roll control appeared sensitive. The pilot reported that lateral control was lighter than on most large airplanes. This lateral-control sensitivity has been improved on the later flights by doubling the bungee force.

The transition from subsonic to supersonic flight has shown two interesting points. The first concerns the somewhat surprising amount of trailing-edge-down elevon deflection required for trim in this flight region. This trim requirement is noted on figure 7 which shows the variation of trim elevon deflection with Mach number. It may be seen that almost 8° of increasing trailing-edge-down elevon deflection is required as the Mach number increases from 0.9 to 1.1. The fact that model tests did not predict this magnitude of pitching-moment change is shown by the dashed "Predictions" curve. The large trailing-edge-down trim requirement is most pronounced in the transonic and low supersonic regions as shown in figure 8. This figure presents the difference between the actual longitudinal trim requirement and the predicted values $\Delta\delta_{e_{TRIM}}$ over the supersonic Mach number range and shows the actual values to be approaching predictions at the higher speeds.

The exact cause of the trim discrepancy is not known at this time. It is expected that stability-derivative investigation during the flight-control research (shown in table in introduction) will shed additional light in this area.

The second point concerns the low static lateral directional stability characteristics with the 0° tip deflection where sluggish airplane response to corrective rudder results in an apparent rudder reversal. This marginal stability is attributed to the large adverse yawing moment produced by the ailerons which is magnified by the trailing-edge-down trim requirements discussed. Drooping the tips to 25° improved this characteristic and fixed the initial tip-droop schedule at a Mach number of 0.95.

The wing tips are deflected to the full-down position at a Mach number of 1.4. Longitudinal and lateral trim changes with wing fold are small and easily controllable.

The supersonic handling qualities are considered adequate with stability augmentation off; however, the initial sensitive lateral control characteristics resulted in small pilot-induced oscillations. The pilot reports less tendency to overcontrol in roll with the increased lateral-control force gradients.

The XB-70 presents satisfactory characteristics with stability augmentation on. There are insufficient data at this point to evaluate the benefits of stability augmentation properly but, on the basis of limited flight data, it would appear that the requirements would be dictated by crew comfort rather than flight safety.

The handling-qualities program will get underway in earnest on airplane XB-70-2, where all facets of the stability and control picture - including the effects of flexibility on the control system characteristics and derivatives - will be studied.

CONCLUDING REMARKS

A review of the initial flight results available from the XB-70-1 shows that, in general, the airplane has performed well, achieving a Mach number of 2.43 at 64,500 feet in 11 flights in less than four calendar months of flight time.

The results obtained to date on the XB-70-1 airplane are providing preliminary information pertinent to a number of research areas of interest to designers of supersonic cruise vehicles. Moreover, these limited data have been sufficient to assure the United States Government of the research potential of the XB-70 flight program which will be expanded in the next several years.

REFERENCE

1. Stickle, Joseph W.: An Investigation of Landing-Contact Conditions for Several Turbojet Transports During Routine Daylight Operations at New York International Airport. NASA TN D-1483, 1962.

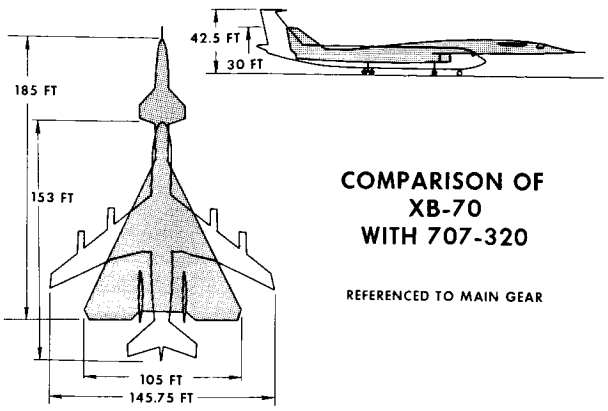

Figure 1

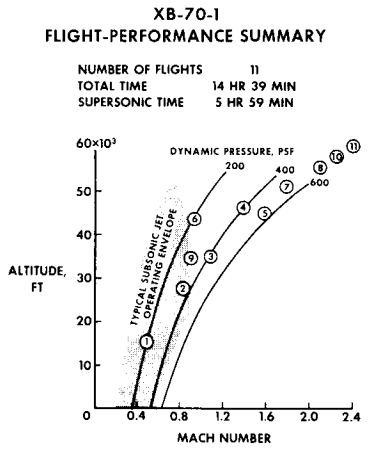

Figure 2

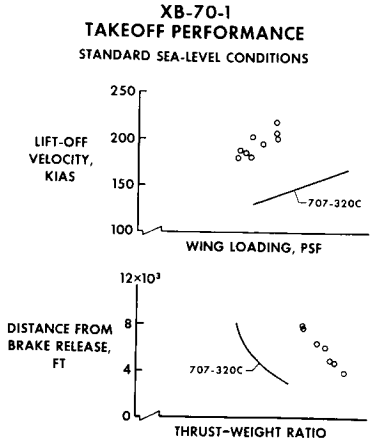

Figure 3

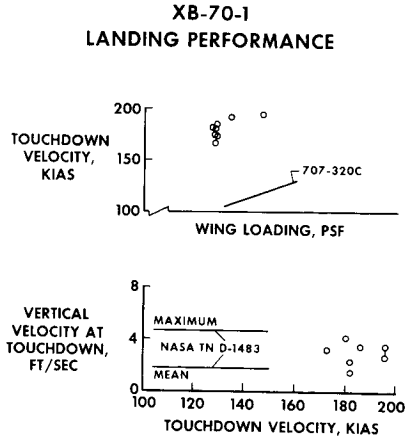

Figure 4

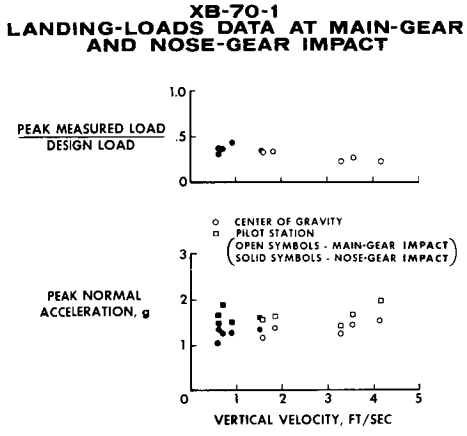

Figure 5

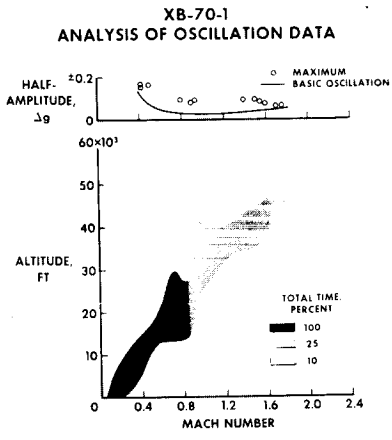

Figure 6

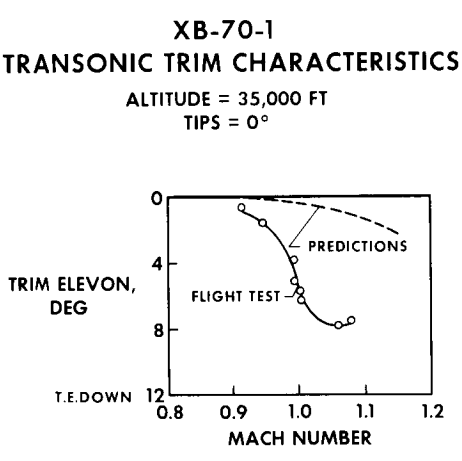

Figure 7

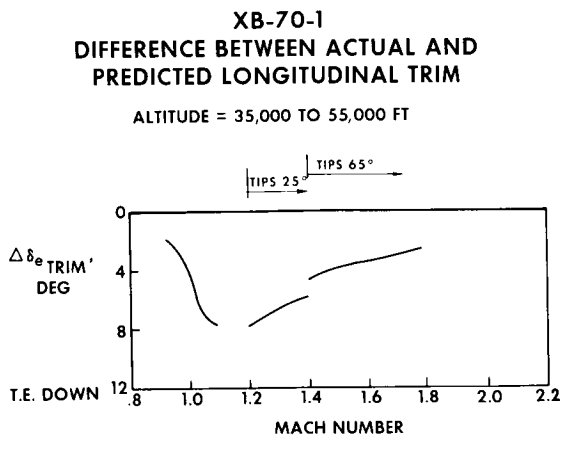

Figure 8

21. CONSIDERATION OF FUEL REQUIREMENTS FOR SUPERSONIC TRANSPORT OPERATION

By Joseph W. Stickle

NASA Langley Research Center

SUMMARY

An analysis of the interaction of operational environment and aircraft characteristics of the supersonic transport (SST) in the areas of design-range and reserve-fuel requirements has been made. Design-range requirements are considered in relation to the effects of wind, temperature, flight-level assignment, and payload variation. An approach toward combining en route and holding reserve requirements while maintaining protection equivalent to that provided subsonic jet transport operations by the present civil air regulation en route plus holding reserves is given. This approach results in a savings in reserve fuel over that required by separate requirements.

INTRODUCTION

There are a number of factors, both environmental and operational, which will affect the fuel requirements of the supersonic transport. A complete understanding of the effects of these factors will not be attained until the aircraft has been in service for some time. Nevertheless, it is necessary to anticipate and account for these factors to the fullest extent possible where they may have an important bearing on the design and ultimate capabilities of the aircraft.

The purpose of this paper is to examine, by using a statistical approach, the interaction of operational environment and aircraft characteristics in the areas of design range and fuel reserves.

The design range is considered in relation to the effects of wind, temperature, flight assignment, and payload variation. Reserve-fuel considerations include en route reserves (accounting for various uncertainty factors in planning mission fuel), holding reserves, and fuel for diversion to an alternate airport. Fuel allowance for en route engine failure is also discussed in relation to the more normal operational reserve requirements.

DESIGN RANGE

The design range, or fuel-carrying capability, of the supersonic transport should provide a rational margin to allow for likely variations of those factors which a dispatcher must account for in planning mission fuel. Here, mission

fuel is considered to be only the fuel required to fly to and land at the destination. Because design range of an aircraft is normally based on standard-day no-wind conditions, the effects of weather and operational factors are expressed in terms of the additional standard-day range increment required over and above the basic trip range. For this analysis, the basic range is taken to be from New York to Paris or 3160 nautical miles.

Atmospheric Effects

One of the primary factors to be accounted for in determining mission fuel is the expected atmospheric conditions en route, that is, winds and temperatures. The statistical characteristics of the east-west effective wind component and temperature differences from the 1962 standard atmosphere are shown for the winter season, December to February, and the summer season, June to August, in table I. The effective means and standard deviations are shown separately for climb and descent and for cruise. The winds and the variability are considerably greater in the winter, particularly at cruise altitudes, than in summer. The summer mean temperatures are warmer, as could be expected, but the standard deviations are somewhat less than in winter.

The increment of still-air range required to account for the effect of wind is, of course, the product of the wind velocity and the flight time. Primary consideration is given to the westbound flights to account for the adverse effects of prevailing head winds.

The effects of temperature were calculated for a Mach 3 supersonic transport configuration having representative climb and cruise performance. In the cruise condition, when the temperature varied above standard, the cruise Mach number was reduced to maintain a constant standard-day Mach 3.0 stagnation temperature.

Both the wind and temperature variations have approximately Gaussian, or normal, distributions. Since the effects of wind and temperature on the incremental range required are nearly linear throughout the range of conditions of interest, the corresponding distributions of incremental range required are also normal. Therefore, the combined effects of wind and temperature were incorporated in the probabilities of requiring given range increments by the usual methods applicable to normal frequency distribution.

Figure 1 gives a comparison between summer and winter of the combined effects of wind and temperature on the design-range requirement. The results indicate that a greater range increment will be required in summer than in winter (the primary reason being the reduced cruise Mach number associated with above-standard temperatures). For example, under summer conditions, about 390 nautical miles is required to compensate for wind and temperature for all but 1 percent of the westbound flights. Under winter conditions, the range increment for the same probability level would be about 320 nautical miles. Therefore, the summer condition is assumed in the following discussion of the effects of other factors. The 1-percent probability level will also be

retained, but only for purposes of illustration. It is not within the scope of this analysis to suggest the probability level that should ultimately be selected for design.

Altitude Assignment

The next factor to be considered is that of altitude assignment. Thus far, it has been assumed that all flights would be made at the optimum cruise altitude. It is very likely, however, that the supersonic transport, as is the case with present jet transports, will, at times, be assigned to flight levels other than optimum. For the purposes of this analysis, three assumptions were made concerning the supersonic transport traffic flow and the effect of off-optimum flight-level performance. These assumptions were:

(1) Three flight levels would accommodate all the one-direction SST traffic, separated, as at present, by 4,000-foot increments.

(2) One-half of the westbound flights would be made at the optimum flight level and the remaining flights distributed 4,000 feet above and below optimum.

(3) The range increment required to compensate for deviations from optimum is the same for flights above optimum as for flights below optimum.

Figure 2 shows the effect of requiring three flight levels to accommodate the westbound SST traffic under summer conditions. The corresponding curve for all flights at optimum from the previous figure is shown for comparison. Again, with the 1-percent probability level, the results indicate that, if three flight levels are required, the increment in design range over and above the basic trip distance should be about 550 nautical miles or about 160 nautical miles greater than if all flights could cruise at optimum.

Payload Variation

The last factor considered in design-range requirements is that of payload variation. In the preceding discussion of the effects of weather and flight-level assignments, it was assumed that a full payload was carried on all flights. However, a 100-percent load factor, for passenger payload at least, is not a practical goal because of the variability in demand for accommodations. Therefore, unless the assumption can be made that the variability in passenger payload can be compensated for by providing excess cargo capacity in the airplane and standby cargo at the airport, the overall load factor will, at times, be substantially less than 100 percent. Average load factors for the SST have been variously estimated between 55 and 70 percent. In this analysis, a mean load factor of 60 percent with a 12-percent standard deviation was chosen. The effects on range capability of the variations of take-off gross weight resulting from this varying payload were computed and combined statistically with the effects of summer wind and temperature conditions and variation in flight-level assignment discussed previously.

The overall effect of these factors on the probability of requiring additional range capability is shown in figure 3. For comparison, the probability curve from figure 2 for the corresponding full payload case is given. For the 60-percent mean load factor, a design range increment of approximately 395 nautical miles should be sufficient for all but 1 percent of the summer westbound flights; whereas, with 100-percent load factor, the range requirement would be about 550 nautical miles at the same probability level.

RESERVE-FUEL REQUIREMENTS

There are a number of factors which introduce some uncertainty in the determination of en route or mission fuel. These factors, together with estimated standard deviations from their predicted values and the corresponding variabilities calculated for en route fuel requirements, are listed in table II. The standard deviation of incremental fuel requirement due to each factor is shown as a percentage of the planned mission fuel. It is indicated that the effect of variations between forecast and actual wind velocity is relatively small for the supersonic transport; whereas, for the subsonic jet, uncertainty in accounting for wind effects has been indicated to be the primary factor contributing to en route reserve requirements. The largest factor for the supersonic transport indicated in table II is the variability in specific fuel consumption. The estimate of 4-percent standard deviation for each engine is one-third greater than values that have been used for subsonic jet engines. This estimate allows for the possibility of more variability with the more complex supersonic engines. With four engines, the overall standard deviation in fuel consumption (hence, the fuel consumed) reduces to 2 percent. The second largest factor indicated in table II is drag variation. This variation is assumed to have a standard deviation of 1.5 percent and is based on observations of speed variations for subsonic transports. The last three factors under the label of en route deviations include deviations from a planned flight profile resulting from air traffic control (ATC), weather avoidance, navigation error, and, in the case of deviations during climb, include the pilot's ability to adhere to a given speed-altitude climb schedule. The climb deviations were recorded deviations in climb fuel as experienced on the Langley fixed-base SST simulator while operating in the joint NASA-FAA supersonic-transport—air-traffic-control program. The vertical cruise deviations are considered as being deviations from the flight-plan cruise altitudes. However, because these deviations normally occur in discrete altitude changes rather than as continuous deviations, it is necessary to treat them separately from the en route factors. The inclusion of vertical cruise deviations in the reserve requirement will be discussed in the section on combined en route and holding requirements. The combined standard deviation of the en route reserve factors amounts to 2.73 percent of the planned mission fuel.

Combined En Route and Holding Requirement

It is apparent that protection in the form of en route reserves is required to allow for those occasions in which the actual en route fuel exceeds the planned en route fuel. On other flights, however, this added fuel would not be

required and would be available as holding fuel at the destination. It would appear logical, therefore, to consider these two reserve requirements together, with the ultimate objective of limiting to a reasonable frequency the need for diversion to an alternate airport because of fuel-limited holding time. To this end, holding-time statistics have been obtained for arriving flights into John F. Kennedy International Airport during the month of May 1963. These data indicate that approximately 37 percent of the arriving flights during this period were delayed - with mean delay of just over 7 minutes. The frequency distribution of these delays was fitted as nearly as possible with the positive half of a normal distribution and the fuel consumption corresponding to these holding times was calculated for two SST configurations. These data were then combined with the previous en route statistics to form probability distributions of exhausting given amounts of reserve fuel.

In the previous discussion of en route reserve factors, the vertical cruise deviations were not included in the combined standard deviation of en route factors. To account for the vertical cruise deviations, the following assumptions were made:

(1) Three flight levels were considered sufficient to accommodate the one-direction SST traffic.

(2) One-half of the flights would be flight planned at the optimum flight level and the remaining half, 4,000 feet above and below optimum.

(3) The maximum deviation from the optimum flight level would be ±6,000 feet.

(4) The frequency distribution of deviations from flight-plan altitudes for subsonic transports operating over the North Atlantic Ocean would be representative of the deviations to be experienced on SST aircraft.

By considering these assumptions, a frequency distribution of deviations from flight-plan altitudes obtained for 417 flights of commercial jet transports operating over the North Atlantic was applied to the three flight levels to obtain the percentage of total flights flown at the optimum altitude and at each 2000-foot increment from optimum. From these percentages and the corresponding added fuel required for each altitude increment, the aforementioned combined en route and holding probability distributions were plotted for each altitude increment and the probabilities were summed together for given values of combined reserve fuel. The total probability distributions of exhausting given amounts of combined en route and holding reserve, including the vertical cruise deviations, is shown in figure 4 where $\Delta W_F/W_{MF}$ is the ratio of the increment in fuel to the total mission fuel. The shaded area represents the spread obtained by including two SST configurations; the dashed curve represents the probability distribution calculated for a subsonic transport and is used in establishing a fix on a probability level suitable for the SST reserve requirement; the vertical dashed line is the calculated civil air regulation en route plus holding reserve for the subsonic transport. It is the intersection of the vertical line with the probability distribution for the subsonic transport that indicates the probability of equaling or exceeding the civil air

regulation reserve. This level (on the order of 1 flight in 800 being required to deviate to an alternate because of fuel-limited holding time) is assumed to be acceptable. The percentage of mission fuel corresponding to the same probability level for the SST aircraft, ranges from 13.25 percent to 14 percent, depending upon the configuration. The total reserve fuel would then be the sum of the combined en route and holding fuel and the fuel required to divert to an alternate airport.

Two-Engine Failure

The final consideration given to reserve fuel is the fuel allowance for a two-engine failure. According to present regulations, should two engines fail simultaneously anywhere along the flight path, sufficient fuel must be provided to proceed to an adequate alternate. If the remaining mission fuel at the time of failure plus the reserve fuel is not sufficient to meet this requirement, the reserve fuel would, in effect, be determined by the two-engine failure cone.

In figure 5, the two-engine subsonic range remaining for a supersonic transport is shown plotted against distance from take-off. In these calculations, a 260-nautical-mile alternate, in combination with an en route and holding reserve of 13.25 percent, was used.

The two dashed 45° lines represent the distance for either returning to the origin or proceeding to the destination. The lower boundary indicates the distance to the nearest adequate alternate airport along the route from New York to Paris. Inasmuch as the range remaining for the SST is above the two dashed lines, it would, in fact, remain within range of either the origin or the destination in the event of a two-engine failure. Therefore, the reserve fuel provided is shown to be sufficient for this requirement.

CONCLUSIONS

The analysis of operational factors in relation to fuel requirements for the supersonic transport has indicated the probabilities of requiring additional design-range capability above the basic trip distance to allow for the effects of atmospheric variations, flight-level assignments, and payload variation.

It is shown, for example, that, with all the factors considered and the assumptions used, an addition of about 395 nautical miles to the basic trip distance from New York to Paris would be sufficient to permit acceptance of all payloads offered except for 1 percent of the flights.

In the area of fuel reserves, it was found that, depending upon the configuration, between 13.25 and 14 percent of the mission fuel would provide equivalent protection to that given subsonic jet transport operations by the combined civil air regulation en route and holding requirements.

It was also found that these reserves, in combination with a planned 260-nautical-mile alternate, would provide ample fuel to proceed at subsonic speeds to an adequate airport in the event of a two-engine failure anywhere en route from New York to Paris.

TABLE I

VARIATION OF ATMOSPHERIC CONDITIONS FROM 1962 STANDARD

SEASON	FLIGHT PHASE	WIND VELOCITY, KNOTS		TEMPERATURE, °F	
		MEAN	STANDARD DEVIATION	MEAN	STANDARD DEVIATION
WINTER	CLIMB AND DESCENT	37 W	±22	-4.3	±10.6
	CRUISE	31 W	±22.6	-2.6	± 9.0
SUMMER	CLIMB AND DESCENT	26 W	±19	4.5	± 8.9
	CRUISE	4 W	±7.7	11.0	± 3.5

TABLE II

EN ROUTE RESERVE-FUEL FACTORS

FACTOR	STANDARD DEVIATION	STANDARD DEVIATION IN PERCENT OF PLANNED MISSION FUEL
WIND ERROR	10 KNOTS	0.57
TEMPERATURE ERROR	3° F	0.86
DRAG	1.5%	1.33
SPECIFIC FUEL CONSUMPTION	4% (EACH ENGINE)	2.00
FUEL GAGE ERROR	0.5%	0.50
EN ROUTE DEVIATIONS:		
1. CLIMB	1,000 LB FUEL FROM PREDICTED	0.56
2. CRUISE (LATERAL)	90 N. MI.	0.24
3. CRUISE (VERTICAL)	CONSIDERED AS SEPARATE FACTOR	
COMBINED STANDARD DEVIATION OF MISSION FUEL:		2.73%

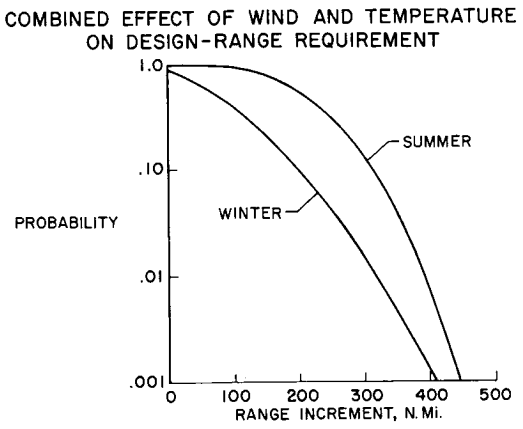

Figure 1

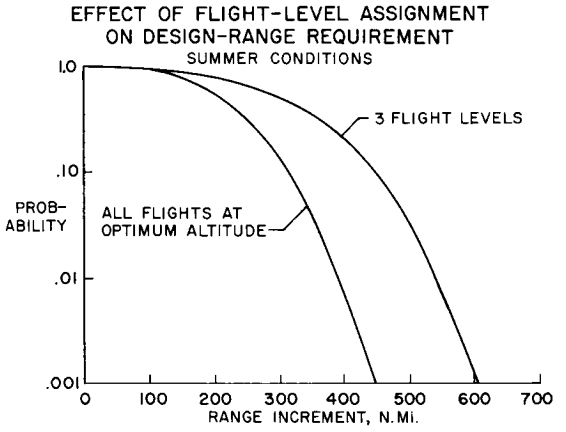

Figure 2

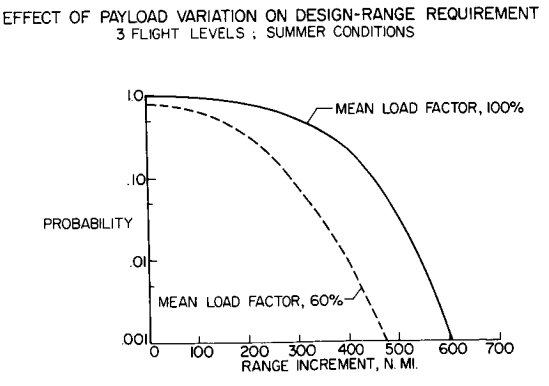

Figure 3

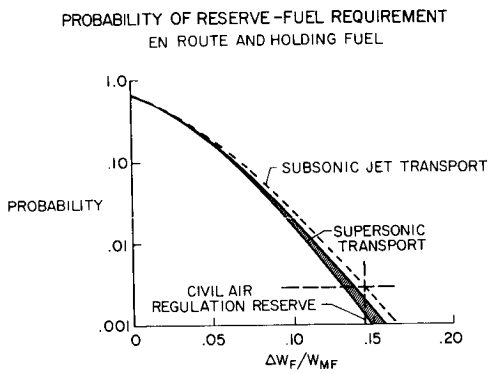

Figure 4

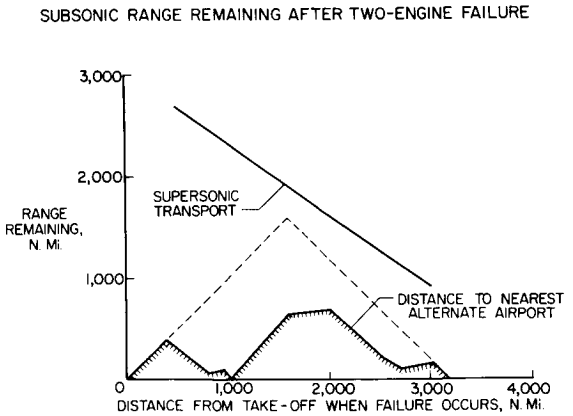

Figure 5

22. THE EFFECT OF YAW COUPLING IN TURNING MANEUVERS OF LARGE TRANSPORT AIRCRAFT

By Walter E. McNeill and Robert C. Innis

NASA Ames Research Center

SUMMARY

A study has been made, using a piloted moving simulator, of the effects of the yaw-coupling parameters N_p and N_{δ_a} on the lateral-directional handling qualities of a large transport airplane at landing-approach airspeed. It is shown that the desirable combinations of these parameters tend to be more proverse when compared with values typical of current aircraft. Results of flight tests in a large variable-stability jet transport showed trends which were similar to those of the simulator data. Areas of minor disagreement, which were traced to differences in airplane geometry, indicate that pilot consciousness of side acceleration forces can be an important factor in handling qualities of future long-nosed transport aircraft.

INTRODUCTION

It is generally recognized that, all else being favorable, an airplane with good handling qualities is a safe airplane from the standpoint of not adding unnecessarily to the pilot's workload during the critical flight tasks. Improved airplane handling qualities have been the subject of much flight and simulator research by various agencies. More recently, emphasis in NASA piloted-simulator work has been directed toward the lateral-directional characteristics of large aircraft, such as the supersonic transport in the landing approach and take-off.

These studies, as well as past work, have pointed out some of the factors which determine that an airplane will handle well in a lateral-directional sense during such critical situations as an instrument landing approach. These factors are: (1) There should be minimum excitation of the lateral-directional, or Dutch roll, oscillation either by pilot control inputs or in rough air. (2) Roll-control power and damping should provide reasonably quick attainment of desired bank angles without overshoot. (3) The spiral stability should be nearly neutral so that the pilot need not hold excessive aileron into or against an established turn. (4) Dihedral effect should be positive but mild in amount. (5) There should be a minimum of sideslip developed in rolling maneuvers, such as turn entries and reversals, so that negligible rudder coordination is required by the pilot; in other words, the airplane should be "two control." It has long been known that during turn entries made with ailerons alone the yaw rate is likely to remain zero momentarily or even to vary in the wrong direction before eventually continuing in the proper direction. In

either case, sideslip angles build up and, in addition to subjecting passengers and crew to uncomfortable side forces, much greater roll-control effort is required if the airplane has an appreciably large dihedral effect. The recent NASA simulator work has shown up this tendency to a degree that can even lead to lateral instability, or a pilot-induced oscillation, when the pilot is maneuvering at low speeds.

The tendency to build up sideslip in the manner just described is accentuated in large airplanes designed for supersonic cruise because of their characteristically long slender configuration having an unusually high yawing moment of inertia; that is, the mass is mostly distributed along the fuselage. For these reasons, the last area of interest (factor (5)) was chosen for further detailed study. It is the purpose of this paper to present some of the results of this study and to show how certain factors influence the yaw coupling and how optimum behavior may be obtained.

SYMBOLS

b	wing span, feet
C_l	rolling-moment coefficient, $\frac{\text{Rolling moment}}{qSb}$
C_n	yawing-moment coefficient, $\frac{\text{Yawing moment}}{qSb}$
I_X	roll moment of inertia, slug-foot^2
I_Z	yaw moment of inertia, slug-foot^2
p	rolling angular velocity, radians per second
q	dynamic pressure, pounds per square foot
S	wing reference area, square feet
V	true airspeed, feet per second
β_1	amplitude of first sideslip excursion during sidestep maneuver, degrees
δ_a	aileron deflection, degrees or radians
ζ	Dutch roll damping ratio
ϕ_1	maximum bank angle during first turn of sidestep maneuver, degrees

$$C_{l_{\delta_a}} = \frac{\partial C_l}{\partial \delta_a}$$

$$C_{n_{\delta_a}} = \frac{\partial C_n}{\partial \delta_a}$$

$$C_{n_p} = \frac{\partial C_n}{\partial \left(\frac{pb}{2V}\right)}$$

$$L_{\delta_a} = \frac{qSb}{I_X} C_{l_{\delta_a}}$$

$$N_{\delta_a} = \frac{qSb}{I_Z} C_{n_{\delta_a}}$$

$$N_p = \frac{qSb^2}{2VI_Z} C_{n_p}$$

P.R. pilot rating

TESTS

Motion Simulator

The simulator used in the present study was the Ames 5-degree-of-freedom motion simulator. A photograph of this device is presented in figure 1. In the cockpit, the pilot was subjected to pitch and yaw angular motions duplicating those which would be encountered in the airplane being simulated. (Roll motions were attenuated to 25 percent of the computed values to avoid unrealistic side forces on the pilot due to cab tilt.) Advantage was also taken of the ability of the device to impose side motions on the pilot during lateral-directional maneuvers by facing the cockpit outward. Large rates of travel around the track, with the attendant noise and extraneous longitudinal forces, were avoided by washing out the acceleration commands to the simulator arm. The resulting maximum lateral excursions of the cab were about 15 to 20 feet.

Cockpit controls and instrumentation typical of those in conventional transport aircraft were available to the pilot. Motion and instrument drive signals were obtained from a 6-degree-of-freedom analog simulation.

Example Airplane

The example airplane chosen for the simulator study was one of the final versions of the SCAT 16 in the landing configuration. The SCAT 16 was originated by the NASA as a possible variable-sweep supersonic transport. Some of the features of the airplane which relate to the study are shown in figure 2. The characteristics which were especially pertinent to the study were the long distance of the pilot ahead of the center of gravity (100 feet) and the large ratio of yawing to rolling moment of inertia (about 6). Most current jet transports have values from approximately 50 to 60 feet for the distance between the center of gravity and the cockpit and of about 2 or 3 for the inertia ratio. This ratio is important since it can be considered as a measure of the resistance of the airplane to applied yawing moments for a given response to roll-control input.

Test Maneuvers

Tasks were chosen for evaluation in the simulator of the lateral-directional behavior of the airplane which would represent the most critical low-speed operating conditions. The instrument landing approach was selected as the main condition upon which to base the study. This condition requires possibly the most concentrated effort by the pilot and is certainly one of the situations in which good handling qualities are needed to help assure safe operation.

There are four of these evaluation tasks. First, the pilot became familiar with the airplane at approach speed in maneuvers such as entries to steady turns, recoveries, roll reversals, steady sideslips, and Dutch roll oscillations. Second, straight instrument landing approaches were made by using deviation information derived from an instrument landing system. Third, the pilot was required, shortly after beginning an approach, to correct an abrupt offset, introduced in the localizer needle, that corresponded to a lateral deviation between 150 and 200 feet. This correction was made by executing a sidestep, or S-turn, maneuver without use of rudder for coordination. Fourth, the sidesteps were repeated by use of coordinating rudder. Figure 3 provides a closer look at the sidestep maneuver. The flight path is shown in plan view, and the variations with time of bank angle and roll rate in response to the pilot's roll-control input during the maneuver are also indicated. The sidestep was chosen as the primary evaluation maneuver because it was readily performed in the simulator and it placed the greatest demand on the pilot for proper phasing of rudder when coordination was desired.

Some flight work reported in reference 1 indicated that the minimum time to perform a sidestep maneuver without exceeding reasonable bank angles was about 10 seconds, which is close to the Dutch roll oscillation periods predicted for most supersonic transports at approach speeds. In order that any possible effects of resonant coupling between the sidestep and the Dutch roll mode be revealed, three nominal Dutch roll periods of 10, 7, and 5 seconds were investigated. (Additional theoretical studies of the sidestep maneuver pertaining to advanced airplane configurations have been reported in ref. 2.)

RESULTS AND DISCUSSION

Simulator Study

The results of the simulator study are presented in figure 4. Plotted one against the other are the aerodymamic derivatives which were chosen as the major variables in the study; they are the yaw due to rolling angular velocity N_p and the yaw due to pilot's aileron-control input for a given roll effort $N_{\delta_a}/L_{\delta_a}$. These parameters were selected on the basis of their strong influence on the amount of self-coordination inherent in an airplane and on the amount of sideslip developed when it is not well coordinated. The ranges of values covered are indicated approximately by the overall shaded areas in the figure. The positive values are called "proverse," indicating a tendency to yaw into the turn, and the negative values of both parameters are termed "adverse," indicating a tendency to yaw away from the turn. These parameters were varied at the three values of Dutch roll period previously mentioned. The Dutch roll damping ratio was set at 0.15, which corresponds to about 7/10 of a cycle to damp to half-amplitude.

Each of the various combinations of these variables was assigned, on the basis of the test maneuvers, a rating according to the widely used pilot-opinion rating scale. (See table I and ref. 3.) It was possible, then, to arrive at boundaries of constant pilot opinion corresponding to ratings of 3.5, which separated satisfactory and unsatisfactory characteristics for normal operation, and of 6.5, which separated acceptable and unacceptable characteristics for emergency operation. (See fig. 4.)

For each value of Dutch roll period, an area of satisfactory combinations of N_p and $N_{\delta_a}/L_{\delta_a}$ was observed to be oriented diagonally and indicated a "trade-off" between these two parameters. The results further indicated that a proverse value (within limits) for either or both of these parameters was desirable. Pilot comments indicate that these satisfactory areas occurred when sideslip excursions were near a minimum without use of coordinating rudder. Essential agreement with the pilot comments is indicated in figure 4 by the dashed lines in the middle of the satisfactory areas inasmuch as they are close to lines of minimum sideslip measured from the sidestep data.

Although it is not customary to design a value of N_p into an airplane (it is a difficult quantity even to measure in a wind tunnel or in flight), the value is somewhat negative for most swept-wing airplanes in the flight condition presently discussed. The value of N_p predicted for the basic SCAT 16 used as the example airplane was -0.1176 in body axes, as indicated in figure 4. The satisfactory areas shown in figure 4, then, represent a significant change from the usual negative value of N_p.

A widening of the satisfactory area is observed at the intermediate period of 7 seconds, indicating a wider latitude or tolerance of variations of N_p or N_{δ_a}. At first glance, this apparent tolerance might tend to confirm the

existence of a resonant coupling effect between the sidestep maneuver and the Dutch roll mode at the periods of 10 and 5 seconds. Comments by the pilots indicate, however, that any resonant coupling which might have been present was nearly undetectable. Measurements of sideslip occurring in uncoordinated sidestep maneuvers in the simulator confirm these pilot comments. The pilots felt that whenever large sideslip excursions were expected, adjustments of pilot-control technique were made which automatically minimized coupling with the Dutch roll oscillation. It should be noted that the boundaries of figure 4 show a similarity to those resulting from work performed on a V/STOL aircraft using a fixed piloted simulator. (See ref. 4.)

Flight Evaluation

In addition to the simulator work discussed in the section entitled "Simulator Study," certain combinations of N_p and $N_{\delta_a}/L_{\delta_a}$ were evaluated by the same pilots in flight under contract with The Boeing Company in their large four-engined jet transport especially adapted for variable-stability testing. Although it would have been desirable to make the flight evaluations by using an airplane similar in geometry to the SCAT 16, the choice of airplane for this purpose was based on availability of a large jet transport capable of artificial variation of the aerodynamic parameters which were of interest (i.e., the yawing-moment derivatives). The flight results, from test maneuvers which were essentially the same as those employed in the simulator, are shown in comparison with the simulator results in figure 5.

The bounded areas indicated as satisfactory, acceptable, and unacceptable are from the simulator, and the plotted points represent the combinations evaluated in flight with the resulting pilot ratings. Data are presented for the three Dutch roll periods of 10, 7, and 5 seconds.

It can be seen that, for the period of 10 seconds, agreement was very good in the area of the lower unacceptable boundary (P.R. = 6.5). In the region in which the simulator results were satisfactory, the flight results showed a slight preference for more proverse values of N_p or $N_{\delta_a}/L_{\delta_a}$. The solid data symbols are for a much higher damping ratio ($\zeta = 0.40$), and a corresponding improvement in rating is noted. For the period of 7 seconds, agreement between simulator and flight is still good, with somewhat more pilot leniency with respect to adverse values of the main variables. For the period of 5 seconds, the limited number of flight data points obtained show an even more generous acceptance of adverse values.

Undoubtedly, some of the apparent leniency shown in flight in certain areas was due to the differences in airplane geometry (for example, the distance from the center of gravity to the cockpit). Another cause for the minor discrepancies might be a lack of precise definition of the stability and control parameters of the basic airplane used in the flight simulation.

The comparison between pilot ratings obtained in the simulator and in flight is shown in a different way in figure 6. Here pilot ratings are plotted

as functions of β_1/ϕ_1, which is the ratio of the amplitude of the first sideslip excursion to the maximum bank angle in the first turn of a sidestep maneuver. The simulator results and the flight results are both indicated. The data for all three values of Dutch roll period are lumped together in this figure. A somewhat lower sensitivity of pilot opinion to β_1/ϕ_1 in flight than in the simulator is readily apparent. The pilots felt that this lower sensitivity of pilot rating to sideslip in flight was mostly due to the absence of significant side acceleration forces at the pilot's cockpit. In the simulator these forces were very noticeable and even became objectionable at the shorter Dutch roll periods. Although the pilots, in establishing their ratings, paid particular attention to the magnitude of the sideslip-angle disturbances in turn entries and reversals, the side acceleration forces undoubtedly had a strong adverse effect on pilot opinion. This effect would be expected when one considers the 2-to-1 ratio which existed between the distance from the center of gravity to the cockpit in the simulation and that of the subsonic jet airplane used in the flight evaluations. As a result of the longer nose length assumed in the simulation, the pilots apparently were more aware of the effects of yawing angular accelerations than they were in the airplane.

These impressions were verified by actual measurement of side accelerations imposed on the pilots during sidestep maneuvers in the simulator and in flight. In the simulator, these side accelerations (for a given amount of sideslip) increased markedly at the short Dutch roll periods, whereas in flight the measured accelerations remained at a low level for all periods tested.

When β_1/ϕ_1 was negative, an indication of excessive yawing into turns, a crossed-control technique was necessary if any rudder coordination at all was attempted. This was considered impractical and therefore was not advocated by the pilots as a normal technique. The proverse characteristics associated with some of the extreme negative values of β_1/ϕ_1 also tended to create objectionable pilot-coupling effects which gave the impression of lateral instability or a decrease in roll damping. These objectionable characteristics are reflected by the extremely steep rise of numerical pilot rating for the negative values of β_1/ϕ_1 in figure 6. Therefore, one should not proceed too far in the positive direction (by design or by artificial stability augmentation) with either of the yaw-coupling parameters N_p or N_{δ_a}.

CONCLUDING REMARKS

A study has been made, through the use of a ground-based piloted simulator and a variable-stability airplane, of the effects of the aerodynamic yaw-coupling parameters on the lateral-directional handling qualities of a large transport airplane at landing-approach airspeed. It has been shown that combinations of these parameters that influence yaw coupling can be found which result in minimal requirements for pilot rudder coordination in turning maneuvers, thus decreasing pilot workload. In order that "two-control" qualities be built into large airplane designs, including the supersonic transport, it has been shown

that the yaw-coupling parameters should be tailored in the proverse direction when compared with those of past and present aircraft. The trends shown in this study agreed in general with results published by other investigators. The trend toward increased nose length should make the pilot more aware of deviations from optimum yaw coupling.

Although it is difficult to control the value of yaw due to rolling in a given configuration, it may be possible during the course of the design to assure that this parameter does not become overly adverse (or even excessively proverse).

If it should prove that even careful aerodynamic design of the airplane cannot result in desirable combinations of these parameters, the alteration of the basic airplane characteristics by means of artificial stability augmentation is an obvious solution.

REFERENCES

1. Perry, D. H.; Port, W. G. A.; and Morrall, J. C.: A Flight Study of the Sidestep Manoeuvre During Landing. R. & M. No. 3347, Brit. A.R.C., 1964.

2. Tomlinson, B. N.: An Extensive Theoretical Study of the Ability of Slender-Wing Aircraft To Perform Sidestep Manoeuvres at Approach Speeds. R. & M. No. 3359, Brit. A.R.C., 1964.

3. Cooper, George E.: Understanding and Interpreting Pilot Opinion. Aeron. Eng. Rev., vol. 16, no. 3, Mar. 1957, pp. 47-51, 56.

4. Dolbin, Benjamin H., Jr.; and Eckhart, Franklin F.: Investigation of Lateral-Directional Handling Qualities of V/STOL Airplanes in Cruising Flight. Rept. No. TB-1794-F-3 (Contract No. P. O. 78839-CAP), Cornell Aeron. Lab., Inc., Dec. 15, 1963.

TABLE I.- PILOT-OPINION RATING SCALE USED IN PRESENT STUDY

Operation	Rating		Description	Primary mission accomplished	Can be landed
	Adjective	Numerical			
Normal	Satisfactory	1	Excellent, includes optimum	Yes	Yes
		2	Good, pleasant to fly	Yes	Yes
		3	Satisfactory, but with some mildly unpleasant characteristics	Yes	Yes
Emergency	Unsatisfactory	4	Acceptable, but with unpleasant characteristics	Yes	Yes
		5	Unacceptable for normal operation	Doubtful	Yes
		6	Acceptable for emergency condition only[1]	Doubtful	Yes
None	Unacceptable	7	Unacceptable even for emergency condition[1]	No	Doubtful
		8	Unacceptable - dangerous	No	No
		9	Unacceptable - uncontrollable	No	No
	Catastrophic	10	Motions possibly violent enough to prevent pilot escape	No	No

[1]Failure of a stability augmenter.

SIMULATOR USED IN STUDY

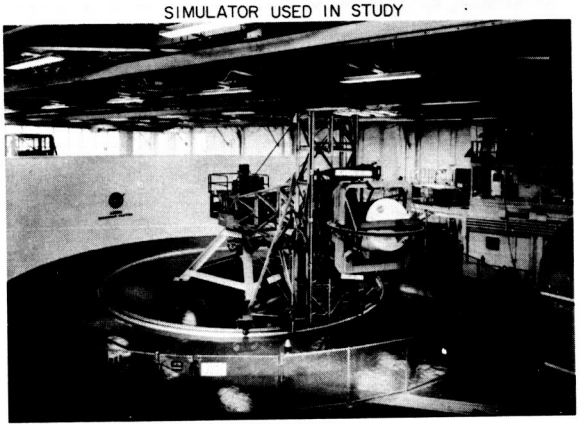

A-31542

Figure 1

CHARACTERISTICS OF BASIC AIRPLANE (SCAT 16)

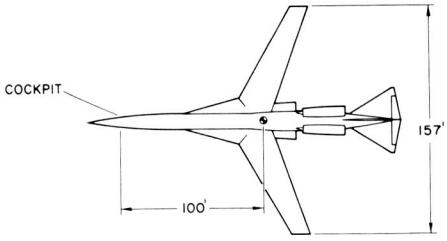

$$\frac{\text{YAW MOM. OF INERTIA}}{\text{ROLL MOM. OF INERTIA}} = \frac{13.4 \times 10^6 \text{ slug-ft}^2}{2.24 \times 10^6 \text{ slug-ft}^2} \approx 6.0$$

APPROACH SPEED 130 knots

Figure 2

SIDESTEP MANEUVER

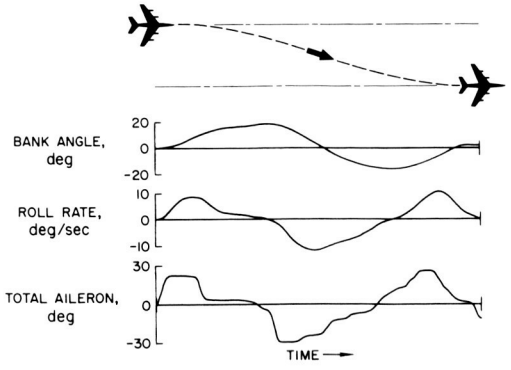

Figure 3

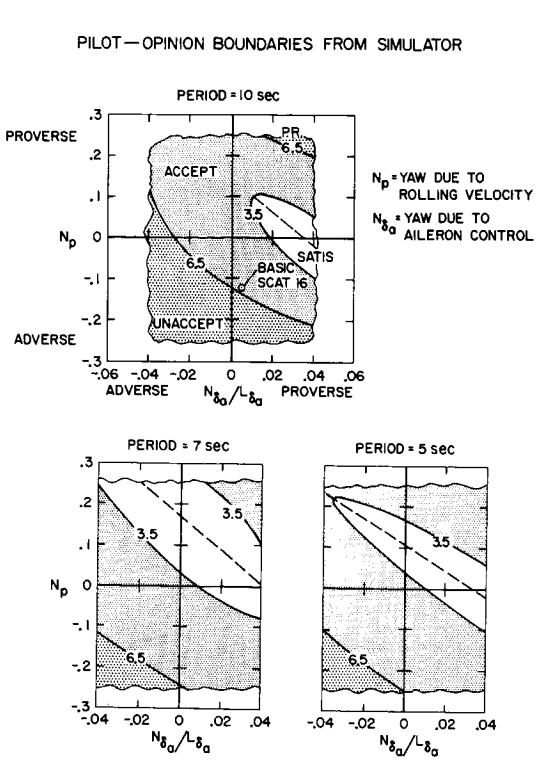

Figure 4

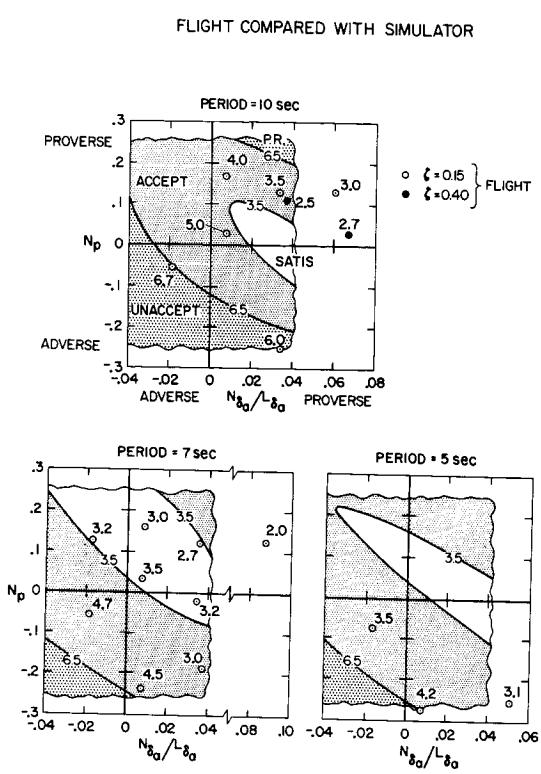

Figure 5

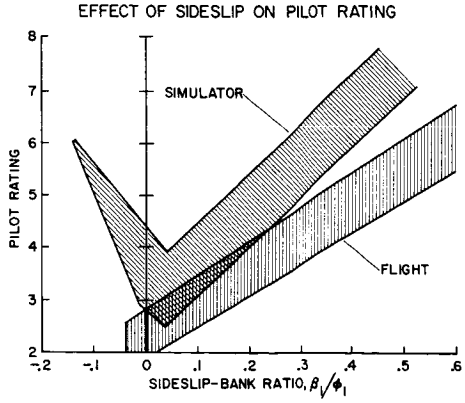

Figure 6

23. AN ASSESSMENT OF A TITANIUM ALLOY FOR SUPERSONIC TRANSPORT OPERATIONS

By George J. Heimerl and Herbert F. Hardrath

NASA Langley Research Center

SUMMARY

An assessment is given of the materials problems and implications regarding the use of Ti-8Al-1Mo-1V alloy sheet for the skin of a supersonic transport. Although the assessment of this alloy in the duplex annealed condition is generally favorable, several questions remain unanswered and new ones continue to arise. The seriousness of the salt stress corrosion problem at 500° F and above under flight conditions cannot be predicted on the basis of current laboratory corrosion tests. A new potential stress corrosion problem at ambient temperatures in the presence of cracks and salt water requires investigation. The ability to withstand a 30,000-hour exposure at 550° F without undue degradation of the material or welds will remain doubtful until more long-time data are available. The substitution of a more corrosion-resistant and stable titanium alloy in the tension critical areas of the structure may prove advisable.

INTRODUCTION

Although a number of titanium alloys have been under consideration for the skin material for a supersonic transport, Ti-8Al-1Mo-1V alloy sheet has been favored for this application because of its relatively high stiffness and strength. This paper will attempt to assess some of the structural materials problems and implications regarding the use of this titanium alloy in terms of current research and knowledge of present-day aircraft materials.

SYMBOLS

K_T	stress concentration factor
M	Mach number
N	number of cycles to failure
S	stress
S_{1g}	nominal 1g stress for level flight at take-off gross weight
S_{MAX}	maximum stress during load cycle

S_m mean stress

δ shortening for salt-coated specimen

δ_o shortening for uncoated specimen

Abbreviations:

SA single anneal

DA duplex anneal

TA triplex anneal

SPECIFIC MATERIALS PROBLEMS

Flight conditions dictate the choice of materials and point to specific materials problems. The general features of the loading and temperature history for a point on the lower surface of the wing in a supersonic flight are shown in figure 1. In this schematic, loads are indicated in terms of the ratio of the stress S during flight to the nominal 1 g stress S_{1g} for level undisturbed flight at take-off gross weight. Most of the significant stress cycles occur during the climb portion of the flight while the aircraft is still at ambient temperature. As gust activity is reduced at high altitudes, few dynamic stress cycles of any consequence are encountered during cruise. During cruise, however, the average temperature of the skin material near the leading edges will vary from about 275° F to 550° F for Mach 2.2 to Mach 3 operation with the maximum running up to about 600° F except in engine areas. Dynamic stresses encountered during descent are less severe because of the reduced fuel load. A significant ground-air-ground cycle also occurs at stations outboard of the landing gear. With the assumption that the material is unaffected by exposure to elevated temperature, fatigue damage will be independent of flight length to a first approximation.

A flight history such as that just discussed involves considerations of material strength, behavior, and life at ambient and elevated temperatures. In the first place, the properties of a new structural material such as Ti-8Al-1Mo-1V alloy need to be established over the temperature range. The principal materials problems resulting from supersonic transport operation are as follows:

(1) Fatigue strength

(2) Fatigue crack propagation

(3) Residual strength

(4) Stability of material and welds

(5) Salt stress corrosion

The properties which require the most consideration from the standpoint of serviceability in the tension critical portion of the structure are the fatigue strength, fatigue crack propagation, and the residual strength. The metallurgical stability of the material and welds must also be known for exposures up to at least 30,000 hours at temperatures up to about 550° F if there is to be any assurance that the structure will be durable. The possibility of salt stress corrosion cracking occurring during cruise must likewise be considered, as this titanium alloy is susceptible to this type of corrosion even for only a slight amount of salt. Creep is not considered to be a problem, except in highly stressed regions such as joints, and is not listed here because it is inconsequential under nominal load and temperature conditions.

STRENGTH AND STABILITY CHARACTERISTICS

Fatigue Strength

Current fatigue data (refs. 1 and 2) for Ti-8Al-1Mo-1V alloy are summarized in figure 2. The bar graphs give the fatigue strength of various specimen configurations and joints at a life of 10^6 cycles for a mean stress of 25 ksi. Data are shown for three temperatures and for the single, duplex, and triplex annealed conditions. No attempt is made to discuss these results in detail. The results can be summarized by saying that the duplex annealed (DA) condition gives the best material and fusion-weld strengths, and elevated temperatures are not detrimental. The relative reduction in strength due to spot-welding and joints is no more than that due to stress raisers in current aircraft structures. This brief look implies that the fatigue characteristics of the new material in the duplex annealed condition do not pose any unusual problems.

Fatigue Crack Propagation

One of the most important considerations in assessing the fail-safe characteristics of a structure is the rate of fatigue crack propagation. Some results (ref. 3) from axial-load fatigue tests of 8-inch-wide specimens with zero to tension loading are shown for Ti-8Al-1Mo-1V alloy sheet (duplex anneal) in figure 3. Crack growth rates are plotted logarithmically in terms of crack lengths. On the left the comparative crack growth at 80° F is shown for the titanium alloy and two common aluminum alloys. The mean stress was 25 ksi for the titanium alloy and 15 ksi for the aluminum alloys. All the curves have approximately the same slope so that the change in crack rate with crack length is about the same for these materials. Crack growth rates for the titanium alloy and the aluminum alloys are also comparable in magnitude. On the right, the effect of temperature on crack growth is shown for the titanium alloy. Crack propagation rates decrease with increase in temperature. Consequently,

fatigue crack progagation does not appear to be any more of a problem at normal and elevated temperatures for this titanium alloy than in present aircraft, unless the material is degraded by long-time elevated-temperature exposure.

Residual Static Tensile Strength

The residual static tensile strength is another important consideration with regard to fail-safe characteristics of a part containing a crack or other damage. Some results (ref. 4) for Ti-8Al-1Mo-1V (duplex anneal) for 8-inch-wide specimens which had been precracked by fatigue loading are shown in figure 4. The ordinate is the ratio of the gross stress at fracture to the ultimate tensile strength at 80° F and the abscissa is the ratio of the initial crack length to the specimen width. On the left, comparisons are shown with two common aluminum alloys at 80° F. The straight dashed line represents the result which would be obtained if the crack had no effect beyond that of removing material. In this comparison, the titanium alloy exhibits slightly better residual strength characteristics than the best of the two aluminum alloys. In addition, the titanium alloy has desirable slow crack growth characteristics; thus, the residual strength at 80° F is no cause for special concern. On the right is shown the effect of low and elevated temperatures on the residual strength of the titanium alloy. The effect of temperature is rather small, although some decrease in strength is indicated at 550° F and -110° F. Cruising conditions should not affect the residual strength appreciably unless the material is changed by long exposure to elevated temperature.

Stability of Material and Welds

One of the main concerns regarding materials for a supersonic transport is their ability to withstand 30,000 hours or more of exposure at elevated temperatures. To answer this question, selected titanium-alloy and stainless-steel sheet specimens of various types were exposed at 550° F, removed from the ovens at intervals, and tested at room temperature (ref. 5). Figure 5 shows the effect of unstressed exposure at 550° F on the notch, tensile, and tensile spotweld strengths of Ti-8Al-1Mo-1V alloy sheet (single anneal) at 80° F. The effect is shown by a change from unity of the relative strength - the ratio of the strength after exposure to that before exposure. The notch strength (sharp ASTM type edge notch, ref. 6) and the tensile strength are relatively unaffected by exposures up to 22,000 hours at 550° F. The tensile spotweld strength, however, decreases about 15 percent for this exposure. Some deterioration of weld strength may therefore be anticipated.

Recent results (fig. 6) of an investigation at the Langley Research Center show the effect of a 24,000-hour unstressed exposure at 550° F on the axial-load fatigue strength at 80° F of Ti-8Al-1Mo-1V alloy sheet (single anneal) for a mean stress of 25 ksi. This figure is a conventional S-N plot in which S_{MAX} is the maximum stress during a load cycle and N is the life in cycles. The data for the unexposed and exposed material (circles and squares, respectively) are given for both unnotched and edge notched ($K_T = 4$) specimens. Examination of these results shows no significant effects of the 24,000-hour exposure on the

fatigue strength for either the notched or unnotched material. These results and those in the previous figure indicate that Ti-8Al-1Mo-1V alloy sheet in the single annealed condition is relatively unaffected by exposure at 550° F, except in the case of the spotwelds. Of concern at the present time, however, is recent evidence at the Langley Research Center of instability of this alloy in the favored duplex annealed condition after exposure for 2000 to 4000 hours at 550° F. More time is required to assess this development.

SALT STRESS CORROSION AT ELEVATED TEMPERATURES

The remainder of this paper discusses the problem of salt stress corrosion of titanium alloys at elevated temperatures, a problem which is receiving considerable attention from the aircraft industry, materials producers, and research laboratories. The information which follows presents some results of an investigation at the Langley Research Center of the severity of the problem, of the effect of various environmental factors, and of the effectiveness of several protective treatments.

Relative Susceptibility and Thresholds

In order to carry out the investigations, many small elastically and residually stressed specimens were salt coated and placed in ovens for exposures up to 20,000 hours at 400° F to 600° F. The amount of stress corrosion damage is determined from room-temperature compression or bending tests of specimens taken from the ovens at regular intervals.

A schematic is included to provide some background on one of the corrosion tests at the Langley Research Center. (See fig. 7.) The self-stressed specimen (on the right) consists of two strips of sheet material which are bent and spotwelded together at the ends in such a way as to induce uniform bending stresses of the desired amount in the curved portions. When an uncoated specimen is loaded in compression (see dashed curve), it develops the maximum shortening δ_o possible without fracturing. On the other hand, if the specimen is salt coated, exposed at elevated temperature until stress corrosion cracking occurs, and then loaded in compression at room temperature (see solid lines), the specimen will fracture and the shortening δ is reduced - the longer the exposure, the less the shortening, and the greater the embrittlement. The shortening and bend ductility of the uncoated specimen are unaffected by the exposure time if the material is stable. In any case, the relative shortening δ/δ_o is a measure of the stress corrosion damage - the smaller the ratio, the more severe the corrosion. A description of the specimen and test and a correlation of the shortening measurements to the crack penetration are given in reference 7.

The severity and extent of this salt stress corrosion problem for Ti-8Al-1Mo-1V alloy sheet is illustrated in figure 8. The relative susceptibility of three titanium alloys at 550° F (ref. 8) is shown on the left. Severe stress corrosion cracking develops within 2000 hours for Ti-8Al-1Mo-1V. Susceptibility is less for Ti-6Al-4V, and Ti-4Al-3Mo-1V is completely resistant up to

7000 hours and more exposure. Thus, Ti-8Al-1Mo-1V is a poor selection as far as elevated-temperature salt stress corrosion is concerned. Only a very thin salt coating is necessary to cause severe damage. On the right, stress and temperature thresholds are shown for Ti-8Al-1Mo-1V alloy for exposures of 400 hours (solid lines) and 1600 hours (dashed lines) for temperatures in the 400° F to 600° F range. For a 400-hour exposure, no stress corrosion occurs until about 500° F is reached, regardless of the stress level. Above this temperature, however, the effect of both temperature and stress becomes critical. The 1600-hour exposure (dashed line) lowers the temperature threshold to about 475° F. Investigation is continuing at the Langley Research Center and some stress corrosion is now being found at 450° F after 5000 hours exposure with a stress of 50 ksi. The seriousness of this problem in supersonic transports is difficult to assess, however, because the flight environment is radically different from laboratory test conditions. With the assumption that laboratory test results apply to flight conditions, a temperature threshold criterion of 500° F at the leading edges would limit transport operation to about Mach 2.7 for unprotected material in order to avoid stress corrosion.

The preceding results are for steady temperature conditions. Under cyclic heating conditions, the situation seems more encouraging. In an investigation in which the total cycle is 180 minutes, maximum temperature is 550° F, and immersion period in $3\frac{1}{2}$ percent salt solution is 10 minutes, no stress corrosion was obtained after 2000 hours at a stress of 25 ksi (information from the Boeing Aircraft Company). On the other hand, some very recent data from the U.S. Naval Research Laboratory, for example, indicate that some titanium alloys may be subject to stress corrosion and embrittlement at ambient temperatures in the presence of cracks and a salt-water environment. This development requires further investigation.

Effect of Environmental Factors

Attempts have been made to determine the effects of some important environmental factors which might provide a clue to the severity of the problem and throw some light on the stress corrosion mechanism. (See ref. 9.) Figure 9 shows preliminary results on the effects of oxygen, pressure, moisture, and surface condition on the salt stress corrosion of Ti-8Al-1Mo-1V alloy (duplex annealed) at 550° F. In these tests the specimens were encapsulated in glass tubes with the desired environment. The effect of oxygen is pronounced. Tests with nitrogen (containing 0.1 percent oxygen) show much less corrosion than with 100 percent oxygen. Moist chlorine is very corrosive, as the specimens failed before they could be removed from the furnace for testing (the curve is illustrative only). The effect of pressure is marked. Tests at 34 mm Hg (equivalent to a 70,000-foot altitude) show much less corrosion than at atmospheric pressure. Tests at 3×10^{-5} mm Hg (378,000-foot altitude) show still less corrosion. The effect of altitude corresponds to a decrease in oxygen and is beneficial. Tests with moist and dry air (dewpoints of 60° F and -40° F, respectively) seemed to show little effect of moisture. The effect of the surface condition, whether polished, in the as-received condition, or anodized (300 to 600 Å thick), likewise seemed to make little difference. Unless an unexpected potent environmental factor such as ozone should change the picture,

these experiments indicate that salt stress corrosion in flight would be less severe than that in most laboratory tests.

Protective Treatments

Elevated-temperature salt stress corrosion cracking can be eliminated by keeping temperatures sufficiently low or by utilizing protective treatments or coatings. Figure 10 shows preliminary results for several protective treatments for Ti-8Al-1Mo-1V alloy sheet (duplex anneal) at 550° F. The specimen shown is a formed 90-degree-bend type with a 1/8-inch radius which develops residual tensile stresses on the inside of the bend. (See ref. 10.) In this case, the relative deflection is a measure of the stress corrosion cracking. The lower curve is the base or reference curve for salt-coated specimens which have not been given any protective treatment. Fine-shot-peening, nickel-plating, and vibratory-cleaning methods all proved effective. The downward slope of the lines does not mean that stress corrosion cracking has occurred, but only that the formed specimen is embrittled somewhat by the exposure - more evidence of the instability of this alloy in the duplex condition. The fine shot peening consisted of a 10-second treatment using 0.002-inch-diameter glass spheres and a pressure of 60 psi. Although the thin nickel plating (1/3 to 1/2 mil) was effective, it tended to peel off when the specimen was bent to any considerable extent. The vibratory cleaning treatment after forming is a conventional cleaning and deburring process. The treatment consisted of placing the formed specimens in a bath containing aluminum oxide prisms and a cleaning solution. The bath was vibrated at 1450 cpm for 8 hours. The reason for the effectiveness of this treatment is not known. Preliminary results for polyimide coatings (1/2 to 1 mil thick) indicate that they are effective to begin with but show signs of degradation after 1000 hours at 600° F. Considerable work needs to be done in this area in order to determine the practicability and durability of various possible treatments.

CONCLUDING REMARKS

The assessment of the serviceability of Ti-8Al-1Mo-1V alloy sheet in the duplex annealed condition for a supersonic transport is generally favorable, although new problems continue to arise, and time may show that some other alloy or condition may prove a better choice, at least for some portions of the structure. This assessment can be summarized as follows:

1. The seriousness of the salt stress corrosion problem at 500° F and above under flight conditions cannot be predicted at present on the basis of current laboratory tests. Until more is known about environmental effects and the stress corrosion mechanism, the possibility of stress corrosion cracking occurring at temperatures above 450° F should be guarded against, particularly in joints and highly stressed parts. Thermal control methods, protective treatments or coatings, or the substitution of a more corrosion resistant alloy are advisable in tension-critical areas in the high-temperature regions near the leading edges and engines.

2. Only qualitative preliminary information is available on the stress corrosion of titanium alloys at ambient temperatures in the presence of cracks and a salt-water environment. An investigation of this new problem is required before any assessment can be made.

3. The ability to withstand 30,000 hours exposure at 550° F has yet to be established for this alloy in the duplex annealed condition. Present indications are that it is not completely stable, and some degradation in material properties and in welds may be expected. Additional time and research are needed for this evaluation.

4. Properties which are important in tension-critical areas - fatigue strength, crack propagation, and residual strength - do not appear to pose any new problems at normal and elevated temperatures except for possible long-time temperature and corrosion effects which have yet to be established.

REFERENCES

1. Gideon, D. N.; Marschall, C. W.; Holden, F. C.; and Hyler, W. S.: Exploratory Studies of Mechanical Cycling Fatigue Behavior of Materials for the Supersonic Transport. NASA CR-28, 1964.

2. Peterson, John J.: Fatigue Behavior of AM-350 Stainless Steel and Titanium-8Al-1Mo-1V Sheet at Room Temperature, 550° F and 800° F. NASA CR-23, 1964.

3. Hudson, C. Michael: Fatigue-Crack Propagation in Several Titanium and Stainless-Steel Alloys and One Superalloy. NASA TN D-2331, 1964.

4. Figge, I. E.: Residual Strength of Alloys Potentially Useful in Supersonic Aircraft. NASA TN D-2613, 1965.

5. Heimerl, George J.; Baucom, Robert M.; Manning, Charles R., Jr.; and Braski, David N.: Stability of Four Titanium-Alloy and Four Stainless-Steel Sheet Materials After Exposures up to 22 000 Hours at 550° F (561° K). NASA TN D-2607, 1965.

6. Anon.: Fracture Testing of High-Strength Sheet Materials: A Report of a Special ASTM Committee. ASTM Bull.
   Ch. 1, no. 243, Jan. Jan. 1960, pp. 29-40.
   Chs. 2 and 3, no. 244, Feb. 1960, pp. 18-28.

7. Heimerl, G. J.; and Braski, D. N.: A Stress Corrosion Test for Structural Sheet Materials. Mater. Res. Std., vol. 5, no. 1, Jan. 1965, pp. 18-22.

8. Braski, David N.; and Heimerl, George J.: The Relative Susceptibility of Four Commercial Titanium Alloys to Salt Stress Corrosion at 550° F. NASA TN D-2011, 1963.

9. Braski, David N.: Preliminary Investigation of Effect of Environmental Factors on Salt Stress Corrosion Cracking of Ti-8Al-1Mo-1V at Elevated Temperatures. NASA TM X-1048, 1964.

10. Pride, Richard A.; and Woodard, John M.: Salt-Stress-Corrosion Cracking of Residually Stressed Ti-8Al-1Mo-1V Brake-Formed Sheet at 550° F (561° K). NASA TM X-1082, 1965.

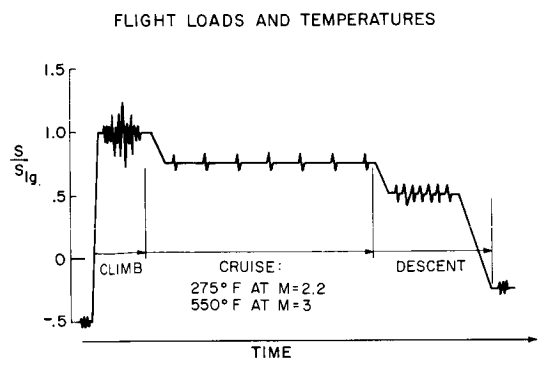

Figure 1

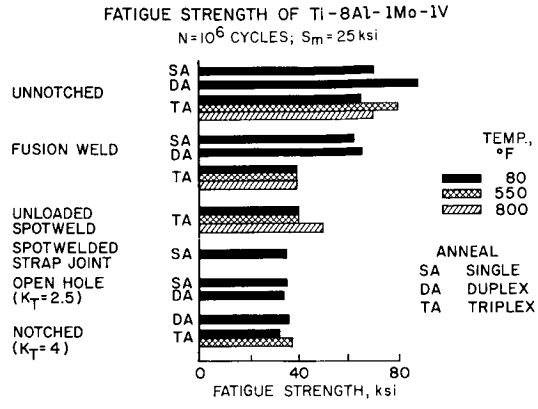

Figure 2

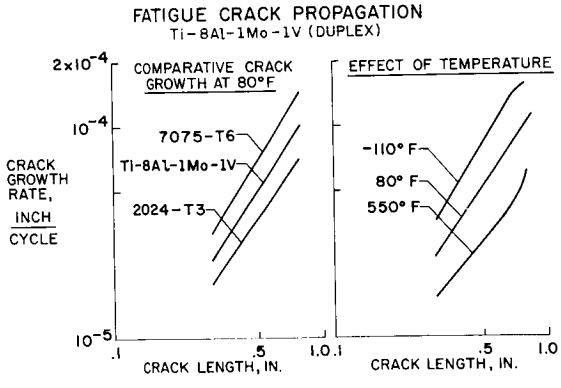

Figure 3

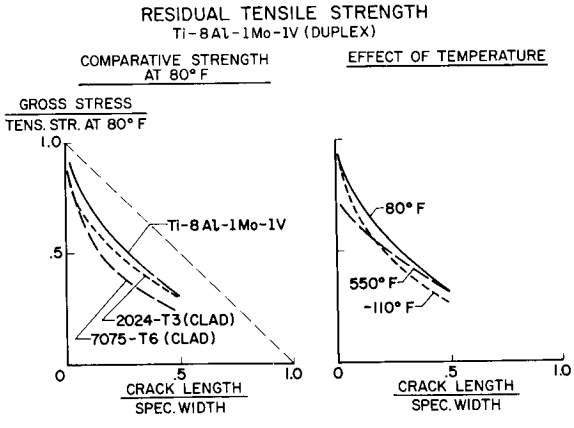

Figure 4

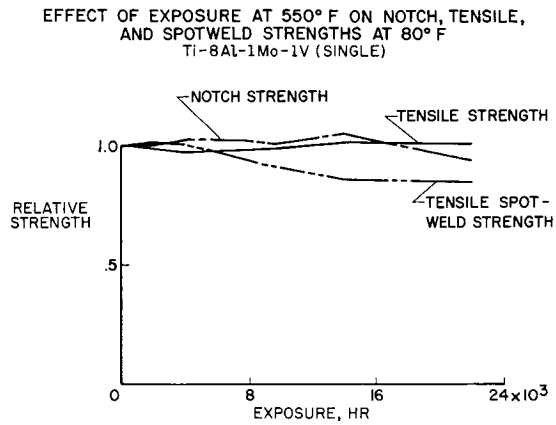

Figure 5

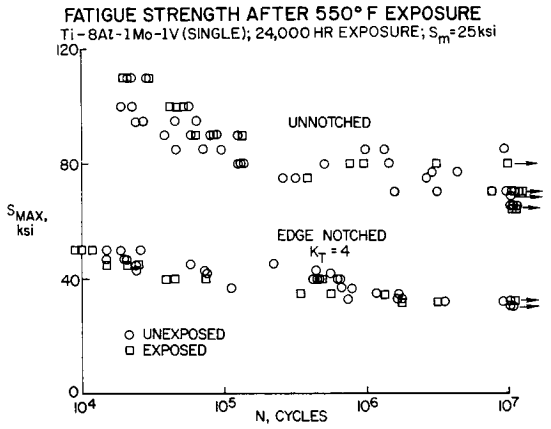

Figure 6

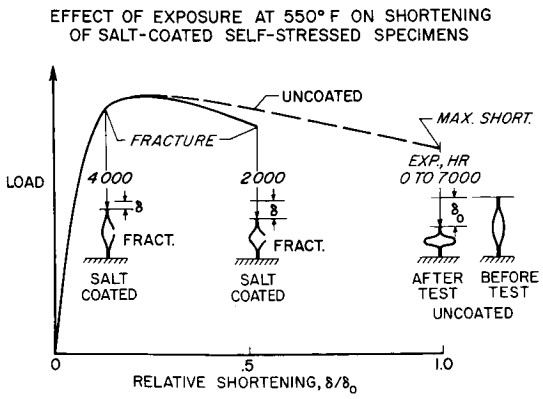

Figure 7

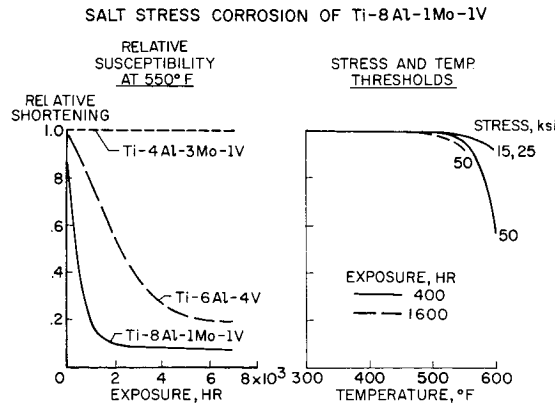

Figure 8

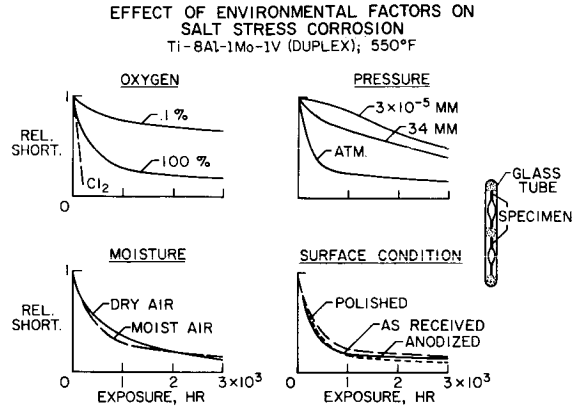

Figure 9

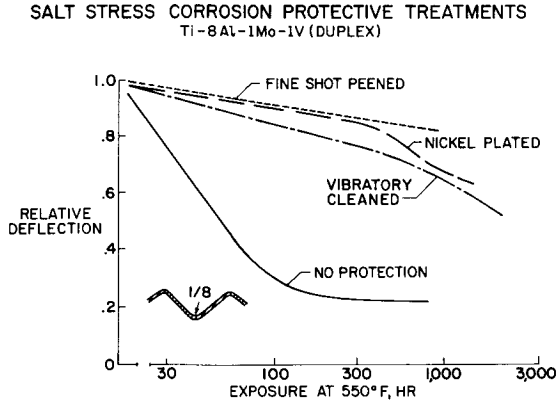

Figure 10

24. IMPLICATIONS OF THE EFFECTS OF SURFACE TEMPERATURE AND IMPERFECTIONS ON SUPERSONIC OPERATIONS

By John B. Peterson, Jr., and Albert L. Braslow

NASA Langley Research Center

SUMMARY

The effects of surface temperature and imperfections on the drag of the supersonic transport are discussed. The relationships among surface temperature, emissivity, and skin friction are reviewed and the importance of manufacturing and maintenance imperfections is indicated.

INTRODUCTION

In the operation of a supersonic transport, considerably more attention should be given to factors that affect drag than has been the case in the operation of present-day subsonic transports because a given increment in drag will produce a larger performance penalty for the supersonic transport than for the present-day subsonic transports. Two factors affecting the drag of the supersonic transport that aircraft operators should be aware of are the effects of surface temperature and surface imperfections.

SYMBOLS

D_{CRUISE}	total cruise drag of supersonic transport
ΔD	drag increment due to imperfections
D_f	skin-friction drag
ΔD_f	increment in skin-friction drag due to roughness
h	aircraft altitude
k	height of imperfection
l	wavelength of bump
L/D	lift-drag ratio of supersonic transport
M	Mach number

T surface temperature

V_∞ free-stream velocity

W_{CRUISE} average cruise weight of supersonic transport

x distance from leading edge in streamwise direction

ϵ surface emissivity

Subscripts:

ad adiabatic wall conditions

SMOOTH smooth surface conditions

DISCUSSION

Surface Temperature

Figure 1 shows how surface temperature affects the skin-friction drag for conditions typical of a supersonic transport. In figure 1, the ratio of the skin-friction drag at a given temperature to the skin-friction drag at the adiabatic temperature is plotted against the surface temperature. Adiabatic surface temperature is shown at 430° F. This value represents the temperature that a perfectly insulated surface reaches because of the frictional heating by the air. The figure shows that a decrease in temperature causes an increase in skin-friction drag. In fact, the skin friction increases about 4 percent for each 100° decrease in temperature because the air density near the surface increases as the temperature decreases and the air, therefore, behaves as though the dynamic pressure were higher and scrubs the surface harder. Since skin friction comprises about one-third of the total drag of a supersonic transport, this effect can be important.

During cruise, the wall temperature of the supersonic transport will be somewhat below the adiabatic value of 430°, since heat is dissipated from the surface both by conduction into the structure and by radiation away from the surface. Figure 2 shows the effect of radiation on the surface temperature. The ability of a surface to radiate heat is determined by a property called emissivity (shown on the figure as ϵ). Surfaces with high emissivity can radiate large amounts of heat and surfaces with low emissivity cannot. Surfaces with an emissivity of 1 are called black bodies and surfaces with an emissivity of 0 are called perfect reflectors. This figure was prepared from the charts of reference 1 in which the interdependence of surface emissivity, surface temperature, and skin friction over a wide range of conditions is presented. It shows that the temperature is reduced by about 90° by a change in emissivity from 0 to 1. This lower temperature in turn causes a higher skin friction. Therefore, an increase in emissivity has the favorable effect of reducing the temperature and the unfavorable effect of increasing the skin friction.

When aerodynamic heating is a problem, a reduction in temperature obtained with high emissivities is generally more important than the increase in skin friction. For this reason, aircraft, such as the X-15 and A-11, have high emissivities to reduce the surface temperature. When heating is less severe and when materials that can withstand the higher temperatures are used, the reduction in skin friction may be more desirable. In these cases, insulation as well as low emissivity may be required to obtain high surface temperatures, although the weight of insulation, of course, must be taken into consideration.

The surface emissivity that is chosen for the supersonic transport, therefore, will be dependent on such factors as Mach number and structural materials selected. In any event, whether the supersonic transport is designed with a low or a high emissivity, it will be important for the aircraft operators to maintain this value within design limits; otherwise, either the surface temperature or the skin friction will be above the design value.

Surface Imperfections

Surface imperfections of the same size will have a higher drag on the supersonic transport than on current subsonic aircraft. This difference occurs because they produce wave drag at supersonic speeds and the supersonic transport operates at higher dynamic pressures. Examples of the drag penalties obtained in experiments at supersonic speeds are shown in figures 3, 4, and 5. These figures were prepared for a typical supersonic transport cruising at Mach 2.7 and an altitude of 65,000 feet with a lift-drag ratio of 8.5 and a cruise weight of 375,000 pounds. Figure 3 shows the drag penalty of 100 linear feet of a sine-wave type of bump on the surface oriented perpendicular to the airstream. This type of surface imperfection can be caused by such factors as aerodynamic heating and loading. In figure 3, the increment of drag increase, as a fraction of the total cruise drag, is plotted against the height of the bump in inches. Two curves are shown for two different wavelengths (10 inches and 20 inches). Although the drag increments are small, these increments can become important, as will be shown later.

Figures 4 and 5 give the drag penalties associated with 100 linear feet of forward- and rearward-facing steps, the types of surface imperfections which occur at skin joints and at the edges of access panels and doors. It should be noted that the supersonic transport will have about 2500 feet of drag-producing steps at skin joints and about 500 feet at access panels and doors. It is seen that a 0.08-inch-high forward-facing step located 10 feet from the leading edge increases the cruise drag by about 0.1 percent. At 100 feet from the leading edge, the drag penalty is, of course, smaller. The step heights considered here are small with respect to the boundary-layer thickness under these flight conditions. Therefore, the drag of rearward-facing steps shown in figure 5 is almost the same as that for forward-facing steps, and the 0.08-inch-high step at the 10-foot station in this case increases the drag a little less than 0.1 percent. These figures indicate why the manufacturer intends to keep close tolerances on surface imperfections due to construction. The aircraft operators should maintain these specifications during operation if the maximum performance is to be retained.

Besides manufacturing imperfections such as shown in figures 3, 4, and 5, general three-dimensional-type surface roughness, such as accumulated dirt, can cause significant increases in the skin-friction drag. In figure 6, the increase in aircraft skin-friction drag, as a fraction of the smooth skin-friction drag, is shown plotted against the grain size of the roughness for closely packed grains distributed over all surfaces. It is seen that there is no drag increase for roughness particles up to a size of 0.007 inch. For larger roughness sizes, there is a rapid increase in skin friction. Similar increases in drag would result from scratches and gouges in the skin surface. These increases are not as easily illustrated, but the information necessary to estimate their drag is available. (See ref. 2.)

Table I was prepared to provide a better feel for the degree of care required in the manufacture and maintenance of the surfaces of the supersonic transport. The drag contributions of various types of surface imperfections are shown for a hypothetical supersonic transport. This transport was assumed to have been constructed and maintained in a manner similar to present-day aluminum fighter airplanes, and the surface imperfections were scaled up from the sizes actually measured on such an airplane in military service. It should be noted that the scale factors used were not equal to the ratio of the sizes of the two airplanes, but were carefully chosen for each type of imperfection to represent a realistic estimate of the imperfections that might be expected on the supersonic transport. As can be seen, even though the drag increment of each of these items is individually small, the total can be a significant part of the cruise drag.

It should be realized, that for each 1-percent increase in drag, the supersonic transport burns about 1000 pounds more fuel during its 3000-mile cruise (the initial cruise weight being assumed as 431,000 pounds and the final cruise weight as 317,000 pounds), and the payload, therefore, is decreased by the same amount. The 3.63-percent increase in drag shown in table I is then equivalent to about a 3500-pound loss in payload capacity as compared with a transport with no imperfections.

The actual transport, of course, will have some degree of both construction and maintenance imperfections. The manufacturer expects to be able to keep the drag of construction imperfections down to slightly more than 1 percent of the cruise drag by use of more advanced construction techniques as compared with present-day practices. They have included this amount of penalty in their performance estimates. The drag increment will increase during service, however, if imperfections from servicing and maintenance procedures are allowed to accumulate. It would probably be to the aircraft operators' advantage, therefore, to review present-day servicing and maintenance procedures for possible improvements in order to minimize this increase in drag.

CONCLUDING REMARKS

It has been shown that surface emissivity has an important effect on surface temperature and skin-friction drag. Therefore, it will be important for the aircraft operators to maintain the surface emissivity within the design

limits; otherwise, either the surface temperature or the skin-friction drag will be higher than the design value. It has also been shown that the drag increments of typical surface imperfections, although individually small, can be very significant when taken together. This condition is especially true of the supersonic transport because small increases in overall drag can have important effects on the payload. It would probably be to the aircraft operators' advantage, therefore, to review their maintenance procedures for the supersonic transport as compared with present-day good practice.

REFERENCES

1. Allen, Jerry M.; and Czarnecki, K. R.: Effects of Surface Emittance on Turbulent Skin Friction at Supersonic and Low Hypersonic Speeds. NASA TN D-2706, 1965.

2. Horton, Elmer A.; and Tetervin, Neal: Measured Surface Defects on Typical Transonic Airplanes and Analysis of Their Drag Contribution. NASA TN D-1024, 1962.

TABLE I

ESTIMATED SURFACE DEFECT DRAG CONTRIBUTION FOR SST
M=2.7

TYPE OF IMPERFECTION	$\frac{\Delta D}{D_{CRUISE}}$
SCRATCHES	0.12%
GOUGES	.01
BUTT JOINTS AND ACCESS DOORS	.21
SURFACE WAVES	.78
RIVETS	.62
SCREWS	.15
PROJECTIONS	.33
HOLES	1.00
CONTROL-SURFACE GAPS	.38
HINGES	.03
TOTAL $\frac{\Delta D}{D_{CRUISE}}$	3.63%
PAYLOAD CHANGE	-3,500 LB

EFFECT OF SURFACE TEMPERATURE ON SKIN FRICTION
M = 2.7; h = 65,000 FT

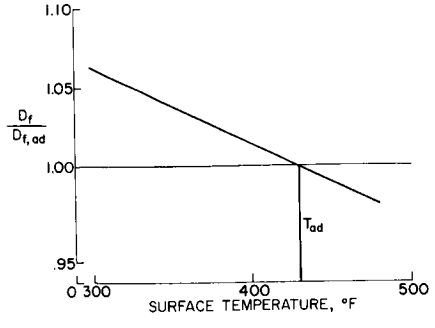

Figure 1

EFFECT OF EMISSIVITY ON SURFACE TEMPERATURE AND SKIN FRICTION

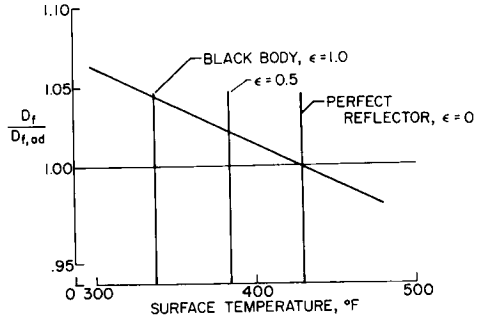

Figure 2

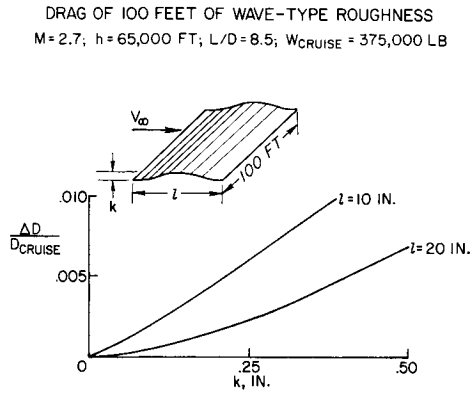

Figure 3

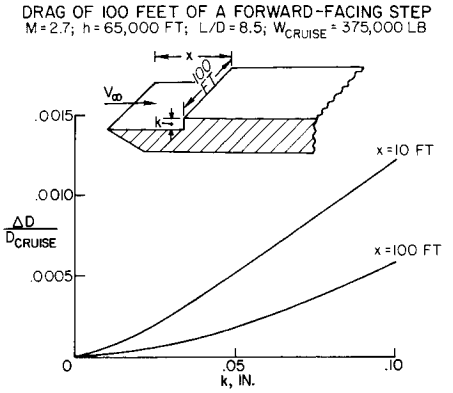

Figure 4

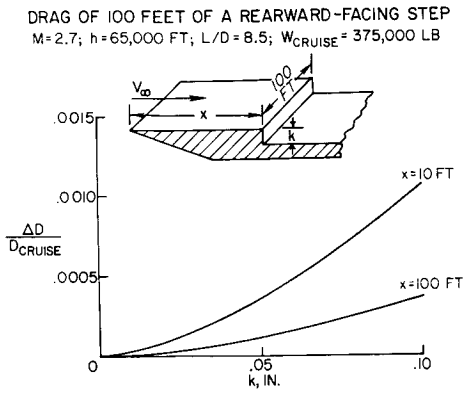

Figure 5

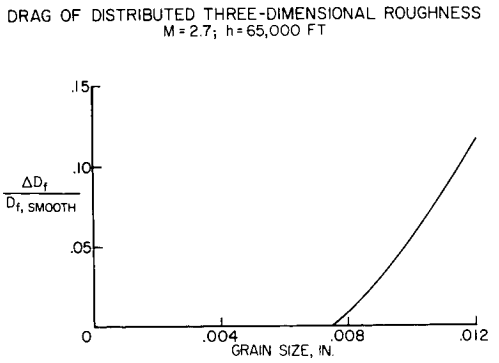

Figure 6

25. PREDICTION OF AIRPLANE SONIC-BOOM PRESSURE FIELDS

By Harry W. Carlson, F. Edward McLean,
and Wilbur D. Middleton

NASA Langley Research Center

SUMMARY

This paper presents a discussion of the sensitivity of supersonic-transport design and operation to sonic-boom considerations and shows the necessity for a study of these problems early in the development program. Methods of predicting pressure signatures are outlined and examples of the correlation of these estimates with wind-tunnel and flight measurements are shown. Estimates of sonic-boom characteristics for a representative supersonic transport show that in the critical transonic acceleration portion of the flight, overpressures somewhat lower than estimated by the use of far-field assumptions may be expected. Promising design possibilities for the achievement of further overpressure reductions are explored.

INTRODUCTION

Successful development of a supersonic transport in a national program and subsequent economical operation of the transport on the world's airlines is critically dependent on sonic-boom considerations, a factor completely new to commercial aviation and one, as yet, not fully understood. In the belief that those concerned with the future of air transport have need of a basic understanding of the sonic-boom phenomena, this paper is presented to outline the present status of sonic-boom research concerned with the formation and propagation of airplane pressure fields. The paper indicates the sensitivity of transport design and operation to sonic-boom considerations, reviews the state of knowledge regarding the prediction of overpressure levels for steady-level flight in still air, and explores the possibilities for sonic-boom minimization.

SYMBOLS

A_E	airplane effective cross-sectional area due to a combination of volume and lift, sq ft
C_L	lift coefficient
h	airplane altitude above sea level, ft
Δh	airplane altitude above terrain, ft

I positive impulse of pressure signature, $\int \Delta p \, dt$, lb sec/sq ft

M Mach number

Δp incremental pressure due to airplane flow field, lb/sq ft

Δp_{max} maximum positive value of Δp, lb/sq ft

t time, sec

W airplane weight, lb

x distance measured along or parallel to airplane longitudinal axis, ft

μ Mach angle

DISCUSSION

Influence of Sonic Boom on Supersonic-Transport Design and Operation

The influence of the sonic boom on the design and operation of the supersonic transport (SST) is shown in figure 1. The figure represents the sonic-boom problem in climb or in cruise depending on the scales assigned. In the plot at the left, it is seen that there is a wide variation in airplane weight for various airframe-engine configurations designed to meet a given set of mission specifications of range, payload, and speed; these weights are critically dependent on allowable design overpressure. Within the shaded area, characteristics for specific design concepts would form a crisscrossing network of curved lines. The large increases in weight necessary to meet the more stringent sonic-boom limitations are the result of the increased engine and wing size required for efficient flight at altitudes permitting lower overpressures. Since the current goals of the national SST program (2.0 psf in acceleration and 1.5 psf in cruise) fall within the vertical leg of the shaded area, careful design is required to achieve overpressures equal to or less than the goals without encountering excessive weight penalties.

When an airplane is developed and delivery is made to the airlines, the operator is faced with the problem illustrated at the right of figure 1. The airplane range (or payload since the two are related) is very sensitive to operational overpressure limitations. The maximum sensitivity falls near the current overpressure design goals. If adverse reaction encountered in operation proves to be greater than anticipated, altering operational procedures to reduce sonic-boom levels could result in serious and even disastrous reductions in supersonic range. On the other hand, if higher overpressures prove tolerable, there is the hazard that the airplane may have been unnecessarily compromised by the size and weight increases required to meet arbitrary sonic-boom limitations. Since the characteristics shown in this plot are dependent on the

airframe-engine design, it is evident that the operators' interest in this area must precede the establishment of design requirements.

Airplane Pressure Field

With sonic-boom considerations playing such a large part in SST development, it is important to review theoretical methods for estimating nominal ground overpressures and to establish their general applicability. Much of the remainder of the paper will be devoted to this purpose, and, finally, theory will be used to study sonic-boom pressure-signature characteristics for a representative SST.

The development of the pressure field about airplanes in supersonic flight is illustrated in figure 2. The flow field is, for the most part, concentrated between a bow shock and a tail shock fanning out from the airplane. Near the airplane, as in the upper pressure signature, there are separate shocks from the individual airplane components such as the fuselage, the wing, and the engine nacelles. This portion of the flow field where the shape of the signature is dependent on the airplane shape is termed the "near field." At larger distances the many shocks evident in the near field have merged and a two-shock system has formed. The "N" wave shown in the lower signature is characteristic of the so-called "far field." Usually, ground measurements of sonic-boom signatures created by airplanes flying at altitudes associated with supersonic speeds resemble the simple N wave. It is this pressure field traveling with the airplane and passing over the ground that creates the sonic-boom problem. In some manner, not completely understood, community acceptance is related to the characteristics of this signature.

Present-day pressure-signature estimation techniques are based on the solution for the flow about bodies of revolution presented in reference 1 and on theoretical work presented in reference 2, which relates airplane geometry and lifting effects to equivalent bodies. With the proper equivalent body used to represent the airplane, the method of reference 1 may be used to describe the flow field at all distances from the airplane. However, in many cases it is convenient and justifiable to make the assumption that a far-field N wave has formed and thus simplify the required calculations. This simplification appears to be valid for all current operational supersonic airplanes except for low-level missions of supersonic fighters.

Development of Airplane Equivalent Body

An outline of the methods used to develop the shape of the equivalent body is shown in figure 3. The area distribution is determined by the projected frontal areas intercepted by Mach planes passing through all airplane components. To this area is added directly an equivalent cross-sectional area due to lift found through a summation of local lifting forces along the airplane axis. Pronounced increases in the rate of growth of this effective area such as those that occur at the airplane nose, the wing-body juncture, and the body closure give rise to high local-flow-field pressures with the resultant

formation of flow-field shocks or pressure jumps. A more detailed discussion of the determination of effective area distributions and the subsequent evaluation of far-field pressure signatures made by using machine-computing techniques is given in reference 3. Machine-computing methods for evaluating near-field signatures have been developed, but have not as yet been published.

Comparison of Theory With Tunnel Signatures

An illustration of the use of the equivalent-body concept in estimating pressure signatures is given in the correlations with wind-tunnel measurements shown in figure 4. Wind-tunnel studies are particularly useful in the evaluation of lift effects which are expected to be of paramount importance for airplanes as large as the SST but which have not been covered to any large extent through flight tests of present airplanes. Data obtained at a Mach number of 1.41 at a distance of 25 inches below a 1-inch model of a delta-canard transport is shown in figure 4 for three values of lift coefficient. Inset sketches corresponding to each of the three signatures show the effective areas used in the estimates. Although tunnel vibration and boundary-layer effects cause considerable rounding of the measured signatures, it may be seen that there is a general agreement with the near-field calculations, and that the increasing influence of wing lift is well accounted for by the theory.

Comparison of Theory With Flight Signatures

The variation of shock strength and signature shape with airplane altitude is shown in figure 5. Measured signatures for the fighter airplane were obtained from three separate flight-test programs (refs. 4, 5, and 6). At an altitude of 60 feet, the signature has a maximum overpressure of nearly 100 psf and has obvious near-field characteristics with separate shocks from the nose, inlet, wing, and fuselage closure. At 48,000 feet, a characteristic far-field N wave has formed with a maximum overpressure less than 1 psf. The theory is seen to give, in general, the shape and magnitude of the signatures. It is not known whether those discrepancies shown are due to an inadequacy of the theory or to distortions in the signatures from unsteady flight and atmospheric effects.

Comparison of Theoretical and Flight Data

Fighter airplane.- Measurements of ground overpressure and signature impulse for this same fighter airplane obtained in the Oklahoma City tests (ref. 7) are shown in figure 6. The measured overpressure is the maximum positive value recorded, and the impulse is the area under the positive portion of the curve. Both overpressure and impulse are used in this figure to indicate that the correlation with theory covers all signature characteristics, and not maximum overpressure only. The data shown here apply to the flight-track station and represent averaged values for all flights within a 1,000-foot altitude band. The theory was determined from the most accurate information available from the airframe manufacturer and employed supersonic area distributions

rather than normal area distributions; thus, it is expected to be somewhat more precise than the theory used in previous correlations. Atmospheric effects for a standard atmosphere have been evaluated by using the method of reference 8. A reflection factor of 1.9 has been assumed. It will be noticed that measured values of both pressure and impulse tend to fall somewhat below the estimates. However it was also noticed during these tests that pressures 5 miles off track tended to be slightly above the theoretical estimates and indicated the possibility of an unexpected and unexplained atmospheric effect.

Bomber airplane.- Flight data for a larger airplane, the B-58 bomber, shown in figure 7 were obtained from the tests conducted at Edwards Air Force Base (ref. 6). A particular effort was made in these tests to insure precise tracking of the airplane; atmospheric disturbances were minimized by performing the tests in the relatively quiet morning air. The data points represent averaged values of overpressure and impulse measured by the flight-track microphone array during a given overpass. The theory which includes both volume and lift effects is shown in the form of a band in order to cover the range of Mach numbers and airplane weights encountered at a given altitude. As can be seen the agreement of experiment and theoretical data is good. An interesting feature of these data is that, although increasing altitude continues to have a beneficial effect on overpressure, there is a minimum impulse reached at about 60,000 feet - an altitude somewhat above that for the most efficient supersonic cruise of this airplane. The increase in impulse beyond 60,000 feet appears to be due to the high angle of attack necessary for sustained flight at the higher altitudes.

Estimated Sonic Boom for a Supersonic Transport

The supersonic transport will be a large airplane; the example considered in this section is larger than the B-58 by about the same factors that the B-58 is larger than the F-104. In each case the length has approximately doubled, and the weight has increased by a factor of about four. Theoretical methods must be relied on for estimates of the sonic-boom characteristics of this airplane. In view of the previously documented correlations of theory with wind-tunnel and flight measurements, it would seem that estimates of nominal steady-flight overpressures may be made with some confidence.

Estimated overpressure characteristics for a representative supersonic-transport configuration are shown in figure 8. A weight of 400,000 pounds and a Mach number of 1.4 were chosen to be representative of conditions at the critical climb portion of the flight; a weight of 350,000 pounds and a Mach number of 2.7 represent conditions in cruise. It has been found (ref. 9) that this and other supersonic-transport designs are long enough and slender enough for near-field flow characteristics to persist to quite large distances from the airplane. Thus, the calculated signatures and maximum overpressures shown here are based on the complete near-field theory. For reference, calculations made by using the assumptions of far-field theory are also shown. Inset sketches show the shape of the pressure signature for a representative $M = 1.4$ climb altitude and a representative $M = 2.7$ cruise altitude. It can be seen that somewhat lower overpressures (about 10 percent) are indicated by the more exact (near-field) theory in the climb or acceleration case. Perhaps more

significant is the fact that in this situation, the shape of the signature is controlled by the shape of the airplane, and thus there exists the possibility of modifying the airplane shape to modify and further reduce maximum overpressures. In effect the modification consists of the creation of a smooth effective area distribution in such a manner as to replace the two shocks shown in the inset sketch by a single bow shock with a succession of very weak shocks behind it.

Estimated Sonic Boom for a Modified Supersonic Transport

Applications of airplane design modifications suggested by near-field considerations are estimated to produce the results shown in figure 9. Theoretical estimates from near-field theory have been made for an airplane employing a modified and enlarged forward fuselage section and are compared with estimates for the original configuration repeated from figure 8. The change in the shape of the signature is shown in the inset sketch. It will be noted that for a design altitude of 40,000 feet, the maximum overpressure in the critical transonic acceleration portion of the flight has been reduced from about 2.2 to about 1.3 psf. Note that although the pressure signature in the vicinity of the tail shock has not been altered appreciably, its pressure jump is less than the modified bow-shock rise. Benefits for the Mach number 2.7 condition, however, do not extend to the altitudes normally associated with cruise, and pressures remain near the 1.5 psf level. Present studies indicate that the required modifications may have little or no detrimental influences on other aspects of airplane performance.

These possibilities are being studied not only by the NASA, but also by the competitors in the national supersonic transport program. Since the modifications do little to alter the total energy content of the pressure-field system but serve mainly to redistribute the energy, an assessment of the resultant benefits in reducing the sonic-boom problem are critically dependent on a knowledge of those characteristics of the pressure signatures which govern the response of people and buildings. Studies of boom minimization directed toward a reduction of the energy content (ref. 10) have shown that in this case, too, configuration effects are important and design requirements for minimization of signature impulse and far-field overpressures have been outlined. The effectiveness of design modifications in minimizing impulse is limited by compromises with other aspects of airplane design.

CONCLUDING REMARKS

This paper has presented a discussion of the sensitivity of supersonic-transport design and operation to sonic-boom considerations and has shown the necessity for a study of these problems early in the development program. Methods of predicting pressure signatures have been outlined and examples of the correlation of these estimates with wind-tunnel and flight measurements have shown good agreement. Estimates of sonic-boom characteristics for a representative supersonic transport have shown that in the critical transonic acceleration portion of the flight, overpressures somewhat lower than estimated by

the use of far-field assumptions may be expected. Promising design possibilities for the achievement of further overpressure reductions have been explored.

REFERENCES

1. Whitham, G. B.: The Flow Pattern of a Supersonic Projectile. Commun. Pure Appl. Math., vol. V, no. 3, Aug. 1952, pp. 301-348.

2. Hayes, Wallace D.: Linearized Supersonic Flow. Rept. No. AL-222, North Am. Aviation, Inc., June 18, 1947.

3. Carlson, Harry W.: Correlation of Sonic-Boom Theory With Wind-Tunnel and Flight Measurements. NASA TR R-213, 1964.

4. Maglieri, Domenic J.; Huckel, Vera; and Parrott, Tony L.: Ground Measurements of Shock-Wave Pressure for Fighter Airplanes Flying at Very Low Altitudes and Comments on Associated Response Phenomena. NASA TM X-611, 1961.

5. Maglieri, Domenic J.; and Morris, Garland J.: Measurements of the Response of Two Light Airplanes to Sonic Booms. NASA TN D-1941, 1963.

6. Hubbard, Harvey H.; Maglieri, Domenic J.; Huckel, Vera; and Hilton, David A. (With appendix by Harry W. Carlson): Ground Measurements of Sonic-Boom Pressures for the Altitude Range of 10,000 to 75,000 Feet. NASA TR R-198, 1964. (Supersedes NASA TM X-633.)

7. Hilton, David A.; Huckel, Vera; Steiner, Roy; and Maglieri, Domenic J.: Sonic-Boom Exposures During FAA Community-Response Studies Over a 6-Month Period in the Oklahoma City Area. NASA TN D-2539, 1964.

8. Friedman, Manfred P.; Kane, Edward J.; and Sigalla, Armand: Effects of Atmosphere and Aircraft Motion on the Location and Intensity of a Sonic Boom. AIAA J., vol. 1, no. 6, June 1963, pp. 1327-1335.

9. McLean, F. Edward: Some Nonasymptotic Effects on the Sonic Boom of Large Airplanes. NASA TN D-2877, 1965.

10. Carlson, Harry W.: Influence of Airplane Configuration on Sonic-Boom Characteristics. J. Aircraft, vol. 1, no. 2, Mar.-Apr. 1964, pp. 82-86. (Also available as NASA RP-208.)

INFLUENCE OF SONIC BOOM ON SUPERSONIC TRANSPORT DESIGN AND OPERATION

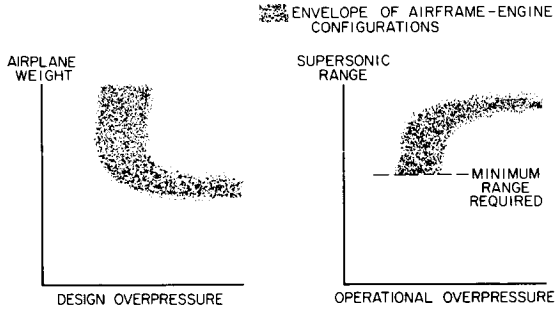

Figure 1

AIRPLANE PRESSURE FIELD

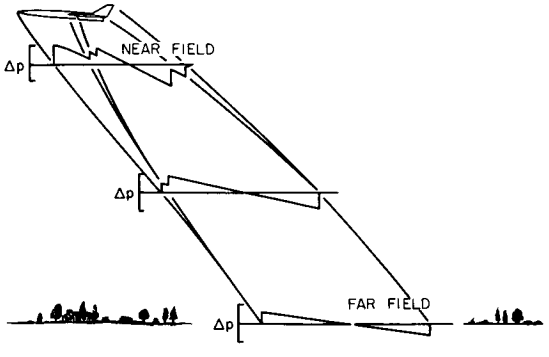

Figure 2

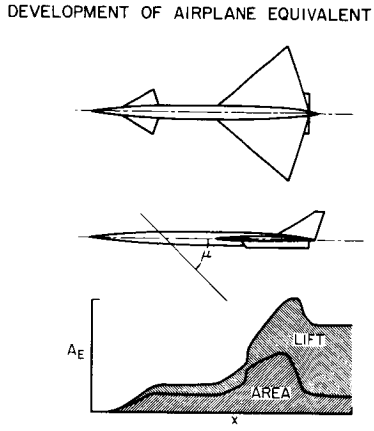

Figure 3

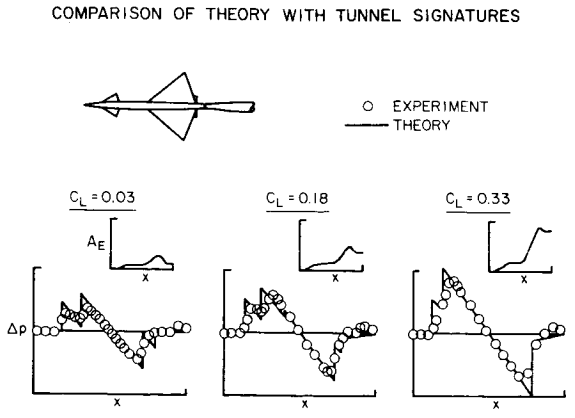

Figure 4

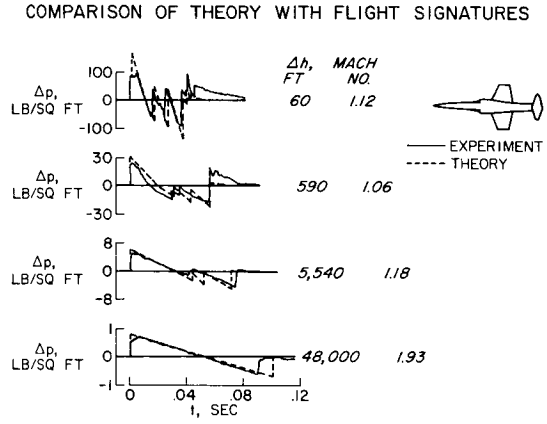

Figure 5

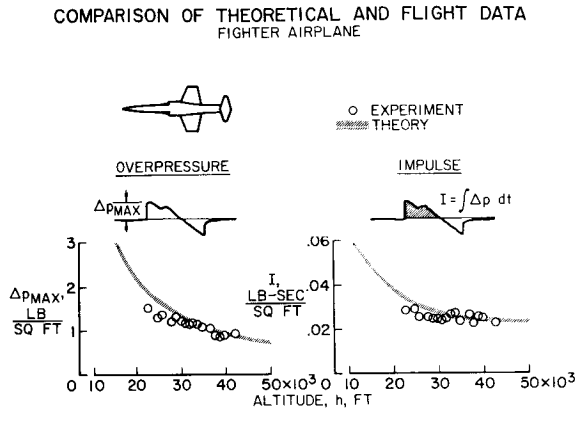

Figure 6

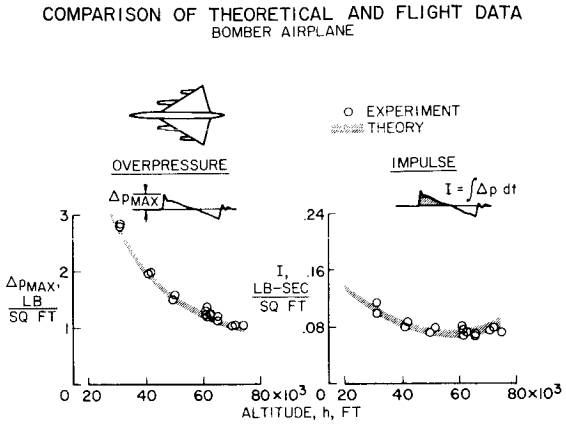

Figure 7

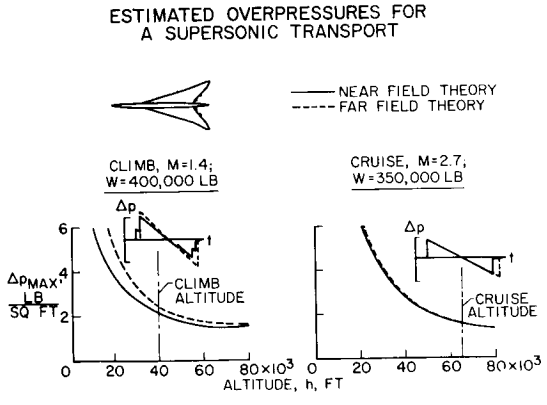

Figure 8

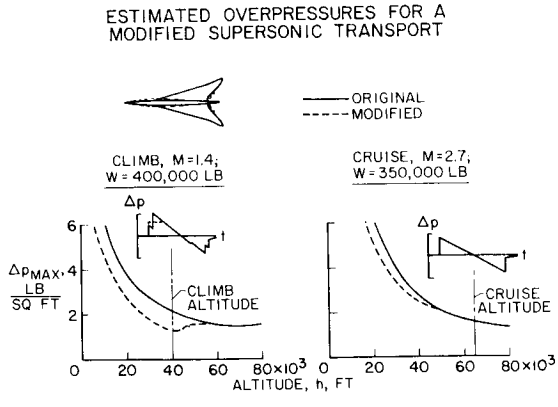

Figure 9

26. SIGNIFICANCE OF THE ATMOSPHERE AND AIRCRAFT OPERATIONS ON SONIC-BOOM EXPOSURES

By Domenic J. Maglieri and David A. Hilton

NASA Langley Research Center

SUMMARY

The information of the paper is in the form of a status report on the state of knowledge of sonic-boom phenomena, dealing first with the pressure buildups in the transonic speed range and with the lateral extent of the pattern in steady flight for quiescent atmospheric conditions. There are also discussions of recent data from flight-test studies relating to atmospheric dynamic effects on the sonic-boom signatures, and finally, brief discussions of the significance of signature shape on the response of people and structures. The acceleration and lateral-spread phenomena appear to be fairly well understood and predictable for current and future aircraft. Variations in the sonic-boom signature as a result of the effects of the atmosphere can be expected during routine operations. From the data evaluated to date, very similar variations in pressure signatures are noted for both fighter and bomber aircraft. The greatest questions still exist in the area of community acceptance of sonic booms. A more definitive answer to the community-acceptance problem will have to await adequate flight experience with larger aircraft.

INTRODUCTION

The scope of the material to be discussed in this paper is illustrated by the sketches of figure 1. Shown schematically in the figure is an airplane flight track extending from subsonic to supersonic speeds. Beneath the flight track are shown sketches of the shock-wave impingement patterns and the associated distributions of N-wave pressures, both along the track and perpendicular to it. The information of the paper is in the form of a status report on the state of knowledge of sonic-boom phenomena, dealing first with the pressure buildups in the transonic speed range (see refs. 1 to 10) and with the lateral extent of the pattern in steady flight for quiescent atmospheric conditions (see refs. 11 to 14). Also, there are discussions of recent data from flight-test studies relating to atmospheric dynamic effects on the sonic-boom signatures (refs. 9, 10, and 14 to 18), and finally, brief discussions of the significance of signature shape on the response of people and structures (see refs. 10, 17, and 19 to 24).

SYMBOLS

M	Mach number
Δp	sonic-boom overpressure, lb/sq ft
Δp_o	sonic-boom overpressure at ground level, lb/sq ft
$\Delta p_{o,calc\ max}$	calculated maximum sonic-boom overpressure on ground track, lb/sq ft
t	period of input, sec
τ	period of structure, sec

EFFECTS OF ACCELERATED FLIGHT

The perspective-view sketches of figure 2 illustrate an aircraft in accelerated, transonic flight and the associated overpressure patterns at the ground. Although the aircraft and shock wave are moving, the ground-exposure pattern is fixed and does not move with the aircraft. For simplicity and clarity, only the bow-wave shock patterns are shown on one side of the ground track. As the aircraft speed increases, the shock waves extend in length until they reach the ground and then extend laterally from the ground track as the aircraft speed further increases. The exposure areas on the ground are defined by the so-called focus and graze lines. Upstream of the focus line, only noise is observed. Pressure buildups occur along the focus line, with the maximum buildup on the ground track. In the region between the focus line and the graze line, multiple booms are observed as a result of the arrival at different times of disturbances from different points along the flight track. The graze line is the line along which the second signature ceases to exist because of atmospheric refraction. Downstream of the graze line, only conventional boom signatures are observed.

An extensive series of ground-pressure measurements has been made for longitudinal aircraft accelerations from Mach 0.9 to about Mach 1.5 at a constant altitude of 37,200 feet with a special array of microphones extending about 23 miles along the ground track. The measured data points from three such acceleration flights are shown at the bottom of figure 3. The data at the zero position represent the so-called superboom condition where pressure buildups occur. The data for the three separate flights were normalized by plotting the highest measured overpressure values at this zero position. The direction of the aircraft is from left to right, as indicated by the sketches at the top along with corresponding tracings of measured signatures. The data points in the figure represent peak overpressures as defined in the sketch. The low-value points to the left of the figure represent noise and are observed as rumbles. The high-value points near the center of the figure correspond to measurements that are very close to the focus point, and thus represent what

are conventionally described as superbooms. To the right of the focus point are two distinct sets of measurements which relate to the region of multiple booms. For convenience in illustrating the trends of the data, solid and dashed lines are faired through the data points. The data points that cluster about the solid curve relate to the first signature to arrive, in all cases, and this eventually develops into the steady-state signature. The data points that cluster about the dashed curve relate, in all cases, to the second signature to arrive. These values generally decrease as distance increases, and eventually this second wave ceases to exist because of the refraction effects of the atmosphere.

The highest overpressures are measured in a very localized region. These values are as high as 2.5 times the maximum value observed in the multiple-boom region and are thus in general agreement with the measured results for lower altitude tests of reference 9. The main multiple-boom overpressure values are of the same order of magnitude as those predicted for comparable steady-state flight conditions. Available overpressure prediction methods (see refs. 2, 3, and 15) give good agreement in the multiple-boom region, but are not considered reliable in the superboom region.

The locations of the superboom and multiple-boom regions are readily predictable (see refs. 3 and 15) provided such information as flight path, altitude, and acceleration rate of the aircraft is available. Based on the experience presented in figure 3, it is believed that the superboom can be placed at a position on the ground to within about ±5 miles of the desired location. The prediction of the location of the superboom can be improved if more detailed weather information is available.

As a matter of further information, it has been suggested that pressure buildups might occur for the graze condition. (See ref. 13.) Such a graze condition is associated with the lower branch of the multiple-boom curve of figure 3 (along the graze line of fig. 2). Based on these results and those of other special graze-condition flights, the possible buildups for the acceleration case are judged not to be significant.

LATERAL-SPREAD PATTERNS

With regard to the steady-flight conditions, some recent experiments have also been conducted in an effort to define more exactly the pressure distribution near the extremity of the shock-wave pattern on the ground. Some sample data are shown in figure 4. Particular emphasis was placed on the region where a grazing condition exists because of atmospheric refraction, as suggested by the ray-path sketch at the top of the figure. Flights were made at altitudes of 52,200 and 37,200 feet and Mach numbers of 2.0 and 1.5, respectively, during quiescent atmospheric conditions, and the results are compared with theory in the data plots at the bottom. The results from the flight at 52,200 feet and a Mach number of 2.0 show that the pressures are generally highest on the track as predicted by theory (ref. 13), and decrease generally as distance increases. The fact that measurements were obtained beyond the theoretically predicted cutoff distance by the method of reference 13 led to more definitive studies

at 37,200 feet and a Mach number of 1.5. (Solid symbols indicate that no boom was observed.) These data, which were obtained from four flights involving various displacement distances of the aircraft from the overhead position, are similar and, in fact, indicate measured signals as much as 15 miles beyond the predicted cutoff distance.

A better understanding of this phenomenon may be obtained from examination of some sample waveforms based on measurements at various distances. Sharply defined shock-wave-type signatures exist generally for the region predicted by the calculations. Near the predicted lateral cutoff, there was no evidence of pressure buildups due to grazing. At distances beyond the predicted cutoff, the signatures lose their identity and associated observations indicate the existence of rumbles, as described previously. Again, it is believed that these rumbles are noise radiated from the extremity of the shock wave as it propagates through the air in the vicinity of the measuring stations.

OTHER EFFECTS OF THE ATMOSPHERE

The propagation of shock waves through the atmosphere may involve the dynamics of the atmosphere as well as the gross refraction effects just described. The data of figure 5 were derived from an accurately calibrated and oriented array of matched microphones along the ground track of the aircraft (ref. 18). The variations in the wave shapes measured during one steady flight of a fighter aircraft are sketched in for the appropriate measurement locations. A wide variation in wave shape occurs even over a distance on the ground of a few hundred feet. This variation in wave shape resulted in substantial variations in the peak ground overpressure, the larger values being associated with the sharply peaked waves and the lower values with the rounded-off waves. Recent studies made under contract have suggested that the effects of the higher altitude disturbances are much less important than those of the lower altitudes (refs. 10, 14, 15, and 17). Recent flight experiments have pointed to the fact that disturbances in the first few thousand feet of the atmosphere may be most significant in affecting the shapes of the sonic-boom signatures measured at the ground. (See refs. 9 and 16.)

Measurements similar in nature to those of figure 5 have been made at specific measuring points for a large number of supersonic flights, and the results are in good qualitative agreement. Some samples of these latter data are shown in figure 6. Sonic-boom signatures for a fighter aircraft are shown at the left. (See ref. 18.) These signatures vary widely from sharply peaked waves at the top to rounded-off waves of sinusoidal appearance at the bottom. Such results are very similar to those shown in figure 5 for conditions of highly turbulent air in the lower atmosphere. The signatures on the right-hand side of the figure have been recently obtained for bomber aircraft and have a noticeably longer wavelength or time duration. The main distortions of the waves in each case are associated with the rapid compression phases, and these distortions are of the same general nature for both short and long wavelengths. The data of figure 6 relate to specific measuring stations for several different aircraft flyovers.

Because of the large number of data points available for a range of flight conditions, it was possible to make statistical analyses of the variations of overpressure. Samples of the overpressure variation data are given in figure 7. In the left-hand plot of the figure are shown overpressure distributions for a fighter aircraft, and in the right-hand plot are similar data for a bomber aircraft. The probability of equaling or exceeding a given ratio of the measured overpressure value to the maximum predicted value for the respective flight conditions (which occurs on the ground track) is shown. All the data have been plotted on log-normal scales, and straight lines have been faired through the data points as an aid in interpretation. For this type of presentation, all the data points would fall on a straight line if the logarithms of the data fitted a normal distribution. For the fighter aircraft, data were obtained on the ground track and at distances up to 10 miles from it; a wider variation in the overpressures occurred for the more remote stations. The probability of encountering high values of pressure was somewhat greater for the lateral stations. In the case of the bomber aircraft, fewer data points were available for analysis and, hence, the statistical sample is not as reliable. Based on the data available, the variation in overpressures for the bomber data, which have markedly longer wavelengths, is noted to be only slightly less than that for the fighter aircraft. Some of the pressure buildups due to atmospheric effects are of the same order of magnitude as those associated with the superboom phenomena. (See fig. 3.)

Although not shown in any of the figures of this paper, the variations in the values of the impulse function, which may be important in response phenomena, were markedly less than the pressure variations illustrated. (See ref. 18.)

RESPONSE PHENOMENA

Humans

With regard to the manner in which the sonic boom affects a community, the point is made that two types of sonic-boom exposures are involved as indicated in figure 8. The first of these is characterized as an outside exposure where the sonic-boom pressure wave impinges directly on the observer. The other is characterized as an inside-exposure situation in which case the sonic-boom pressure loading is first imposed on the exterior surfaces of the building. The observer is then exposed to a rather complex series of stimuli including auditory, vibratory, and visual inputs. The nature of the acoustic inputs for both of these exposure situations (see ref. 18) is summarized in figure 9.

The top trace represents the outside-exposure situation, whereas the bottom two traces represent the inside-exposure situation. The basic question which arises is, What are the significant features of the wave with regard to community response? In general, the ear is sensitive to the rapid changes in pressure associated with the two compressions and is not sensitive to the slowly varying pressure in between. Studies conducted by E. J. Richards at the University of Southampton which relate directly to the outside situation have

shown that the overpressure values and the initial rise time were both important with regard to loudness judgments. Of these two factors, the rise time was dominant.

A microphone inside a room records a pressure variation in that room similar to that of the middle trace. This record has the gross features of a damped sine wave, the frequencies of which correspond to the fundamental vibration-mode frequencies of the main framing members of the building. Although this inside pressure variation is of large amplitude, it usually occurs at a characteristic frequency at which the human ear is not very sensitive. Superposed on this middle trace is an audible acoustic input. In order to better define the audible acoustic input to an inside observer, simultaneous measurements were made with a microphone system having a response similar to that of the human ear. The objective was to eliminate the dominant low-frequency components that the ear does not normally respond to in order to better define the high-frequency components to which the ear is much more sensitive. Such audible acoustic signals are believed to be associated with the vibration of small building components and miscellaneous items of furnishings and equipment. The exposure for the inside observer is strongly shaped by the response of the building. The results of studies to date (refs. 19, 20, and 23) have suggested strongly that building vibrations play a dominant role in determining the judgments of community observers in sonic-boom exposure situations.

Buildings

The significant factors in the response of structures to sonic-boom signatures are illustated in figure 10. Represented by the sketches at the top of the figure are such features of the input as the overpressure, the impulse, and the period. In the case of the structure, the most significant feature is the period of its first natural vibration mode as indicated by the sketch on the right. Analytical studies presented in reference 21 and some additional studies conducted by David H. Cheng at the Langley Research Center have suggested that the ratio of the period of the input to the natural-vibration period of the structure determines the manner in which the structure responds and that maximum response occurs when this ratio is approximately unity. The plot at the bottom of the figure represents a brief summary of the situation for various combinations of the period of the input and the natural-vibration period of the structure; for instance, for a short period input, as in the case of a fighter aircraft, and a long period response, such as for a large structure, the impulse is believed to be the significant feature of the input. On the other hand, for a long period input or for a very large airplane and a short period of the structure as in the case of small components of a building, the overpressure is believed to be the significant feature of the input. Many of the structures which are of concern in a community are of such a nature that they do not clearly fall into either of the two categories shown in figure 10, and hence it must be concluded that both the overpressure and impulse are significant.

CONCLUDING REMARKS

In conclusion, some recent results obtained with the aid of fighter and bomber aircraft have been presented in an attempt to show the significance of the atmosphere and aircraft operation on sonic-boom exposures. The acceleration and lateral-spread phenomena appear to be fairly well understood and predictable for current and future aircraft. Variations in the sonic-boom signature as a result of the effects of the atmosphere can be expected during routine operations. From the data evaluated to date, very similar variations in pressure signatures are noted for both fighter and bomber aircraft.

The greatest questions still exist in the area of community acceptance of sonic booms. A more definitive answer to the community-acceptance problem will have to await adequate flight experience with larger aircraft.

REFERENCES

1. Maglieri, Domenic J.; and Lansing, Donald L.: Sonic Booms From Aircraft in Maneuvers. NASA TN D-2370, 1964.

2. Lansing, Donald L.: Application of Acoustic Theory to Prediction of Sonic-Boom Ground Patterns From Maneuvering Aircraft. NASA TN D-1860, 1964.

3. Lansing, Donald L.; and Maglieri, Domenic J.: Comparison of Measured and Calculated Sonic-Boom Ground Patterns Due to Several Different Aircraft Maneuvers. NASA TN D-2730, 1965.

4. Lina, Lindsay J.; and Maglieri, Domenic J.: Ground Measurements of Airplane Shock-Wave Noise at Mach Numbers to 2.0 and at Altitudes to 60,000 Feet. NASA TN D-235, 1960.

5. Warren, C. H. E.: The Propagation of Sonic Bangs in a Nonhomogeneous Still Atmosphere. Paper No. 64-547, Intern. Council Aeron. Sci., Aug. 1964.

6. Lilley, G. M.; Westley, R.; Yates, A. H.; and Busing, J. R.: Some Aspects of Noise From Supersonic Aircraft. J. Roy. Aeron. Soc., vol. 57, no. 510, June 1953, pp. 396-414.

7. Rao, P. Sambasiva: Supersonic Bangs. Aeron. Quart., vol. VII.
   Part 1. pt. I, Feb. 1956, pp. 21-44.
   Part 2. pt. II, May 1956, pp. 135-155.

8. Kerr, T. H.: Experience of Supersonic Flying Over Land in the United Kingdom. Rept. 250, AGARD, North Atlantic Treaty Organization (Paris), Sept. 1959.

9. Hubbard, Harvey H.; Maglieri, Domenic J.; Huckel, Vera; and Hilton, David A.: Ground Measurements of Sonic-Boom Pressures for the Altitude Range of 10,000 to 75,000 Feet. NASA TR R-198, 1964.

10. Anon.: Proceedings of NASA Conference on Supersonic-Transport Feasibility Studies and Supporting Research - September 17-19, 1963. NASA TM X-905, 1963.

11. Lina, Lindsay J.; Maglieri, Domenic J.; and Hubbard, Harvey H.: Supersonic Transports - Noise Aspects With Emphasis on Sonic Boom. 2nd Supersonic Transports (Proceedings). S.M.F. Fund Paper No. FF-26, Inst. Aeron. Sci., Jan. 25-27, 1960, pp. 2-12.

12. Maglieri, Domenic J.; Parrott, Tony L.; Hilton, David A.; and Copeland, William L.: Lateral-Spread Sonic-Boom Ground-Pressure Measurements From Airplanes at Altitudes to 75,000 Feet and at Mach Numbers to 2.0. NASA TN D-2021, 1963.

13. Randall, D. G.: Methods for Estimating Distributions and Intensities of Sonic Bangs. R. & M. No. 3113, British A.R.C., 1959.

14. Kane, Edward J.; and Palmer, Thomas Y.: Meteorological Aspects of the Sonic Boom. SRDS Rept. No. RD64-160 (AD 610 463), FAA, Sept. 1964.

15. Friedman, Manfred P.: A Description of a Computer Program for the Study of Atmospheric Effects on Sonic Booms. NASA CR-157, 1965.

16. Maglieri, Domenic J.; and Parrott, Tony L.: Atmospheric Effects on Sonic-Boom Pressure Signatures. Sound, vol. 2, no. 4, July-Aug. 1963, pp. 11-14.

17. Hubbard, Harvey H.; and Maglieri, Domenic J.: Noise and Sonic Boom Considerations in the Operation of Supersonic Aircraft. Paper No. 64-548, Am. Inst. Aeron. Astronaut., Aug. 1964.

18. Hilton, David A.; Huckel, Vera; Steiner, Roy; and Maglieri, Domenic J.: Sonic-Boom Exposures During FAA Community-Response Studies Over a 6-Month Period in the Oklahoma City Area. NASA TN D-2539, 1964.

19. Pearsons, K. S.; and Kryter, K. D.: Laboratory Tests of Subjective Reactions to Sonic Boom. NASA CR-187, 1965.

20. Borsky, Paul N.: Community Reactions to Sonic Booms in the Oklahoma City Area. AMRL-TR-65-37, U.S. Air Force, Feb. 1965.

21. Arde Associates: Response of Structures to Aircraft Generated Shock Waves. WADC Tech. Rept. 58-169, U.S. Air Force, Apr. 1959.

22. Mayes, William H.; and Edge, Philip M., Jr.: Effects of Sonic Boom and Other Shock Waves on Buildings. Mater. Res. Std., vol. 4, no. 10, Nov. 1964, pp. 588-593. (Available also as NASA RP-385.)

23. Nixon, Charles W.; and Hubbard, Harvey H.: Results of USAF-NASA-FAA Flight Program to Study Community Responses to Sonic Booms in the Greater St. Louis Area. NASA TN D-2705, 1965.

24. Parrott, T. L.: Experimental Studies of Glass Breakage Due to Sonic Booms. Sound, vol. 1, no. 3, May-June 1962, pp. 18-21.

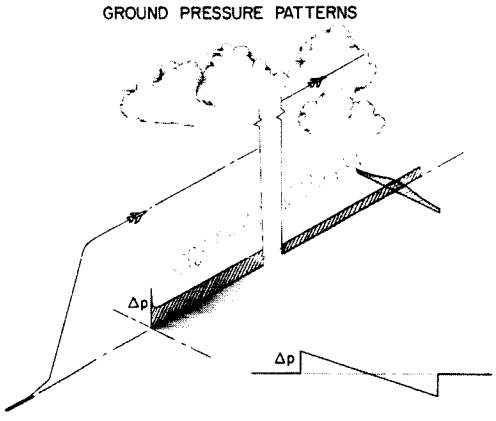

Figure 1

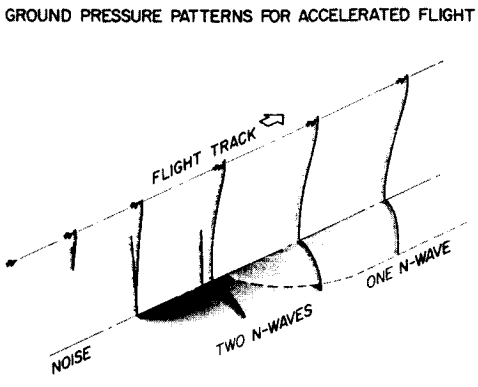

Figure 2

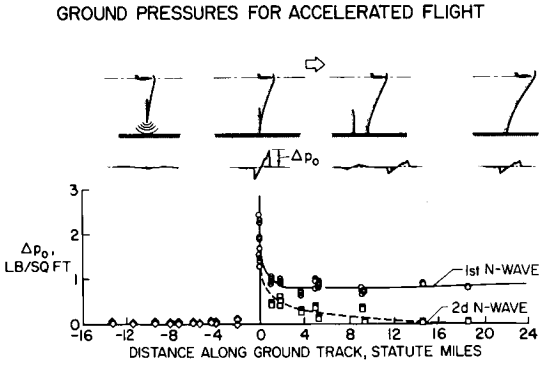

Figure 3

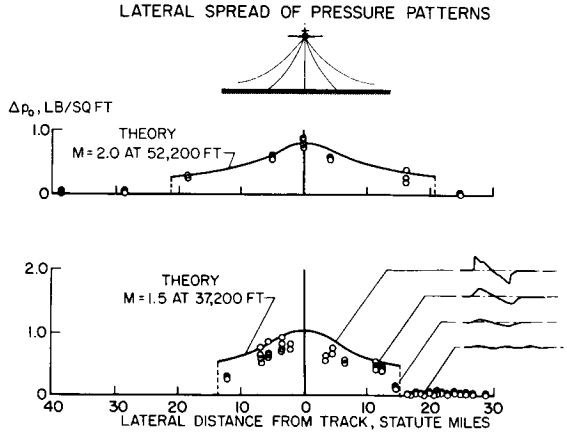

Figure 4

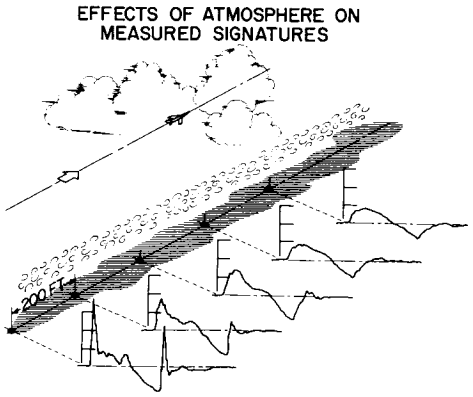

Figure 5

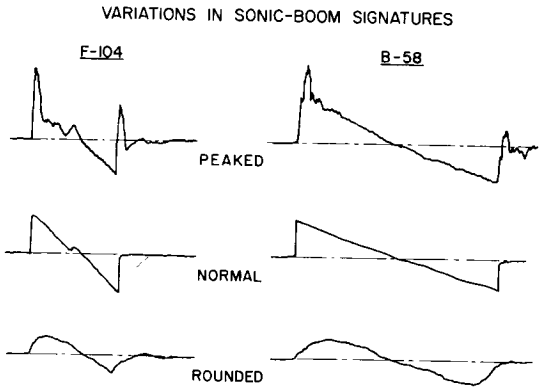

Figure 6

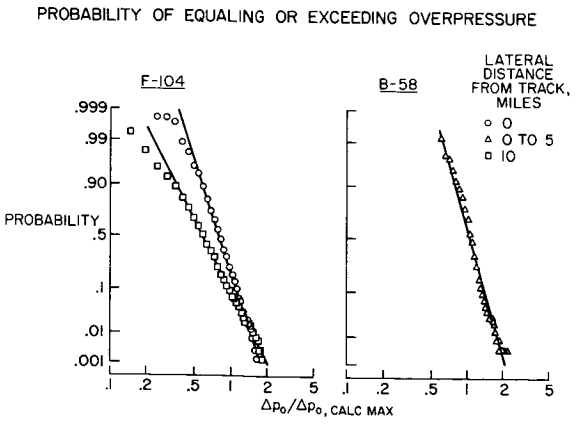

Figure 7

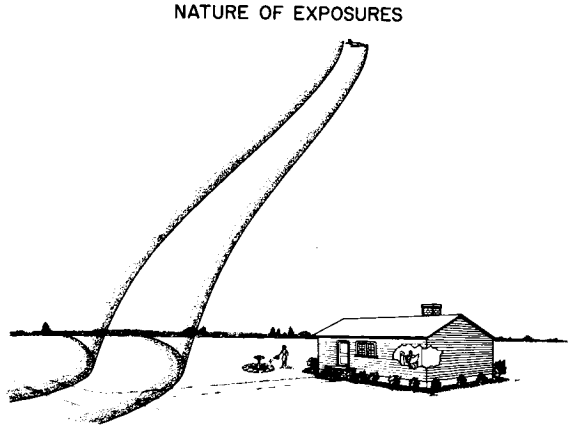

Figure 8

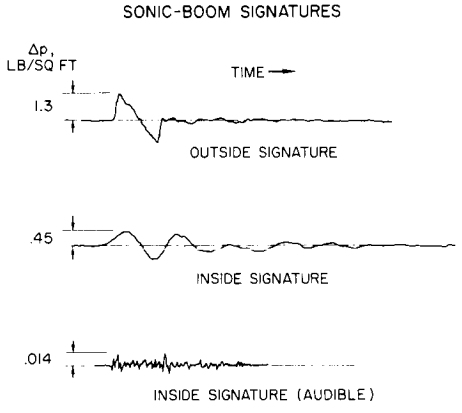

Figure 9

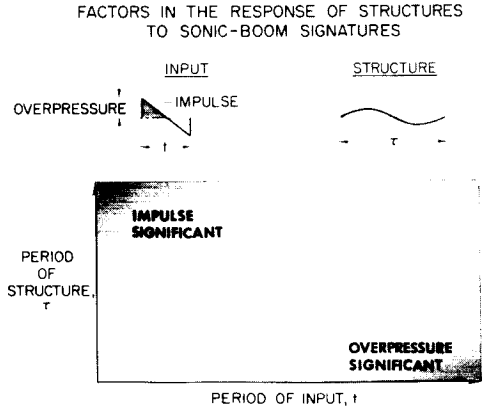

Figure 10

27. OPERATIONAL EXPERIENCES OF GENERAL AVIATION AIRCRAFT

By Joseph W. Jewel, Jr., and Walter G. Walker

NASA Langley Research Center

SUMMARY

An investigation is currently under way to determine the operational practices and load experiences of general aviation aircraft performing five basic types of operations: twin-engine executive, single-engine executive, personal, instructional, and commercial survey. Limited data obtained to date from aircraft engaged in these operations indicate that aircraft are generally being operated within the limits to which they were designed.

INTRODUCTION

The National Aeronautics and Space Administration, at the request of the Federal Aviation Agency, has recently undertaken an extensive V-G/VGH program on a variety of general aviation aircraft to obtain current information on the operating practices and the flight loads experienced by these aircraft during normal operations. Information being obtained from this program is handled in a manner similar to that obtained from the V-G/VGH transport programs in that the specific data are treated as proprietary between the operators and NASA. Only the generalized results are made available to organizations outside of NASA. Since conclusive, or statistically significant, results are not available at this early stage of the program, the purpose of this paper is to present the scope of the program and to illustrate the type of data that are being obtained.

SYMBOLS

V_A	design maneuver speed, knots
V_C	design cruise speed, knots
V_D	design dive speed, knots
V_{NE}	placard never-exceed speed, knots
V_S	design stall speed, knots
W_{MAX}	design gross weight, pounds
W_{MIN}	minimum design weight, pounds

DISCUSSION

Program Description

The scope of the program is indicated in table I. Five basic types of operations are included in the program: twin-engine executive, single-engine executive, personal, instructional, and commercial survey. Business and personnel transport operations are covered by the first two categories; flying club and general flying by the third; instructional and student flying by the fourth; and forest patrol, pipeline survey, and commercial fish spotting by the last operation.

The number of aircraft in each operation which are instrumented with either an NASA V-G or an NASA VGH recorder are listed in the columns on the right of table I. Generally, three VGH and nine V-G recorders were assigned to each type of operation. However, since most of the high-performance, or turbine-powered, planes fall in the twin-engine executive class, an additional five VGH recorders were assigned to this operation. The eight V-G recorders in this category were assigned to two types of twin-engine piston-powered aircraft. The total program will involve 64 aircraft - 20 instrumented with VGH recorders and 44 with V-G recorders - from which it is expected that 64,000 hours of data will be obtained in a period of from 4 to 6 years. As the program now stands, 2225 hours of data from VGH recorders and 3904 hours of data from V-G recorders have been collected for a total of 6129 recorded hours.

Figure 1 shows the location of the 46 aircraft instrumented to date with 20 VGH recorders and 26 V-G recorders. These aircraft are based throughout the continental United States to avoid biasing the data as coming from any one geographical area. The aircraft chosen for the program range in size from small, light, training planes weighing less than 1500 pounds to twin, jet-powered, executive transports weighing about 20,000 pounds. Owners of these aircraft were personally contacted, briefed on the purpose and aims of the program, and asked to participate in the program until 1000 hours of flight data were obtained over a period that at least covered the four seasons. Normally, an attempt was made to instrument planes that were flown a minimum of 300 hours per year.

VGH Data

The largest data sample - 888 hours - obtained to date from a single aircraft came from an airplane used in commercial fish-spotting operations. This paper, therefore, deals primarily with VGH data from the commercial fish-spotting operation. A limited amount of V-G data from each of the other four types of operations is also shown.

The airplane used for the fish-spotting operation was a small, high-wing monoplane having a take-off gross weight of about 1500 pounds. The data sample contained 211 flights having an average length of 4 hours and 13 minutes. Most

of the flights were over water, extending out over the Atlantic Ocean from the Eastern Seaboard between New Jersey and South Carolina.

The percent time that the aircraft was flown in various altitudes and airspeed intervals is shown in figure 2. Most of the flights were below altitudes of 3000 feet, with the majority of the time being spent between altitudes of 500 and 2500 feet. The distribution of airspeeds shows that the largest number of flights were flown between 50 and 70 knots.

Although the airspeed distribution shown in figure 2 indicates the percent time flown in various airspeed intervals, it does not give the relationship between the speeds actually flown and the design limit speeds. This information is given in figure 3 which shows the percent time flown above given speeds and indicates the design cruise speed, the design dive speed, and the placard never-exceed speed. For this operation, neither the design dive speed nor the never-exceed speed was reached. The design cruise speed was equaled, or exceeded, only one hundredth of 1 percent of the flight time.

The maneuver acceleration experience for the fish-spotting operation is given in figure 4. The outline of the shaded area represents the maximum positive and negative maneuver accelerations recorded by the instrumented aircraft in 10-knot speed intervals. The solid outline defines the design positive and negative maneuver accelerations required by Federal Aviation Regulations (ref. 1) for this particular airplane. This outline is designated the design maneuver envelope and was constructed assuming the aircraft was flying at its maximum gross weight. The dashed line represents a section of the positive design maneuver envelope based on the aircraft minimum design weight. The curved sections of the envelopes are stall lines computed from the maximum static lift coefficients. The vertical lines represent the design stall speed, the design maneuver speed, the design cruise speed, the design dive speed, and the placard never-exceed speed. In general, the instrumented airplane maneuver accelerations were well within the design limits. The figure does show, as would be expected, that positive maneuver accelerations were larger than negative maneuver accelerations.

The gust acceleration experience of the fish-spotting airplane is shown in figure 5. The outline of the shaded area in the center of the figure indicates the maximum positive and negative gust acceleration encountered in 5-knot speed intervals and the solid outline defines the design gust envelope based on the maximum gross weight of the aircraft. This envelope was constructed in accordance with Federal Aviation Regulations (ref. 1) which require that the aircraft be designed to withstand positive and negative 30-foot-per-second effective gusts U_e at speeds up to the design cruise speed and positive and negative 15-foot-per-second effective gusts at the design dive speed. The dashed curve is the positive limit for the design gust envelope based on the aircraft minimum design weight. None of the gust accelerations experienced by the instrumented aircraft exceeded the design gust limits.

Figure 6 shows the percent time the aircraft was flown in rough air in each 1000-foot-altitude interval. Rough air is defined here as turbulent areas containing gust velocities on the order of 2 feet per second. Data from altitudes above 3000 feet are not shown since the sample size was considered too

small to yield valid results. The solid line shows the predicted rough air based on transport operations defined in reference 2. The variation in rough air encountered by the fish-spotting operation is in good agreement with that predicted by reference 2.

V-G Data

Examples of V-G data taken from aircraft engaged in the remaining four types of operations are shown in figure 7. One thousand four hundred and ninety-six hours were recorded by three aircraft of the same type engaged in twin-engine executive operations, 341 hours were recorded by two aircraft of the same type engaged in single-engine executive operations, 315 hours were recorded by one airplane engaged in personal operation, and 453 hours were recorded by two aircraft of the same type engaged in instructional operations. In each plot, the load factor is plotted against the indicated airspeed in knots. The design flight envelopes, based on the composite gust and maneuver design envelopes for the maximum gross weight, are shown in each plot by the solid lines. Portions of the positive flight envelope, based on the minimum design weight, are indicated by the dashed lines. Design stall, maneuver, cruise, and dive speeds and the placard never-exceed speeds are designated by the vertical lines. The outlines of the shaded areas show the maximum normal accelerations and the associated airspeeds recorded by the instrumented airplanes.

An examination of figure 7 shows that, although the design cruise speed was exceeded by aircraft in all four types of operations, the placard never-exceed speed was equaled or exceeded only during instructional-type operations. In general, most of the loads experienced by aircraft in the four operations were contained within the design flight envelopes. One airplane in the twin-engine executive operations did experience an acceleration that exceeded the design flight envelope; however, this acceleration was below the ultimate load factor. The exceedance of the positive stall line between 60 and 80 knots by aircraft in instructional operations probably resulted from dynamic overshoot during accelerated maneuvers made in training operations.

CONCLUDING REMARKS

An investigation is currently under way to determine the operational practices and load experiences of general aviation aircraft performing five basic types of operations: twin-engine executive, single-engine executive, personal, instructional, and commercial survey. Limited data obtained to date from aircraft engaged in these operations indicate that aircraft are generally being operated within the limits to which they were designed.

REFERENCES

1. Anon.: Airworthiness Standards: Normal, Utility, and Acrobatic Category Airplanes. Federal Aviation Regulation Part 23, Rules Service Co. (Washington, D.C.), Feb. 1, 1965, pp. C-74 - C-77.

2. Press, Harry; and Steiner, Roy: An Approach to the Problem of Estimating Severe and Repeated Gust Loads for Missile Operations. NACA TN 4332, 1958.

TABLE I

SCOPE OF GENERAL AVIATION PROGRAM

TYPE OF OPERATION	NUMBER OF AIRCRAFT WITH-	
	VGH RECORDER	V-G RECORDER
TWIN-ENGINE EXECUTIVE	8	8
SINGLE-ENGINE EXECUTIVE	3	9
PERSONAL	3	9
INSTRUCTIONAL	3	9
COMMERCIAL SURVEY	3	9

- DESIRED TOTAL: 64,000 FLIGHT HOURS
- RECORDED TO DATE:

VGH RECORDS: 2,225 FLIGHT HOURS
V-G RECORDS: 3,904 FLIGHT HOURS
TOTAL: 6,129 FLIGHT HOURS

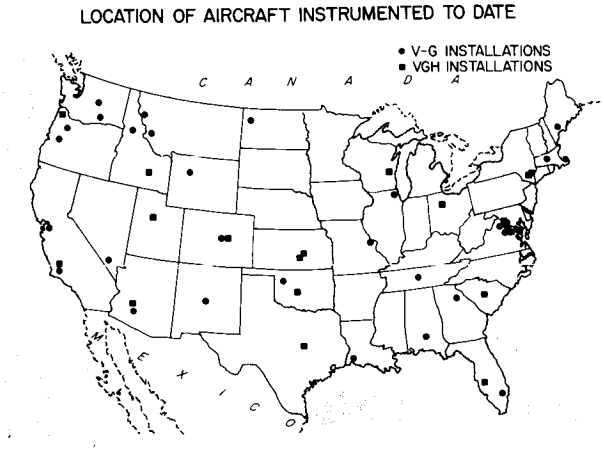

Figure 1

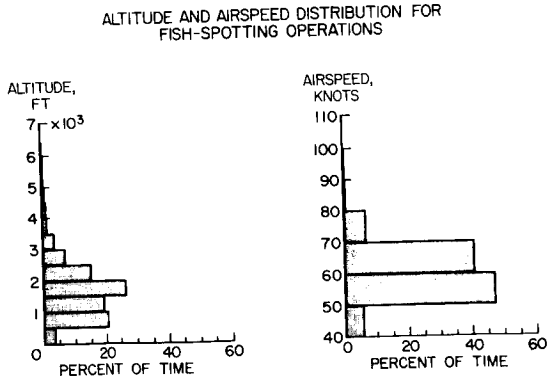

Figure 2

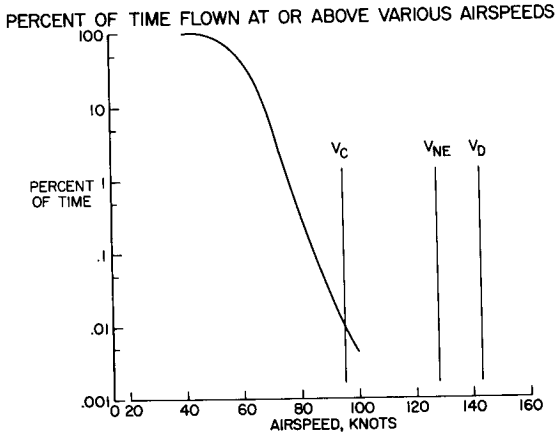

Figure 3

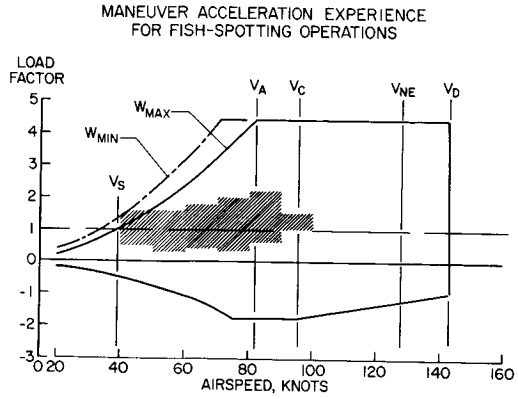

Figure 4

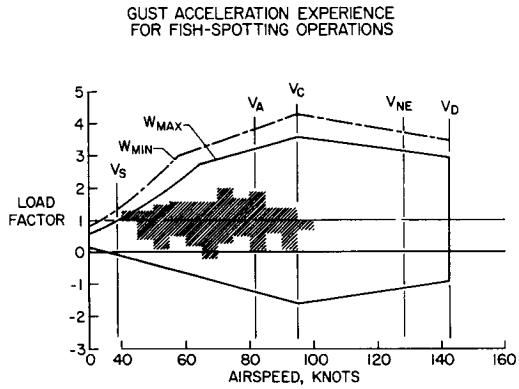

Figure 5

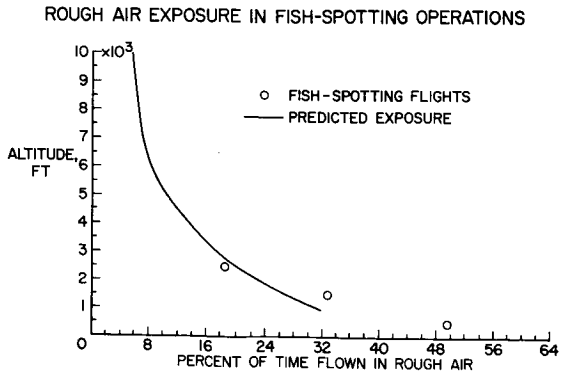

Figure 6

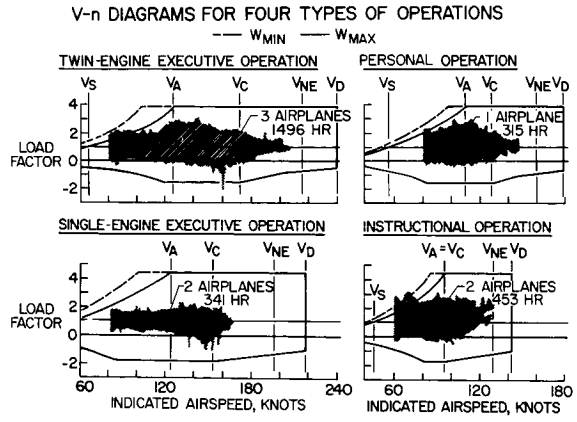

Figure 7

28. AIRPLANE SPINNING

By James S. Bowman

NASA Langley Research Center

SUMMARY

A summary on spinning is presented to point out the state of the art and the most important parameters, and to show the effects of these parameters on the spin and spin-recovery characteristics. The discussion presented applies to the fully developed spin. The principal factors in spinning are mass distribution, which is by far the most important single parameter, and tail design, which is particularly important for conditions of zero or near-zero loading. By knowing the mass distribution and tail design, it is possible in many cases to predict whether an airplane has satisfactory spin-recovery characteristics. In other cases, however, it is necessary to make spin tests to assure satisfactory recovery.

INTRODUCTION

The purpose of this paper is to present a summary on spinning which will indicate the state of the art, point out the most important parameters, and show the effects of these parameters on the spin and spin-recovery characteristics. The discussion presented applies to the fully developed spin.

Spinning is a subject that has not been very amenable to theoretical analysis, and consequently most spin studies have been conducted by experimental procedures. At the NASA Langley Research Center much experience has been gained from spin-tunnel tests. In this connection, spin tests have been made of models of nearly 400 different airplane designs over a period of 30 years, and very good correlation between the model tests and full-scale spin tests has been established (refs. 1 to 3).

SYMBOLS AND ABBREVIATIONS

S	wing area, sq ft
b	wing span, ft
ρ	air density, slugs/cu ft
μ	airplane relative-density factor, $\frac{m}{\rho S b}$

m	mass of airplane, slugs
I_X, I_Y	moments of inertia about X and Y body axes, respectively, slug-ft^2
W	weight, lb
TDR	tail damping ratio
URVC	unshielded rotor volume coefficient
TDPF	tail damping power factor, (TDR)(URVC)

DISCUSSION

Mass Distribution

The airplane mass distribution has an almost overriding effect on the spin and spin recovery. The mass distribution is the way in which the mass of an airplane is distributed along the fuselage and wings. The aerodynamic factors are also important; however, the effects of the aerodynamic factors on the spin and recovery depend on the mass distribution.

The developed spin involves a balance between the aerodynamic forces and moments and the inertia forces and moments acting on an airplane; an illustration is presented in figure 1 to show the balance of moments in pitch. The sketch on the left indicates that in a spin, an airplane has a nose-down aerodynamic moment. The sketch on the right shows a system of weights representing an airplane from a mass standpoint. As this system of weights rotates about the spin axis, the weights cause a nose-up inertia pitching moment; this nose-up inertia moment balances out the aerodynamic nose-down pitching moment. There are corresponding balances of aerodynamic and inertia moments about the other axes.

Since the moments in a spin depend on the inertia as well as the aerodynamic characteristics of the airplane, the effectiveness of any control in terminating a spin depends not only on the aerodynamic moments the control creates, but also on the inertia moments it induces. These inertia moments are a function of the mass distribution of the airplane; and, in this way, the mass distribution is directly related to the airplane spinning.

The mass distribution of airplanes can be grouped into three general loading categories, as indicated in figure 2. Shown on the right is the case of an airplane that has more of its weight distributed along the wings than along the fuselage by virtue of having wing fuel, wing-mounted engines, wingtip tanks, wing-mounted military stores, and so forth. This type of weight distribution is referred to as a wing-heavy loading; and in this case, the roll

moment of inertia is greater than the pitch moment of inertia. Shown on the left is the case of an airplane that has most of its weight distributed along the fuselage. This type of weight distribution is referred to as a fuselage-heavy loading; and in this case, the roll moment of inertia is less than the pitch moment of inertia. Shown in the middle of the figure is the case of an airplane that has roll and pitch moments of inertia which are about equal; this condition is referred to as a zero loading.

The loading of the airplane can dictate what controls are required for recovery (ref. 4). The deflection of the rudder against the spin is always recommended, but it may not be satisfactory. For the case of the wing-heavy loading, down elevator is the primary recovery control; whereas, for the fuselage-heavy loading, the aileron is the primary recovery control. In the latter case, the aileron needs to be deflected with the spin - for example, stick right for a spin to the right. The zero loading is an uncertain condition as far as recovery is concerned. It is difficult to tell exactly what the effect of the control might be, but almost invariably the proper recovery procedure is to move the rudder against the spin and, then, at a short time later move the elevator down.

Figure 2 might be taken to indicate that the prediction of spin recoveries is simple; however, for two reasons, it is not quite so simple. First, the exact range of loading for each category shown in figure 2 cannot be predicted; and second, although the controls that should be moved for recovery and the direction that they should be moved can be predicted from the mass distribution, whether the controls will have enough aerodynamic effectiveness to give a satisfactory recovery cannot be predicted in many cases.

Tail Design

Figure 2 shows that mass distribution is a critically important factor. Another very important factor is tail design, which is particularly important for airplanes in the zero or near-zero loading condition, where the rudder is a primary recovery control. The factors entering into tail design from spin considerations are illustrated in figure 3. The sketches show an airplane in the spinning attitude. There is a dead-air region over much of the vertical tail caused by the stalled wake of the horizontal tail. It is obvious that in order to have good rudder effectiveness for recovery, there must be a substantial amount of rudder area outside this dead-air region. This rudder area may be either above or below the dead-air region. Another factor which enters into tail design from the spin standpoint is that there should be a substantial amount of fixed area beneath the horizontal tail to provide damping of the spinning motion. It is important to have both of these factors - rudder power and damping. The sketch at the left in figure 3 illustrates a good tail design; whereas, the sketch at the right illustrates a poor tail design with the rudder entirely within the dead-air region and with very little fixed area beneath the horizontal tail.

A criterion for tail design was determined empirically many years ago (refs. 5 and 6) on the basis of spin-tunnel tests with about 100 different

designs. This criterion is called the tail-damping power factor, which is a measure of the damping provided by the fixed area beneath the horizontal tail and the control power provided by the unshielded part of the rudder. The formula for determining the tail-damping power factor is given in figure 4.

The tail-damping power factor required to insure satisfactory recovery is given in figure 5. Figure 5 shows the tail-damping power factor plotted against mass distribution. All of the data are in the area of zero or near-zero loading, where the rudder is a primary recovery control and the tail design is of particular importance. The scale on the abscissa was chosen to point out the fact that in this discussion of tail design, only a limited part of the total range of mass distributions that have been found to exist for all airplanes applies.

The plot shows boundaries indicating the minimum values of the tail-damping power factor required to insure satisfactory recovery. The hatched side of the boundaries is the unsatisfactory side. The solid lines are for recovery by rudder alone, and the broken line shows the boundary for recovery by rudder and elevator. The boundaries are presented in terms of the parameter μ, which is the airplane relative-density factor. This factor is a common parameter used in airplane stability work and is a measure of the density of the airplane relative to the density of the air in which it is flying. The airplane density is expressed as the mass of the airplane divided by an arbitrary volume obtained by multiplying the wing area by the span. The value of μ, then, is the ratio of this arbitrary measure of airplane density to the actual air density.

Figure 5 presents boundaries for values of the relative-density factor of 35, 15, and 6. The value of 6 is representative of that for light single-engine personal-owner airplanes, and the value of 35 is representative of that for executive jets and jet trainers. This group of boundaries, then indicate that the tail-damping power factor required for satisfactory recovery is dependent on both the mass distribution and the airplane relative-density factor. These boundaries can be used as design charts to determine whether a particular tail design will insure satisfactory recovery for the range of variables shown on the chart.

Use of the data presented in figure 5 will be made in a discussion on how the satisfactory spin-recovery characteristics of an airplane may deteriorate as the airplane weight is increased. The data in figure 5 for $\mu = 15$ are replotted in figure 6; however, in figure 6, the scales have been expanded. Boundaries for satisfactory spin recovery are shown for values of the airplane relative-density factor of 15 and 20. Point 1 in figure 6 is representative of an airplane originally designed to have a relative-density factor of 15. In other words, the airplane was designed so that the tail was just barely satisfactory from a spin-recovery standpoint. Then, over the years the airplane gross weight is increased by one-third because of design changes or changes in operating practices. This increase in weight increases the value of μ to 20, and the airplane characteristics would then be on the unsatisfactory side of the boundary. If some of this weight increase were in the form of wing-tip tanks or heavier engines on the wing, the airplane characteristics would be

even more unsatisfactory, as shown by point 2. Such changes in spin-recovery characteristics from satisfactory to unsatisfactory have actually happened in the past as a result of a weight increase over that of the basic airplane design.

Figure 7 gives a summary of the most important factors in spinning and indicates the state of the art at the present time. The mass-distribution scale at the bottom of the figure applies to both the plot at the bottom and the table at the top. The extent of the mass-distribution scale is intended to include the loading of all aircraft of any type which have been encountered to date. The table at the top of the figure shows again that from the mass distribution, the primary recovery controls and the way they should be moved can be predicted.

A small range of mass distribution for which spin-recovery characteristics can be predicted is shown at the bottom of figure 7. For the zero or near-zero loading condition, tail-design criteria are available for assuring satisfactory recovery for values of the relative-density factor up to about 35. Actually, heavily loaded fighter aircraft can have a relative-density factor as high as 100, but values up to 35 include many types of airplanes in the lightweight military or general aviation category. For the extreme loadings on both ends of the scale, no criteria have been developed for predicting the effectiveness of the controls for satisfactory recovery. Predictions can be made occasionally in these areas, but in most cases of fuselage-heavy or wing-heavy loadings, full-scale spin tests or model spin-tunnel tests must be made to determine whether the controls are powerful enough to give a satisfactory recovery.

CONCLUDING REMARKS

For the fully developed spin, the principal factors are mass distribution, which is by far the most important single parameter, and tail design, which is particularly important for conditions of zero or near-zero loading. Other factors such as general aerodynamic configuration and high-lift devices have some effect, but these effects are only minor perturbations. If the mass distribution and tail design are known, it is possible in many cases to predict whether an airplane will have satisfactory spin-recovery characteristics. In other cases, however, it is necessary to make spin tests to assure satisfactory recovery.

REFERENCES

1. Seidman, Oscar; and Neihouse, A. I.: Comparison of Free-Spinning Wind-Tunnel Results With Corresponding Full-Scale Spin Results. NACA WR L-737, 1938. (Formerly NACA MR, Dec. 7, 1938.)

2. Berman, Theodore: Comparison of Model and Full-Scale Spin Test Results for 60 Airplane Designs. NACA TN 2134, 1950.

3. Neihouse, Anshal I.; Klinar, Walter J.; and Scher, Stanley H.: Status of Spin Research for Recent Airplane Designs. NASA TR R-57, 1960. (Supersedes NACA RM L57F12.)

4. Neihouse, A. I.: A Mass-Distribution Criterion for Predicting the Effect of Control Manipulation on the Recovery From a Spin. NACA WR L-168, 1942. (Formerly NACA ARR, Aug. 1942.)

5. Neihouse, A. I.: Tail-Design Requirements for Satisfactory Spin Recovery for Personal-Owner-Type Light Airplanes. NACA TN 1329, 1947.

6. Neihouse, Anshal I.; Lichtenstein, Jacob H.; and Pepoon, Philip W.: Tail-Design Requirements for Satisfactory Spin Recovery. NACA TN 1045, 1946.

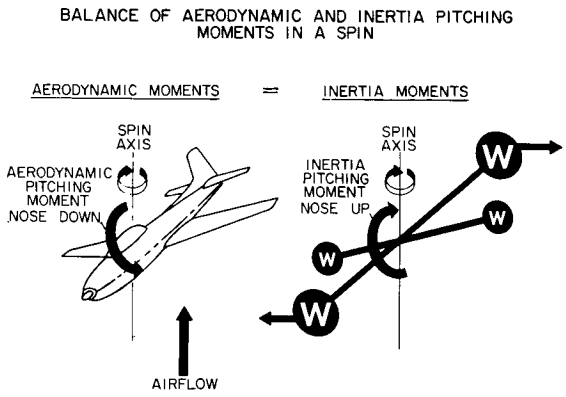

Figure 1

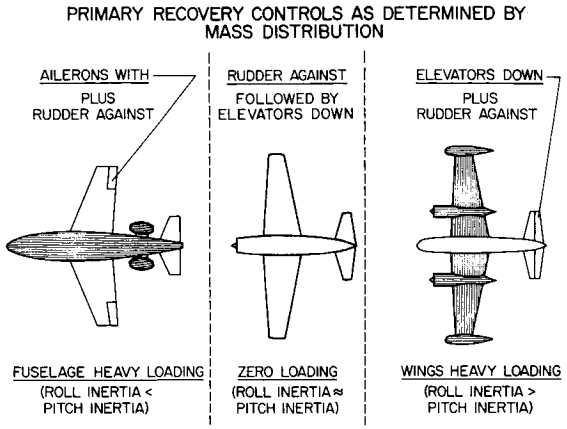

Figure 2

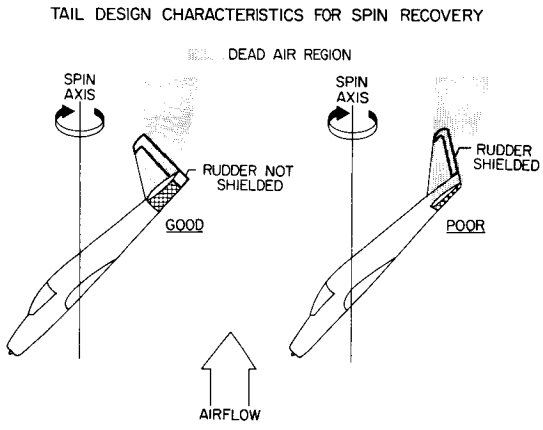

Figure 3

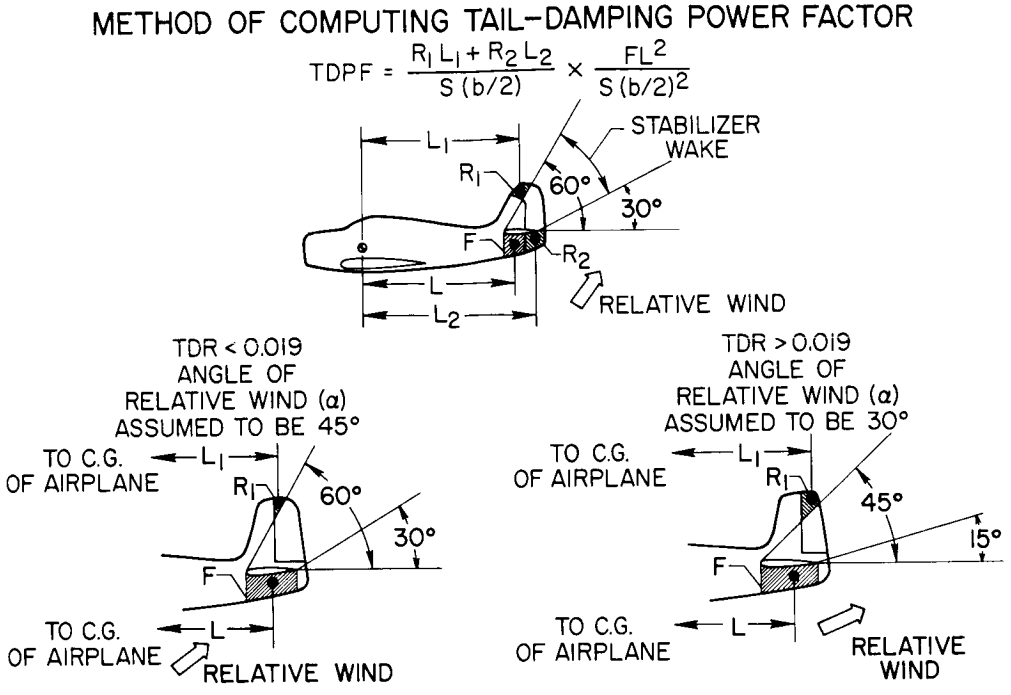

Figure 4

TAIL DESIGN REQUIREMENTS

$$\mu = \frac{\text{AIRPLANE DENSITY}}{\text{AIR DENSITY}} = \frac{m/Sb}{\rho}$$

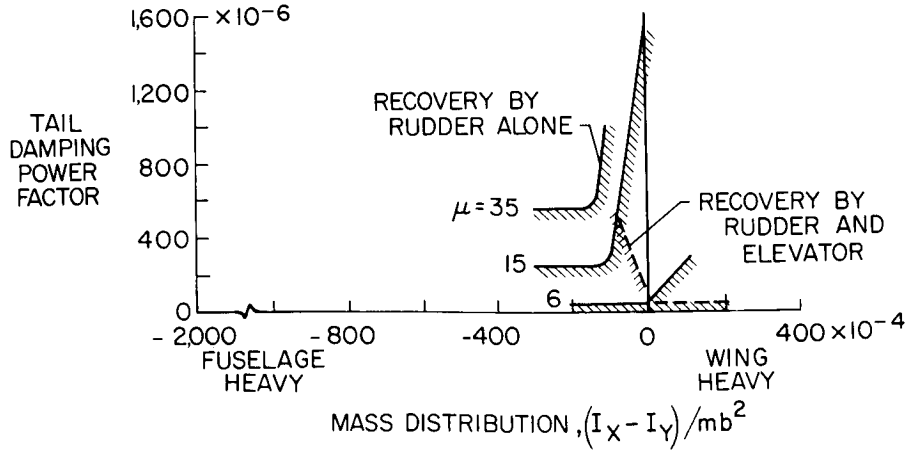

Figure 5

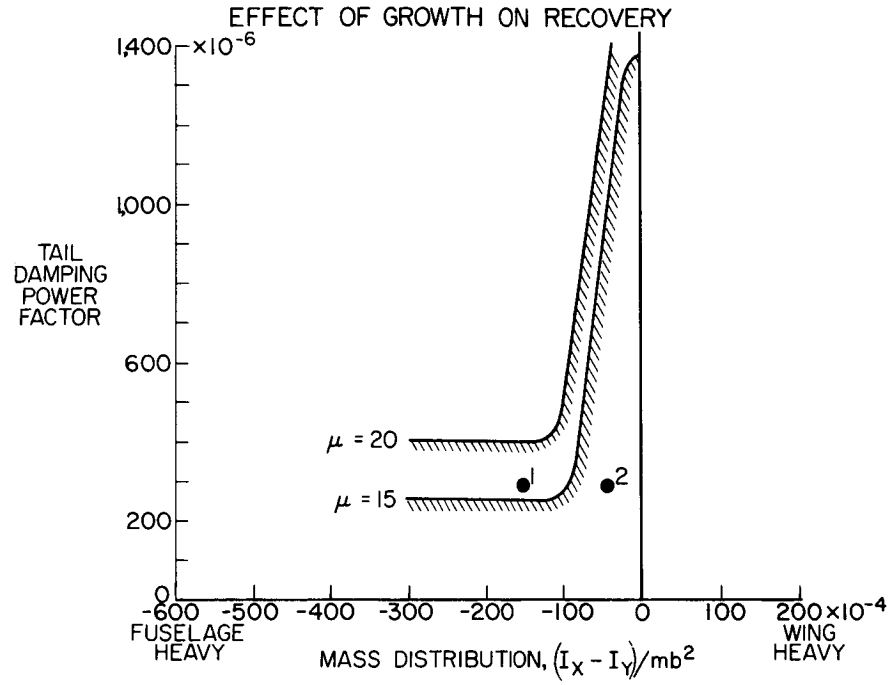

Figure 6

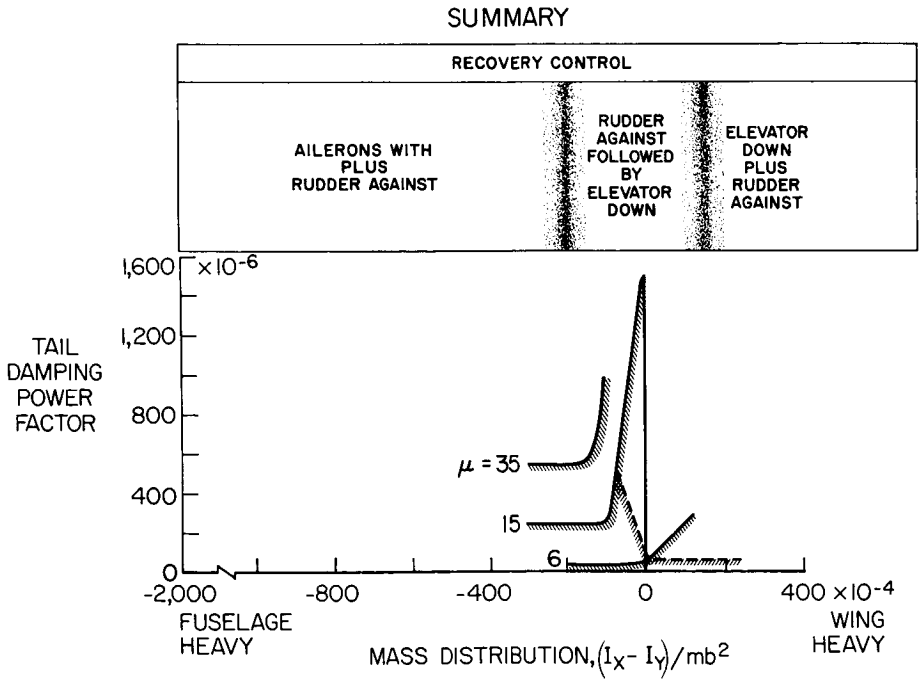

Figure 7

29. OPERATING PROBLEMS PECULIAR TO V/STOL AND STOL AIRCRAFT

By John P. Campbell

NASA Langley Research Center

SUMMARY

This paper covers the unique features and different modes of operation of V/STOL and STOL aircraft which result in new operating problems and serves to introduce the papers which deal in more detail with some of the more important V/STOL and STOL operating problems.

INTRODUCTION

By way of introduction, some definitions should be given in order to avoid the confusion which sometimes has arisen in the use of the terms VTOL, STOL, and V/STOL. VTOL, of course, means vertical take-off and landing. STOL refers to short take-off and landing, where there is no VTOL capability and some take-off and landing run is always required. The term V/STOL indicates the capability to perform either vertical or short take-offs and landings. An airplane of this type has VTOL capability but may operate much of the time as an STOL airplane for improved economy and a greater margin of safety in event of engine failure. Actually, the terms VTOL and V/STOL can be used interchangeably since all VTOL configurations currently under consideration can perform running take-offs and landings.

DISCUSSION

Some fundamental relationships between lift and power required for conventional and V/STOL aircraft are illustrated in figure 1. The lift, in percent of weight, and the power required for level flight are plotted against airspeed for both types of aircraft. In the lower plot, the solid-line curve represents a typical variation of power required for a conventional airplane, extending from the stalling speed to the top speed of the airplane. The upper plot shows that, for this speed range, the airplane is supported entirely by aerodynamic lift provided by the wing. On the other hand, for the V/STOL aircraft which can operate below conventional wing stalling speeds on down to hovering flight, the aerodynamic lift is gradually replaced by powered lift as hovering is approached. In this speed range where powered lift must be used - the so-called transition speed range - the power required for the V/STOL airplane, indicated by the dashed-line curve, rises rapidly to a maximum for the hovering flight condition. The STOL, or short take-off and landing, aircraft only go part of

the way up the power-required curve to obtain a modest reduction in stalling speed from a modest increase in power.

The high power required by the V/STOL aircraft in hovering flight is one of the basic characteristics leading to new operating problems. Other important characteristics of V/STOL aircraft in hovering and transition flight are the vertical slipstream for hovering flight, the special provisions made for performing the conversion from the hovering to the cruise configuration, and the inherent deficiencies in aerodynamic stability and control in hovering and low-speed flight. Each of these characteristics and their related operating problems will now be considered.

High Power Required

The high power required in hovering flight results in higher fuel consumption, greater noise, and greater slipstream effects. The magnitude of the increases depends upon the type of propulsion system as illustrated in figure 2. Fuel consumption is shown plotted against slipstream velocity for hovering and cruising flight for various types of V/STOL aircraft having the same gross weight (W = 40,000 pounds). It is apparent that the fuel consumption for hovering is very high for the higher performance V/STOL types, particularly for the turbojet configurations. The significance of this characteristic in terms of operating procedures is that the hovering times of these aircraft must be kept to an absolute minimum, and it is not realistic to consider long periods of vertical climb or descent during take-off and landing operations.

In general, the noise associated with the various V/STOL propulsion systems varies in roughly the same manner as power required and fuel consumption. That is, helicopters are generally the quietest and jet aircraft, the noisiest. Some of the operational considerations involved with the noise problem will be discussed subsequently.

Vertical Slipstream for Hovering

Slipstream effects are greater with V/STOL aircraft both because of the higher power required and the vertical direction of the slipstream for hovering flight. As illustrated in figure 3, there can be important effects on the surroundings in the take-off and landing areas as the high-velocity vertical slipstreams impinge and flow outward in all directions. There are also important effects on the aircraft itself as the slipstreams come together and recirculate about the airframe and propulsion system. Slipstream flows are never as steady and symmetrical as those in the simple and idealized illustration of figure 3. The problems resulting from slipstream impingement and recirculation are covered in detail in paper no. 31 by Kuhn and paper no. 32 by Rolls.

Provisions for Conversion

V/STOL aircraft must, of course, be designed so that the slipstream or jet exhaust can be directed downward for hovering and rearward for cruising flight.

There are a number of methods of accomplishing this conversion of configuration in order to perform the transition, as illustrated in figure 4. There are V/STOL types, such as the helicopter, which merely tilt forward to fly forward. There are some in which only the thrust unit itself tilts, with the fuselage remaining essentially horizontal at all times, and others which have swiveling nozzles to direct the jet exhaust downward for hovering or rearward for cruising flight. In addition, there are types which have one propulsion system for hovering and another for cruising flight.

The significant point here in terms of operating problems is that the additional operations to be carried out in accomplishing the conversion maneuver make the piloting task more difficult in the transition flight range and increase the time required in the landing approach pattern. In paper no. 30, Reeder shows that the degree of complexity of the conversion maneuver has a direct bearing on the difficulty of the piloting task.

Aerodynamic Stability and Control Deficiencies

The inherent aerodynamic stability and control deficiencies of V/STOL aircraft are illustrated in figure 5 which shows typical variations of aerodynamic stability and control with airspeed from hovering through the transition to cruising flight. In this illustration the V/STOL airplane is assumed to have satisfactory aerodynamic stability and control in cruising flight and at the upper end of the transition range represented by the end points of the curves. Since all these parameters vary with the dynamic pressure in the airstream, they drop off rapidly as the airspeed is decreased in the transition. There is no aerodynamic control effectiveness at all in hovering unless the control surface is in a high-velocity slipstream. It is usually necessary, therefore, to provide an additional control system for V/STOL aircraft specially for the hovering and low-speed flight conditions. In hovering flight, all V/STOL aircraft have neutral static stability - that is, there is no stability of attitude. As for dynamic stability, jet V/STOL types are about neutrally stable in hovering but other V/STOL types usually have dynamic instability in the form of unstable pitching and rolling oscillations. This lack of static and dynamic stability does not prevent V/STOL aircraft from being flown under visual flight conditions, but it does lead to certain undesirable handling characteristics which must be improved by stability augmentation to insure satisfactory operation during instrument flight. Paper no. 30 by Reeder and paper no. 33 by Anderson, Quigley, and Innis cover some of the operating problems associated with these characteristics for both V/STOL and STOL aircraft.

Noise

One approach to alleviating the V/STOL noise problem is to get the aircraft to and from altitude in a shorter distance by using steeper take-off and landing profiles as pointed out in paper no. 4 by Hall, Champine, and McGinley and paper no. 9 by Hubbard, Cawthorn, and Copeland. Figure 6 shows typical take-off and landing profiles for conventional and V/STOL aircraft. For the conventional airplane, a 3° approach and a 6° climbout are considered normal. V/STOL aircraft, with their slower approach speeds and greater power available

for climbout, will be able to operate on much steeper flight paths - at 6^{o} or more on the approach and 10^{o} or more in the climbout. These steeper flight profiles are expected to be used by STOL as well as V/STOL aircraft.

Comparisons of the noise levels of conventional and V/STOL transports using these take-off profiles are shown in figure 7. Values are shown of perceived noise level in decibels (PNdB) which would be noted by observers on the ground directly below the airplane - that is, at various points along the ground track. These PNdB values are plotted as a function of distance from the start of the take-off roll. The horizontal dashed line at 112 PNdB represents what has been judged an acceptable noise level in some communities for daylight and early evening take-off operations. The solid lines represent the calculated noise of 40-passenger turboprop and turbofan V/STOL transports from lift-off and through the climbout to an altitude of about 2000 feet. At distances beyond about 1 mile from the start of take-off roll their noise appears to become acceptable. In order to relate this to the conventional transport noise with which most people are familiar today, the shaded bands have been added to represent measured PNdB levels for large conventional turbojet, turbofan, and turboprop transports. These bands start at the point of lift-off for the conventional transports - that is, at about $1\frac{1}{2}$ miles from the start of take-off roll. On the basis of this plot, it would appear that, in operations from a conventional airport, V/STOL transports would produce less community noise problems than present-day transports. That is, their noise would be less at any given distance from the start of take-off roll. But, of course, to justify their use, V/STOL transports will have to operate from small close-in airports or heliports which are likely to be closely surrounded by noise-sensitive areas of the community. In such operations, the airport boundary will be reached at distances less than a mile from the start of the take-off roll, so it is going to be difficult to avoid unacceptable PNdB levels in approaches and climbouts over the surrounding community. In addition to the community noise problem in the general vicinity of the airport, the noise levels will also be higher on the airport itself, especially during vertical take-off and landing operations, and this may well lead to requirements for some new approach to the airport noise problem.

CONCLUDING REMARKS

This paper has brought out some of the unique features and different modes of operation of V/STOL and STOL aircraft which result in additional operating problems. Subsequent papers bring out some of the important factors to be considered in dealing with these problems.

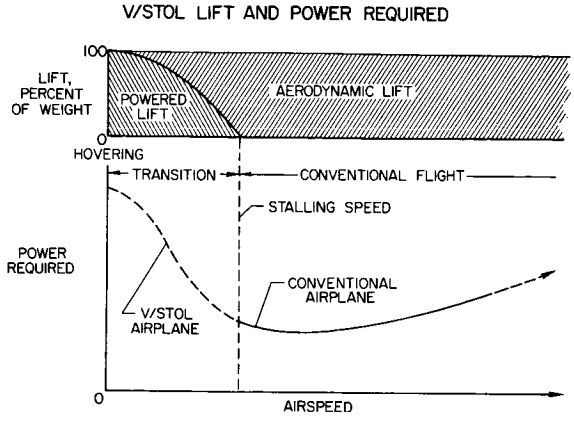

Figure 1

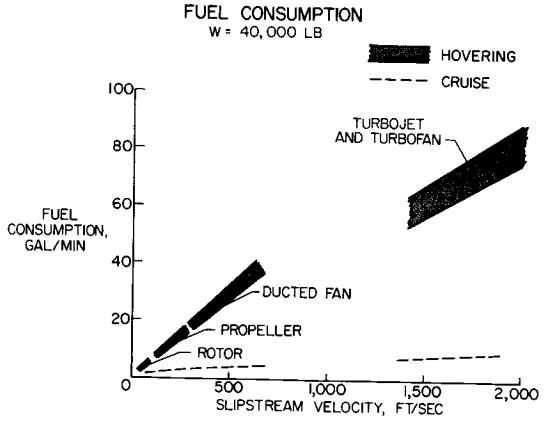

Figure 2

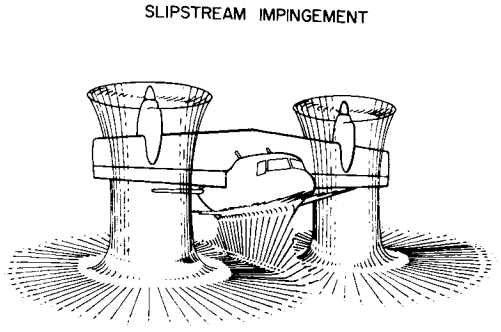

Figure 3

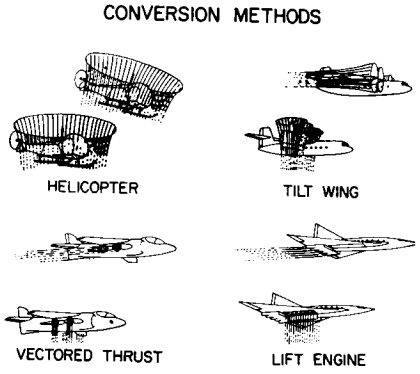

Figure 4

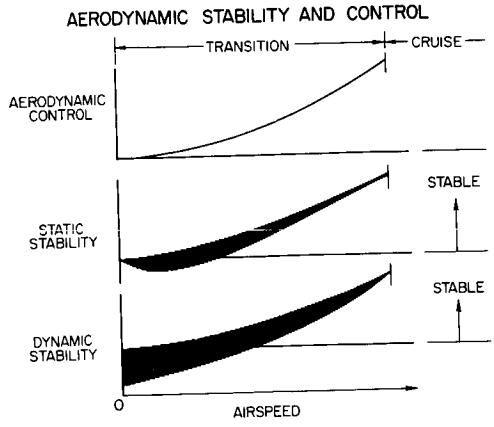

Figure 5

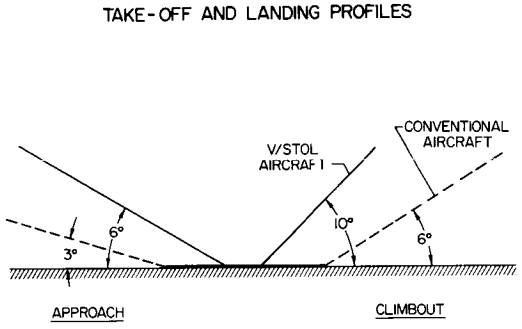

Figure 6

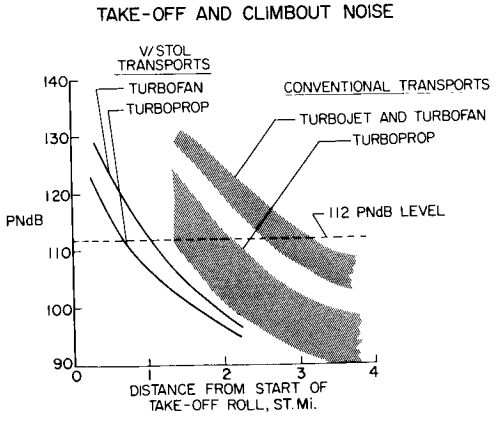

Figure 7

30. V/STOL AIRCRAFT OPERATION IN THE TERMINAL AREA

By John P. Reeder

NASA Langley Research Center

SUMMARY

Some aspects of V/STOL operation in a terminal area have been presented. A V/STOL instrument approach with present-day displays and guidance systems requires about 5 minutes at low speeds, but this time could be cut to $1\frac{1}{2}$ to 2 minutes if the displays and guidance systems were improved. In order to keep approach-pattern time to a minimum, the conversion process should be simplified by interconnecting as many operations as possible with one control. Adequate vectoring for the lifting system, attitude stabilization to prevent excessive wandering, and automatic glide-path control for approaches over 6° will probably be required also.

INTRODUCTION

V/STOL aircraft have the potential for: (a) operating safely to lower weather minimums than conventional airplanes, and (b) permitting better utilization of airspace in a terminal area and, thus, a greater volume of traffic at any one time. To realize this potential, V/STOL aircraft must utilize their low-speed capability. This paper is a discussion of some aspects of this terminal area operation. Additional discussion may be found in reference 1.

THE ENVIRONMENT

The V/STOL environment considered is illustrated in figure 1 which shows possible routings of V/STOL aircraft into a terminal airport such as the John F. Kennedy International Airport. Note the scale of miles in the lower right corner. The shaded areas are the present major airport control and approach zones. The arrowed lines are the V/STOL aircraft inbound routes. They lie generally underneath conventional airplane traffic. The V/STOL traffic slows to below airplane speeds, maneuvers into approaches into the wind and generally parallel to airplane traffic, and uses its own guidance and landing facilities. Two landing facilities are indicated on opposite sides of the airport. Vertical approaches are not considered feasible for the near future. The patterns are, therefore, drawn to scale for an approach speed of about 50 knots. The half circles represent the intercept of 6° glide paths at an altitude of 1,000 feet.

Figures 2 and 3 show the V/STOL instrument approach pattern and profiles, necessitated by presently available pilot displays and guidance systems, in more

detail and compared with that for an airplane. The patterns illustrated in figure 2 are not optimum ones but are the least advantageous ones as dictated by winds, direction of arrival, local restrictions, or limitations of guidance equipment.

V/STOL instrument-flight experience to date, primarily with helicopters, has emphasized that the pilot must perform one task at a time and keep variables to a minimum during the alinement stages of the instrument approach. The alinement legs are thus straight, as shown in figures 2 and 3, and flight is at essentially constant speed. Time is the important factor in establishing alinement. The size of the pattern compared with that for an airplane thus varies directly as the approach speed. The pattern size is further reduced by the use of the steeper glide path.

During the downwind leg of the pattern, the V/STOL aircraft converts to a speed as near the final approach speed as possible which is adequate for maneuvering. This leg is long enough to allow adequate time on the inbound leg. A cross-wind leg of 1/2 minute is allowed for unknown wind effects. Flight experience has shown that about 1 minute is required to establish alinement with the inbound track before acquiring the glide path. The glide path requires about $1\frac{1}{2}$ minutes to stabilize before breakout, after which a visual deceleration to a vertical landing is performed.

The important thing to be noted from this pattern is that the V/STOL aircraft will be spending about 5 minutes at low speeds. This fact is very significant for the jet type, particularly, as it requires operation for this length of time at 85 to 95 percent of hovering thrust at a very high rate of fuel consumption. In fact, one such approach will reduce the range of a jet type by about one-third. Consequently, missed approaches cannot be tolerated. Propeller types would not suffer as much since the power required at 50 knots is reduced to about one-half that for hover.

Since the pilot can convert to a vertical landing in perhaps $1\frac{1}{2}$ minutes in visual flight, the solution to reducing the time in the approach lies in the development of improved pilot displays and guidance systems.

PILOTING PROBLEMS IN SLOW FLIGHT

The V/STOL aircraft has been assumed to have simple conversion procedures and good handling qualities so that these factors do not influence the time required or the speeds chosen. In actual practice, however, it is very possible that piloting problems associated with slow flight will result in increased times and airspace required or in increased risk of missed approaches, despite the benefits of improved displays. This condition must be avoided through adequate design. Some piloting problems of concern are (a) complexity of the conversion, (b) handling qualities, and (c) effect of winds.

Complexity

With regard to the first of these problems, the time required for conversion and the safety in performing it depend heavily on the degree of complexity or the number of factors the pilot must be concerned with during the process. Conversion by simply tilting a lift-thrust system to select any speed between hover and airplane flight has proved to be acceptably simple, at least in visual flight. As an example of increased complexity for a jet type, the addition of separate lifting engines adds the tasks of opening doors, starting and checking numerous engines, and adjusting a second set of throttles when preparing for landing or low-speed maneuvering. Figure 4 illustrates the methods of controlling a descent with a simple lift-engine configuration compared with a pure vectored-thrust type. For the former, the rate of descent is controlled with lift-engine throttles, and the speed is controlled by attitude and cruise engine thrust, if the engine is not at idle. There is a danger in this case of stalling the wing or encountering pitch-up conditions. In the case of the pure vectored-thrust type, the descent can be controlled primarily by vectoring the thrust as required and keeping the angle of attack α at any value desired. In addition, some throttle adjustments will be required.

To reduce complexity, the lift-engine configurations must be simplified in the number of operations required by having a single control for opening inlet doors and starting all engines for instance. Also, control of aircraft speed and descent will be improved and simplified by provision of vectoring on the lift engines in both forward and rearward directions. The objective should be to approach the inherent simplicity and flexibility in operation of the pure vectored-thrust arrangement.

Handling Qualities

When handling qualities are considered, the characteristic of slow flight which has caused the greatest problem during precision instrument approaches is illustrated in figure 5 which shows the effect of speed on heading control during a 6° approach with a helicopter. The increased wandering at 25 knots compared with 65 knots is very apparent, despite the fact that the helicopter was stabilized with a moderate amount of rate damping about all axes. The pilot's workload was very high at 25 knots because of the high rate of instrument scanning required. His rate of eye motion was found to be four times higher than that for a similar approach performed visually. Because the pilot was working at maximum capacity, it was not unusual for the aircraft to "get ahead of the pilot" and for the course-indicating needles to go off scale, the pilot having become "lost."

The wandering in heading illustrated in figure 5 results from the increased rate at which the flight-path direction changes at low speed for a given change in aircraft attitude. This effect is illustrated in figure 6 by the rate of turn which develops from a 5° bank upset as a function of speed and by assuming that the aircraft weathercocks into the relative wind. Note that below 30 knots the rate of turn due to this upset is higher than the standard rate of turn generally used for maneuvering during instrument flight.

The only satisfactory solution to this general low-speed instrument-flight problem seems to lie in attitude stabilization with maneuvering capability provided through the normal controls.

Effect of Winds

Winds have a large effect on V/STOL aircraft during low-speed operation, particularly during an instrument approach. One significant effect is that of wind gradients and gusts on glide-path control when the glide path is steeper than 3°. Figure 7 shows approaches in a gusty wind at 25 knots on glide paths of 7° and 18° with a helicopter. The larger power corrections required for the 18° approach are apparent. Pilot comments indicate that the power corrections required for 7° were noticeably increased over those for 3°, and that the greatly increased corrective action required at 18° was very troublesome. In the case of a jet V/STOL, the problem may be exaggerated by the lack of damping along the vertical axis at low speed.

One solution to this problem is to limit glide-path angles to about 6° for operations of the first generation of V/STOL aircraft. For steeper angles in the future, automatic control of the glide path will probably be required.

CONCLUSIONS

A study of the problems involved with V/STOL aircraft operation in a terminal area has indicated the following conclusions:

(1) A V/STOL instrument approach with presently available pilot displays and guidance systems requires about 5 minutes at low speed, an ideal aircraft being assumed. Vastly improved pilot displays and guidance systems could cut the time required to $1\frac{1}{2}$ to 2 minutes.

(2) To insure that the approach pattern time is the minimum possible and that there will be no missed approaches, the following must be considered:

(a) The conversion process must be kept simple by interconnecting as many operations as possible through one control, and by providing adequate vectoring capability for the lifting system.

(b) Attitude stabilization probably will be required to insure against excessive wandering of V/STOL aircraft in the instrument approach.

(c) Automatic glide-path control will probably be required for approaches over 6°.

REFERENCE

1. Reeder, John P.: The Impact of V/STOL Aircraft on Instrument Weather Operations. NASA TN D-2702, 1965.

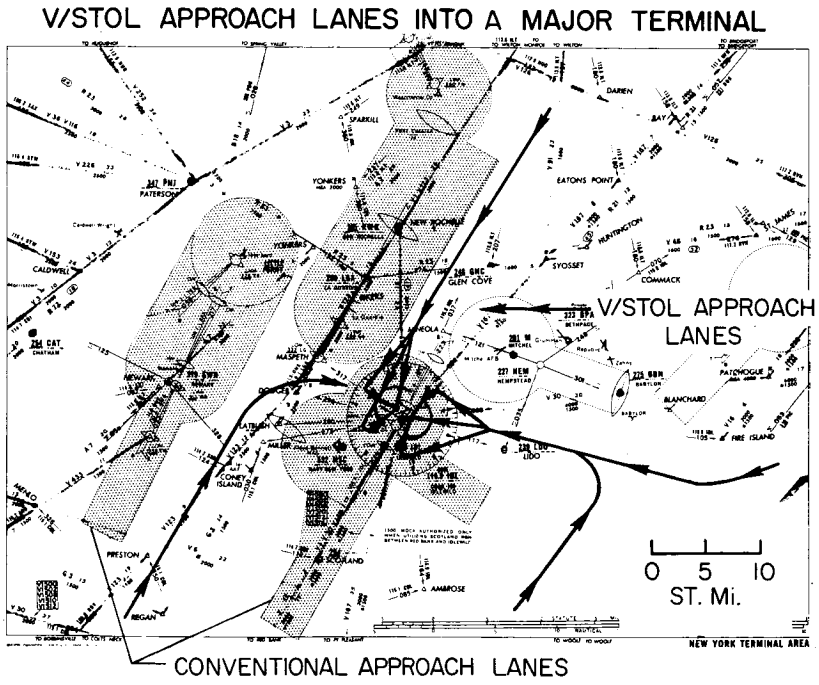

Figure 1

NOMINAL INSTRUMENT APPROACH PATTERNS

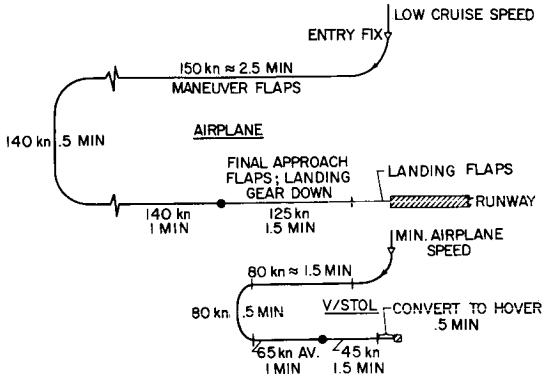

Figure 2

NOMINAL INSTRUMENT APPROACH PROFILES

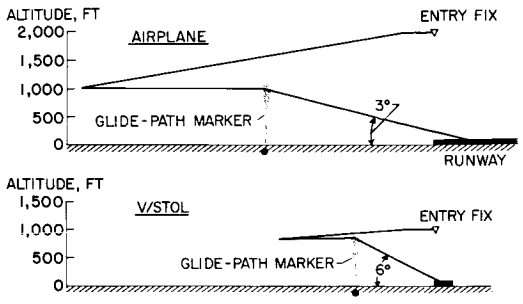

Figure 3

DESCENT CONTROL WITH TWO LIFT-PROPULSION CONFIGURATIONS

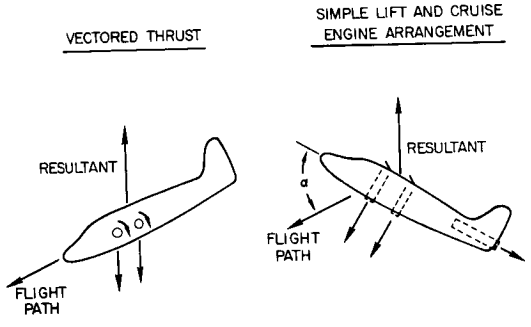

Figure 4

EFFECT OF FLIGHT SPEED ON HEADING CONTROL
FOR A HELICOPTER
APPROACH ANGLE, 6°

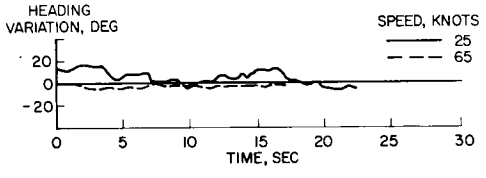

Figure 5

RATE OF TURN RESULTING FROM 5° BANK UPSET

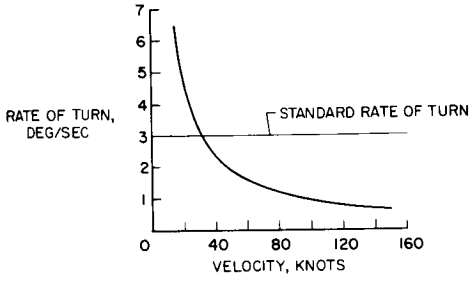

Figure 6

POWER CHANGES DUE TO WIND GUSTS FOR A HELICOPTER
AIRSPEED, 25 KNOTS; GUSTY WIND

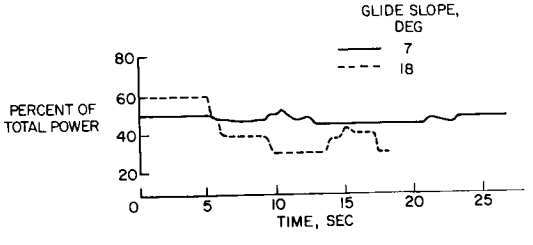

Figure 7

31. GROUND EFFECTS ON V/STOL AND STOL AIRCRAFT

By Richard E. Kuhn

NASA Langley Research Center

SUMMARY

Ground effects on V/STOL and STOL aircraft arise from the fact that these aircraft support themselves by deflecting air downward. The presence of the ground interrupts this downward flow with attendant effects on both the ground and the aircraft.

In general, ground effects on transport aircraft in the 50,000-pound class will not be significant at heights above about 20 to 30 feet and velocities above about 40 to 50 knots. At lower heights and velocities, the aircraft will experience self-induced disturbances and hot-gas ingestion due to the recirculated slipstreams, and lift losses and trim changes in STOL operations.

The effects of self-generated turbulence will not be serious if adequate control is provided, and this annoyance to the pilot can be reduced by providing artificial damping. The avoidance of ground-erosion damage involves proper preparation and housekeeping of the landing site for high-disk-loading vehicles and proper operating procedures to avoid running into debris. Research is still in progress to obtain a better understanding of hot-gas ingestion and means of reducing it; its effects can be minimized by vectoring the exhaust rearward and using a short running take-off. The lift losses and trim changes in STOL operations will require an extra margin of power and velocity to compensate for this problem. Ground effects may preclude some operations such as hovering over loose sand with jet aircraft, but, in general, operational procedures can be devised to minimize adverse ground effects.

INTRODUCTION

The ground effects on V/STOL aircraft are associated with the fact that a hovering aircraft supports itself by accelerating air vertically downward. An STOL aircraft, if it achieves its low speed by means of power, deflects air downward at a large angle to the direction of flight. When either aircraft is close to the ground, the impingement of this downward flowing stream of air has effects on the ground and personnel as well as on objects in the vicinity, and the deflection of these downflows by the ground alters the aerodynamic forces on the aircraft.

This paper will review both the effects of the slipstream on the ground and the effects of the ground on the aircraft. (Refs. 1 and 2 present related

discussions.) For the purpose of this discussion, the types of flow involved can be divided into three classes as shown in figure 1:

(a) Single slipstream
(b) Multiple slipstreams
(c) STOL aircraft

In the case of the single-slipstream configuration (as shown in the upper left-hand corner), the flow impinges on the ground and flows radially outward in all directions. So long as the ground remains reasonably smooth, the flow adheres to the ground and is not reflected onto the aircraft. The outward flowing sheet of air entrains the stationary air above it and this entrainment of air causes the characteristic lift loss frequently discussed in connection with ground effects (refs. 3 to 5). The lift-loss problem, however, is not discussed in this paper.

In the case of multiple slipstreams (shown in the upper right-hand corner of fig. 1), the flows from the slipstream are deflected upward where they meet after flowing along the ground. The problems of self-generated turbulence, hot-gas ingestion, and debris damage are associated with this upflow.

In the STOL aircraft case (as shown in the sketch at the bottom of fig. 1), the presence of the ground deflects part of the flow that would normally proceed downward at a large angle to the stream, forward along the ground, and thereby causes a loss in lift. Also, the flow direction at the tail of the aircraft is altered by the presence of the ground and causes a change in longitudinal trim of the aircraft.

SYMBOLS

d	diameter, ft
h	height above ground, ft
q	dynamic pressure, lb/sq ft
T	exhaust temperature, ^{o}F
ΔT	inlet-temperature rise, ^{o}F
V	velocity, knots
ΔV_V	increase in sinking speed, fps
W	gross weight, lb
θ	vector angle, deg

DISCUSSION

Surface Erosion and Debris Damage

One of the most significant problems of V/STOL aircraft hovering in ground effect is that of the effects of disk loading on the ground erosion and effects of the outward flowing air on personnel, objects, and other aircraft in close proximity to the hovering aircraft. Ground erosion and the forces on objects in the vicinity are proportional to the dynamic pressure of the outward flow of air along the ground. The outflow from a helicopter-type configuration with a disk loading of 10 lb/sq ft and from a buried-fan configuration with a very high disk loading (500 lb/sq ft) are compared in figure 2. The dynamic pressure of this outward flowing sheet of air is a maximum very near the surface of the ground at any particular radial station. In the lower part of the figure, this maximum dynamic pressure is plotted as a function of radial distance from the center line of the aircraft (calculated from the data of refs. 6 and 7.) For both configurations, the dynamic pressure reaches a maximum near the edge of the slipstream and falls off rapidly outboard. Immediately under the aircraft, the configuration with the higher disk loading produces the higher dynamic pressure. In this region the effects of disk loading predominate. However, outboard of the extremities of the aircraft, both configurations produce essentially the same dynamic pressure. In this region, the problems of the downwash from the hovering aircraft are a function of the gross weight of the aircraft only and are independent of disk loading. It can also be noted in the sketches at the top of figure 2 that the outward flowing sheet of air from the high-disk-loading configuration is appreciably thinner than that for the low-disk-loading configuration. This result is due to the fact that the high-disk-loading vehicle achieves its lift by accelerating downward a much smaller mass of air to a much higher velocity. This smaller mass of air produces a thinner sheet along the surface.

The effects of high disk loadings then are confined to the immediate area of impingement of the slipstream, and it is in this area that the problems of ground erosion are most serious. The flow paths of the debris created by the erosion of the ground surface by a hovering VTOL aircraft are shown schematically in figure 3. When the sublayer is not eroded, the loose particles on the surface of a hard ground are blown radially outward from the point of impingement. If, however, the dynamic pressure is higher or the ground surface is softer, erosion of the surface can take place, and, after a short period of time, a depression is created which results in particles being projected upward into the air where they may be drawn back into the lifting system. This problem was experienced by the X-14 aircraft hovering over wet sod and is discussed in more detail in paper no. 32 by Rolls. In both cases (with penetration and without penetration) the lighter particles are carried aloft by the turbulent eddy currents above the primary outward flowing sheet of air along the surface.

The question of whether the ground will be eroded depends on the disk loading of the vehicle as well as on the type of terrain over which the aircraft is operating. Figures 4 and 5 show the tolerance of various types of terrain to the temperature and to the dynamic pressure of the jet or slipstream

from the hovering aircraft (refs. 6, 8, and 9). Sand and loose dirt begin to erode at dynamic-pressure levels of the order of only 3 lb/sq ft. Even helicopters have a problem when hovering over loose dirt and sand, and those with the higher disk loadings will soon dig a hole in this type of surface. The primary concern in the case of crushed rock is with loose particles over the top of a hard sublayer and, in this situation, the tolerance to dynamic pressure is a function of the mass of the rock. The tolerance of sod to dynamic pressure depends upon the moisture content and root structure. Dry sod has been known to withstand the blast from turbojet engines for relatively long periods of time; however, wet sod will erode after very short exposure.

The exposure time is of considerable importance in the question of erosion of the ground. Some work on this has been done by Rolls-Royce, Ltd., using a vertically mounted lift engine installed in a Meteor aircraft by taxiing the aircraft over various types of terrain. Very few of these data are published but results indicate that the problems of ground erosion can be reduced appreciably by using a very short running take-off - that is, by accelerating the aircraft forward with jets pointed aft and deflecting the jets down for lift-off after the aircraft has started moving.

The effects of temperature on the problems of erosion are shown in figure 5. Road asphalt will melt at relatively low temperatures and is not a suitable surface for hot-jet configurations. Normal concrete will also erode under the action of turbojet engines after a short period of time. Apparently the hot exhaust expands the moisture within the concrete causing it to crack and chip. Special water-cured concrete can be produced which will withstand the full exhaust temperature of nonafterburning turbojet engines. There are, in addition, some newer materials such as epoxy and polyester resin-bonded glass fibers being investigated by the U.S. Air Force (ref. 10) and industry that can withstand considerably higher temperatures for prolonged periods of time. Some experience with these newer materials has been obtained from tests with the X-14 airplane as discussed in paper no. 32 by Rolls.

So far, the present discussion has considered only the problems of erosion from the single-jet case. Additional problems can be created by the upflows created where the spreading flows from multiple slipstreams meet on the ground. Both the VZ-2 propeller-driven tilt-wing aircraft shown in figure 6 and the X100 tilt-propeller configuration have experienced debris damage associated with these flows (refs. 11 and 12). For both configurations, with the thrust axis nearly vertical, the slipstreams impinge on the ground and meet along the center line of the aircraft producing a fairly large volume of flow in the fore-and-aft direction near the center line of the aircraft. When aircraft damage was encountered, this airflow was carrying with it rocks and debris which were thrown up into the path of the aircraft due to random collisions with other debris. Because of the forward motion the aircraft ran into this debris. This occurred at high-power conditions with an incidence of about 70° and a speed of about 20 knots. This problem was not encountered at zero airspeed with the thrust line vertical because the debris was thrown away from the aircraft. The problem would also not be encountered for very low thrust incidences, as in a conventional configuration, where all the slipstreams would be directed behind the aircraft and there would be no debris projected forward for the aircraft

to encounter. The problems of ground erosion and debris damage will sometimes require special site preparation and will require operational procedures to avoid running into debris.

Hot-Gas Ingestion

The problem of hot-gas ingestion can also be aggravated by the upflows created by two impinging slipstreams. Figure 7 shows data obtained on a full-scale model of the XV-5A fan-in-wing configuration in the Ames 40- by 80-foot tunnel (ref. 13). The fans in the wing are powered by the exhaust from turbo-jet engines which drive the fans through tip turbines; thus, the hot gases from the turbines are on the outer edges of the slipstreams from the fans. After the flows impinge on the ground, the hot gases are on the upper surface of the outward flowing sheet of air. The model was fitted with a nose fan as well as two wing fans and at the point where the nose-fan and main-fan slipstreams meet, air is projected vertically upward carrying with it the hot exhaust gases. Also, with a forward velocity in the tunnel, the air that flows forward past the nose fan is also returned to the inlets to both the engines and the fans. The inlet-temperature rise reaches a maximum at wind speeds of the order of 40 knots. These data apply to the aircraft either hovering in a head wind or decelerating for a landing. In these flight conditions, the slipstream would be nearly vertical. One method of minimizing this problem, at least for the take-off condition, is to use a running take-off by accelerating the aircraft forward with the slipstream from the fans vectored rearward. In this case, the point of mixing of the two slipstreams is moved farther aft and the general rearward flow of air pulls most of the hot gas under the wing.

Because of the turbulences of the flow, the temperature at any point in the inlet fluctuates greatly and is not easy to measure. The data shown in figure 7 and presented in reference 13 represent the peak temperatures measured. The average temperature rise would be considerably lower, perhaps less than one-half of the values shown. In some jet VTOL investigations, however, even higher temperature rises (up to 50° F) have been encountered. Good data on inlet-temperature increase due to hot-gas ingestion are required because an average rise of 10° F will cause a thrust loss of $2\frac{1}{2}$ to 3 percent on a jet lift engine and 7 to 8 percent on a lift fan. Research is continuing on operational techniques and on methods of designing the aircraft, such as shielding the inlets, to minimize hot-gas ingestion.

Self-Induced Disturbances

Another problem arising due to the impingement of multiple slipstreams on the ground and their reflection to the aircraft is that of self-induced turbulence. (See refs. 14 and 15.) Some flight records illustrating this for the VZ-2 tilt-wing aircraft are shown in figure 8, which presents the aircraft motion in terms of angular velocity about the three axes and the pilot's work load in terms of control travel, as a function of time for the aircraft hovering in and out of ground effect. In ground effect the aircraft motions are much

greater than out of ground effect and the pilot is forced to use almost full control about all three axes in maintaining control of the aircraft.

Self-induced disturbances have been experienced by several aircraft including three of the four shown in figure 9, which also shows the flow pattern on the ground. For the VZ-2 airplane, the meeting of the two slipstreams creates an upflow along the center line of the aircraft. For the XV-5A airplane with three fans, the upflow lines form a Y-pattern. For the P.1127 airplane with four jets, the upflow lines form an X-pattern. The self-induced disturbances arise because these upflow lines do not stay fixed but move in response to control inputs and motions of the aircraft, thus altering the circulation of flow onto the aircraft causing a further disturbance which, in turn, causes further motion. All these aircraft experienced self-induced turbulence, the P.1127 being least affected because of its higher wing loading. The X-14 aircraft, although having a lower wing loading than either the P.1127 or the XV-5A aircraft, suffered least from the problems of self-induced turbulence primarily because the two jets involved were very close together and essentially acted as one. The jets, therefore, did not create any significant upflow that would disturb the aircraft.

One problem that can aggravate the effects of self-induced turbulence is that of reduction of control effectiveness in close proximity to the ground. This problem has been encountered on tilt-wing aircraft such as the VZ-2 where the trailing-edge ailerons, with the wing in the vertical position, are deflected differentially to produce yawing moments on the aircraft in hovering flight. (See fig. 10.) Plain ailerons suffer a significant loss in control effectiveness below a height of about 1 diameter. Recent data, however, have indicated that the control effectiveness in proximity to the ground can be increased appreciably by using a slotted aileron. This configuration allows air to flow through the slot to control the flow on the upper surface of the flap; thus, much higher flap deflections can be used with the slotted aileron than with the plain ailerons.

Ground Effects in STOL Operation

Both the VZ-3RY deflected-slipstream aircraft (ref. 16) and the VZ-2 tilt-wing aircraft (ref. 17) have experienced significant losses in lift in ground proximity in short landings.

Figure 11 shows schematically the flow around the wing and the impingement of the flow on the ground. Part of the air is projected forward along the ground, and this forward flowing sheet of air tends to lower the pressure under the wing and to cause a loss in lift and a forward inclination of the lift vector. The loss in lift has created problems for the pilots; however, the forward component of force has not been troublesome. For the VZ-2 aircraft, adequate power was available to compensate for the loss in lift. In order to investigate this problem, however, some special flights were made in which the aircraft was set up in a trimmed condition out of ground effect at a low rate of sinking speed. Power and attitude were maintained constant to ground contact. The increase in sinking speed at the point of ground contact is shown

in figure 11 as a function of the approach speed. The ground effect did not become significant until speeds below about 30 knots were reached and only became critical at speeds below about 20 knots.

These losses in lift have been attributed to the recirculation of flow through the propellers (ref. 16); however, experience from wind-tunnel tests has shown that it is not the loss in propeller thrust due to this recirculation that is important in this loss in lift. The propeller forces are affected by the recirculating flow but the loss in lift has been encountered on blowing-flap and jet configurations as well. In fact, wind-tunnel data have shown that blowing-flap configurations may experience even larger losses in lift than the propeller-driven configurations for which flight experience is available.

A change in trim due to the proximity to the ground may also be encountered in STOL operation. The angle of flow with respect to the horizontal tail is changed by the presence of the ground giving rise to a nose-up trim change as the aircraft leaves the ground on a take-off. This trim change was encountered on the VZ-2 tilt-wing aircraft at about the same tilt angles and speeds at which the loss in lift was experienced. The pilots reported that under normal conditions both the lift loss and trim change could be controlled. These two problems may be more serious in rough air or during instrument operations.

CONCLUDING REMARKS

Figure 12 presents the approximate height and airspeed conditions under which ground effects may be encountered by transport V/STOL and STOL aircraft in the 50,000-pound class. In general, ground effects should not be significant at heights above about 20 to 30 feet and at airspeeds above about 40 to 50 knots.

The effects of self-generated turbulence will not be serious if adequate control is provided, and this annoyance to the pilot can be reduced by providing artificial damping. The avoidance of ground-erosion damage involves proper preparation and housekeeping of the landing site for high-disk-loading vehicles and proper operating procedures to avoid running into debris. Research is still in progress to obtain a better understanding of hot-gas ingestion and means of reducing it; its effects can be minimized by vectoring the exhaust rearward and using a short running take-off. The lift losses and trim changes in STOL operations will require the pilot to hold an extra margin of power and velocity in the landing approach to compensate for this problem. Ground effects may preclude some operations such as hovering over loose sand with jet aircraft, but, in general, operational procedures can be devised to minimize adverse ground effects.

REFERENCES

1. Campbell, John P.: Ground Proximity Effects Associated With V/STOL Aircraft. NASA paper presented at the Eighth Anglo-American Aeronautical Conference (London, England), Sept. 3-14, 1961.

2. Schade, Robert O.: Ground Interference Effects. NASA TN D-727, 1961.

3. Spreemann, Kenneth P.; and Sherman, Irving R.: Effects of Ground Proximity on the Thrust of a Simple Downward-Directed Jet Beneath a Flat Surface. NACA TN 4407, 1958.

4. Wyatt, L. A.: Static Tests of Ground Effect on Planforms Fitted With a Centrally-Located Round Lifting Jet. C.P. No. 749, Brit. A.R.C., 1964.

5. Vogler, Raymond D.: Interference Effects of Single and Multiple Round or Slotted Jets on a VTOL Model in Transition. NASA TN D-2380, 1964.

6. Kuhn, Richard E.: An Investigation To Determine Conditions Under Which Downwash From VTOL Aircraft Will Start Surface Erosion From Various Types of Terrain. NASA TN D-56, 1959.

7. O'Bryan, Thomas C.: An Investigation of the Effect of Downwash From a VTOL Aircraft and a Helicopter in the Ground Environment. NASA TN D-977, 1961.

8. Vesigot, J. P.; and Gire, E.: Terrain de decollage ou atterrissage pour avion VSTOL. Symposium on Vertical/Short Takeoff and Landing Aircraft. Pt. II. AGARDograph 46, June 1960, pp. 355-370.

9. Grotz, C. A.: Simulated VTOL Exhaust Impingement on Ground Surfaces. Symposium on Vertical/Short Takeoff and Landing Aircraft. Pt. II. AGARDograph 46, June 1960, pp. 419-426.

10. Vasiloff, A.: Test Results of Research for Rapid Site Preparation for VTOL Aircraft. APL-TDR-64-104, U.S. Air Force, Nov. 1964.

11. Pegg, Robert J.: Damage Incurred on a Tilt-Wing Multipropeller VTOL/STOL Aircraft Operating Over a Level, Gravel-Covered Surface. NASA TN D-535, 1960.

12. O'Bryan, Thomas C.: An Experimental Study of the Effect of Downwash From a Twin-Propeller VTOL Aircraft on Several Types of Ground Surfaces. NASA TN D-1239, 1962.

13. Kirk, Jerry V.; Hickey, David H.; and Hall, Leo P.: Aerodynamic Characteristics of a Full-Scale Fan-In-Wing Model Including Results in Ground Effect With Nose-Fan Pitch Control. NASA TN D-2368, 1964.

14. Reeder, John P.: Handling Qualities Experience With Several VTOL Research Aircraft. NASA TN D-735, 1961.

15. Gustafson, F. B.; Pegg, Robert J.; and Kelley, Henry L.: Aerodynamic Observations From Flight Tests of Two VTOL Aircraft. NASA Conference on V/STOL Aircraft - A Compilation of the Papers Presented. NASA, Nov. 1960, pp. 149-169.

16. Turner, Howard L.; and Drinkwater, Fred J. III.: Some Flight Characteristics of a Deflected Slipstream V/STOL Aircraft. NASA TN D-1891, 1963.

17. Pegg, Robert J.; Kelley, Henry L.; and Reeder, John P.: Flight Investigation of the VZ-2 Tilt-Wing Aircraft With Full-Span Flap. NASA TN D-2680, 1965.

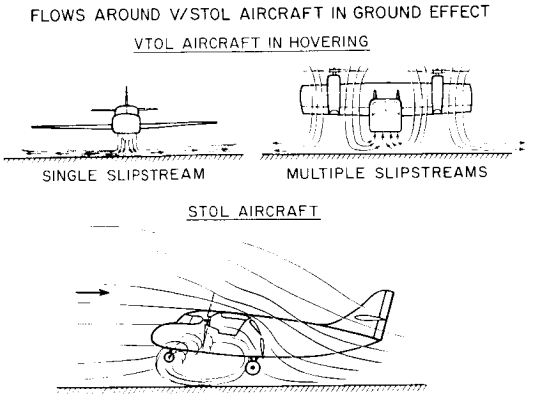

Figure 1

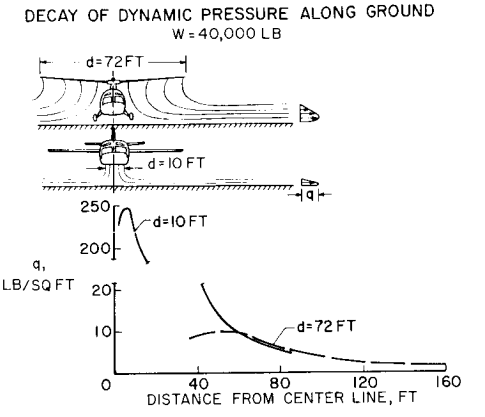

Figure 2

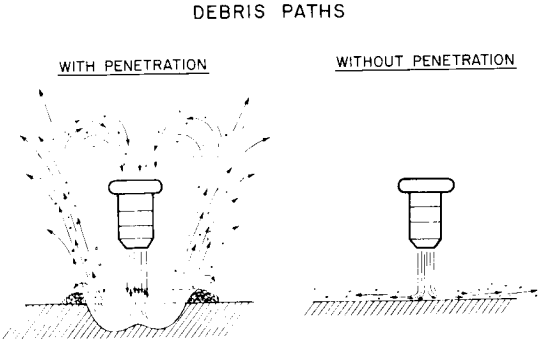

Figure 3

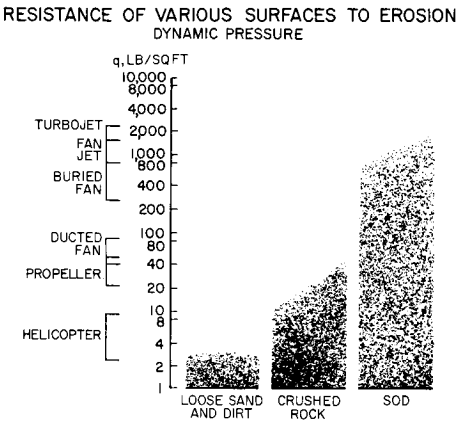

Figure 4

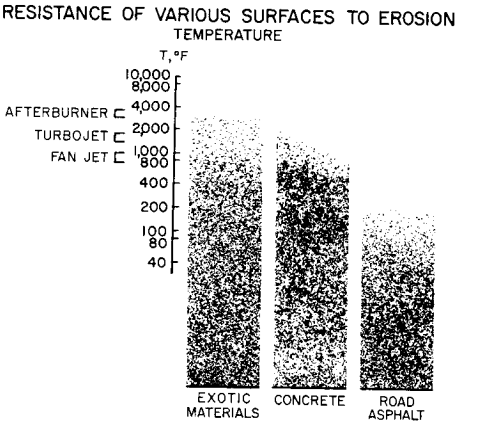

Figure 5

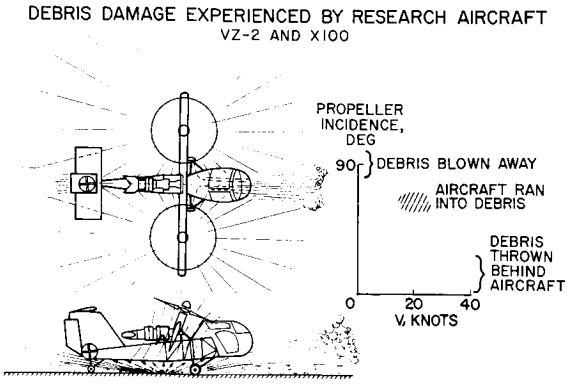

Figure 6

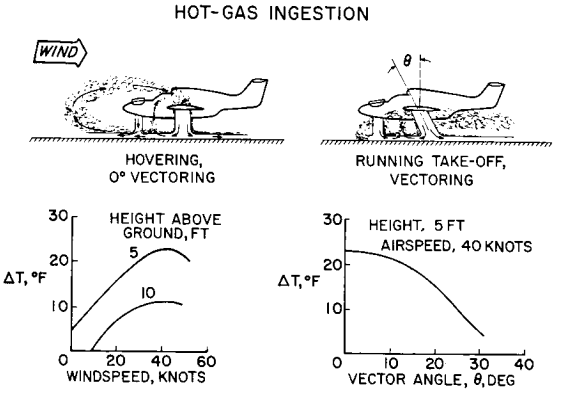

Figure 7

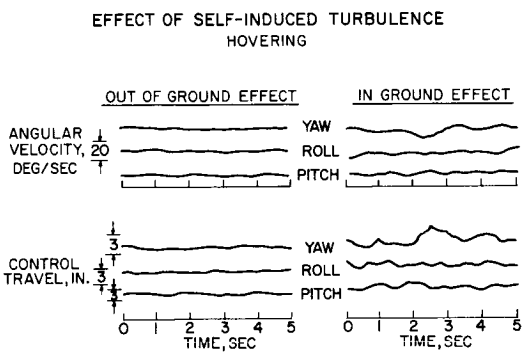

Figure 8

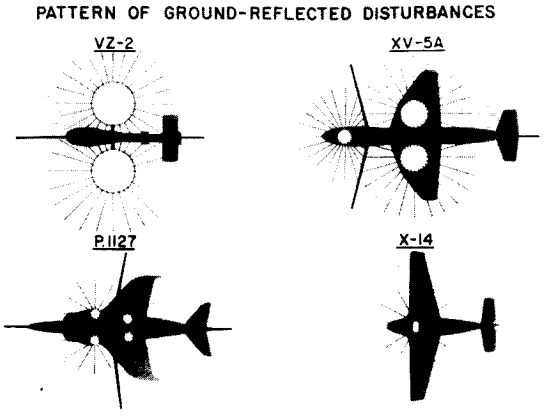

Figure 9

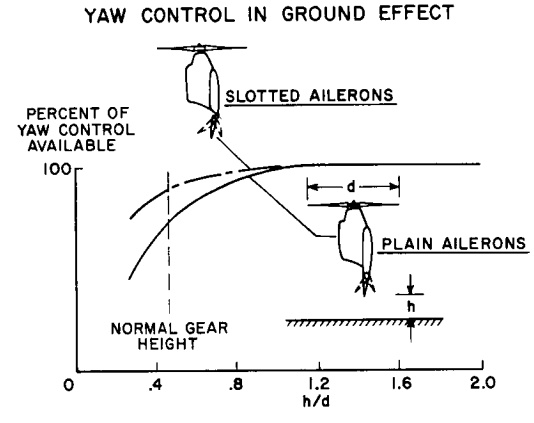

Figure 10

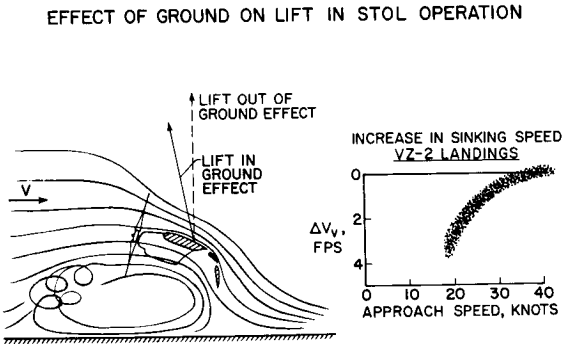

Figure 11

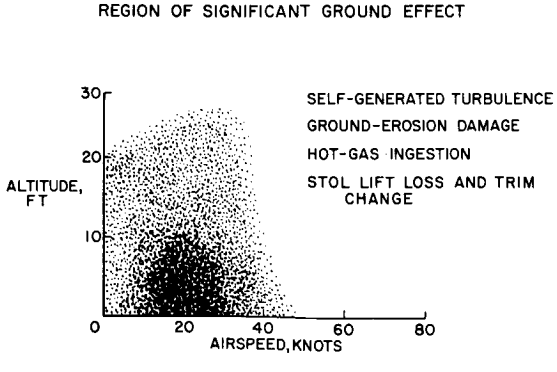

Figure 12

32. OPERATIONAL EXPERIENCES WITH THE X-14A DEFLECTED-JET VTOL AIRCRAFT

By L. Stewart Rolls

NASA Ames Research Center

32

SUMMARY

During $5\frac{1}{2}$ years of flight research with a deflected-jet VTOL aircraft, a number of operational problems were experienced and investigated. These experiences can be grouped into two general categories: (1) the effects of the jet engine and its operation and (2) the restrictions imposed upon the pilot's operation due to reduced visual reference. This report is an examination of these problems and, in some cases, presents possible solutions to these problems.

INTRODUCTION

Since the late 1950's, numerous agencies both in this country and abroad have been flying various forms of vertical take-off and landing aircraft. The majority of these flight activities were directed toward developing satisfactory pilot control and handling qualities. Whereas these quantities are extremely important, the extension of the VTOL aircraft beyond an experimental oddity to an operational aircraft requires an examination of the operational problems associated with this class of aircraft and of the solutions found to these problems.

During the $5\frac{1}{2}$ years of research flying of a deflected-jet VTOL research vehicle (the X-14A) at the Ames Research Center, there were certain areas of operation in which difficulties were encountered that might limit the operational utility of the concept. These experiences have shown that the environmental surroundings have a significant influence on both the operation of a VTOL aircraft and the ability of the pilot to complete a prescribed mission. The factors discussed in this report which influence the operation of the aircraft include hot-gas ingestion, suck-down, and ground erosion. The factors affecting the pilot are exemplified by his loss in orientation through the lack of sideward or backward velocity indications while hovering at altitude and, at night, by his poor judgment of vertical velocity while hovering.

DESCRIPTION OF EQUIPMENT

The X-14A research aircraft used in this investigation was constructed by the Bell Aircraft Company (now a part of Bell Aerosystems Company) under

contract to the U.S. Air Force and had successfully completed hovering and transitional flight prior to its transfer to the NASA in late 1959. Following a brief initial flight program at the Ames Research Center, the aircraft was extensively modified to improve its performance and enlarge its research capability. The information in this report was obtained from flight tests of the modified aircraft, which is shown in hovering flight in figure 1. The X-14A VTOL aircraft utilizes the vectored-thrust principle of vertical lift. The exhaust gas from two horizontally mounted General Electric J85-5 turbojet engines is directed through a cascade system of exit diverters, as shown in figure 2. The exhaust gas may be directed vertically or horizontally by the positioning of the outer set of cascades. During hover and slow-speed flight, control of the aircraft attitude is maintained by the use of reaction jets at the wing tips and tail; air for these controls is bled from the compressor of the turbojet engines. A set of servo-operated valves in conjunction with a pilot's control panel provides a variable stability and control capability in the aircraft. A more detailed description of the test vehicle and the test procedures is presented in references 1 to 3.

RESULTS AND DISCUSSION

The experience of operating a deflected-jet VTOL aircraft has indicated that the operational difficulties can be grouped into two general categories; the first is primarily the effects of the jet engine and its operation, and the second is the results from the restrictions imposed upon the pilot's operation due to the environment in which he is flying.

Engine Jet Effects

Hot-gas ingestion.- The susceptibility of a turbojet-engine thrust output to inlet-air temperature can result in a critical operation of a jet-lift VTOL aircraft. The large quantities of hot exhaust gases which circulate around the aircraft during hover can, under certain conditions, be ingested into the inlets with a corresponding loss in thrust. The flow of these exhaust gases about the vehicle and the effect of wind on this flow is illustrated in figure 3. Also, if the distribution of hot gases across the inlet is nonuniform, it could cause the temperature sensor to signal erroneous commands to the fuel control and increase the probability of compressor stall. In addition, a nonuniform temperature variation could impose an additional stress problem for the compressor blades. The effect of ingesting hot gases into the engines on the thrust is shown in figure 4. The thrust reduction with temperature increase is shown in the left side of this figure. The dashed line represents the thrust required from each engine to lift the aircraft off the ground. The data indicate that for inlet temperatures greater than 80° F the aircraft will not become airborne. The right side of the figure shows that a headwind causes an increase in the hot-gas ingestion, as indicated by the increase in inlet temperature. When this increase in inlet temperature results in a thrust available - that is, less than the thrust required for lift-off - the pilot must decide whether (1) to operate the engines momentarily above the temperature limit, knowing that the thrust requirements decrease with height, (2) to

burn off fuel until a sufficient weight reduction is made to allow lift-off, but with a reduced flight capability, or (3) to lift off with a cross wind or tail wind even though difficulty in attitude control is increased.

Ground effect.- The air entrained by the engine exhaust flows across and around the surfaces of the aircraft so that a negative pressure field is created, resulting in a suck-down when the aircraft is less than about 20 feet above the ground. Therefore, a thrust greater than the weight of the aircraft is required to lift the aircraft vertically off the ground. The magnitude of this effect in the X-14A is illustrated in figure 5, in which the thrust required to hover at various fixed heights is shown. The rapid increase in the thrust-required curve as the aircraft approaches the ground is a severe problem for this type of vehicle because it dictates a greater installed thrust and also accounts for the long landing gear on the X-14A. In order that there be a better understanding of this effect, the wing-root fairings were removed from the X-14A; thus, a more direct inflow of the entrained air was permitted, with the possibility of a corresponding decrease in the negative pressure field. Flight tests for this condition did not show any change in the suck-down magnitude. The removable fairings were near the trailing edge of the wing and a considerable distance from the jet.

Also, the instability resulting from this condition makes the pilot's task of learning the take-off and landing maneuvers more difficult. In the X-14A the instability is symmetrical, and no attitude-control problem is induced; however, in some aircraft in which the lifting units are dispersed from the center, an unstable rolling moment is experienced.

The ground effects of jet-lift aircraft have been studied in various facilities. (See ref. 4.) A comparison of the X-14A data and the computed requirements based upon these tunnel tests is shown in figure 6. The data near the ground are in fair agreement, but the effect of the ground is felt to a much greater height in the airplane than the model tests would indicate. Because of this difference, the actual penalty in operating a VTOL airplane may be small, since only a limited amount of time would be spent in this altitude range.

Ground erosion.- Extreme difficulty may be encountered when operating a VTOL aircraft near an unprepared surface. The downwash velocities associated with these hovering vehicles are usually high enough to cause ground erosion and to cause debris to be thrown in all directions about the aircraft. The jet-lift aircraft is most critical in this regard because of the extremely high jet velocities which are directed toward the ground. When the X-14A approaches an unprepared surface, a dust cloud similar to that of figure 7 results. In this particular view, the X-14A is hovering alongside the runway at a height of about 45 feet above a barren field of loose dirt, and the dust cloud extends to a height of about 35 feet. It is obvious that a landing on this type of surface is undesirable and probably could not be made without severe damage to the aircraft or the engine compressors.

Ground erosion also occurred when the aircraft has hovered at low altitude over a grass-covered field. On this occasion the aircraft was hovered at various heights over a moist field of native rye type of grass. No

sign of ground erosion or browning of the grass was observed as long as the airplane was at a height greater than about 15 feet. When the hovering height was lowered to a jet-exhaust height of about 6 feet and held for about 5 seconds, a large section of the soil exploded into the air and a sizable amount was ingested into the jet engines. Figure 8 illustrates the magnitude of the crater caused by the rapid hurling of earth into the air. Inasmuch as this event occurred during an interval of 1 or 2 seconds, it was impossible for the pilot to remove the aircraft from this position prior to the ingestion of the dirt and subsequent compressor damage. The P.1127 in England has operated from turf fields, but in the X-14A incident, the roots of the grass did not stabilize the soil sufficiently to withstand the jet.

Full utilization of VTOL aircraft will require that the vehicle can be operated from other than hard concrete landing surfaces. Thus, either a method to reduce the jet-exhaust velocities or a means of quickly preparing a suitable surface for landing is required. Both these approaches are being pursued in an attempt to free the jet VTOL from the restriction of operating only over a concrete surface. To examine methods to minimize the ground-erosion effect of the jet exhaust, the NASA has contracted for a study of several nozzle shapes designed to increase the mixing between the jet exhaust and the surrounding air. (See ref. 5.) Some of these nozzles are shown in figure 9. The experimental results obtained with these nozzles are shown in figure 10 in terms of the variation of the maximum dynamic pressure in the jet q_x/q_N with distance downstream from the nozzle x/D. These data also show the nozzle velocity coefficients, which are the ratios of the actual to the ideal nozzle thrust. The jet dynamic pressure has been shown in the past to be a determining factor in ground erosion. The achievement of values less than 0.3 is a desirable goal and should permit VTOL operation with pure jet aircraft from a wide variety of sod conditions. To relate these distance ratios to an aircraft, it is felt that values of x/D from 2 to 3 will be the range used in fighters, whereas values up to 8 will be used on high-wing transports with lift engines in pods on the wing. Figure 10 indicates that a dynamic pressure ratio of 0.3 is possible within this x/D range for some of these nozzles. Studies of these nozzles in the presence of a wing and fuselage, however, indicate that the rapid mixing of the jet and surrounding air might increase the thrust loss of the airplane-engine combination. Further studies of these nozzles are necessary to document their usefulness more fully and to weigh the beneficial and undesirable characteristics. Inasmuch as these nozzle shapes are similar to those studied in the past for noise reduction, some beneficial noise reduction may also result from their use.

The X-14A was used as a test vehicle during a field test of a method for rapid preparation of a landing area for VTOL aircraft. The method used in this test was developed by the U.S. Air Force and Ling-Temco-Vought and consisted of spraying alternate layers of fiber-glass yarn and a chlorinated polyester resin. Test samples of this pad were successfully evaluated in a laboratory rig and withstood afterburning temperatures and exhaust velocities. Figure 11 shows the pad under construction on a test site alongside the taxiway at Moffett Field. This figure illustrates the two separate operations used to build up the landing pad: (1) spraying the fiber-glass yarn and (2) covering it with the polyester resin. The pad was first prepared to cover a

25-foot-diameter area; however, an attempted landing on this pad indicated that a larger pad would be required. An additional surface, 18 feet wide but thinner, was laid around the original pad to serve as a dust cover. The pad was prepared on the same barren dirt field which resulted in the dust cloud shown in figure 7. Four hours after the pad preparation commenced, the pad was ready for the aircraft. The X-14A made a series of approaches, landings, and take-offs from the prepared surface. (See fig. 12.) This method of preparing a landing area for jet VTOL aircraft shows some merit, and further field tests are planned by the U.S. Air Force. A complete description of the field tests with the X-14A is contained in reference 6.

Environmental Restrictions

The second major category is associated with the hovering of a VTOL aircraft under varied visibility conditions. For this discussion, the vehicle is assumed to have satisfactory control power and damping characteristics. In order to operate a hovering vehicle successfully, the pilot must be able to assay his situation rapidly and accurately. Consequently, until now hovering flights have been restricted to situations in which the pilot has good visual reference to supply his much needed attitude information. This problem has been demonstrated during flight tests of the X-14A when, for safety reasons, the vehicle was hovered at an altitude from 2500 to 3000 feet during check flights of control-system changes or for early indoctrination flights for new pilots. The lack of visual reference at altitude makes it extremely difficult for the pilot to determine sideward or backward motion. The pilots who are more familiar with the X-14A use other inputs, such as the position of the angle-of-attack vane or the reversal of elevator control force, to supply information concerning the motion of the aircraft. The difficulty of this task has been illustrated by the unscheduled maneuvers which have been performed by pilots during their check flights because of their inability to detect airplane motion. These maneuvers have included attitude changes along the pitch or roll axis of greater than 180°. Fortunately, with its light wing loading, recovery can be executed in the X-14A with only a nominal loss in altitude.

One test objective required that a flight be made at night. A lighted area around the landing spot and a lighted hangar with the door open was provided to serve as an attitude reference. The pilot reported difficulty in judging height and height rate. It was not until he was high enough to line up distant lights that he was confident about height control. This problem may be more severe on the X-14A because of the low value of vertical damping which intensifies the height-control problem. During normal hovering periods when there are good visual references, the pilot has no difficulty maintaining his height. However, when the references are reduced, the control of height becomes more difficult and it is harder for the pilot to maintain the vehicle at the desired altitude. Helicopters can hover at night, but with their high vertical damping the task of controlling height is not as critical as that for the X-14A; however, helicopters experience problems during sonar operations over the sea on dark nights when the pilot loses orientation due to the lack of references. Thus, the experiences in the X-14A have shown that sensitive displays of high resolution will have to be developed if a VTOL is to hover successfully during periods of reduced visibility.

CONCLUDING REMARKS

Examination of the experiences in flight testing a deflected-jet VTOL aircraft, the X-14A, has indicated possible operating problems. Hot-gas ingestion and suck-down are problems which will cause difficulties for some VTOL concepts. Test results have indicated possible approaches for minimizing the ground erosion by using either special nozzle shapes to reduce downwash velocities at ground level or by preparing the ground surface to withstand the velocities. Operation during periods of reduced visual references demonstrated the need for sensitive pilot displays of high resolution for VTOL operation.

REFERENCES

1. Rolls, L. Stewart; and Drinkwater, Fred J., III: A Flight Determination of the Attitude Control Power and Damping Requirements for a Visual Hovering Task in the Variable Stability and Control X-14A Research Vehicle. NASA TN D-1328, 1962.

2. Rolls, L. Stewart; Drinkwater, Fred J., III; and Innis, Robert C.: Effects of Lateral Control Characteristics on Hovering a Jet Lift VTOL Aircraft. NASA TN D-2701, 1965.

3. Pauli, Frank A.; Hegarty, Daniel M.; and Walsh, Thomas M.: A System for Varying the Stability and Control of a Deflected-Jet, Fixed-Wing VTOL Aircraft. NASA TN D-2700, 1965.

4. Schade, Robert O.: Ground Interference Effects. NASA TN D-727, 1961.

5. Higgins, C. C.; and Wainwright, T. W.: Dynamic Pressure and Thrust Characteristics of Cold Jets Discharging From Several Exhaust Nozzles Designed for VTOL Downwash Suppression. NASA TN D-2263, 1964.

6. Vasiloff, A.: Test Results of Research for Rapid Site Preparation for VTOL Aircraft. APL-TDR-64-104, U.S. Air Force, Nov. 1964.

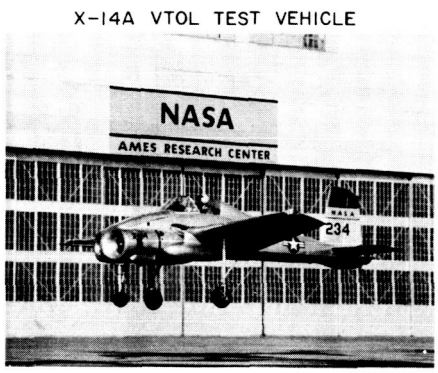

Figure 1 A-28473-9

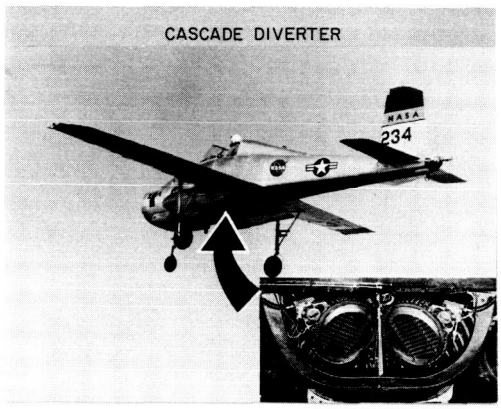

Figure 2 A-34382-2

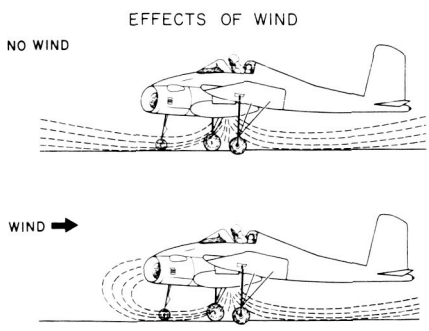

Figure 3

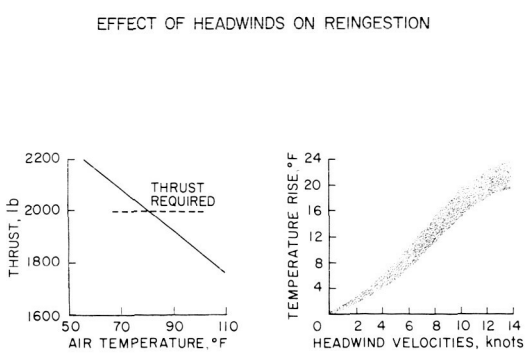

Figure 4

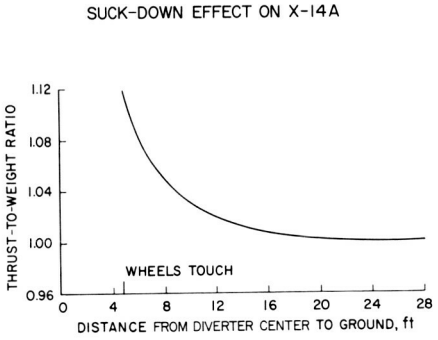

Figure 5

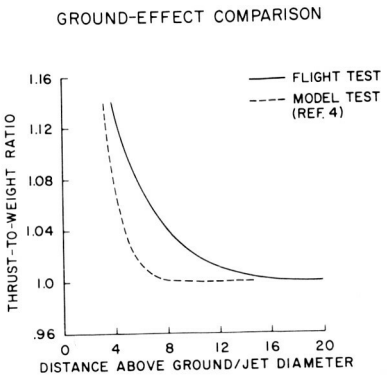

Figure 6

Figure 7 A-32780-27

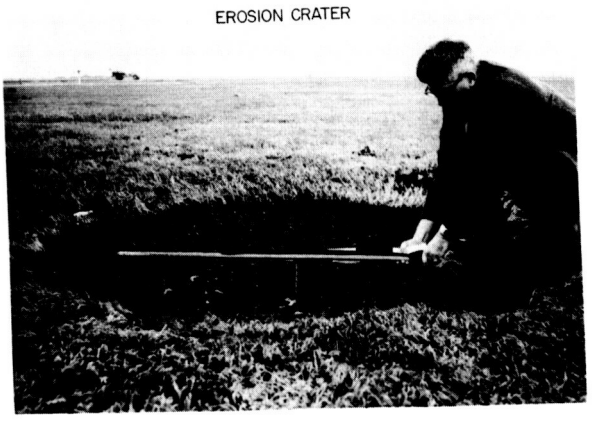

Figure 8 A-30386

NOZZLE SHAPES

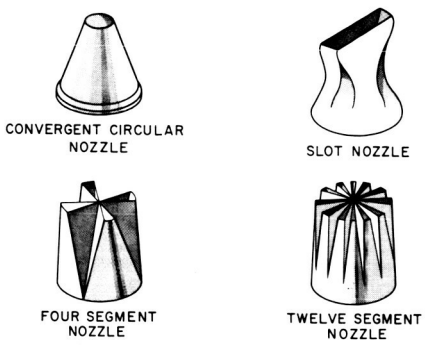

Figure 9

EFFECT OF NOZZLE SHAPE ON VELOCITY DECAY

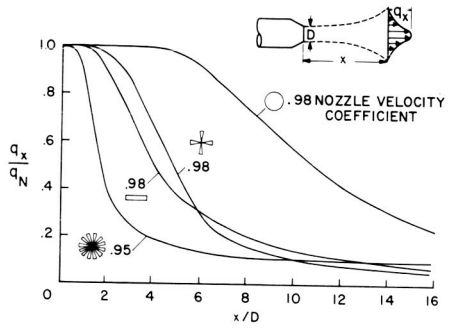

Figure 10

PREPARATION OF PLASTIC LANDING PAD

Figure 11 A-32780-28

X-14A LANDING ON PLASTIC PAD

Figure 12 A-32780-8

33. SOME PERFORMANCE AND HANDLING-QUALITIES CONSIDERATIONS FOR OPERATION OF STOL AIRCRAFT

By Seth B. Anderson, Hervey C. Quigley,
and Robert C. Innis

NASA Ames Research Center

SUMMARY

Studies of a number of STOL aircraft show that relatively high maximum lift-coefficients and large increases in lift due to power are within the present state of the art. With these lift characteristics, approach speeds of the order of 60 knots for aircraft of moderate wing loading can be realized. Full advantage of the STOL performance of aircraft such as those discussed herein may not be realized on a routine operational basis, however, without some form of damping augmentation system because of lateral-directional handling considerations, particularly for large aircraft operating under instrument flight conditions. Satisfactory characteristics can be obtained by use of only a servodriven rudder. Additional experience is needed to determine how the STOL aircraft is to be operated before more firm requirements for augmentation systems can be established.

INTRODUCTION

The requirement for STOL airplanes which can operate out of small fields and yet retain high cruise performance has continued with increased emphasis for both military and commercial operation. Aircraft requiring STOL operation are

(1) COIN (counter-insurgency) fighter

(2) Short-haul transport

(3) HLS (heavy logistics) transport

Short-field landing distance depends on approach speed as indicated in figure 1. Shown are the approximate approach speeds and landing distances for the aforementioned aircraft. Although each of these aircraft has been identified as an STOL type, the landing distance ranges from 800 feet for the COIN aircraft to 4,000 feet for the HLS transport. Since approach speed is dependent on wing loading and lift coefficient, and since these aircraft require high wing loading for efficient cruise, the expected short-field requirements can be met

only by operation at high lift coefficients. In addition, to realize maximum STOL performance, engine power must be used to augment aerodynamic lift. The amount of engine power used is a measure of the degree of STOL operation, the ultimate being VTOL. As a result, the STOL aircraft must operate in an environment of low dynamic pressure which results in reduced control and damping and where engine power effects on stability are more important.

SYMBOLS

C_L	lift coefficient
$C_{L_{max}}$	maximum lift coefficient
N_p	yawing moment due to roll rate
$N_{\delta a}$	yawing moment due to aileron deflection
P	period, sec
r	rate of turn, rad/sec
t	time, sec
V	velocity, knots
β	angle of sideslip, deg
$\dot{\beta}$	rate of sideslip, deg/sec
δ_a	aileron deflection angle, deg
δ_r	rudder deflection angle, deg
ϕ	angle of bank, deg

DESCRIPTION OF TEST AIRCRAFT

For a number of years NASA has investigated STOL aircraft to obtain information on performance, handling qualities, and operational characteristics. Because of very high lift systems and controls designed for low-speed operation, it was possible with the test aircraft to probe further into STOL flight than heretofore had been possible. (See refs. 1 to 6.) Once the problems and limitations of these aircraft are understood, the possibility of further expanding the low-speed envelope for the HLS or any future STOL aircraft may be realized. In addition, if good handling qualities are provided, the

performance of the skilled test pilot can become routine for the operator of STOL aircraft.

RESULTS AND DISCUSSION

The main points learned from the operating experience with the test aircraft that may apply to the three previously mentioned aircraft fall in the following three areas:

(1) Lift performance

(2) Limitations in low-speed operation

(3) Solutions to handling-qualities problems

Lift Performance

Lift performance of the STOL aircraft is shown in figure 2 in terms of lift coefficient and speed. The values of $C_{L_{max}}$ corresponding to maximum power, approach power, and idle power as well as the values of C_L for approach are shown. Relatively high values of maximum lift have been obtained with these STOL aircraft, and the use of engine power is primarily responsible for the large increase from the basic lift. The 367-80 jet aircraft had little direct lift due to power. The immediate question that comes to mind is, How much of this available lift is actually usable to the pilot not only under ideal test flying conditions, but also for routine day-to-day operation? The selected values of C_L for approach, although far removed from maximum lift, are above the value of $C_{L_{max}}$ at minimum power for the slipstream configurations. For STOL operation these approach lift coefficients represent a marked reduction in approach speeds over those used by conventional aircraft for which the approach C_L is based on the idle-power stall speed multiplied by 1.3. For example, the conventional approach speed would be about 80 knots for the 941 aircraft.

Operational Envelope

One major reason for limiting the amount of lift used (flying slower) is that of obtaining desirable descent rates or steep flight path angles. Figure 3 shows the flight path angle plotted against speed for the 941 aircraft at various engine powers. The shapes of the curves are representative of all the test aircraft. All the aircraft had adequate descent capability, that is, 800 feet per minute or 6° flight path angles provided that low engine power was used in approach. As soon as engine power is increased above idle to reduce speed, the values of L/D increase and the approach path becomes shallower. The point to be emphasized is that if improvements beyond the values shown are required for the deflected-slipstream aircraft, they must be obtained either by increasing the basic or idle-power lift capability or by increasing the slipstream turning

and the engine power as is the case for the VZ-3RY or the tilt-wing aircraft such as the XC-142. In these cases the stall or minimum-speed line would be displaced towards the lower speed region.

Handling Qualities

Assuming that the existing landing performance of the test aircraft is satisfactory, another reason for limiting the amount of lift used is the fact that the aircraft must have satisfactory handling characteristics so that it can be controlled precisely along its intended flight path. Unsatisfactory handling qualities which would compromise performance in a day-to-day operation were common to all the aircraft to some degree. In general, it was possible for test purposes to approach at a speed slower than the minimum speed dictated by stability and control considerations. Of the various handling qualities, the lateral-directional characteristics were the most troublesome and, therefore, were considered to require immediate attention particularly for instrument flight operation.

Sideslip Control

The item of primary concern common in varying degrees to all aircraft tested was control of sideslip angle. Shown in figure 4 is the effect of airspeed on the variation of the sideslip-bank ratio $\Delta\beta/\Delta\phi$ with directional period for rudder-fixed turn entries. These curves were determined by using the characteristics of the basic 367-80 aircraft. Large sideslip angles are easily generated at the low speeds of STOL operation because of low values of directional stability. Since the yawing moment needed to turn the aircraft must be generated by sideslip if the rudder is not used, a large part of the increase in sideslip is due to the increased turn rate associated with flight at lower airspeeds. The pilot is concerned about controlling sideslip angle for a number of reasons: (1) Sideslip excursions occurring during turn maneuvers result in heading errors. (2) Precise control of sideslip is needed during decrab for cross-wind landings. (3) Fin stalling may occur at large angles of sideslip.

During turn entries at low speeds, large yawing moments can be generated by (1) aileron deflection and (2) roll velocity. Since these yawing moments can be large and adverse at high lift coefficients, their influence is greater in STOL aircraft because they increase the requirement to use the rudder to reduce sideslip during turning. A time history of the rudder requirements for a coordinated (sideslip equals zero) turn maneuver of the C-130B aircraft at 70 knots is presented in figure 5. The difficulty of (1) applying the correct amount of rudder deflection and (2) properly phasing the rudder and aileron is illustrated by these data. Even for a small-turn entry at a bank angle of only -10°, appreciable amounts of rudder deflection at different times are required to maintain zero sideslip.

Lateral-Directional Period

Rudder coordination becomes more difficult as the lateral-directional period becomes longer since the aircraft behavior will be slow or sluggish and the rise time of the response will appear as lag to the pilot. The lag makes it difficult for the pilot to predict the final response of the aircraft to his input. The relationship of pilot rating to period for two aircraft configurations obtained from simulator tests and verified by flight results in the speed range of 55 to 85 knots is shown in figure 6. Pilot rating deteriorated with increasing period; the poorest rating was obtained with the swept-wing configuration, primarily because of the inherently larger adverse yawing moment due to roll rate and because of other characteristics such as poor Dutch-roll damping associated with this planform. In general, the unaugmented aircraft were rated unsatisfactory for periods greater than 7 seconds. Marked improvements were obtained for both the swept-wing and the straight-wing configurations by using damping augmentation. The lateral-directional period of an aircraft is a function of both its size and the airspeed at which it is operated. Thus for the C5-A type aircraft, the period can be as long as 15 seconds if operated at speeds of the order of 85 to 90 knots.

Damping Augmentation Systems

Solutions to the lateral-directional problem involving the use of damping augmentation which obviously would be needed for operation of the larger aircraft, particularly under IFR conditions, are examined. Since the primary problem previously discussed has been identified as that of controlling large sideslip excursions which accompanied landing-approach maneuvers, consideration was given to a damping system which would utilize the rudder to counteract the yawing moments produced by aileron deflection, roll rate, and yaw rate. Simulator studies and flight tests of stability and damping systems were made in the UF-XS, NC-130B, and 367-80 aircraft. These studies showed that reducing adverse yaw due to aileron deflection did not by itself improve pilot rating, nor did a conventional yaw damper improve the pilot rating sufficiently. Sideslip-rate damping, referred to a $\dot{\beta}$ damping, was more successful as a means of controlling sideslip as shown in figure 7 for the NC-130B aircraft. For a turn at a bank angle of 10°, $\dot{\beta}$ damping markedly reduced the peak sideslip angle; the final steady-state value of β was less, and a greater turn rate resulted. The basic deficiency in applying a yaw damper to the sideslip problem of STOL aircraft is that in a turn entry the yaw damper applies a rudder deflection opposite to that required in the turn and thereby increases sideslip. A washout type of yaw damper would, of course, reduce the steady-state sideslip, but would have little or no effect on the peak value of sideslip.

In addition, there is a need to offset the unfavorable (negative) yawing moment due to roll velocity since inherent values of N_p for most aircraft are unfavorable. Both flight and simulator tests have shown that with low directional stability (periods greater than 10 seconds) the desired gain of a yawing-moment augmenter is quite critical.

The results of a damping augmentation system, which considered all the points learned from the operating experience with STOL aircraft, are shown in

figure 8. These results for the NC-130B aircraft show that large reductions in peak sideslip angle for a given bank angle were obtained by the use of the augmentation system which provided $\dot{\beta}$ damping, a favorable value of N_p, and compensation for adverse values of N_{δ_a}. In the NC-130B airplane, the maximum authority (that is, percent of total rudder deflection) was 25 percent and was limited by the characteristics of the servosystem used. Even with the augmentation system, maneuvering had to be limited to a 15° bank angle if sideslip was to be restricted to 5°. Further reduction in sideslip could be achieved provided increased rudder authority is acceptable.

CONCLUDING REMARKS

In summary, relatively high maximum lift coefficients and large increases in lift due to power, which are within the present state of the art, result in approach speeds of the order of 60 knots for aircraft of moderate wing loading. Full advantage of the STOL performance of aircraft such as those discussed herein may not be realized on a routine operational basis, however, without some form of damping augmentation system because of lateral-directional handling considerations, particularly for large aircraft operating under instrument flight conditions.

Satisfactory characteristics can be obtained by use of only a servodriven rudder.

Additional experience is needed to determine how the STOL aircraft is to be operated before more firm requirements for augmentation systems can be established.

REFERENCES

1. Turner, Howard L.; and Drinkwater, Fred J., III.: Some Flight Characteristics of a Deflected Slipstream V/STOL Aircraft. NASA TN D-1891, 1963.

2. Innis, Robert C.; and Quigley, Hervey C.: A Flight Examination of Operating Problems of V/STOL Aircraft in STOL-Type Landing and Approach. NASA TN D-862, 1961.

3. Quigley, Hervey C.; and Innis, Robert C.: Handling Qualities and Operational Problems of a Large Four-Propeller STOL Transport Airplane. NASA TN D-1647, 1963.

4. Quigley, Hervey C.; Innis, Robert C.; and Holzhauser, Curt A.: A Flight Investigation of the Performance, Handling Qualities, and Operational Characteristics of a Deflected Slipstream STOL Transport Airplane Having Four Interconnected Propellers. NASA TN D-2231, 1964.

5. Booda, Larry: Japan Seeks Markets for New Projects. Aviation Week and Space Technol., vol. 80, no. 11, Mar. 16, 1964, pp. 276-283.

6. Gratzer, L. B.; and O'Donnell, T. J.: The Development of a BLC High-Lift System for High-Speed Airplanes. Paper No. 64-589, Am. Inst. Aeron. Astronaut., Aug. 1964.

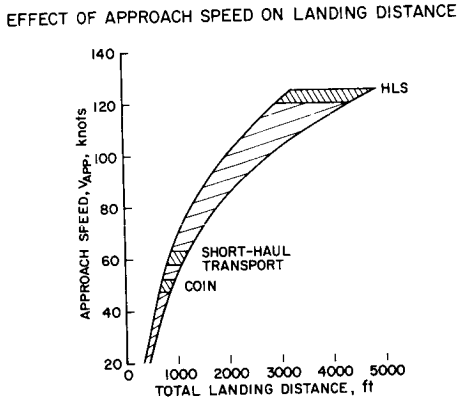

Figure 1

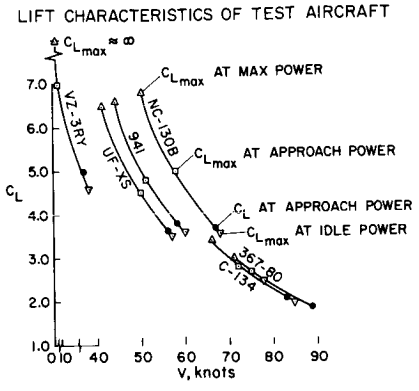

Figure 2

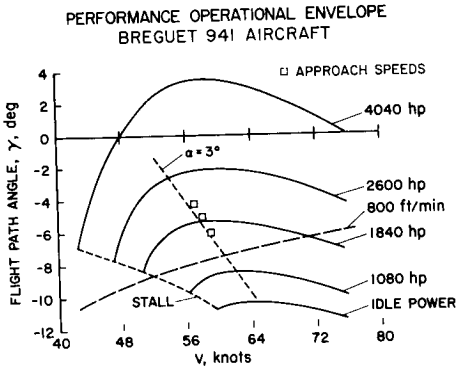

Figure 3

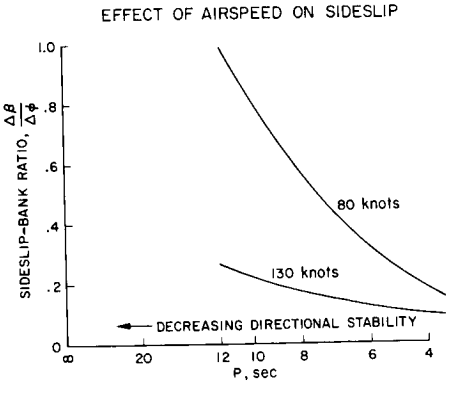

Figure 4

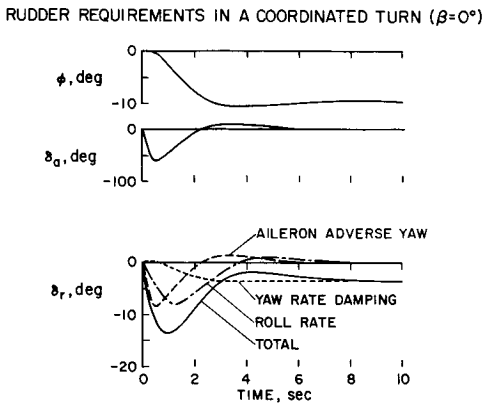

Figure 5

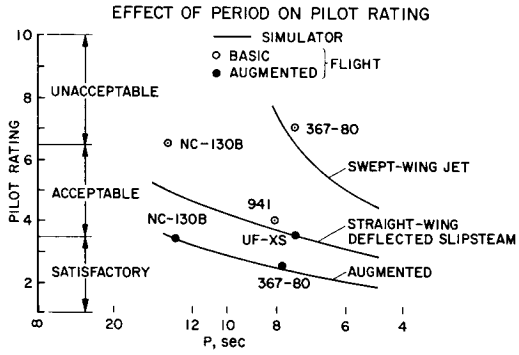

Figure 6

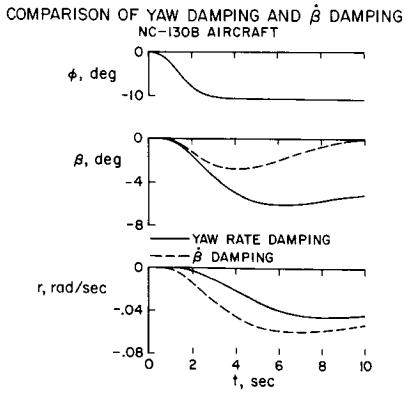

Figure 7

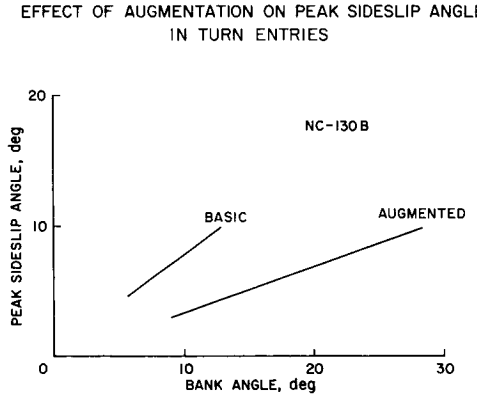

Figure 8

34. LOW-SPEED FLIGHT CHARACTERISTICS OF A POWERED-LIFT JET TRANSPORT DURING THE LANDING APPROACH

By Robert O. Schade and Harold L. Crane

NASA Langley Research Center

SUMMARY

A flight-test program to determine the flight characteristics of large jet transports equipped with powered-lift systems indicated the following results: Speed margins appear to be primarily related to power-on stall speeds. At these speed margins, the maneuver margins were adequate and did not appear to be a problem or limiting factor during powered-lift operation. No large detrimental effects on handling qualities were apparent but in some areas stability augmentation would be required to obtain satisfactory flight characteristics. Use of the powered-lift airplane would result in a sizable increase in the noise levels; these increases are primarily the result of higher engine power settings in the approach.

INTRODUCTION

In recent years, the development of the high-speed jet transport has emphasized the need for high lift to reduce the approach and landing speeds. Lower approach and landing speeds are desirable from the standpoint of reducing landing distance, lowering weather minimums, and obtaining greater safety.

One method of improving the lift capabilities of these aircraft is to use a powered-lift system such as boundary-layer control or "blown flaps." Before such systems can be considered for future application or operational use, however, a considerable amount of research will be required in the areas of performance margins, handling qualities, and engine noise. In order to obtain some information in these three areas, the Langley Research Center has recently completed a flight-test program to determine the flight characteristics of a large powered-lift jet transport in the landing approach.

AIRPLANE AND EQUIPMENT

The airplane used in the investigation was the original Boeing 707 prototype, modified to provide high-lift capability and to improve flying qualities at low speeds. (See ref. 1.) The general arrangement of the airplane is shown in the photograph of figure 1.

The 35° swept wing was modified with leading-edge devices which included a fixed slat from the wing tip to the inboard engine pylon and a fixed cambered Kreuger type of flap from the inboard pylon halfway to the fuselage. A

simple hinged, trailing-edge flap was used that extended from the fuselage to 68 percent of the wing semispan. The average ratio of flap chord to wing chord was 22.2 percent and the maximum flap deflection was 85°.

The powered-lift system is illustrated in figure 2. In operation, the boundary-layer-control air was bled from each of the four JT3D engine compressors into two separate ducting systems. Each ducting system covered the full span of the flaps. The blowing nozzles alternated between these two distribution ducts to minimize the loss of lift in the event of failure of one of the systems. These nozzles blew through an ejector at the knee of the flap, and entrained secondary air; thereby the blowing momentum was increased by approximately 30 percent.

In order to operate the engines at the high powers required for the powered-lift system and still obtain the low thrust settings required for the landing-approach condition, a thrust modulation system was used. The normal clamshell-type thrust reversers located in each of the four engine primary tailpipes were modified to be continuously variable through their entire operation range from maximum thrust to essentially zero thrust by a set of four levers located on the pilot's console. This thrust modulation system offered a very fast-acting speed control during the landing approach when compared with the response of the normal throttle control. The system was used in place of the normal throttle control during all powered-lift conditions.

TEST PROCEDURES

Configurations

The configurations tested in the investigation included the basic airplane and the airplane with various amounts of powered lift. This paper includes only two of the configurations - the basic airplane without the powered-lift system in operation for a base line to determine the effects of powered lift and a configuration with full powered lift to obtain indications of the maximum changes in flight characteristics.

Evaluation Tasks

Preliminary evaluation tests were made under conditions of Visual Flight Rules (VFR) at a safe altitude to insure safety of procedures and to define the desired flight conditions for the final landing-approach evaluation tests.

After these tests, final pilot evaluation was obtained under conditions of simulated (hooded) Instrument Flight Rules (IFR) during approach to landing. Hooded approaches were used in order to provide a precision pilot task representative of those that are used during actual operations.

For the basic task, an intercept of the localizer was made approximately 8 miles from the runway at an altitude of 1500 feet. The airspeed and flight conditions were then stabilized. At the intercept of the glide slope,

approximately 5 miles from the runway, the descent was initiated and the pilot attempted to fly the prescribed flight path as closely as possible down to approximately 200 feet and, if conditions were favorable, to continue visually to touchdown. Some tests were made with the localizer offset 200 feet from the runway center line. After the simulated IFR breakout at 200 feet of altitude, the pilot performed a visual sidestep maneuver in order to line up with the runway.

All final evaluations were made with the minimum safe approach speeds at which the pilots felt they could make consistent approaches and landings. These selected minimum safe approach speeds enabled the pilots to evaluate the minimum, or limiting, conditions related to the performance criteria and to study handling-qualities characteristics in the speed area where problems were likely to be most severe. Flight tests were conducted under good ceiling and visibility weather conditions with light to moderate winds of 10 knots or less and gusts below 5 knots.

RESULTS AND DISCUSSION

Criteria for Performance Margins

The performance margins established by the Federal Aviation Agency (FAA) for present-day commercial transport airplanes (see ref. 2) are illustrated in figure 3. The requirements specify a minimum approach speed of 1.3 times the power-off stall speed V_{STALL}. By using this minimum approach speed, the resulting maneuver margin - which is the difference between the lift required and the maximum lift available - is 0.44g. This difference means that the airplane, when flying at 1.3 times the power-off stall, has a maximum pull-up maneuver capability of 0.44g from level flight. These speed and maneuver margins have proven to be adequate for conventional aircraft.

For powered-lift airplanes, the use of speed and maneuver margins based on power-off stall speeds may no longer be applicable because powered-lift systems require essentially full power to operate. Another factor which also must be considered is that the maximum lift coefficient $C_{L,MAX}$ for powered-lift airplanes is no longer constant over the speed range because of the variation in blowing momentum with forward speed (as forward speed decreases with a given power setting, the same amount of blowing becomes effectively larger in relation to the airspeed).

It may be noted that the designated stall speed shown in figure 3 is a minimum, steady-flight speed which is actually beyond the stall or below the lift coefficient C_L required for 1 g flight. In this condition, the airplane is not capable of 1g flight and is experiencing a normal acceleration close to 0.1 g downward. In this low-speed flight investigation, all stall speeds were referred to the 1g stall or the minimum speed at which the airplane can develop lift equal to the weight of the airplane.

Powered-lift speed and maneuver margins.- The results of the flight tests to establish criteria for speed and maneuver margins are shown in figure 4 where the minimum safe approach speeds selected by the three test pilots (the shaded area) is given for the range of gross weights flown during the flight tests. For comparison, similar data are shown for the basic airplane. The data for the basic airplane are shown in relation to the normal 1g stall speed, and the data for the powered-lift airplane are shown in relation to the power-on 1g stall speed. The pilots' selected minimum safe approach speeds for the basic airplane were at, or just below, 1.2 times the stall speed for the range of gross weights flown and indicated a close relationship between the minimum approach speeds and the stall. If the difference between the FAA stall speed and the stall speed used in this investigation is taken into account, this relationship becomes essentially the same as the FAA specified minimum-approach-speed criteria of 1.3 times the stall speed. Except for the power-on stall speed being used, the relationship for the powered-lift airplane was the same as that for the basic airplane; that is, the pilots' selected minimum safe approach speeds were about 1.2 times the power-on stall speed.

The minimum safe approach speeds for the powered-lift airplane resulted in maneuver margins of 1.42g. This maneuver margin, which was essentially the same as that obtained for present-day airplanes, was adequate and, as would be expected, did not appear to be a problem or limiting factor.

Pitch attitude.- Although the stall speed was apparently the most significant single factor in establishing the minimum approach speed for the powered-lift airplane, there was another factor that was of concern to the pilots - the pitch attitude of the airplane during powered-lift operation. During approach and landing, the nose-down attitude caused the pilots concern that, during the landing flare, the airplane would touch down nose wheel first with a resulting rebounding of the aircraft.

Illustrated in figure 5 are typical test results showing the body attitude for the basic airplane and the airplane with powered lift. Shown as the shaded area is the pilots' established, desired pitch attitude range for operation of the aircraft. This attitude range represents an area in which the airplane would not inadvertently touch down nose wheel first nor tail skid first during the landing flare. From the flight-test data shown in figure 5, it can be seen that the airplane body pitch attitude varied from the high side of the desirable range for the basic airplane to below, or outside, the desirable range for the powered-lift airplane. The nose-down pitch attitude during powered-lift operation was of sufficient concern to the pilots that they would have preferred lower approach speeds in order to raise the nose. However, the lower approach speed could not be utilized because of the close proximity to stall.

Handling Qualities

A considerable portion of the flight-test time of this investigation was used to determine the effects of powered-lift operation on the handling qualities of the airplane. Shown in figure 6 are some typical flight-test results which indicate that there were no large detrimental effects on the flight characteristics of the airplane resulting from use of powered lift. It appears from this

figure that the task of flying the simulated IFR approach could be done just as well, or perhaps even better, with powered lift. This tendency was further indicated by the more accurate landings that were made during powered-lift operation. Illustrated in figure 7 are the results for the actual airplane touchdown points in relation to a runway target touchdown point on the runway 1500 feet from the runway threshold. Zero indicates the target touchdown point, negative values are for landings that undershot the target, and positive values are for landings that overshot the target. It can be seen that, at the lower approach speeds with the powered-lift airplane, the dispersion from the target tends to be less. It appears that this was the result of the considerably lower approach speeds of the powered-lift airplane which gave the pilot more time to make corrections and to aline the airplane with the target before touchdown.

Handling-Qualities Problem Areas

Although there were no large detrimental effects on flight characteristics resulting from the use of powered lift, there were some areas in which the handling qualities did noticeably deteriorate. These areas were related to Dutch roll, lateral directional cross coupling, and longitudinal trim changes in ground effect. It is felt that the deterioration of the handling qualities in these three areas was not a function of the particular test airplane but rather inherent problem areas which must be considered during the operation of jet transports with blown-flap powered-lift systems.

Dutch roll.- In the flight tests, the Dutch roll oscillations, which were lightly damped for the basic airplane, become unstable for the powered-lift airplane. Since the unstable Dutch roll motion was undesirable from the standpoint of obtaining good pilot evaluation, a series of tests were conducted to establish what stability augmentation would be required to stabilize this motion satisfactorily. These results indicated that a $C_{n_{\dot{\beta}}}$ sideslip rate damper, which gave yawing moment in response to rate of sideslip, adequately damped the Dutch roll motion. The function of this sideslip rate damper is very similar to that of a normal yaw damper except that it measures the rate of change of sideslip angle rather than the rate of change of azimuth heading.

Cross coupling.- During powered-lift operation, it became apparent that there was a large amount of adverse lateral directional cross coupling (adverse yaw due to roll); this was particularly true at the lowest speeds that were flown. A combination of two stability augmentation systems was used to minimize the cross-coupling effects: a $C_{n_{\delta a}}$ turn coordinator which gave yawing moment in response to aileron control to counteract the adverse yaw due to aileron deflection; and a $C_{n_{\dot{\phi}}}$ roll decoupler which gave yawing moment in response to rolling to counteract adverse yaw due to rolling.

With these augmentation systems operating, the adverse sideslip due to roll was essentially eliminated at the minimum approach speeds used for powered-lift configurations.

Ground effects.- The airplane also exhibited a large nose-down longitudinal trim change in ground effect. This change resulted in considerably larger elevator deflections being required by the pilot during the landing flare than those normally used for the basic airplane. This trim change appears to be the result of the large change in downwash angle at the tail. It is believed that, because of the relatively large angles of downwash associated with the high-lift operation of powered-lift systems, this trim change will be an inherent problem with aircraft of this type.

Engine Noise

Engine noise is considered a problem with conventional jet aircraft during the landing approach. With the powered-lift airplane, the noise problem becomes more acute since high engine power is required during the landing approach for operation of the powered-lift system.

Some indications of the magnitude of this engine noise problem were obtained during the flight program. The results of these tests are shown in figure 8 as a comparison of the relative perceived noise levels (PNdB) for the basic airplane and the powered-lift airplane. The noise values were measured approximately 0.8 mile from touchdown during 3° glide-slope landing approaches. Zero time indicates the airplane is overhead; plus values indicate airplane noise before it is overhead; and minus values indicate airplane noise after it has passed overhead. It can be seen that the use of powered lift with its high power settings increased the maximum peak noise level approximately 10 PNdB. Basically, this increase in noise is the result of the high engine power setting, and the methods of reducing the noise levels on the landing approach would be the same as those used during the take-off. Two possible methods would be lower thrust levels (by better blowing efficiency) and use of steeper approach paths above the normal 2.5° or 3.0°.

In addition, figure 8 shows that the duration of the higher intensity noise is much longer for the airplane with powered lift than that for the basic airplane. The results of reference 3 indicate that, if this increased duration were taken into consideration, it would tend to increase the ratings of perceived noise level in decibels (PNdB) further. For example, doubling the duration of the same noise level would increase the PNdB ratings by approximately 4.5. The apparent increase in noise level with longer duration was very noticeable to the people located below the powered-lift airplane during the landing approaches.

CONCLUDING REMARKS

An investigation has been conducted to provide some preliminary information concerning the low-speed flight characteristics of large jet transports equipped with powered-lift systems.

In relation to possible criteria for performance margins for powered-lift airplanes, the speed margins appear to be primarily related to power-on stall

speeds. At these speed margins, the maneuver margins were adequate and did not appear to be a problem or a limiting factor during powered-lift operation.

Although there were no large detrimental effects on handling qualities resulting from the use of powered lift, there were some areas in which the handling qualities had deteriorated sufficiently that they needed stability augmentation to obtain satisfactory flight characteristics.

The powered-lift airplane showed sizable increases in noise levels which were primarily the result of the higher engine power settings in the approach.

REFERENCES

1. Gratzer, L. B.; and O'Donnell, T. J.: The Development of a BLC High-Lift System for High Speed Airplanes. Paper No. 64-589, Am. Inst. Aeron. Astronaut., Aug. 1964.

2. Anon.: Airworthiness Standards: Transport Category Airplanes. Federal Aviation Regulation Part 25, Rules Service Co. (Washington, D.C.), Feb. 1, 1965.

3. Kryter, Karl D.; and Pearsons, Karl S.: Some Effects of Spectral Content and Duration on Perceived Noise Level. NASA TN D-1873, 1963.

TEST AIRPLANE

L-2431-1

Figure 1

BLC FLAP INSTALLATION

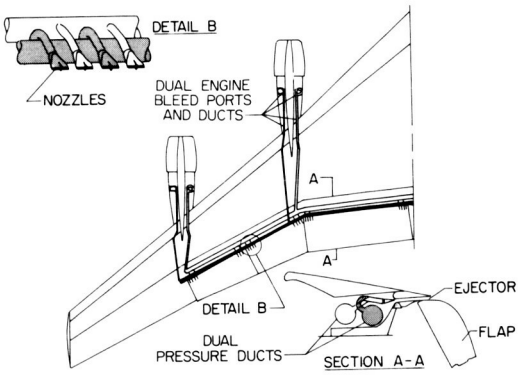

Figure 2

ILLUSTRATION OF SPEED AND MANEUVER MARGINS

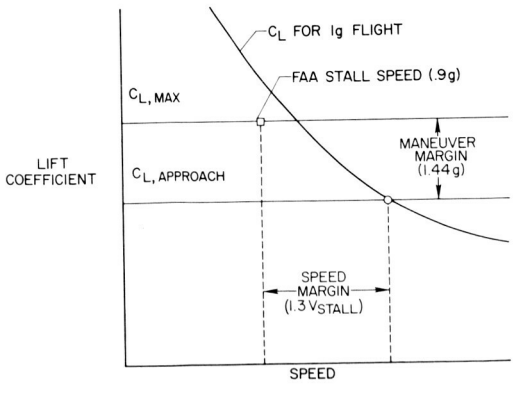

Figure 3

POSSIBLE CRITERIA RELATED TO SPEED AND MANEUVER MARGINS

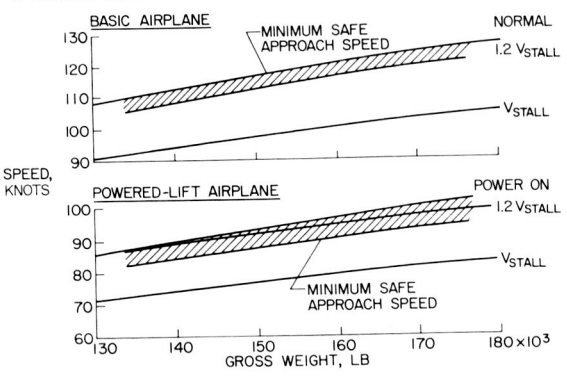

Figure 4

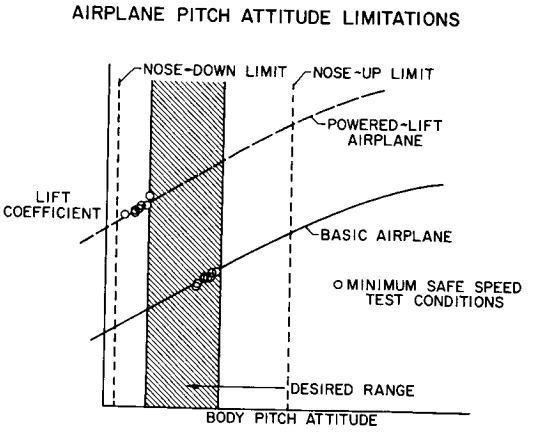

Figure 5

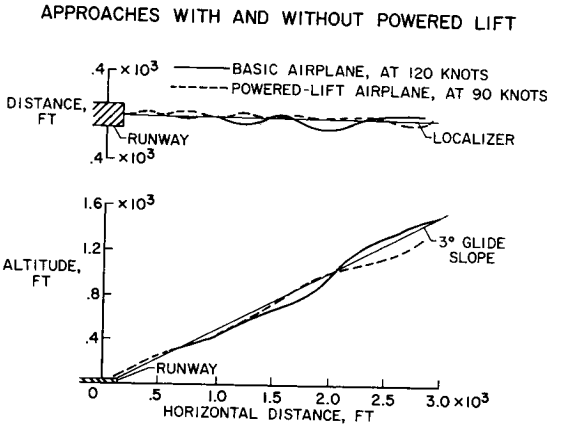

Figure 6

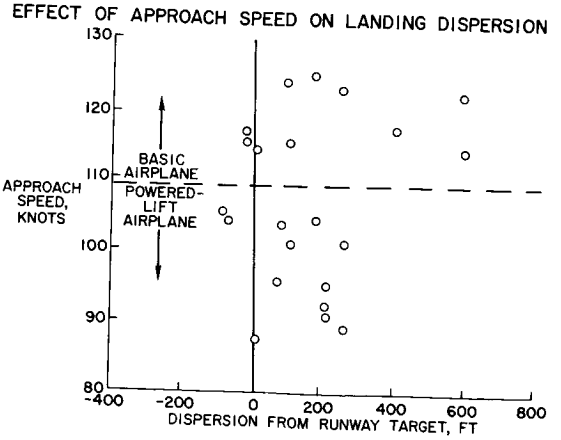

Figure 7

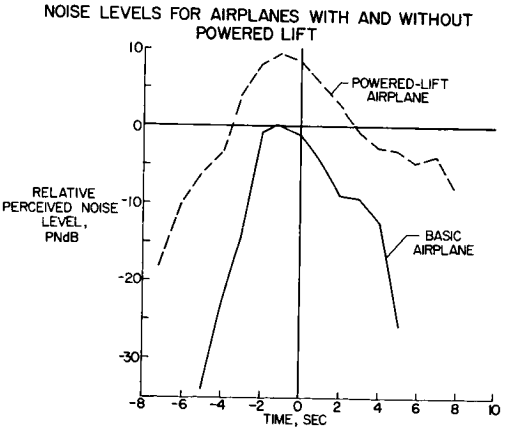

Figure 8

NASA-Langley, 1965